Assay Development Towards the Characterisation of the Bifunctional Activity of *P. aeruginosa* and *E. coli* Class A PBPs

Amy Mae O'Reilly

Thesis submitted in partial fulfillment of the requirements for the degree of Doctor of Philosophy in Mathematical Biology and Biophysical Chemistry

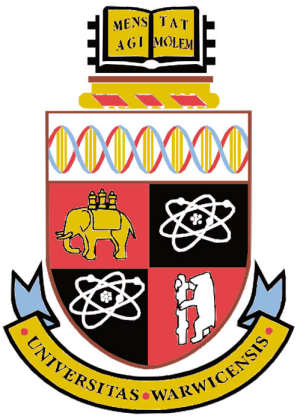

The University of Warwick

Department of Chemistry

March 2017

Thesis Contents

Chapter 1 Introduction

Chapter 2 Materials and Methods

Chapter 3

The Cloning, Expression and Purification of PBPs and their Associated Proteins

Chapter 4

The Kinetic Analysis of the Transglycosylation Activity of *E. coli* PBP1A and *P. aeruginosa* PBP1A using a Continuous Fluorescence Assay

Chapter 5
A Discontinuous Spectrophotometric Assay for The Detection of Transglycosylase-Dependent Undecaprenyl Pyrophosphate Production

Chapter 6

The Study of Transpeptidation in Class A Penicillin Binding Proteins from *E. coli* and *P. aeruginosa*

Chapter 7

Discussion, Conclusions and Future Work

Acknowledgements

I would like to thank my supervisors, Prof. Tim Bugg and Dr. David Roper. Thanks to Tim who is always really positive about my research and results and I appreciate his efforts in critiquing this thesis before submission. A huge thank you goes to Dr. Adrian Lloyd for his patience, his willingness to share results and collaborate on multiple areas of this project. Adrian went out of his way to help in all aspects of the bringing together of this thesis.

Thanks to Anita, Julie and Smita for help with compound synthesis. I appreciate the numerous flasks of media supplied by Cerith and Mark, totalling over 1000 Litres of media over 3.5 years. I would like to thank fellow lab members: Claire, Christine, Ailidh and Mussa for being fantastic bench partners. Kat, Steve, Conor, Greg and Mike for pub Fridays, DannyMc for consecutive secret santa exchanges and Kyle for sophisticated dinner parties. Thanks to Chris for all the films, cooking sessions and Family Guy episodes we shared. Thank you to Soph and Adrian for being so accommodating and flexible.

Thank you to my advisory panel for keeping my project on the straight and narrow. A particular mention to Dr. Ann Dixon for her support and interest in my progression. A huge heart-felt thank you to Prof. Alison Rodger who awarded me the EPSRC funding to conduct this research. I appreciate everything that comes with the Doctoral Training Centre family, from life-long friendships and team-building to weekly seminars and multi-disciplinary problem solving. Thank you to Naomi for organising the greatest annual conferences.

Finally, a big love to Rich who has always been there for support no matter what and has been extremely patient during the write up of this thesis.

There may be times when we are powerless to prevent injustice,
but there must never be a time when we fail to protest.
Elie Weisel, 1928-2016 Nobel Laureate.

This thesis is dedicated to Dr. Adrian Lloyd.
Without his overwhelming support and trust,
this thesis would not have been written.

"Strong people stand up for themselves; stronger people stand up for others”
Steve Oedekerk, 2006.

Declaration

This thesis is submitted to The University of Warwick in support of my application for the degree of Doctor of Philosophy. It has been composed by myself and has not been submitted in any previous application for any degree. The work presented (including data generated and data analysis) was carried out by myself and any deviation from this is acknowledged in the text.

Abstract

Pseudomonas aeruginosa is a Gram-negative species of bacteria that is of high clinical importance and is on the ESKAPE list of pathogens, causing the most serious nosocomial infections World-wide. Current antibiotics in clinical use against *P. aeruginosa* include carbenicillin, cefepime, ceftazidime, and the fluoroquinoline ciprofloxacin. The multi-drug resistant (MDR) phenotype exhibits widespread resistance to β-lactams and antibiotics from multiple classes often need to be administered in conjunction with β-lactamase inhibitors.

Penicillin binding proteins (PBPs) are essential for cell viability and are important antibiotic targets, with the Class A bifunctional PBPs synthesising the principle component of the bacterial cell wall, peptidoglycan. The focus of this project was to investigate the kinetics of transglycosylation and transpeptidation mechanisms with a view to improving our understanding of bacterial cell wall synthesis, maintenance and regeneration.

In this project, the function of Class A PBPs 1A and 1B from *Escherichia coli* and *P. aeruginosa*, with particular focus on PBP1A has been investigated. Transglycosylation and transpeptidation have been probed from multiple angles using orthogonal assays and fluorescently-labelled and native lipid substrates, as well as Lipid II structural variants. *P. aeruginosa* PBP1A transglycosylase and transpeptidase activities are demonstrated continuously, and compared to the model organism equivalent, *E. coli* PBP1A. The continuous monitoring of activity gave insights into the possibility of two catalytic sites for transglycosylation: a donor and an acceptor site. Data was fitted to different kinetic models to elucidate the best fit for extracting meaningful kinetic parameters.

The data acquired over the course of this project suggests that *P. aeruginosa* PBP1A and *E. coli* PBP1A exhibit similar functional behaviour to each other, with *E. coli* PBP1B showing distinct activity from PBP1A. *Pa*PBP1B activity was not detected at a level required to kinetically characterise the enzyme and it is possible that this PBP has an as yet undetermined stimulatory cofactor. The assays developed and optimised in this thesis will pave the way for further in-depth studies of *P. aeruginosa* PBP1A, which could be used to screen for putative inhibitor compounds and potentially identify certain characteristics required for antimicrobial efficacy.

Over the past 4 years, major leaps in our knowledge of assay development, the transglycosylase and transpeptidase activities of Class A PBPs and substrate features and requirements for transglycosylase and transpeptidase donors and acceptors have thus far and will continue to unravel the unique and fascinating mechanistic intricacies of the bifunctionality of PBPs.

Abbreviations

2YT	2 x yeast trypone media
A_{xxx}	Absorbance
ATP	Adenosine 5'-triphosphate
AU	Absorbance Unit
BCA	Bicinchoninic acid
BODIPY	Boron dipyrromethene dye
BSA	Bovine Serine Albumin
C_{55}-PP	Undecaprenyl pyrophosphate
CD	Circular dichroism
CHAPS	3-[(3-Cholamidopropyl) dimethylammonio]-1-propanesulfonate
CMC	Critical Micellar Concentration
Da	Dalton
DAAO	D-amino acid oxidase
Dans	dansylated
DAP	D-aminopimelic Acid
DDM	*n*-Dodecyl-β-D-maltopyranoside
DEAE	Diethyl-aminoethyl
DMSO	Dimethyl Sulphoxide
DNAaseI	Deoxyribonuclease I enzyme
dNTPs	deoxy
Ec	Escherichia coli
ECL	Electrochemiluminescence
EGTA	ethylene glycol-bis(β-aminoethyl ether)-N,N,N',N'-tetraacetic acid
EDTA	Ethylenediaminetetraacetic acid
FRET	Fluorescence resonance energy transfer
GlcNAc	N-acetylglucosamine
HEPES	4-(2-hydroxyethyl)-1-piperazineethanesulfonic acid
HMW	High molecular weight
HPLC	High-Performance Liquid Chromatography
HRP	Horseradish peroxidase
IC_{50}	Inhibitory concentration

IMAC	Immobilised Metal-Affinity Chromatography
IPTG	Isopropyl-β-D-thiogalactopyranoside
K_{cat}	Michaelis-Menton Constant
K_D	Dissociation constant
K_m	Michaelis-Menton Constant
kpsi	kilopound per square inch
LB	Luria Broth
LDAO	Lauryldimethylamine oxide
Lipid I	Undecaprenyl pyrophosphoryl-N-acetylmuramyl-L-Alanyl-D-Glutamyl-L-Lysyl-D-Alanyl-D-Alanine
LII	Undecaprenyl pyrophosphoryl-N-acetylmurmayl (Nacetyl-glucosaminyl)- L-Alanyl-D-Glutamyl-X-D-Alanyl DAlanine
mAU	Milli-absorbance unit
MESG	7-methyl-6-guanosine
MurNAc	N-acetylmuramic acid
m/z	Mass to charge ratio
NADH	Nicotinamide adenine dinucleotide
Pa	Pseudomonas aeruginosa
PAGE	Polyacrylamide electrophoresis
PBP	Penicillin Binding Protein
PCR	Polymerase chain reaction
PEP	Phosphoenol pyruvate
PgpB	phosphatidylglycerophospate phosphatase B
pI	Isoelectric point
Pi	Inorganic phosphate
PMSF	Phenyl methyl sulphonyl fluoride
PNP	Purine Nucleoside Phosphorylase
RFU	Relative Fluorescence Units
SDM	Site-Directed Mutagenesis
SDS	Sodium dodecyl sulfate
TAE	Tris acetate ethylenediaminetetraacetic acid
TEV	Tobacco etch virus protease
TG	Transglycosylase

TM	Transmembrane domain
TP	Transpeptidase
Tris	Tris(hydroxymethyl)aminomethane
TX-100	Triton X-100
UDP	Uridine diphosphate
v/v	volume to volume ratio
w/v	Weight to volume ratio

List of Tables

Chapter 1 Introduction

Chapter 2 Materials and Methods

Chapter 3 The Cloning, Expression and Purification of PBPs and their Associated Proteins

Chapter 4 The Kinetic Analysis of the Transglycosylation Activity of *E. coli* PBP1A and *P. aeruginosa* PBP1A using a Continuous Fluorescence Assay

Chapter 5 A Discontinuous Spectrophotometric Assay for The Detection of Transglycosylase-Dependent Undecaprenyl Pyrophosphate Production

Chapter 6 The Study of Transpeptidation in Class A Penicillin Binding Proteins from *E. coli* and *P. aeruginosa*

List of Figures

Chapter 1 Introduction

Chapter 3 The Cloning, Expression and Purification of PBPs and their Associated Proteins

Chapter 4 The Kinetic Analysis of the Transglycosylation Activity of *E. coli* PBP1A and *P. aeruginosa* PBP1A using a Continuous Fluorescence Assay

Chapter 5 A Discontinuous Spectrophotometric Assay for The Detection of Transglycosylase-Dependent Undecaprenyl Pyrophosphate Production

Chapter 6 The Study of Transpeptidation in Class A Penicillin Binding Proteins from *E. coli* and *P. aeruginosa*

Chapter 7 Discussion, Conclusions and Future Work

Chapter 1 Introduction

1.1 Gram-Positive vs Gram-Negative Bacterial Cell Envelopes

The exclusivity of the cell wall to bacteria has resulted in its exploitation as a valid target for antimicrobials, particularly β-lactams such as penicillin and cephalosporins. Antimicrobial inhibition of cell wall synthesis can be targeted to several steps in the pathway, by antibiotics including Fosfomycin, Cycloserine, Bacitracin, Vancomycin glycolipids and β-lactams. Increasing prevalence of antibiotic resistance has fuelled research into novel targets for antibacterial drugs.

1.1.1 The Gram-Positive Bacterial Cell Wall

Gram-positive cells contain an inner cell membrane called the plasma membrane, which follows the most widely accepted model for membrane structure: the fluid mosaic model. The structure is dynamic and flexible, containing peripheral and integral membrane proteins. This membrane comprises of a phospholipid bilayer with hydrophilic surfaces and hydrophobic interior, with most bacterial membranes lacking sterols. It provides a selectively permeable barrier that keeps the cytoplasm separate from the external environment. The plasma membrane is the site for metabolic processes such as lipid synthesis, cell wall synthesis and harbours chemo-response receptor molecules (Silhavy *et al.*, 2010).

Surrounding the plasma membrane is a thick layer of the organic polymer peptidoglycan (**Figure 1.1 a**), a mesh-like structure that maintains structural integrity under osmotic stress and pressure. The cell wall of Gram-positive bacteria defines the cell shape and is made up of 90% peptidoglycan, as well as large amounts of teichoic acids that are not present in Gram-negative bacteria. As Gram-positive cells have no membrane outside of their thick peptidoglycan layer, they are more susceptible to antibiotics.

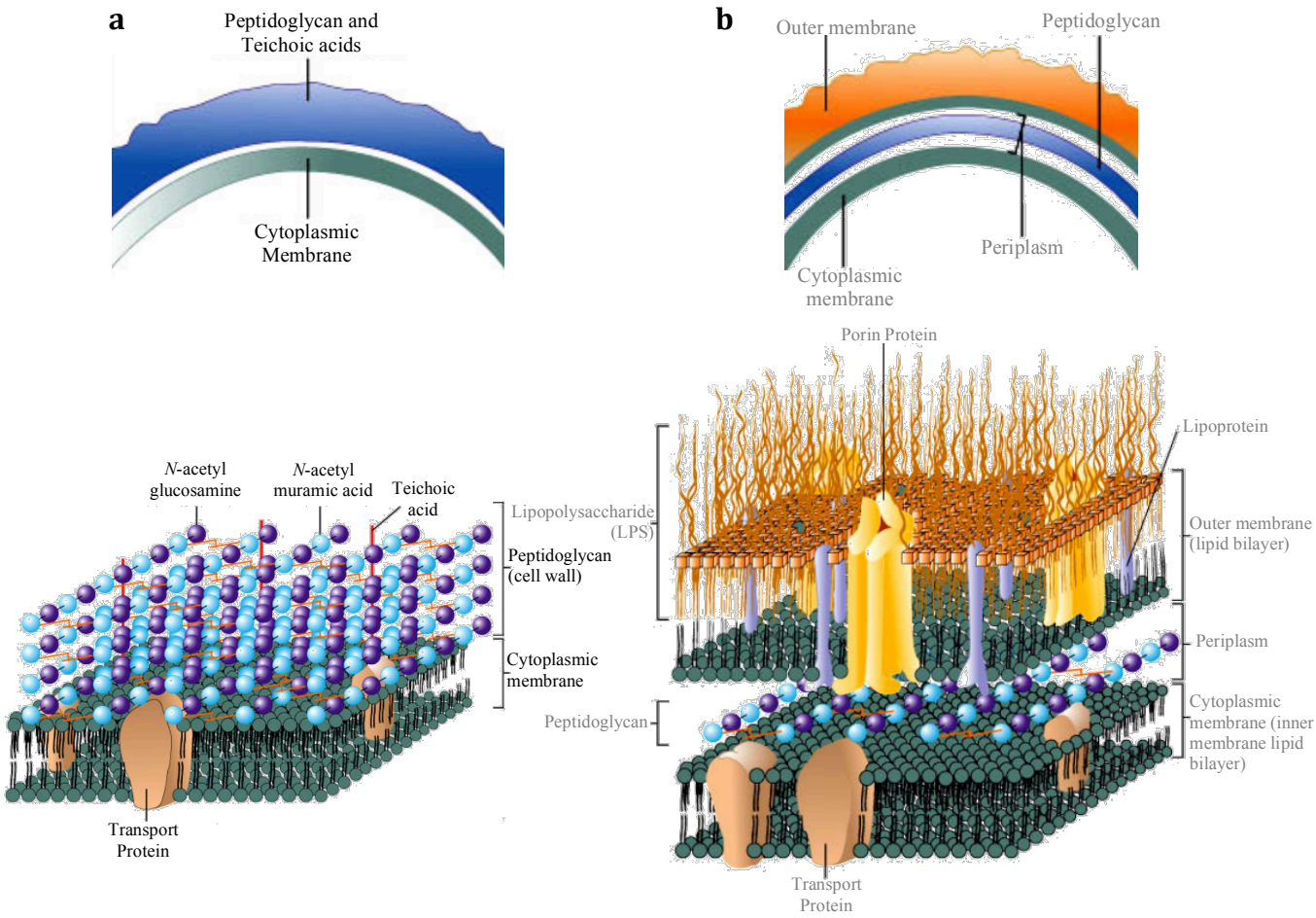

Figure 1.1 The Structural Architecture of (a) Gram-Positive and (b) Gram-Negative Bacterial Cell Envelopes (Adapted from Prescott, Harley & Klein's Microbiology 7th Ed, 2008).

1.1.2 The Gram-Negative Bacterial Cell Wall

This thesis is focused on the Gram-negative bacteria *Escherichia coli* and *Pseudomonas aeruginosa*. The Gram-negative bacterial cell envelope is thinner, less compact and more chemically complex than in Gram-positive cells. The cell envelope of Gram-negatives is comprised of an outer membrane, a cell wall, and an inner (cytoplasmic) membrane (**Figure 1.1 b**). The outer membrane is a distinguishing feature of Gram-negative bacteria, where the outer leaflet is composed of the glycolipid lipopolysaccharide and the inner leaflet contains phospholipids. The outer membrane serves as a semi-permeable molecular sieve preventing lysis-promoting molecules such as Penicillin G and lysozyme from entering the cell (Silhavy, *et al.*, 2010). It comprises of a plasma membrane, a layer of peptidoglycan surrounding the plasma membrane and an outer cell wall. The peptidoglycan layer in Gram-negatives is extremely thin (~ one

layer thick) being only 5-10% of the cell wall, making them much more challenging for antibiotics to penetrate. Cross-linking in Gram-negative peptidoglycan is mostly by direct 3-4 cross-linking between adjacent peptide stems, whereas in Gram-positive peptidoglycan, peptides can be cross-linked by additional amino acids due to potential peptide stem side-branching (amidation). Modification of the peptide stem alters the efficacy of antibiotics, as well as transpeptidase specificity (Münch *et al*., 2015). The Gram-negative cell envelope has to have more advanced mechanisms to evade destruction by β-lactams as they have a thinner peptidoglycan layer compared to Gram-positive bacteria. The β-lactam antibiotics penicillin and cephalosporins interfere with the cross-linking between peptides in peptidoglycan, compromising cell wall integrity. Gram-negative bacteria are known to have developed a higher resistance to antibiotics compared to Gram-positive bacteria, *Pseudomonas spp*. in particular (Miller, 2016).

An outer membrane composed of lipids, lipoproteins and lipopolysaccharides (LPS) surround the thin layer of peptidoglycan, with no teichoic acids in Gram-negative cell walls. This outer membrane is more permeable than the plasma membrane as it is composed of large LPS molecules and porins, which form channels through which small molecules (600-700 Da) can pass (van den Berg, *et al.*, 2015). LPS can be harmful and are classified as endotoxins, however, they are necessary as they prevent antibiotics from entering the periplasm in Gram-negative bacteria (Delcour, 2009).

1.2 Targets for Antibiotics

Antibiotics target major metabolic processes including folate synthesis, DNA and RNA synthesis, protein synthesis and cell wall biosynthesis (Walsh 2003), some of which are summarised in **Table 1.1**.

Table 1.1 A List of Antibiotics and their Mode of Action Against Metabolic Processes in Bacterial Cells. The first year of the commercial availability of each antibiotic class is shown and examples from each class are given, with the mode of action (not an exhausted list). Adapted from (Lewis, 2013).

Year	Antibiotic Class	Examples	Mode of Action
1935	Sulphonamides	Sulpadimethoxine, sulphamethoxazole	Folate Synthesis: Blocks folate metabolism which is essential in DNA replication
1940	β-lactams	Penicillin, cephalosporins, carbapenems, monobactams	Peptidoglycan biosynthesis: Mimics D-Ala-D-Ala peptidoglycan chain and inhibits cross-linking
1944	Aminoglycosides	Streptomycin	Protein Synthesis: Bind to 30S ribosomal subunit and blocks translation
1945	Tetracyclines	Chlortetracycline	Protein Synthesis: Bind to 30S ribosomal subunit and blocks translation
1948	Phenicols	Chloramphenicol	Protein synthesis: Binds to 50S ribosomal subunit of ribosome and blocks translation.
1949	Polymyxins	Colistin	Cell membrane: Permeabilises the cell membrane, allowing components to diffuse out
1952	Macrolides	Erythromycin A	Protein Synthesis
1958	Glycopeptides	Vancomycin	Peptidoglycan biosynthesis: Binds to the D-Ala-D-Ala peptide chain of peptidoglycan precursors
1962	Quinolones and Fluoroquiolones	Ciprofloxacin. Cefotaxime, Nalidixic Acid	DNA synthesis: Binds to DNA gyrase, blocking DNA replication
1963	Rifamycins	Rifampycin	RNA Synthesis: Binds to RNA polymerase and prevents attachment to DNA
1984	β-lactamase inhibitors	Clavulanic acid, Penicillanic acid sulfones	Target β-lactamases
1998	Streptogramins	Quinupristin	Protein synthesis: Binds to 50S ribosomal subunit of ribosome and blocks translation.
2000	Oxazolidinones	Linezolid	Protein Translation
2003	Lipopeptides	Daptomycin (Cubicin) Cubist Pharmaceuticals	Cell membrane: Binds to and depolarises the cell membrane
2011	Fidaxomicins;	Fidaxomicin	Binds to RNA polymerase and specifically targets *C. difficile*
2012	Diarylquinolines;	Bedaquiline	Inhibits ATP-Synthase

1.2.1 Protein Synthesis as an Antibiotic Target

Protein synthesis in bacteria is unique from that in Eukaryotes, and is a complex and viable target for antibiotics. The ribosome is central to protein synthesis, made up of two subunits: a 30S and 50S that associate to form a 70S ribosome upon protein synthesis. Initiation, elongation and termination are all targeted by streptogramins, macrolides and phenicols, which target the 50S subunit. Aminoglycosides (E.g. Kanamycin A) target the 30S subunit and cause misreading of the mRNA, incorporating the incorrect amino acids. Tetracyclines bind to part of the rRNA in the 30S subunit and compete with tRNA for the acceptor binding site. Chloramphenicol and tetrahydropyrimidinones block translation, while Oxazolidinones (e.g. Linezolid) inhibit the ribosomal peptidyl transferase activity (Arenz & Wilson 2016).

1.2.2 DNA and RNA Synthesis

The RNA polymerase initiation complex that precedes transcription can be disrupted by oxazolidinone drugs, and rifampicin also binds to the RNA polymerase initiation complex, inhibiting RNA synthesis. DNA gyrase is unique to bacteria/prokaryotes and is inhibited by the quinolone family. The fluoroquinolone ciprofloxacin A targets and inhibits the DNA synthesis enzymes Topoisomerase IV and DNA gyrase (Fournier *et al.*, 2000).

1.2.3 Cell Wall Biosynthesis

The exclusivity of the cell wall to bacteria has resulted in its exploitation as a valid target for antimicrobials, particularly β-lactams such as penicillin and cephalosporins. Antimicrobial inhibition of cell wall synthesis can be targeted to several steps in the pathway, by antibiotics including Fosfomycin, Cycloserine, Bacitracin, Vancomycin glycolipids and β-lactams. Increasing prevalence of antibiotic resistance has fuelled research into novel targets for antibacterial drugs, which is the focus of this body of research. A list of antimicrobial agents that target a variety of biosynthetic mechanisms in the bacterial cell wall are summarised in **Table 1.2**.

Table 1.2 A Summary of Antimicrobial Agents that Target the Bacterial Cell Wall

Antimicrobial Agent	Cell Wall Target
	Inhibitors of Muramyl-Pentapeptide Synthesis
Fosfomycin	The *N*-acetylmuramic acid component of the bacterial cell wall is derived from *N*-acetyl glucosamine by the addition of a lactic acid substituent derived from phospheenolpyruvate. The pyruvyl transferase enzyme involved is MurA and is inhibited by fosfomycin.
D-Cycloserine	The first three amino acids of the pentapeptide chain are added individually, but the terminal two residues D-alanyl-D-alanine are added as dipeptide. This dipeptide is produced by racemization of L-Ala to D-Ala and subsequent ligation by a D-ala-D-ala ligase (DDlb). Both of these reactions can be inhibited by D-cycloserine as it is a structural analogue of D-alanine.
	Inhibitors of reactions occurring at or in the membrane
Ramoplanin	Ramoplanin is a lipoglycodepsipeptide active against Gram-positive bacteria. It inhibits the uptake of *N*-acetylglucosamine by growing cells with a resultant accumulation of UDP-Mur*N*Ac-pentapeptide. Inhibition is of *N*-acetyl-glucosaminyl-transferase (MurG) that adds *N*-acetyl glucosamine to the undecaprenyl-muramyl-pentapeptide.
Bacitracin	The lipid carrier involved in transporting the cell wall UDP-Mur*N*Ac pentapeptides across the membrane are C_{55} isoprenyl phosphates. In the transport process the lipid acquires an extra phosphate moiety and to continue in another cycle of transport it must be dephosphorylated. Bacitracin is a cyclic peptide that binds to the isoprenyl pyrophosphate and prevents dephosphorylation.
	Inhibitors of chain cross-linking and formation of the cell wall structure
β-Lactams	β-Lactams are based around a thiazolidine ring structure and mimic the D-Ala-D-Ala stem peptide of peptidoglycan. To prevent the final cross-linking reactions in peptidoglycan biosynthesis that gives the peptidoglycan sacculus its characteristic rigidity. β-Lactams specifically inhibit the transpeptidase domain of penicillin-binding proteins (PBPs) by acting as suicide substrates, which form inactive acyl-enzyme complexes. This results in the accumulation of a pool of inactivated PBPs incapable of catalysing transpeptidation with resulting cell lysis.
Vancomycin	Vancomycin targets lipid II, the substrate molecule for transglycosylase/ transpeptidase. The cup shaped vancomycin molecule binds with high affinity to the *N*-acyl-D-Ala-D-Ala termini of the uncross-linked pentapeptide by the use of five hydrogen bonds in its concave binding pocket. This steric hindrance prevents subsequent transglycosylase / transpeptidase activity.

1.3 Mechanisms of Antibiotic Resistance in Bacterial Pathogens

Resistance mechanisms include the breakdown of β-lactams by β-lactamases, which are present in the periplasm of the Gram-negative cell envelope. Permeability of the outer membrane can be altered due to altered porins in the outer membrane, preventing access of β-lactams to the cell. Also, PBPs are showing increasing signs of reduced affinity to β-lactams in particular (Moya *et al.*, 2009).

1.3.1 Reduced Antimicrobial Uptake and Active Export by Efflux Pumps

For inhibition of DNA topoisomerases, RNA polymerase, protein synthesis and the cytoplasmic stage of peptidoglycan biosynthesis, navigation through the plasma membrane is required (two in the case of Gram-negatives) and then accumulation in the cytoplasm. The outer membrane in Gram-negatives provides a selective barrier to antimicrobials, excluding most hydrophobic molecules and macromolecules but the presence of hydrophilic porins allows slow absorption through the membrane (Kumar & Schweizer, 2005). Efflux pumps are found in all bacteria but most cannot respond to an antibiotic without specific mutations. Active efflux pumps and selective uptake work in synergy to reduce the ability of antimicrobials penetrating the cell wall. Gram-negative cells can reduce the permeability of their outer membrane and can also lower the antibiotic concentration near the targets using efflux proteins. *P. aeruginosa spp* does not contain the porin OprD, and also contains the active β-lactamase AmpC, which confers resistance to the β-lactam Imipenem (Ochs *et al*., 1999). *P. aeruginosa* absorption efficiency of drug molecules through outer membrane porins is 10-100 fold less than those in *E. coli* (Hancock and Speert, 2000).

1.3.2 Modification of the Antibiotic

Two examples of antibiotic modification are enzymatic modification of aminoglycosides and hydrolysis of β-lactams by β-lactamases (Walsh, 2004). Many antibiotics have hydrolytically susceptible chemical bonds (e.g. esters and amides), whose integrity is essential to biological activity. Aminoglycosides inhibit translocation of the tRNA and functional groups can be irreversible attached to the antibiotic *via N*-acetylation, *O*-phosphorylation or *O*-adenylation by the acetyl-, phosphoryl- and

adenyltranserases, respectively (Shaw, *et al.*, 1993). Modification reduces their affinity to the ribosomal RNA.

Amidase enzymes have evolved to cleave the β-lactam ring of penicillins and cephalosporins. Also, β-lactamases hydrolytically cleave the β-lactam ring using either an active site serine nucleophile or a nucleophilic water molecule (activated via a Zn^{2+} centre). The β-lactam ring mimics the terminal D-Ala-D-Ala of the peptide stem, acting as a pseudosubstrate. β-lactamases have a similar active site structure to the transpeptidases and they also hydrolyse the β-lactam ring, so the β-lactam can no longer act as a suicide substrate for the inhibition of PBPs (Philippon *et al.,* 1989). The spread of β-lactamase genes has been increased by their integration in to mobile genetic elements – plasmids and transposons. Multi-drug resistance cassettes can confer resistance not only to β-lactams, but to aminoglycosides, macrolides, sulphonimides and chloramphenicol.

1.3.3 Modification of the Antibiotic Target

Interaction of the β-lactam with a PBP involves a rapid transformation of a non-covalent complex, blocking PBP function. Many PBPs have evolved with decreased antibiotic affinity including the transpeptidase *S. aureus* PBP2a, which confers resistance to Methicillin as its rate constant for transpeptidation is reduced 1000-fold (Lim & Strynadka, 2002). The glycopeptide antibiotic vancomycin has a concave binding pocket that is a heptapeptide core, forming five Hydrogen bonds with the D-Ala-D-Ala terminus of the pentapeptide, stalling peptidoglycan synthesis. Resistance to vancomycin occurs in some strains including Vancomycin-Resistant *Enterococci* (VRE) due to the van*HAX* and van*RE* genes structurally altering the D-Ala-D-Ala target to D-Ala-D-Lac (Walsh *et al.*, 1996). Vancomycin binds to D-Ala-D-Lac with only four Hydrogen bonds, reducing affinity by 1000-fold and causing resistance.

1.3.4 The Emergence of Antimicrobial Resistant (AMR) Superbugs

Penicillin was initially introduced in to clinical use in 1948 and the first resistant isolate was found in 1950. By the end of the 1950s, MDR strains of *S. aureus* were widespread, with MRSA being isolated in 1960 (Moellering 2012). In 2014, MRSA was responsible

for 80,000 infections, and 11,285 deaths in the USA (Centre for Disease Control, USA 2014). The ESKAPE pathogens (*Enterococcus faecium*, *Staphylococcus aureus*, *Klebsiella pneumoniae*, *Acinetobacter baumannii*, *Pseudomonas aeruginosa*, and *Enterobacter* species) are the leading cause of nosocomial (hospital-acquired) infections throughout the world. Most of them are multidrug resistant isolates, which is one of the greatest challenges in clinical practice (Santajit & Indrawattana, 2016). Roughly 400 deaths per year are attributed to these infections (Data from Centre of Disease Control, 2013, USA). Some strains of MDR *P. aeruginosa* have been found to be resistant to nearly all antibiotics, including aminoglycosides, cephalosporins, fluoroquinolones, and carbapenems.

1.4 Peptidoglycan as the Molecular Scaffold

The bacterial cell is encompassed inside a cell wall that is essential for its viability. This sacculus is composed of multiple layers of a carbohydrate polymer peptidoglycan. Peptidoglycan (murein) is the principal constituent of the bacterial cell wall and is responsible for rigidity of the cell against internal osmotic pressure. The biosynthetic pathway of peptidoglycan is intricate with multiple complexes involved (**Figure 1.2**). Peptidoglycan a regular mesh-like structure of numerous glycan strands cross-linked for extra tensile strength (Barreteau, *et al.,* 2008). During bacterial growth, the murein layer is continually being replenished at a very high rate.

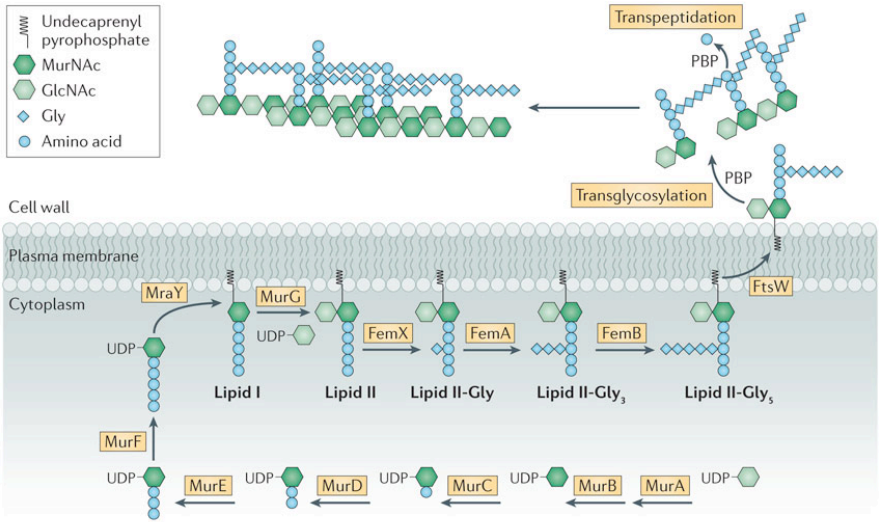

Figure 1.2 A Schematic of the Peptidoglycan Synthesis Pathway (Adapted from Pinho *et al.,* 2013). Beginning with the Mur ligases in the cytoplasm, becoming associated with the periplasmic membrane, being 'flipped' across the membrane by FtsW / MurJ / RodA or a synergy of the two, before undergoing polymerisation by PBPs.

1.4.1 Cytoplasmic Steps of Peptidoglycan Synthesis

The biosynthesis of peptidoglycan is a multistep pathway of 11 steps, divided into 3 main phases: (1) Formation of UDP-*N*-acetyl muramic acid (UDP Mur*N*Ac) (2) a pentapeptide chain is added sequentially to UDP Mur*N*Ac by four ATP-dependent amide bond ligases (**Figure 1.3**) (3) transport through the cytoplasmic membrane and incorporation into the growing peptidoglycan layer.

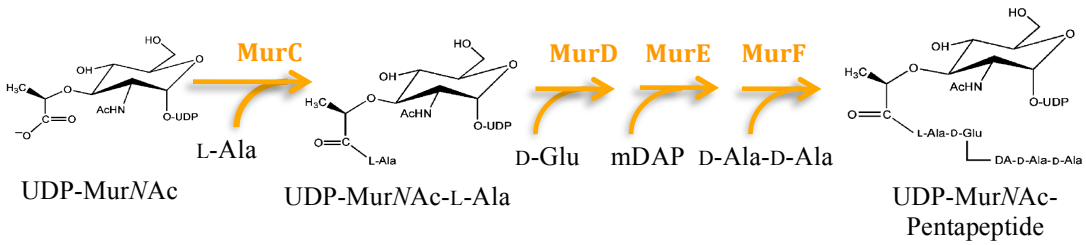

Figure 1.3 The Cytoplasmic Steps of Peptidoglycan Biosynthesis. The four Mur ligases: Mur C, D E and F catalyse the sequential addition of the pentapeptide side chain to the D-lactyl group of UDP-Mur*NA*c.

Peptidoglycan is formed by polymerisation and cross-linking of a lipid II monomer into a mesh structure. Lipid II (undecaprenyl-P-P-Mur*N*Ac-[pentapeptide]-Glc*N*Ac) is formed in the cytoplasmic phase and is 'flipped' to the other cytoplasmic surface via a 'flippase' mechanism performed by either FtsW (Mohammadi *et al.* 2011), or MurJ (Sham *et al*., 2014), or a synergistic effort by both. The extracellular processing of the monomer Lipid II occurs, with the membrane-associated transglycosylation reaction, followed by transpeptidation.

1.4.2 Lipid-Linked Steps of Peptidoglycan Synthesis

Peptidoglycan is comprised of alternating *N*-acetylglucosamine (*N*AG) and *N*-acetylmuramic acid (*N*AM) residues linked by β1-β4 Carbon-bonds and serves as a protective layer unique to bacteria (Lovering, *et al.,* 2007). Polymerisation of each glycan strand is catalysed by transglycosylation and cross-linking between glycan chains is catalysed by transpeptidation. In the case of bifunctional peptidoglycan synthases (more commonly referred to as Penicillin-Binding Proteins or PBPs), these two functions can be performed by one bifunctional PBP. *N*-acetylmuramic acid has a pentapeptide stem attached to its D-lactyl group that helps form the bridge between two glycan chains. The structure of the pentapeptide in Gram-negative bacteria is commonly

L-Ala-D-Glu-*meso*DAP-D-Ala-D-Ala. The cross-linking bridge is formed between L-alanyl-γ-D-glutamyl-*meso*-2,6-diaminopimelic acid of one glycan and the forth D-alanine on the new glycan. The most common form of cross-linking extends between the residue at position 3 of one peptide stem (the acyl acceptor) to the D-Ala at the forth position of another peptide stem (the acyl donor), known as 3-4 cross-linkage (Lovering *et al.*, 2012). *meso*DAP contains both an L- and a D-stereocentre. In peptidoglycan, the L-stereocentre is incorporated into the peptide backbone, whereas the cross-linking side-chain contains the D-stereocentre of *meso*DAP.

1.4.3 The Mechanism of Transglycosylation

Transglycosylation is the polymerisation of the monomer unit LII in to linear glycan strands, catalysed by the transglycosylase domain of Penicillin Binding Proteins (PBPs). The initial reaction in transglycosylation is the linking of two LII molecules together to form Lipid IV. After which, the successive addition of a single LII unit on to the growing end of the glycan chain forms an extended glycan chain (**Figure 1.4**). These two reactions are similar, differing only in the length of substrate used. The terms transglycosylation donor and acceptor differentiate between the growing chain (donor) and the incoming LII unit (acceptor). The transglycosylases are processive enzymes anchored to the membrane by a TM alpha-helix, which have a donor site where the growing glycan chain resides and an adjacent acceptor site for the incoming lipid II monomer. As a result the enzyme active site is comparatively long and extended and must accommodate at least four sugar binding sites. Similar active site architecture is seen in lysozyme which also binds alternating *N*-acetyl-glucosamine and *N*-acetylmuramic acid repeat units and there are structural similarities between the two (Lovering *et al.* 2012). The carrier lipid, undecaprenyl pyrophosphate is released with each addition of LII. Transglycosylation remains an important target mechanism for novel bacterial cell wall inhibitor design.

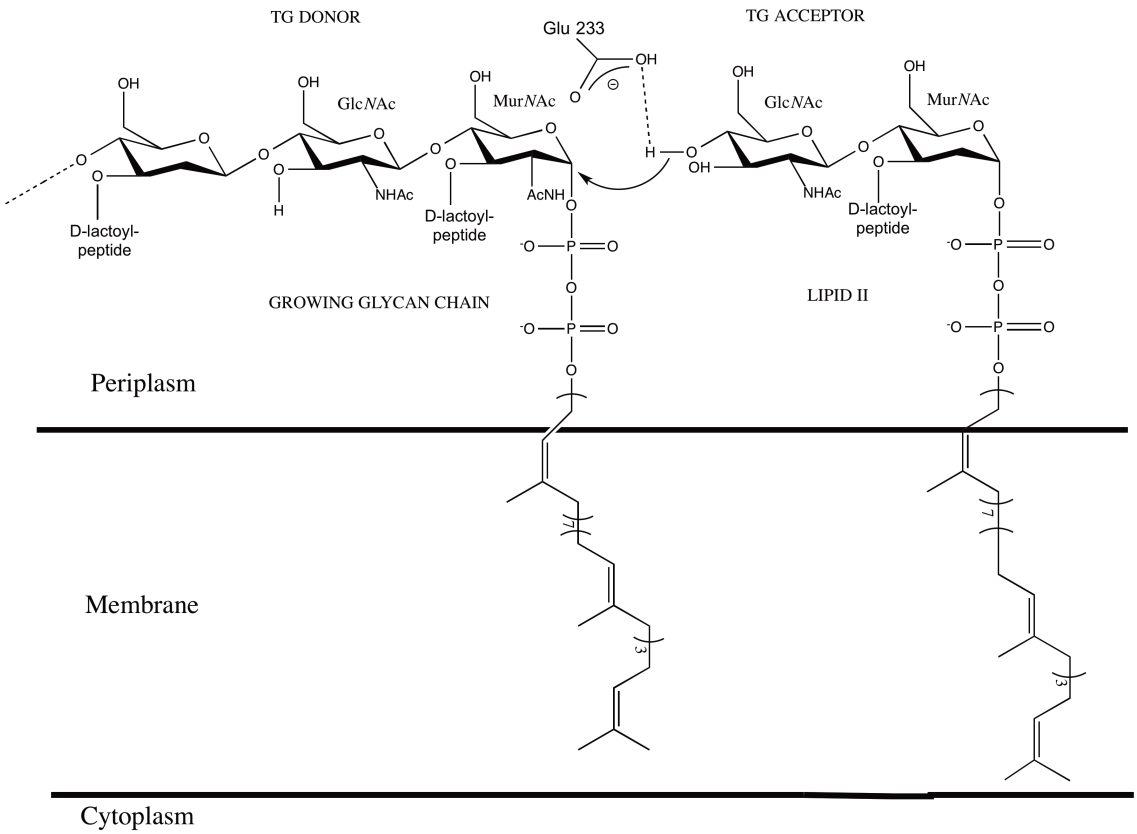

Figure 1.4 Transglycosylation: The Mechanism. The transglycosylase domain of Penicillin-Binding Proteins (PBPs) catalyse the polymerisation of Lipid II in to elongated linear peptidoglycan polymers. The growing glycan chain attached to undecaprenyl pyrophosphate is the glycosyl donor substrate and is transferred to the 4-OH group of the Glc*N*Ac unit of the incoming LII, which is the glycosyl acceptor substrate. β-1-4 C-linked *N*-acetylmuramic acid-*N*-acetylglucosamine [(*N*AG-*N*AM)$_n$] polymers are formed by transglycosylation.

1.4.4 Known Inhibitors of Peptidoglycan Transglycosylation

The natural product moenomycin has been used for several decades in agriculture without reports for resistance (Butaye *et al*. 2003). The search for novel inhibitors targeting the same mechanism is required, with improved pharmacokinetic properties for human use. The structure, biosynthesis and chemical properties of moenomycin have been reviewed extensively (Ostash and Walker 2010). The latest advancements in inhibitors of transglycosylation include those based on moenomycin and its analogues, as well as analogues of lipid II. The lantibiotic mersacidin inhibits peptidoglycan synthesis at the level of transglycosylation (Brötz *et al.,* 1997).

1.4.4.1 Moenomycin: The 'blueprint' Transglycosylase Inhibitor and a Structural Tool

The moenomycins are a family of glycolipid antibiotics naturally produced as a complex of related compounds by *Streptomyces ghananensis* with moenomycin A representing the major component with antimicrobial activity (Welzel 2005, Ostash & Walker 2010). The structure of moenomycin consists of a pentasaccharide of units B, C, D, E and F with a chromophore (unit A) and a C_{25} lipid chain connected to the F saccharide *via* a phosphoglycerate linker (**Figure 1.5**).

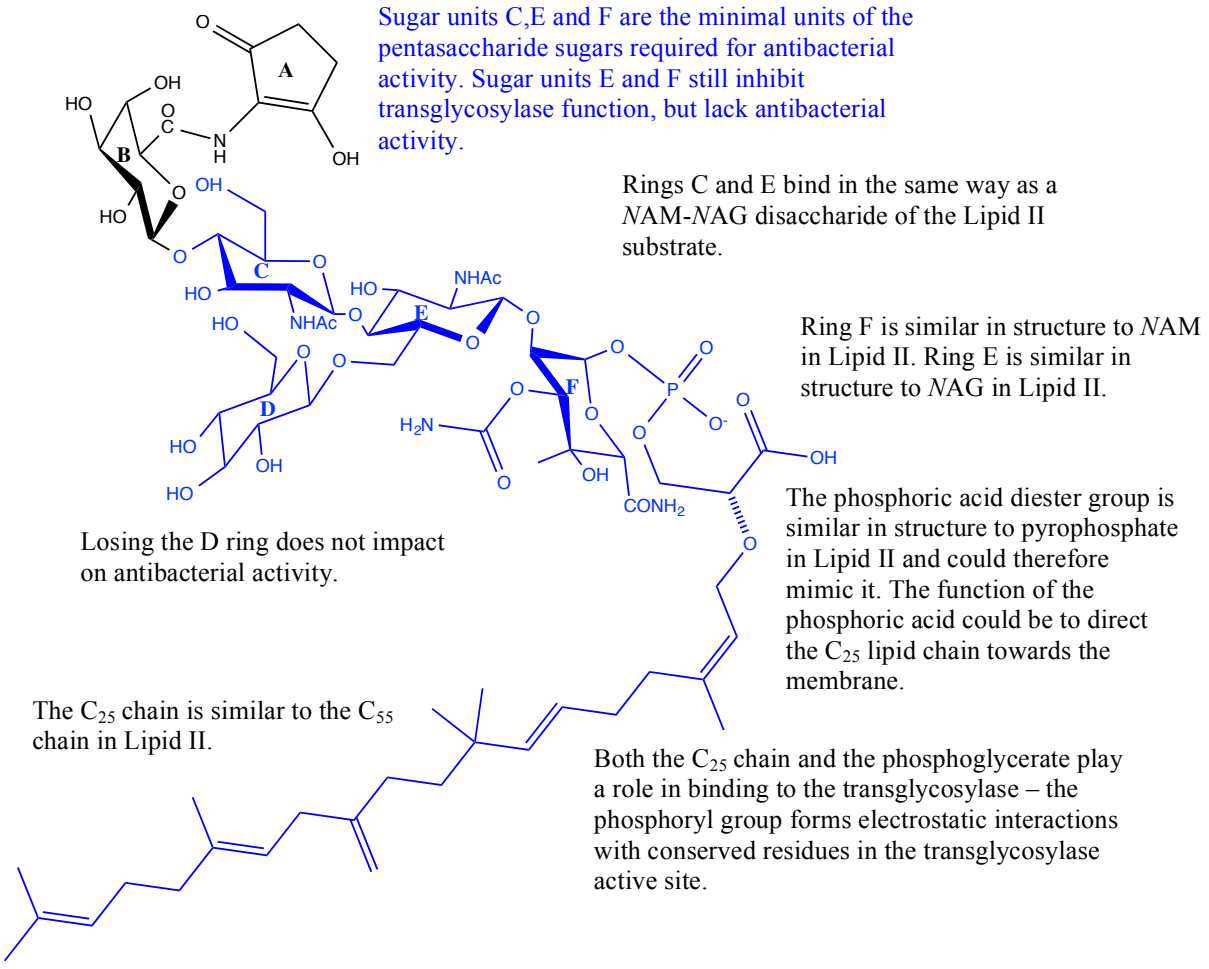

Figure 1.5 The Chemical Structure of Moenomycin A. The only known potent inhibitor for bacterial transglycosylases. The region highlighted in blue is the minimal inhibitory pharmacophore, which is often used as a scaffold for the design of new potential inhibitors.

The C_{25} chain is required for antimicrobial action and the moenomycin structure resembles that of the Lipid IV product formed within the transglycosylase active site. Moenomycin has amphiphilic properties due to the hydrophilic nature of the A to F carbohydrate units, the phosphate group of the phosphoglycerate linker and the folded

hydrophobic domain formed by the lipid chain. Structure-activity relationships have been carried out on the moenomycin A molecule through selective degradation of the moenomycin structure and the synthesis of di- and trisaccharide analogues, resulting in an understanding of the minimal pharmacophore for moenomycin (Welzel *et al*., 1987, Yang *et al*., 2004, Ostash & Walker 2010). The degradation of moenomycin to chemical entities retaining the carbohydrate units C, E and F, inhibit transglycosylation and thus have antibacterial activity (Möller *et al*., 1993, El-Abadla *et al.,* 1999). Degradation to retain the E and F carbohydrate units only still inhibits transglycosylase function but lacks antibacterial activity (Welzel *et al*., 1987). The C_{25} lipid chain is required to achieve full antibacterial activity of moenomycin, but is also the origin of its long half-life and contributes to its poor bioavailability and incompatibility for human consumption (Ostash & Walker 2010). Decreasing the length of the lipid chain slowly reduces the inhibitory ability of moenomycin (El-Abadla *et al.,* 1999), most likely due to loss of ability to anchor itself into the cytoplasmic membrane. Modifying or truncating the lipid chain of moenomycin improves pharmacokinetic properties but the loss of activity needs to be compensated by maintaining essential polar active-site contacts or by utilisation of other hydrophobic chemophores with acceptable properties.

1.4.4.2 The Binding of Moenomycin and Lipid II to Transglycosylases

The two natural molecules known to bind to the transglycosylase domain of PBPs are moenomycin and lipid II. The structural differences between lipid II and moenomycin must be responsible for the inhibition of transglycosylase, as lipid is the natural substrate for transglycosylation and moenomycin is the most potent inhibitor. Understanding how these two molecules interact and bind to the transglycosylase domain is fundamental in pursuing structural analogues of these molecules for inhibition. The LII molecule has two phosphates, whereas moenomycin only has one phosphate. The acid group on the lipid chain of moenomycin binds to the cytoplasmic membrane and is thought to mimic the second phosphate group of the growing peptidoglycan strand (Kempin *et al*., 1995).

Moenomycin A binds with high affinity to the transglycosylase domain of several Class A PBPs and is the most potent inhibitor of the transglycosylase function of PBPs with MICs in the region of 0.01-0.1 μg/mL (Welzel 2005). The mode of inhibition of

moenomycin is unique in that it directly (and reversibly) binds to the active site of the transglycosylase domain, preventing lipid II polymerisation. Moenomycin first binds to the cytoplasmic membrane *via* its lipid chain, followed by selective binding to the sugar moiety to the donor site of the transglycosylase. The transglycosylase domain contains five motifs representative of the GT_{51} fold-family (Lairson *et al*., 2008) and are conserved among both mono- and bi-functional PBPs.

Six residues in the transglycosylase domain have been identified as important in the interaction with moenomycin in *Aquifex aeolicus* PBP1A (Yuan *et al.,* 2007, Yuan *et al.,* 2008), and are likely to be conserved across other species. It is also thought that the C_{25} chain of moenomycin interacts with the transmembrane (TM) segment of *E. coli* PBP1B (Cheng *et al.,* 2008), increasing the binding affinity 5-fold of moenomycin to the transglycosylase domain, highlighting the importance of the TM domain in transglycosylases for activity.

The only structural information available at present for the interaction of lipid II with the transglycosylase domain is that derived from the X-ray crystal structure of *S. aureus* mono-functional glycosyltransferase with an analogue of Lipid II (Huang *et al.,* 2012). Many inhibitors that bind to transglycosylases occupy the donor site, mimicking the elongating chain of polymerized lipid II (Lovering & Strynadka, 2008). Lovering and co-workers have proposed that moenomycin structurally mimics Lipid IV (Lovering, *et al*., 2007, Lovering & Strynadka, 2008), further supported in that Lipid IV and moenomycin are suggested to bind to the same site on the transglycosylase domain (Gampe *et al.,* 2011) and that lipid IV may bind to *E. coli* PBP1B with a higher affinity than lipid II (Shih *et al*., 2011).

1.4.4.3 Moenomycin Analogues as Transglycosylase Inhibitors

Finding that the moenomycin degradation products exhibit inhibitory activity against transglycosylases prompted a study in 1999 by Sofia *et al*, to develop a combinatorial library of 1300 analogues of the disaccharide core of moenomycin (Sofia *et al*., 1999). These disaccharide analogues explored modifications at C2 of the E ring and C3 of the F ring (the critical interaction points with the transglycosylase domain). Modifications included aromatic groups attached to the E and F rings and a lipid tail of 12 rather than

25 carbons. Three compounds showed particular promise TS30663, TS30153 and TS30888, with some being more active than the EF disaccharide (**Table 1.3**). These compounds were orders of magnitude less potent than the parent molecule moenomycin, but had IC_{50} values in the range of 10-15 μM (Goldman & Gange 2000). These putative inhibitors also exhibited activity against the moenomycin-resistant strain *Entercoccus faecium*, highlighting that simple degradation compounds show potency against clinically relevant pathogens. The IC_{50} values obtained are within a similar range to other cell wall inhibitors such as bacitracin, vancomycin and ramoplanin. These compounds showed differing activities against transglycosylases in different species, suggesting that they may target different subsets of the transglycosylases (Ostash & Walker 2005) as is also seen for β-lactams which show differing activities against PBPs in various species (Miller *et al*., 2004).

A new member of the moenomycin group AC326-alpha was introduced in 2000 whose moenocinol chain is cyclic, giving a diumycinol chain. Branched chain lipids show more potent antibacterial activity than linear chained lipids. Putative inhibitors could be designed to mimic moenomycin and could exhibit antibacterial activity to cyclic lipid chains. Halliday *et al*., presented a class of compounds made by Alchemia in 2006, based on the disaccharide scaffold of Sofia *et al.*, with a focus on maintaining the important transglycosylase binding regions. The hits had MIC values of 1-4 μg/mL, against a broad range of Gram-positive organisms (Sofia *et al*., 1999, Halliday *et al.*, 2006). One example compound from this class: ACL 19273, showed direct binding and inhibition of the transglycosylase domain, potentially binding to either the acceptor or donor site of the transglycosylase (Halliday *et al*. 2006). Inhibitors that bind to the transglycosylase acceptor site, which may be the case for these small disaccharides, are binding to the contrary site to where moenomycin binds. Determining whether inhibitors bind to the donor or acceptor site of the transglycosylase is important is elucidating their mode of action.

Table 1.3 A Summary of Analogues and Small Molecule inhibitors of Moenomycin and Lipid II, exhibiting inhibitory activity against the transglycosylase function in PBPs, with some compounds additionally showing modest antibacterial activity.

Reference	Compound Name
	Moenomycin Analogue Inhibitors
Sofia *et al.,* 1999	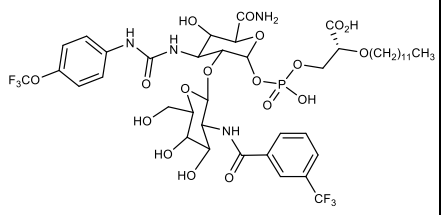 TS30153
	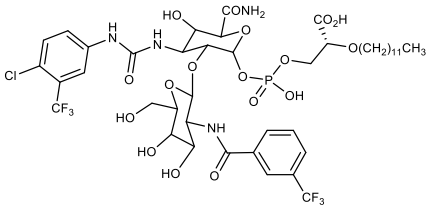 TS30663
	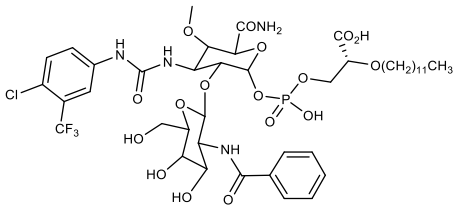 TS30888
He *et al.,* 2000	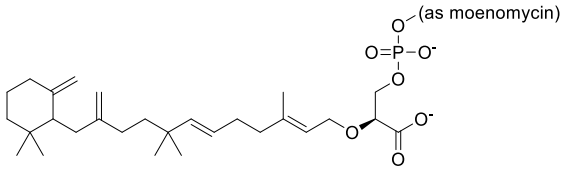 AC326-α
Halliday *et al.,* 2006	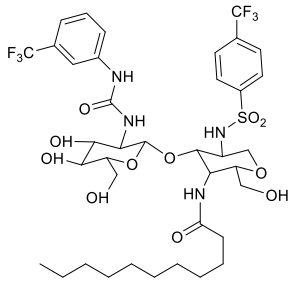 ACL 19273
Cheng *et al.,* 2010	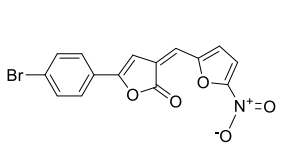 HTS-6
	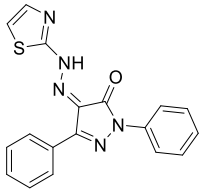 HTS-7
	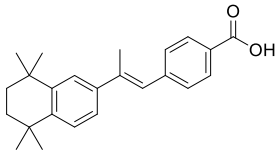 HTS-8
Gampe *et al.,* 2013	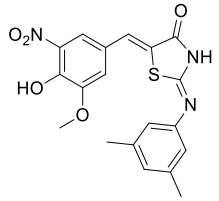 Compound 10

Lipid II Analogue Inhibitors		
Garneau *et al.,* 2004	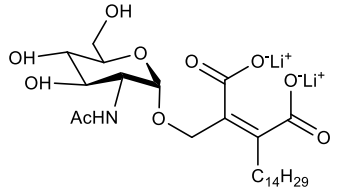 Compound 5	
Cheng *et al.,* 2010	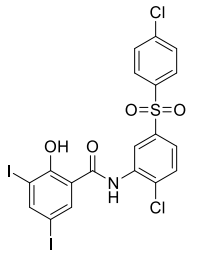 Compound 24	
Huang *et al.,* 2012	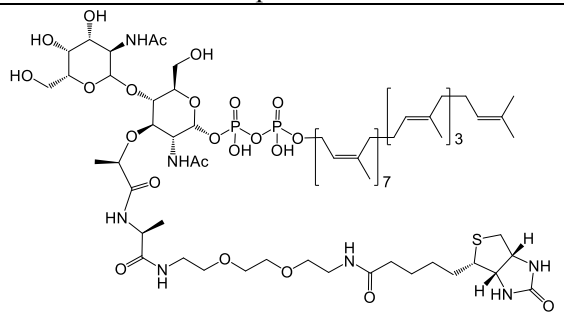 Analogue 3	
Huang *et al.,* 2012	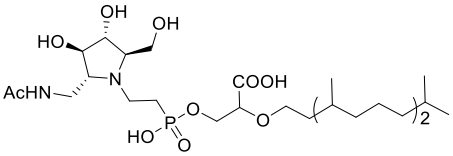 Compound 31	
Dumbre *et al.,* 2012	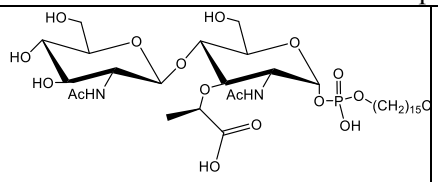 Compound 21	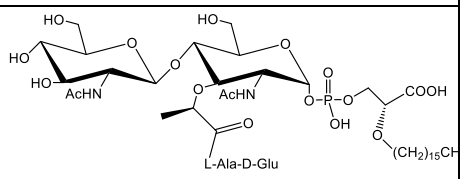 Compound 62
Huang *et al*., 2013	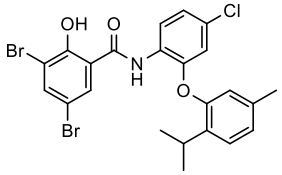 Compound 19	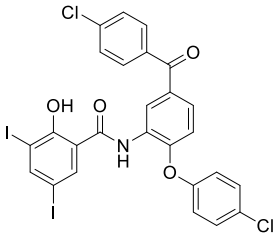 Compound 20
	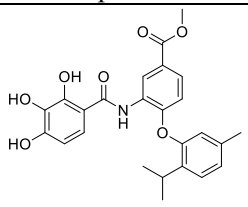 Compound 24	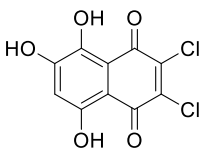 Compound 25

1.4.4.4 Lipid II Analogues as Transglycosylase Inhibitors

In the early 1990's, efforts were focused on synthesizing transglycosylase inhibitors based on monosaccharide and disaccharide analogues of lipid II, but most were not very active (Hecker *et al.,* 1990, Qiao & Vederas 1993, Brooks *et al.* 1995). A combination of mono- and disaccharide analogues of lipid II and moenomycin were synthesised by Garneau *et al* based on the active part of moenomycin and combining with structural features of lipid II (Garneau *et al.*, 2004). A lipid II monosaccharide analogue, Compound 5, was designed to mimic the pyrophosphate of lipid II with a dicarboxylate group. Modest activity with just monosaccharide analogues was exhibited, with 28 % inhibition of transglycosylases at 100 μM (Garneau *et al.*, 2004). Clearly the potency of such compounds is weak and it may be that monosaccharide analogues do not have comparable complexity to moenomycin, to sufficiently inhibit transglycosylases (Derouaux *et al.,* 2013).

Lipid I and lipid II substrate analogues (both mono- and disaccharides) were synthesised by Dr. M. Terrak and co-workers (Terrak 2008, Dumbre, *et al*., 2012, Derouaux *et al*., 2013) to test the consequences of variations in the lipid chain length, the pyrophosphate and the length of the peptide stem. The disaccharide analogues were 2-fold better inhibitors than their cognate monosaccharides and also as the length of the peptide stem increased from no peptide to L-Ala- D-Glu, to L-Ala- D-Glu- D-Lys, inhibition decreased. This was attributed to the presence of a peptide preventing high affinity binding between the Glc*N*Ac and the transglycosylase. Analogues were tested to highlight important moieties for the future designing of substrate-based inhibitors with two hits: C16-phosphoglycerate-Mur*N*Ac-Glc*N*Ac (Compound 21) and C16-phosphoglycerate-Mur*N*Ac-(L-Ala- D-Glu)-Glc*N*Ac (Compound 62). The most active being Compound 62, which showed both inhibitory activity against the transglycosylase as well as antibacterial ability.

The role of the pentapeptide moiety in lipid II and its mode of interaction with the transglycosylase has been explored (Shih *et al*., 2012). Lipid II analogues with an assortment of peptide stems were synthesised to analyse their capabilities as transglycosylase substrates. Modifications include incorporating a fluorescent NBD label into position 3 of the peptide and incorporating a D-lactyl group at the hydroxyl

group of Mur*N*Ac. Surface Plasmon Resonance (SPR) binding studies were conducted to determine the binding affinity of these lipid II analogues to transglycosylase. The three main conclusions from this work were (1) the terminal D-Ala-D-Ala is *not* essential for substrate binding and does not significantly interact with the transglycosylase domain, (2) the fluorescent probe NBD on the ε-amino group of the 3rd position lysine does not affect binding affinity to transglycosylase and (3) the minimum structural requirement for the peptide moiety in lipid II as a transglycosylase substrate is D-lactyl-L-Ala. Further research has shown that only the D-lactyl in the Mur*N*Ac is required for the substrate binding to transglycosylase (Dumbre *et al.,* 2012).

1.4.4.5 Prospects for New Transglycosylase Inhibitors

Developing new drugs with antibacterial properties by inhibition of peptidoglycan transglycosylation is of current interest to both academia and the pharmaceutical industry. Currently most compounds discovered have greater potency against Gram-positive bacteria than Gram-negatives, presumably due to easier access to the thicker peptidoglycan layer in Gram-positives. Progress on the development of transglycosylase inhibitors has been slow historically due to the complexity of the active site of the enzymes, lack of suitable assays for high throughput screening, provision of suitable substrates for such assays and the difficulties surrounding the reconstitution of activity of these membrane proteins. The availability of lipid II substrate from chemo-enzymatic and total chemical synthesis domains allows transglycosylases from various species to be studied along with a growing literature detailing molecular architecture interactions within the active site. Further understanding of substrate specificity will aid the design of future substrate analogues, common features of which are becoming apparent.

The development of glycolipids and glycopeptides as putative transglycosylase inhibitors has shown that there are new prospects for the combinatorial biosynthesis of phosphoglycolipid antibiotics (Ostash *et al*., 2013) and there are new generation glycopeptides currently in clinical development that inhibit the transglycosylation process (Yim *et al*., 2014). In addition, research is on-going to determine the exact inhibitory mechanism of moenomycin on transglycosylases, with a drive towards finding novel inhibitory compounds with distinct structural features to moenomycin. Total synthesis of moenomycin A has been achieved (Taylor *et al.,* 2006) and the

biosynthetic pathway of moenomycin variants can be theoretically generated which could help in the quest to design new compounds with better pharmacokinetics (Ostash *et al.,* 2007).

There is now the capability to synthesize structurally diverse substrates and to homogenate synthetic and biological compounds by either enzymatic modification of synthetic analogues or by chemical modification of biosynthetic intermediates. These capabilities enable the better comprehension of the role of lipid II in binding to the transglycosylase domain and help to optimise structures for the transglycosylase donor and acceptor sites. These sites have different requirements for lipid chain length, which is important for the processivity of the transglycosylase, with the donor site requiring a C_{20} lipid chain and the acceptor site tolerating shorter lipids (Perlstein *et al.*, 2010), so there is a compromise between lipid chain length and antibiotic activity. Walker and coworkers have predicted that lipid II with four successive *cis* isoprene units in a 35-carbon chain is the best transglycosylase substrate (Ye *et al.*, 2001). Investigating the optimal substrate for transglycosylases such as lipid IV or longer as potential substrate inhibitors may be a worthwhile focus and could be fruitful for being able to closely mimic moenomycin, without the poor pharmacokinetics (Shih, *et al.*, 2011). Despite the evolution of structurally diverse substrates, there is still more room to understand transglycosylase-substrate mimics.

There are now in the region of 15-20 structures of transglycosylase enzymes in the protein databank, with a small subset being below 2.5 Å resolution and thus reliable for structure based drug design efforts. Further knowledge of the catalytic mechanism and *in-vivo* regulation of transglycosylation activity may provide further insight into the chemistry of potential novel lead compounds required for effective chemotherapeutic intervention. With the growing awareness to the need for novel antimicrobials by both the public and policy-makers, the development of new approaches within academia and Pharma to design novel inhibitors is on the horizon.

1.4.5 The Mechanism of Transpeptidation

Transpeptidation involves a donor substrate and an acceptor substrate, cross-linked to each other by the action of PBPs. The donor substrate is the incoming strand, and is

often a glycan chain polymer of multiple disaccharide subunits. The acceptor is an adjacent strand that forms a 3-4 cross-link with the donor strand, creating a mesh-like structure of high tensile strength. Transpeptidation occurs when the PBP recognises the D-alanyl-D-alanine dipeptide on the end of the pentapeptide stem, forming an acyl-enzyme intermediate at the active site serine. The terminal D-alanine on the acceptor strand acts as a nucleophile and resolves the acyl-enzyme intermediate, releasing the terminal D-alanine and the PBP from the original donor strand. The cross-link is formed between the fourth D-alanine on the donor strand and the third *meso*DAP residue on the acceptor strand (**Figure 1.6**). The acyl-enyme intermediate undergoes either aminolysis *via* a DD-transpeptidase to yield cross-linked peptidoglycan, or hydrolysis *via* the DD-carboxypeptidase function of the enzyme, limiting cross-linking (Spratt, 2008) (DD-carboxypeptidase function discussed in Section 1.4.6.1).

Transpeptidation requires polymerised LII as its substrate and therefore the transglycosylase product is likely to have an influence on the transpeptidase active site. Certain HMW PBPs require simultaneous peptidoglycan synthesis or a pre-formed uncross-linked peptidoglycan polymer (Born *et al.*, 2006). The level of cross-linking is lower in Gram-negative bacteria (25-50% cross-linked stem peptides), compared to 70-90% in Gram-positive bacteria (Bugg, 1999).

Figure 1.6 A Schematic of the Transpeptidase Mechanism The PBP is acylated and donates a proton from its active-site serine to the terminal D-alanine of the donor strand. An acyl-enzyme intermediate is formed and the terminal D-alanine is released from the donor. An acceptor strand deacylates the PBP, with the amine group on its third position *meso*DAP residue acting as a nucleophile and donating a proton back to the active site serine of the PBP. The ester bond between the PBP and the donor strand is broken and the PBP is released, forming a 3-4 cross-link between residue 3 on the acceptor peptide stem (*meso*DAP) and residue 4 on the donor peptide stem (D-alanine).

1.4.5.1 PBP Acylation

As the PBP docks onto the donor strand, the position 4 D-alanine of the pentapeptide stem acylates the active site Serine. A proton is removed from this Serine and transferred to the amine group of the terminal D-Alanine on the donor strand. The peptide bond between the two D-alanines is broken and the terminal alanine is released, harbouring the proton donated from the PBP active-site serine. An acyl-enzyme intermediate is formed, linking the PBP to the penultimate D-alanine of the donor strand *via* an ester bond. Acylation occurs by nucleophilic attack of a serine residue onto the carbonyl carbon of the β-lactam ring or of the penultimate D-Ala of the pentapeptide substrate to form a covalent acyl-enzyme complex. The second order rate constant of acylation is widely used as a measure of the potency of an antibiotic.

1.4.5.2 PBP Deacylation

For cross-linking to occur between two stem peptides, the terminal D-alanine of the acceptor peptide stem acts as a nucleophile. Its amine group attacks the acyl-enzyme ester bond, giving a proton back to the active-site serine in the PBP, releasing the complex, forming a peptide bond cross-link between the position 3 *meso*DAP of the acceptor stem, and the position 4 alanine of the donor stem. The third amino acid in the peptide stem that contains the reactive amine for transpeptidation varies between bacterial species, but the overall mechanism is conserved.

Deacylation occurs when an incoming amino group of a neighboring peptide, or a water molecule attacks the acyl-enzyme complex, breaking the acyl-enzyme bond and allowing release of the product. The kinetics of deacylation between PBP and β-lactam is a lot slower than deacylation between PBP and stem peptide (Nicola *et al.,* 2010).

DD-Transpeptidase enzymes belong to a group of enzymes called transferases because they transfer away the D-Ala from the terminal position of the pentapeptide: the PBP is transferred from the active site serine hydroxyl group and added to the amine leaving group. An acyl-enzyme intermediate is formed and the second substrate comes in and displaces the enzyme from the complex. Both of these steps are nucleophilic substitution (SN_2) reactions. In the first step the -OH group of the active site serine

residue acts as the nucleophile and in the second step, the incoming substrate (D-DAP) is the nucleophile. The concentration of water is extremely high (55 M) compared to that of the acceptor (mM) and water is smaller and fits into the active site easier than the transpeptidase acceptor. However in the case of most transferases, they transfer the intermediate to the incoming second substrate rather than water because the active site has under-gone conformational change that closes the active site to water, and makes it more complementary to the substrate (”induced fit”). In DD-carboxypeptidation, water acts as the nucleophile rather than the D-DAP residue of the in-coming substrate (Section 1.4.6.1).

The active site of transpeptidase domains contains an SxxK motif with a catalytic serine and base lysine, characteristic of the acyl-transferase superfamily of proteins (Goffin & Ghuysen, 1998). The first serine is the essential nucleophile and is spatially central in the catalytic active site, key to the acylation and deacylation steps (Figure 6.1). There are 3 conserved motifs in total with the other two being SxN or SxD, and KTG or KSG. The motifs occur at equivalent places and with roughly the same spacing along the polypeptide chains and they have spatial proximity to each other in the 3D structure (Goffin & Ghuysen, 2002).

The discovery of antibiotics against class A HMW PBPs has been hampered by lack of mechanistic information about these enzymes. The mechanism of the reaction between a PBP enzyme and D-Ala-D-Ala in peptidoglycan are the same as the mechanism of the interaction between PBP and β-lactam antibiotics, as β-lactams mimic the D-Ala-D-Ala moiety (Section 1.4.7). The transpeptidase reaction of almost all PBPs is less stringent for the acceptor substrate and can use various D-amino acids (Pollock *et al.*, 1972), allowing their incorporation (exchange) into peptidoglycan (Sauvage & Terrak, 2016).

1.4.6 Peptidoglycan Recycling and Maintenance

Although transpeptidation is the final step in cell wall synthesis, the cell wall is dynamic and constantly being maintained, remodeled and regenerated to maintain integrity. Gram-negative bacteria have evolved an elaborate process for peptidoglycan recycling, initiated in the periplasm by lytic transglycosylases. Products of lysis (muropeptides) are transferred to the cytoplasm to continue recycling mechanisms.

Peptidoglycan recycling occurs during cell wall growth, maturation, maintenance and also in response to antibiotics. Lytic transglycosylases catalyse the fragmentation of the glycosidic bond between *N*AG and *N*AM residues. Upon transfer of muropeptides to the cytoplasm, it is reformed *de novo* via the peptidoglycan biosynthesis pathway, merging recycling, recovery and remodeling with biosynthesis.

In Gram-negative pathogens, cell wall recycling has been linked to β-lactamase induction (Johnson *et al.*, 2013). Muropeptides regulate β-lactamase induction, including AmpC β-lactamase and AmpG in *P. aeruginosa* specifically (Zhang *et al.*, 2010). Inhibitors of cell wall recycling could be combined with cell wall-targeting β-lactams to overcome resistance, which could be necessary in AmpC β-lactamase hyper-producing *P. aeruginosa* in cystic fibrosis (Mark *et al.,* 2011).

1.4.6.1 The DD-Carboxypeptidase and DD-Endopeptidase Function of PBPs

Transpeptidases and carboxypeptidases have similar mechanisms: transpeptidases contain two domains (HWM PBPs), while many carboxypeptidases contain one domain (LMW PBPs), but not all. The mechanism of DD-carboxypeptidases and transpeptidases is very similar, the only deviation being what acts as the nucleophile (**Figure 1.7**). The nucleophile in carboxypeptidation is water, releasing a tetrapeptide, whereas in transpeptidation the nucleophile is the third-position *meso*DAP/Lys in the acceptor peptide stem. Transpeptidases and carboxypeptidases are known as Penicillin-binding proteins (PBPs). DD-Carboxypeptidases are enzymes that remove the terminal D-alanine from muramylpentapeptide and DD-endopeptidases hydrolyse the cross-links between glycan chains. The protein family of DD-peptidases have the same active site functional groups, a common protein fold and the SxxK motif.

Transpeptidation occurs by the enzyme recognising the D-alanyl-D-alanine dipeptide on the end of the peptide stem, forming an acyl-enzyme intermediate at the active site serine and releasing D-alanine. This covalent acyl-enzyme intermediate is attacked by a nucleophile. In carboxypeptidation, the nucleophile is water and the tetrapeptide is released whereas in transpeptidation, the nucleophile is an amine from a stem peptide on an adjacent peptidoglycan polymer, and the cross-linked product is formed.

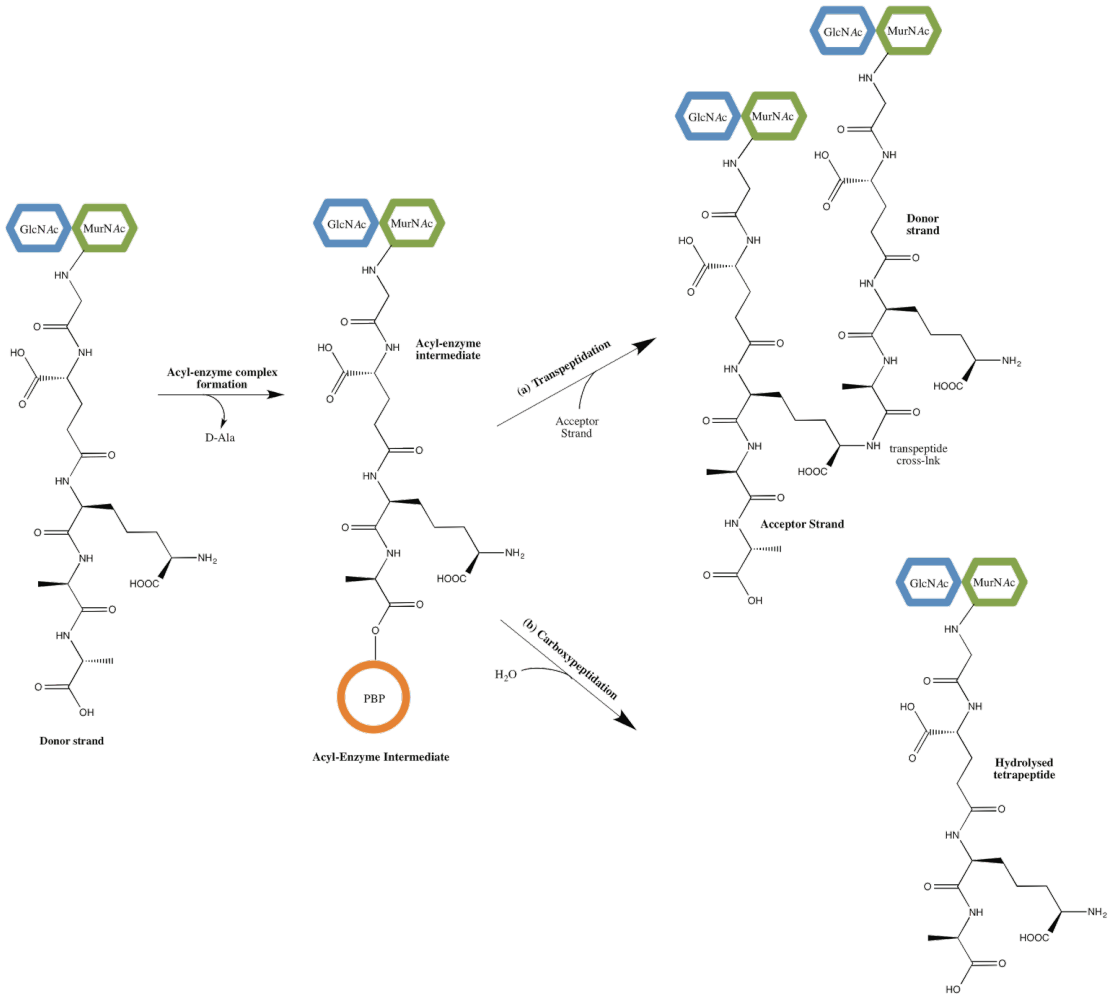

Figure 1.7 DD-Carboxypeptidation vs Transpeptidation. **(a)** The active site serine attacks the forth D-Ala residue **(b)** an acyl enzyme intermediate is formed in which the PBP active site effectively takes the place of the terminal D-Ala residue **(c)** the pentapeptide stem is hydrolysed to a tetrapeptide lacking the final D-Ala. In the case of carboxypeptidation, H_2O acts as a nucleophile to attack the ester bond, releasing the tetrapeptide, uncross-linked to any acceptor (Thesis of T. B. Clarke, Warwick 2008).

1.4.7 Antibiotics Targeting Transpeptidation: The Structural Similarity of β-lactams to D-Ala-D-Ala

The interaction between β-lactams and transpeptidases are more extensively characterised than transpeptidation reactions involving natural substrates, as the substrates required to study transpeptidation are hard to make. The final two amino acid residues in the pentapeptide stem of peptidoglycan have structural similarity to that of β-lactams such as penicillin G, in particular, the CO-N bond in both species. When the PBP enzyme interacts with its usual substrate D-Ala-D-Ala, the D-Ala-D-Ala acylates the active site serine residue in the PBP, and allows the terminal D-Ala to serve as the leaving group. In contrast, when penicillin interacts with the active site serine, it leaves

the leaving group covalently tethered to the acyl-enzyme species on the PBP (Tipper & Strominger 1965).

Penicillin is an acylated cyclic dipeptide of L-cysteine and D-valine and is viewed as an analogue to the acylated D-alanyl-D-alanine in the pentapeptide stem (Pratt, 1952). The structure of penicillin is similar to that of D-alanyl-D-alanine therefore can bind to the active site of the transpeptidase as a 'pseudosubstrate' and inhibit the activity of the PBP. The active site of the PBP is acylated by penicillin and then deacylates very slowly and subsequently cannot perform its cross-linking function. PBPs break the amide bond in the lactam ring of β-lactam antibiotics, where the penicillin moiety is transferred to a serine in the active site of the PBP (Ghuysen, 1991). The amide bond of the β-lactam ring of penicillin is the equivalent of the peptide bond in D-alanyl-D-alanine (**Figure 1.8**). Nucleophilic attack on β-lactams by the active site serine residue of a PBP leads to the β-lactam ring opening, leaving the antibiotic covalently attached to the serine, blocking further transpeptidase activity and leads to cell death. β-lactamase can hydrolyse 10^3 penicillin molecules/second, rapidly destroying the drug before it reaches it target enzymes (Walsh, 2000).

a Penicillin G (6-aminopenicillanic acid)

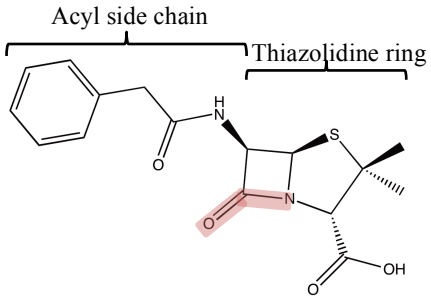

b D-alanyl-D-alanine

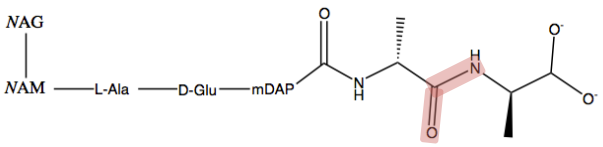

Figure 1.8 The Structure of (a) Penicillin G (6-aminopenicillanic acid) and (b) the D-alanyl-D-alanine end of the Peptidoglycan Strand. (Tipper & Strominger 1965). Variations of the penicillin acyl side chain improve activity against Gram-negative bacteria, particularly the aminopenicillins such as Amoxicillin and Ampicillin. Non-β-lactam inhibitors of transpeptidation include lactivicin analogues, being amongst the most potent.

1.5 The Penicillin Binding Proteins

Each bacterial species has a set of PBPs that are involved in the late stages of peptidoglycan synthesis and are targets for β-lactam antibiotics. PBPs are acyl-serine transferases, the actions of which are mediated by an active-site serine moiety. PBPs

catalyse the final stages of murein biosynthesis and help to modify and shape of peptidoglycan exoskeleton by removing the terminal D-alanine residue from pentapeptide stems (Vollmer *et al*., 2008). The morphology of a bacterial cell is dependent on the composition and synthesis of the peptidoglycan layer. PBPs modify the exoskeleton and work with cytoskeleton proteins to manipulate the structure, through specific protein localisations and interactions. PBPs are named for their affinity for penicillin, which mimics the peptide side chain structure and blocks cell wall synthesis. However, they could be more appropriately named as 'Peptidoglycan Synthases', as their role is mainly as the drivers behind bacterial cell wall biosynthesis.

1.5.1 Classification and Topology of PBPs

Penicillin-Binding Proteins (PBPs) are initially classified according to molecular weight and are then further classified according to function. PBPs are initially divided into high molecular weight (HMW, Mr >60,000) and low molecular weight (LMW, <60,000) PBPs. HMW PBPs are further divided in to Class A PBPs (bifunctional) and Class B PBPs (monofunctional transpeptidases) (**Figure 1.9 a**). Generally, two HMW PBPs are necessary for the bacterium to survive, one Class A and one Class B. LMW PBPs are shapeless mutants (Popham & Young, 2003) and not essential for survival of the bacterial cell. The role of LMW PBPs serves more to recycle peptidoglycan in preparation for the incorporation of nascent peptidoglycan by HMW PBPs. Peptidoglycan synthesis and incorporation is mainly by HMW PBPs 1-3. HMW Class A bifunctional PBPs are the focus of this PhD (**Figure 1.9 b**), which carry out both transglycosylation and transpeptidation.

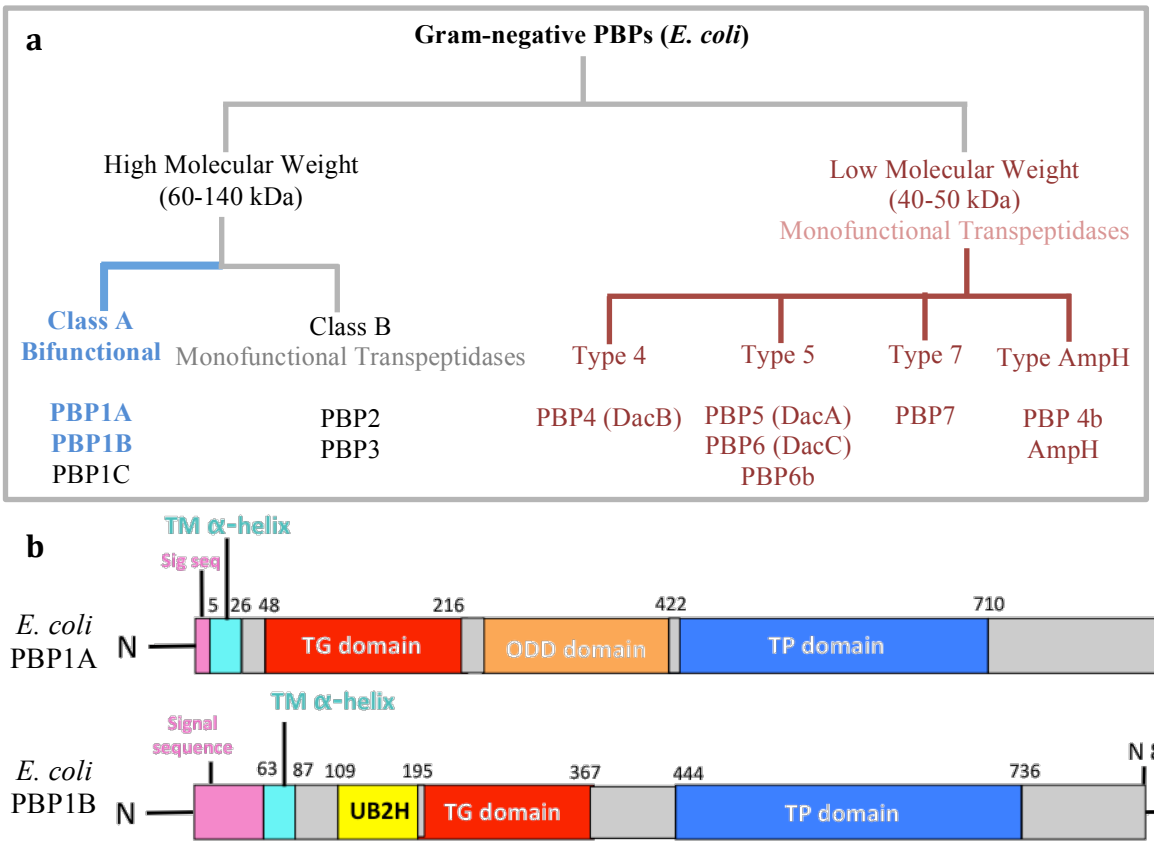

Figure 1.9 (a) The Classification of Gram-negative PBPs (using *E. coli* as the model). The topology of HMW Class A PBPs (blue) consist of a cytoplasmic tail, a transmembrane anchor, and two domains joined by a β-rich linker located on the outer surface of the cytoplasmic membrane where peptidoglycan synthesis takes place. The C-terminal of all HMW PBPs has a transpeptidase domain. LMW PBPs (red) are sometimes classified based on their migration through SDS-PAGE in to Classes A, B and C. Here they have been divided based on amino acid sequence alignment and knowledge of their structure and function (Massova & Mobashery, 1998). Type 4 and Type 7 PBPs are DD-endopeptidases, Type 5 PBPs are strict DD-carboxypeptidases and Type AmpH are of unknown function, except PBP4b has shown weak DD-carboxypeptidase activity (Vega & Ayala, 2006). **(b) A Schematic representation of the two Class A bifunctional PBPs: *E. coli* PBP1A and PBP1B**. NB: The ODD domain (Outer Docking Domain) of *E. coli* PBP1A is located between the transglycosylase and the transpeptidase domains, whereas the UB2H domain in *E. coli* PBP1B is after the TM helix, prior to the transglycosylase domain.

The *E. coli* genome has two major bifunctional Class A penicillin binding proteins, *E. coli* 1A and 1B. *E. coli* PBP1A serves to polymerise LII monomer units into polymers of a length of ~20 disaccharide units. All bacteria contain at least one PBP from each class. Gram-negative cocci tend to have one peptidoglycan-synthesising machinery i.e. the divisome at the septum, whereas Gram-negative rods have two: the elongation machinery in addition, so they have at least two Class A PBPs and two class B PBPs. *Chlamydiae* peptidoglycan is a particular case as it doesn't have any class A PBPs.

There are even some bacteria without peptidoglycan and PBPs: *Rickettsia*, *Mollicutes* and *Dehalococcoides*.

1.5.2 Membrane Proteins as Drug Targets

Membrane proteins include receptors, ion channels, transporters, and enzymes, and constitute a significant fraction (20 %-30 %) of the proteome (Fagerberg *et al.*, 2010). However they are highly underrepresented, and make up less than 1% of all protein structures solved. As of January 2017, there were 1194 published reports of membrane protein structures (671 unique) solved by NMR or crystallographic techniques.

1.5.3 Using Detergents to Study Membrane Proteins

Detergents are required for the solubility of membrane proteins and are needed to extract PBPs from their periplasmic associated environment. Despite Class A PBPs only having a single transmembrane (TM) domain, the transglycosylase domain is also embedded within the cytoplasmic membrane, to maintain a hydrophobic environment for its Lipid II substrate. Mainly non-ionic detergents are used to solubilise PBPs in this thesis. Non-ionic detergents are neutrally charged. The most common of the synthetic anionic surfactants are based on the straight chain alkylbenzene sulfonates, which produce electrically negative colloidal ions in solution. Cationic detergents produce electrically positive ions in solution. Amphoteric detergents are capable of acting either as anionic or cationic detergents in solution depending on the pH of the solution.

1.5.4 *E. coli* PBP1A

E. coli PBP1A is a bifunctional PBP with both transglycosylase and transpeptidase functionality. Its structure has not been solved crystallographically yet, but the transglycosylase domain of *Aquifex aeolicus* PBP1A structure was solved in 2007 (Yuan *et al.*, 2007). The *A. aeolicus* transglycosylase domain has also been crystallised in complex with Moenomycin (Fuse *et al.*, 2010). *E. coli* PBP1A is likely to follow a similar structural pattern to *H. influenzae* PBP1A which was crystallised in December 2016 (Minasov *et al.,* 2017). The structure of *E. coli* PBP1A is likely to consist of an N-terminal single α-helical TM domain, a transglycosylase domain, an Outer Docking

(ODD) Domain and a C-terminal transpeptidase domain. *E. coli* PBP1A interacts with the cell-elongation-specific Class B monofunctional transpeptidase PBP2 *in vivo* and localises mainly to the cylindrical wall of the cell, helping with cell elongation. It helps govern cell shape and inactivating PBP2 in *E. coli* causes cells to lose their rod shape and grow as enlarged spheres that eventually die unless compensatory mutations or conditions. PBP2 also binds to the outer-membrane lipoprotein LpoA, where the lipoprotein also helps in cell elongation. LpoA is attached to the outer-membrane and hangs down in to the periplasm to interact with PBP1A. The ODD domain of *E. coli* PBP1A and LpoA are restricted to γ-proteobacteria.

1.5.5 *E. coli* PBP1B

E. coli PBP1B is a major Class A bifunctional PBP that has been heavily studied over the past quarter century, as it is the workhorse of peptidoglycan synthesis, synthesising glycan chains *de novo*. *E. coli* PBP1B consists of five domains: (i) an N-terminal TM α-helix (residues 64-87) (ii) a UvrB domain 2 Homolog (109-200) (iii) a membrane-associated transglycosylase domain (203-367) (iv) a linker region connecting the transglycosylase and transpeptidase domains (391-443) (v) a C-terminal transpeptidase domain (444-736).

The X-ray crystal structure of *E. coli* PBP1B was solved in 2009 by Sung *et al.* The single α-helix TM region functions as both a signal sequence for secretion and a stop transfer signal that serves as a membrane anchor. It stabilises the PBP-membrane interaction, but stable protein-membrane interaction is not critical for normal function of *E. coli* PBP1B. Removal of the TM domain does not affect the structure of the transglycosylase domain in the binding site (Sung *et al.*, 2009). The function of transglycosylases is similar to that of lysozyme (Terrak *et al*., 1999), in that lysozyme cleaves the β1-4 glycosidic bond between Glc*N*Ac and Mur*N*Ac peptidoglycan units, which are initially generated by transglycosylases. The 2009 crystal structure shows the transglycosylase domain to be located at a site near to where the cell membrane would be, in relation to the overall structure of the enzyme. If this structural model is accurate, it would support the theory that the proximity of the enzyme to the membrane would assist in its interaction with the membrane bound substrate (Sung *et al.*, 2009). The recent crystal structures of transglycosylase domains in complex with moenomycin and

various β-lactams have highlighted essential interactions but their significance in structure based drug design efforts (King *et al.,* 2016).

The transglycosylase domain is mostly α-helical and is responsible for polymerising LII in to linear glycan strands. It is part of a group of glycosyl transfer proteins ordered by sequence homology in to the CAZY (carbohydrate-active enzymes) classification of enzymes. Peptidoglycan glycosyl transfer proteins are in family 51 (GT_{51}), characterised by five conserved motifs and the use of LII. 80 % of the CAZY database are bifunctional PBPs and 20 % are monofunctional. The transglycosylase domain is comprised of two regions - a larger globular 'head' and a smaller, flexible 'jaw' region, separated by a cleft (Lovering *et al.,* 2007). The globular head subunit has homology to lysozyme and the flexible jaw has high hydrophobicity and interacts with the lipid bilayer and the lipidic substrate. Positioning of the two subunits forms a cleft lined with residues that are conserved, shown in *E. coli* PBP1B (Terrak *et al.*, 2008), *S. aureus* MGT and *A. aeolicus* PBP1A, with several similar structural features between members of the TG_{51} family (Lovering *et al.*, 2008) **(Figure 1.10a**). These residues are clustered in to five motifs (**Figure 1.10 b** and **c**), with the first three motifs residing in the cleft. The cleft contains the catalytic residues, with motifs 1 and 3 harbouring the two conserved glutamic acid residues and motif 2 being involved in substrate recognition. Motifs 4 and 5 play a structural role in the cleft.

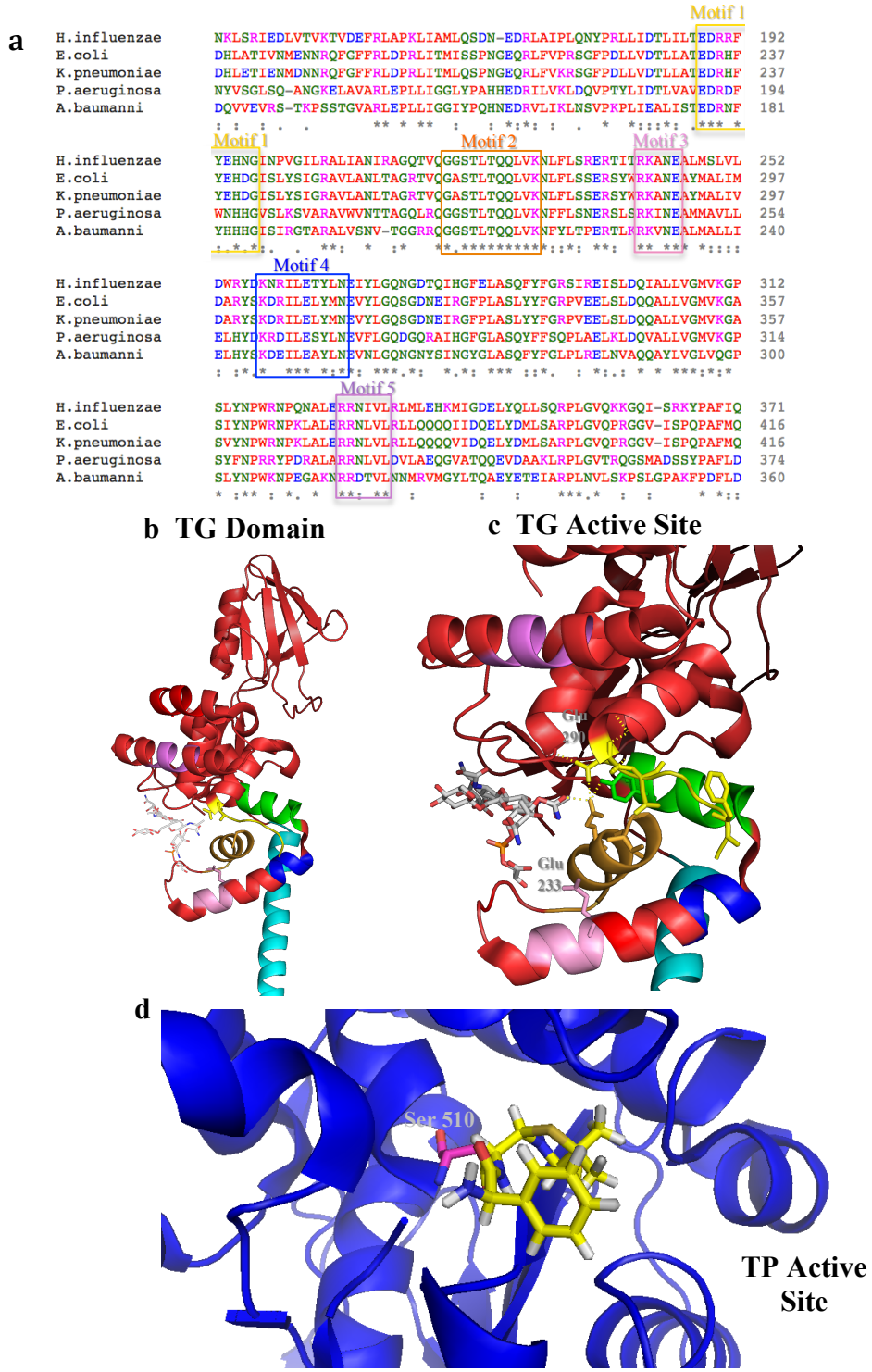

Figure 1.10 The Conserved Motifs in the TG51 Structural Family, with this *E. coli* PBP1B Domain Bound to Moenomycin A, Residing in the Catalytic Cleft. (a) The alignment of the five conserved TG_{51} motifs in Gram-negative species **(b)** The full transglycosylase domain and α-helix of *E. coli* PBP1B, the beginning of the linker region between the transglycosylase and transpeptidase domains is in purple TM α-helix = cyan, transglycosylase domain = red the five conserved motifs are shaded as follows: Motif 1 = yellow, motif 2 = orange, motif 3 = pink, motif 4 = blue, motif 5 = violet. **(c)** The active site cleft of the transglycosylase domain. Conserved residues include the catalytic glutamates E233 in motif 1 and E290 in motif 3 (Terrak *et al.*, 2008). **(d)** The *E. coli* PBP1B transpeptidase domain (blue) containing the β-lactam ligand, ampicillin (yellow), bound to the catalytic active site Serine 510 (magenta). (King *et al.*, 2016).

The amino acids tryptophan and tyrosine are found at higher frequency at a lipid-water interface in membrane proteins (Yau *et al.,* 1998) and were found at the bottom of the transglycosylase domain, indicating that it is partially embedded in the lipid bilayer. The residues in the transglycosylase domain that interact with transglycosylase inhibitors such as Moenomycin and are also conserved between other transglycosylases are critical in antibiotic drug design.

The UvrB Homology (UB2H) domain interacts with the MltA protein. It also interacts with the lipoprotein LpoB along with the transpeptidase domain, which stimulates its cross-linking ability. *E. coli* LpoB and the UB2H domain of *E. coli* PBP1B are further restricted within γ-proteobacteria to the enterobacteria (Typas *et al*., 2010) and so are not present in *Pseudomonas spp* species. PBP1B-LpoB may work in parallel with the Tol-Pal complex to aid membrane constriction.

Three-dimensional structures of the four proteins of interest in this thesis: *E. coli* and *P. aeruginosa* PBP1A and PBP1B have not been solved yet, apart from the full-length *E. coli* PBP1B protein (King *et al.*, 2017, Sung *et al.*, 2009) (**Figure 1.11 b**). The transpeptidase domain of *P. aeruginosa* PBP1A has been crystallised with a sideromimic conjugated compound in its transpeptidase serine active site (Starr *et al*., 2014). The transglycosylase domain is missing due to intrinsic flexibility and tryptic cleavage. No structures at all have been solved for *E. coli* PBP1A or *P. aeruginosa* PBP1B. There is a total of two Class A PBPs from species other than *E. coli* and *P. aeruginosa*, for which structures have been resolved: the transglycosylase domain only of the bifunctional PBP1A from the thermophilic species *Aquifex aeolicus* (Yuan *et al.*, 2007) and the full-length bifunctional PBP1A from the Gram-negative *Haemophilus influenzae* (Minasov *et al.,* 2017) (**Figure 1.11 a**).

a *H. influenzae* PBP1A

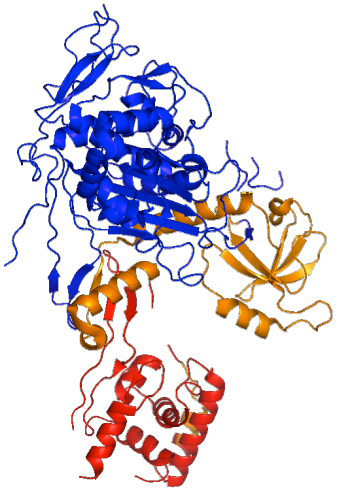

b *E. coli* PBP1B

Figure 1.11 The Crystal Structures of the Two Gram-Negative Class A Bifunctional PBPs (PBP1A and 1B). (a) *H. influenzae* PBP1A and (b) *E. coli* PBP1B. In *E. coli* PBP1B, the enzyme resides in the periplasmic space between the inner and outer membranes of *E. coli* cells, with the transmembrane α-helix anchoring the PBP to the membrane. The transglycosylase domain is at the N-terminal and the transpeptidase domain is at the C-terminal. The transglycosylase active site glutamic acid residue is at position 233 and the transpeptidase active site is residue 510. Cyan = TM domain, red = transglycosylase domain, orange = ODD domain in *Hi*PBP1A, yellow = UB2H domain in *Ec*PBP1B, blue = transpeptidase domain. *H. influenzae* PBP1A has been crystallised without its TM domain. PDBs: 3VMA & 5HL9 for *Ec*PBP1B (Sung *et al.,* 2009, King *et al*., 2017) and 5U2G for *H. influenzae* (Minasov *et al.,* 2017) (The 5U2G structure was deposited on to the Protein Data Bank (www.rcsb.org) in December 2016, but the associated article has not yet been published, thus the domain colouring of *Hi*PBP1A in (a) has been estimated at this time).

1.5.6 *P. aeruginosa* as a Clinically Important Pathogen

Pseudomonas aeruginosa was chosen as a species to study, as it is a Gram-negative of high clinical relevance with a major resistance problem. The *P. aeruginosa* enzymes earlier in the peptidoglycan synthesis pathway has been mostly characterised, but its PBPs have not. There is a need for high-through-put assays that could be used for screening, therefore part of the project was to investigate different assay methods for PBPs.

P. aeruginosa is one of the most common Gram-negative micro-organisms isolated from nosocomial isolates in recent years. It commonly causes hospital-acquired infections (HAIs) including pneumonia, bloodstream, urinary tract and surgical-site infections. More than 6,000 (13%) of the 51,000 health care-associated *P. aeruginosa* infections that occur in the U.S. each year are multi-drug-resistant (MDR) (Rossolini *et*

al., 2014). The associated PBPs could play a crucial role in β-lactam resistance in MDR Gram-negative bacteria. *P. aeruginosa* colonises on the surface of medical equipment in surgical theatres and infects patients during surgery; this pathogen also infects the wounds of burns victims, and persistently occupies the lungs of Cystic Fibrosis patients. It is an opportunistic pathogen for which treatment options are limited, but include broad-spectrum β-lactams (carbapenems) and is of increasing concern in clinical situations. Some Gram-negative organisms including *P. aeruginosa* have mechanisms for evading the action of β-lactam antibiotics including the acquisition of β-lactamases, provoking the emergence of MDR strains.

1.5.7 *P. aeruginosa* PBP1A

Pseudomonas aeruginosa have a full compliment of PBPs as *E. coli*, including the Class A PBPs 1A and 1B, three Class B enzymes (PBP2, PBP3, and PBP3a: orthologues of the corresponding enzymes in *E. coli*) and the Class C PBPs 4 and 5. *Pa*PBP3 shares 42% sequence identity with the corresponding protein in *E. coli* and has been identified as the primary target of a number of β-lactams used to treat pseudomonal infections, including the cephalosporin analogues cefsulodin (Gotoh *et al.,* 1990) and ceftazidime (O'Callaghan *et al.*, 1980), piperacillin (Godfrey *et al.,* 1981), and the parenteral carbapenem, doripenem (Davies *et al.*, 2008). PBP1A follows the same structural format as *E. coli* PBP1A: The TM helix followed by a domain of unknown function, known in *E. coli* PBP1A as the 'ODD' domain. This is followed by a transglycosylase domain, linked by a β-rich linker to a transpeptidase domain. The interface between the transglycosylase and transpeptidase domains comprises of 6 sequential β-strands, with two serving as a linker between the two domains. The transpeptidase domain has a similar fold to other transpeptidases and serine β-lactamases. Within the transpeptidase domain, there is an oligosaccharide/ nucleotide-binding (OB) fold, as in *A. baumanii* (Han *et al.,* 2011). The crystal structure of the transpeptidase domain of *Pa*PBP1A was solved in 2014 (PDB: 4OON) with a sideromimic-conjugated compound bound to its transpeptidase domain (Starr *et al.*, 2014), achieved after proteolysis with trypsin. The construct crystallised was the full-length PBP minus the N-terminal TM domain: residues 36-822, to a resolution of 3.20 Å. The transglycosylase domain cannot be seen in the crystal structure due to intrinsic flexibility and tryptic cleavage.

1.5.8 *P. aeruginosa* PBP1B

Very little is published on *Pseudomonas aeruginosa* PBP1B, including any structural or functional information. It has been assumed thus-far that this enzyme behaves similarly to *E. coli* PBP1B and is likely to have a similar structure, with the main difference being that there is no LpoB protein present in Pseudomonas species and the LpoB protein is thought to have evolved along with the UB2H domain, as in *E. coli* PBP1B. Therefore it is also unlikely that *Pa*PBP1B has a UB2H like that in *E. coli*.

1.5.9 *P. aeruginosa* Resistance to β-Lactams

Many β-lactam antibiotics are used in combination with β-lactamase inhibitors, as there is such widespread β-lactam resistance. *Pseudomonas aeruginosa* cells exhibit resistance to β-lactams through over-expression of AmpC and OprD, as well as efflux pumps. Six *P. aeruginosa* nosocomial isolates were studied for resistance mechanisms, all of which lacked OprD and over-expressed AmpC, and five of them showed modified PBP profiles such as diminished expression of PBP1A and modified binding affinities to β-lactams (Moya, *et al.*, 2012). Ceftaroline (a cephalosporin B-lactam) has a broad-spectrum activity against Gram-positive pathogens and several Gram-negative pathogens, with the notable exceptions of *P. aeruginosa* (and extended spectrum β-lactamase (ESBL)-producing *Enterobacteriaceae*). Current antibiotics active and in use against *Pseudomonas aeruginosa* infections include the carbenicillin, the cephalosporins cefepime and ceftazidime and the fluoroquinolone ciprofloxacin.

1.5.10 Proteins that Interact with PBPs

PBP1B in particular makes a series of important protein-protein interactions (PPIs) that are important in cell metabolism providing a network of interactions. PBP1A is involved in adding new sugar units to the peptidoglycan sacculus during cell elongation. PBP1B localises to the septum of a bacterial cell during cell division, forming a complex machinery of enzymes as part of the Z-ring, the driving force behind constriction of the cell wall. Both of these activities require a plethora of enzymes to work together to coordinate these fundamental processes (**Figure 1.12**). Cell division proteins such as FtsN interact with PBP1B, building a network of protein interactions

that work together to polymerise peptidoglycan including during enlarging of the sacculus during cell division. FtsN interacts with *E. coli* PBP1B (Müller *et al.*, 2007) as well as PBP3 (FtsI) (Bertsche *et al.,* 2006) and FtsW (Fraipont *et al.*, 2011; Derouaux *et al.*, 2013, Derouaux *et al.*, 2008). FtsN is thought to initiate cell division and divisome assembly, being the final component in the divisome complex (van der Ploeg *et al.*, 2013). FtsW was recently shown to impair the polymerisation and peptide cross-linking of PBP1B (Leclerq *et al*., 2017). *Pa*PBP3 is essential for growth in *P. aeruginosa* (Chen *et al.,* 2017) and has an essential role in cell division in both *P. aeruginosa* and *E. coli*. The β-lactams ceftazidime, ceftolozane and Imipenem all target *Pa*PBP3 and Imipenem targets *Pa*PBP2 in addition to *Pa*PBP3.

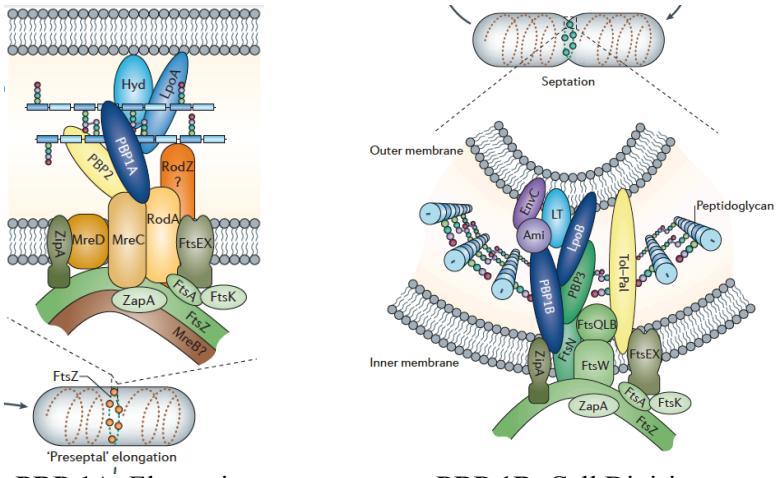

PBP 1A: Elongation **PBP 1B**: Cell Division

Figure 1.12 The 'Divisome' machinery and 'Elongasome' complexes involved in both (a) Cell Elongation and (b) Cell Division (Adapted from Banzhaf *et al*., 2012). Cell wall synthesis has recently been thought to be mediated by Shape, Elongation, Division, Sporulation (SEDS)-family proteins working within the cytoskeletal machines. The SEDS family of proteins represent a diverse set of peptidoglycan synthases, which exhibit weak similarity to O-antigen ligases involved in synthesis of LPS in Gram-negative bacteria (Cho *et al.*, 2016 & Meeske *et. al*., 2016).

1.5.10.1 The LpoA and LpoB Lipoproteins

Lpo proteins are associated with the outer-membrane and protrude down in to the periplasmic space, interacting with the PBPs. LpoA or LpoB are absolutely required for *in vivo* and *in vitro* activity of PBP1A and PBP1B, respectively. This has been proven in *E. coli* thus far (Typas *et al.*, 2010, Paradis-Bleau *et al.,* 2010), and each Lpo lipoprotein stimulates its transpeptidase function. The structures of *E. coli* LpoA and LpoB were solved by solution NMR in 2014 by Jean *et al*., 2014, and Egan *et al*., 2014,

respectively. LpoA stimulates transpeptidase activity, which in turn stimulates transglycosylation. LpoB stimulates transglycosylase activity, stimulating transpeptidase activity in-turn. γ-proteobacteria regulate peptidoglycan synthesis by co-evolving interacting proteins and their PBP docking domains (Typas *et al.*, 2010).

Little is known about the role of the N-terminal domain of LpoA, but structurally it is rich in α-helicies (H1-H12) with helix-turn-helix tetra-tripeptide repeat (TPR)-like motifs, adopting a TPR-like fold. LpoA interacts with the PBP1A ODD domain, stimulating both transglycosylase and transpeptidase domain activity, through conformational change. The C-terminus of LpoA has two extended flexible, unstructured regions that do not interact with PBP1A. As of consequence of this flexibility, it is not very stable and the ODD domain of PBP1A is also not very stable. There is very little flexibility between the N and C termini of LpoA, owing to a rigid linker between the two domains. The full LpoA protein is a long elongated shape and spans the entire outer membrane through the periplasm.

LpoA and LpoB are unrelated in amino acid sequence and have very different molecular weights. LpoA is 700 amino acids long (>70 kDa) and LpoB is 200 amino acids long (20 kDa). LpoA and PBP1A are involved in the elongosome, LpoB and PBP1B are involved in the divisome, with YbgF (recently renamed CpoB in *E. coli*) being involved in outer membrane invagination, as part of the Tol-Pal complex (Gray *et al.,* 2016). YbgF coordinates PBP1B and TolA during outer membrane constriction and cell division. YbgF forms a trimer in solution and modulates the activity of PBP1B *via* its interaction with LpoB, with LpoB and YbgF sharing the UB2H domain of *Ec*PBP1B (Krachler *et al*., 2010).

1.6 Underexploited Targets for Antimicrobials

Peptidoglycan transglycosylases are under-exploited as antimicrobial drug targets, despite their key and clear role in an area of bacterial metabolism that is a validated target for a number of existing antibiotics. Moreover, since most pathogens have at least two transglycosylase activities required for peptidoglycan biosynthesis that utilise the same mechanism, resistance to novel compounds would require simultaneous and multiple compensatory mutations.

Antimicrobial peptides are an alternative avenue to explore; they are less vulnerable to bacterial resistance than conventional antibiotics (Lohner, 2017). It takes 30 passages of *P. aeruginosa* in a sub-MIC peptide to increase its resistance by 2-4 fold (Marr *et al.*, 2006). The lack of diversity in the sequence and targets of conventional antibiotics renders them more susceptible to resistance. Peptides have multiple targets so can cause cell lysis via various mechanisms, whereas conventional antibiotic target a specific enzyme or function in the cell. A class of antimicrobial peptides called structurally nano-engineered antimicrobial peptide polymers (SNAPPS) exhibit sub-μM activity against Gram-negatives, including ESKAPE and colistin-resistance MDR pathogens, showing toxicity against *Acinetobacter baumannii in vivo* (Lam *et. al.*, 2016).

Some of the most promising opportunities for antibiotic discovery and development are (i) antibiotic compounds that were discovered decades ago but left unexplored because of their limited therapeutic prospects and (ii) adjuvants that act synergistically with existing antibiotics to overcome established mechanisms of antibiotic resistance (Farha & Brown, 2013).

1.7 Strategies for Novel Antibiotic Discovery

Improvements in protein structure-activity relationships determination has enabled rational drug design, as well as robotic liquid handling has encouraged high through put screening of biochemical assays. The development of 'big data', improved data storage and manipulation capabilities, coupled with improved genome-mining strategies such as Genome Wide Association Study (GWAS) and metagenomics is aiding in identifying precise deletions that may prevent the drug target from being susceptible to current resistance mechanisms (Brown & Wright, 2005).

Bacterial proteases that are responsible for the cell's stress response and pathogenicity have been ear-marked as underexplored targets with potential (Culp & Wright 2016). Also an antibiotic resistance platform (ARP) that contains a set of resistance elements has recently been developed that can be used for both the identification of antibiotic adjuvants and for antibiotic dereplication (natural product screening) and identifying inhibitors of resistance (Cox *et al*., 2017).

Yeast-2-hybrid and bacterial-hybrid experiments are being used to generate networks of genetic interactions, which can be used to predict functional interactions, drugs targets or combinations of drugs that inhibit interacting proteins (Babu *et al.*, 2011). A network of chemical and genetic interactions that resist disruption can be built using antibiotic adjuvants (non-antibiotic compounds that enhance or suppress antibiotics). These interaction networks offer new target for adjuvants (Brown, 2016).

Microbes in the environment target cell wall synthesis by a variety of ways, making natural products the best sources of antibiotic. Natural products dominate the history of antibiotics, especially those produced by microorganisms. Although it is challenging to chemically synthesise natural product derivatives in the laboratory as they are chemically complex. Synthetic compounds are traceable (unlike natural products) and are easier to scale-up. A successful example being synthetic fluoroquinolones, but very little has been generated this was in the past 3 decades. Screens of natural products identify bioactive (but already known) compounds, screens of synthetic libraries find potent ligands that have poor bioactivity (Brown, 2016). One solution is the development of synthetic libraries with the chemical diversity and properties of natural products (Kim *et al*., 2014). It is also important to avoid resistance by using combination therapy, i.e. synergistic combinations (Worthington & Melander, 2013). Teixobactin was ineffective against wild type *P. aeruginosa* and *E. coli*, however, an *E. coli* strain with a defective outer-membrane had an MIC of 2.5 μ g/ml, suggesting that outer membrane-permeabilising adjuvants may increase the potency of Teixobactin against Gram-negatives, including *P. aeruginosa* (Lamers & Burrows, 2016).

1.7.1 Recent Developments in Compounds Against MDR *P. aeruginosa*

Currently, the only clinically approved PBP1b specific β-lactam is cefsulodin, in which clinical utility is restricted to *Pseudomonas aeruginosa* (Sarkar *et al.,* 2012). The monobactam Aztreonam in conjunction with the β-lactamase-inhibitor Avibactam was not lethal towards the β-lactamase-producing *P. aeruginosa* (Testa *et al*., 2015). However, a novel siderophore cephalosporin (S-649266) showed superior *in vitro* activity over its β-lactam comparators against MDR *P. aeruginosa* (Kohira *et al.*, 2016). Synergy was also observed between the siderophore sulfactam BAL30072 and

carbapenems against both MDR *Enterobacteriaceae* and *P. aeruginosa* isolates (Mushtaq *et al.,* 2013). The aminoglycoside Plazomicin demonstrated synergistic *in vitro* activity with carbapenems against *P. aeruginosa* and *A. baumannii* isolates (Walkty *et al.*, 2014) but Eravacycline, like tetracycline, showed limited activity against *P. aeruginosa* (Sutcliffe *et al*., 2013).

1.7.2 Recently Approved Antimicrobials

Zerbaxa is a combination product containing ceftolozane, a cephalosporin antibacterial drug, and tazobactam, a beta-lactamase inhibitor. Zerbaxa is used to treat complicated urinary tract infections, including kidney infections. It is used in combination with metronidazole to treat intra-abdominal infections like Avycaz. Developed by Cubist, (now Merck) clinically available 2014.

Dalvance (USA) / Xydalba (Europe) is a lipoglycopeptide belonging to the same class a vancomycin, one of the few treatments against MRSA. Developed by Allergan, clinically available May 2014.

Sivextro is an oxazolidinone-class antibiotic used to treat acute bacterial skin infections, developed by Cubist (now Merck), clinically available June 2014.

Avycaz is a combination of ceftazidime, a cephalosporin, and avibactam, a β-lactamase inhibitor, to treat complicated intra-abdominal infections, used in combination with metronidazole. Developed by Allergan, available February 2015.

Zinplava (bezlotoxumab) treats recurrent *Clostridium difficile* infections in patients receiving antibacterial treatment. Developed by Merck, approved October 2016.

1.7.3 Teixobactin - The Latest Discovery

Most antibiotics are natural products derived from microbes in the soil and Teixobactin is no different. Teixobactin is natural product antibiotic isolated by Ling *et al.*, in Boston, USA in 2015. The chemical was found in soil and has shown to be active against tuberculosis, septicemia, *C. difficile* and could potentially be available in the

next 5 years. An electronic chip was used to grow microbes in soil and isolate the naturally produced chemical compound from an uncultured soil microorganism similar to *Aquabacteria*. The compound exhibited antimicrobial ability, binding to both Lipid II and Lipid III. This novel technique allows compounds to be isolated from soil, harbouring microorganisms that do not grow under 'normal' laboratory conditions. It is currently believed that bacteria will not become resistant to Teixobactin for at least 30 years as it targets lipid molecules as well as having multiple methods of attack. Trials thus far have revealed no side effects in mice. This antibiotic is being scaled-up ready for clinical trials in humans (Ling *et. al.*, 2015). Teixobactin was ineffective against wild type *P. aeruginosa* and *E. coli*; however, an *E. coli* strain with a defective OM had an MIC of 2.5 μ g/ml, suggesting that OM permeabilising adjuvants may increase the potency of teixobactin against Gram-negatives, including *P. aeruginosa*.

1.8 Antimicrobial Resistance (AMR) Public Policy

The World Health Organisation (WHO) have published reports named 'The Evolving Threat of Antimicrobial Resistance' (2012) and 'AMR: Global Report on Surveillance' (2014), which both discuss better tracking and monitoring of antibiotic use, reducing the use of antibiotics in animal husbandry and improving infection prevention in hospitals (WHO Report, 2014). Recommendations from the UK Chief Medical Officer's 2013 Annual Report echoed many of the political commitments outlined in the 2012 WHO Report, such as widening education on antibiotics, challenging the irresponsible use of antibiotics, tightening the laws in agriculture to avoid over-use for the sake of prevention, improving data recording to retrieve true observations on prescription statistics and to encourage the investment in innovative solutions (Chief Medical Report, UK 2013). The Economist James O'Neill released a report on the socio-economic impact of AMR (J. O'Neill Report, May 2016). The problem of AMR needs to be confronted through collaboration from multiple funding bodies, including WHO, NHS, DEFRA, Food Standards Agency as well as agricultural bodies. In 2007 the European Centre for Disease Prevention Control (ECDC) began an annual 'Antibiotic Awareness Day' each November to raise the profile of the scale of the problem. The European Commission is set to publish a 'New Action Plan' to combat antimicrobial resistance in 2017. In the USA, the FDA introduced the GAIN (Generating Antibiotics Incentives Now) Act, which extends by five years the exclusivity period during which

antibiotics can be sold without generic competition. This additional period of exclusivity increases the potential for profits from new antibiotics by allowing the Pharma industry more time to recoup investment costs.

1.9 Thesis Aims and Outlines

To further investigate the transglycosylase function of Class A bifunctional PBPs, using *E. coli* Class A PBPs as the model organism for which to compare to *P. aeruginosa* PBPs. Very little literature has been published on *P. aeruginosa* PBPs, possibly as they may have proven challenging to isolate and purity and additionally due to the pathogenicity of the *P. aeruginosa* PA01 strain generating caution. The transpeptidation activity of these PBPs will also be analysed using previously known techniques as well as novel assay developments and optimisation. The known interacting partner proteins to PBPs will also be investigated as to their stimulatory or inhibitory impact on the transglycosylase and transpeptidase function of *P. aeruginosa* PBPs.

The main aim of this thesis is to develop spectrophotometric assays to enable the rapid, kinetic characterisation of the PBP transglycosylase and transpeptidase activities, whilst concomitantly establishing conditions in which these activities can be detected. The assays used to characterise these activities will be developed extensively. Enabling such assays to be used in a high-throughput manner will aid the screening of potential inhibitor compounds to elucidate future antimicrobial candidates.

Chapter 2
Materials and Methods

2.1 Chemical Reagents and Buffers

All chemical reactions were sourced from the following, unless otherwise stated: Avanti Polar Lipids, Alabaster, AL, USA, Affymetrix (formerly Anatrace); Maumee, Ohio, USA, Calbiochem, USA, Fisher Scientific USA, GE Healthcare; Little Chalfont, Buckinghamshire, UK, Integrated DNA Technologies, Coralville, Iowa, USA, Invitrogen Life Technologies Ltd., Paisley, UK, New England Biolabs (UK) Ltd; Hitchin, Hertfordshire, UK, Promega Corporation; Madison, Wisconsin, USA, Sigma-Aldrich Company Ltd.; Dorset, UK.

All buffers were prepared in MilliQ purified water. Buffers for chromatography and spectrophotometric measurements were also filtered using a 0.2 mm filter. pHs were determined using a WPA pH meter CD720 with pH 4.0, pH 7.0 and pH 10.0 buffer standards supplied by Hanna Instruments. For chromatography, buffers were filtered prior to use with a 0.2 μm filter.

2.2 Growth and Maintenance of Bacteria

2.2.1 Bacterial Strains

Table 2.1 Bacterial strains used for cloning and protein overexpression.

Competent Cell Line *E. coli* Strain	Genotype	Reference
TOP10	F$^-$ *mcrA* Δ(*mrr-hsdRMS-mcrBC*) φ80*lacZ*ΔM15 Δ*lac*X74 *deo*R *rec*A1 *ara*D139 Δ (*ara-leu*)7697 *gal*U *gal*K *rps*L (Str^R) *endA1 nupG*	Grant *et al*., (1990)
DH5-α	F$^-$ *endA1 glnV44 thi-1 recA1 relA1 gyrA96 deoR nupG Φ80dlacZΔM15 Δ(lacZYA-argF)U169, hsdR17(rK - mK+), λ–*	Hanahan, 1985
BL21 (λDE3)	F$^-$ *omp*T *hsd*S$_B$ (r$_B^-$ m$_B^-$) *gal dcm rne*131 (λDE3) An *E. coli* strain with DE3, a λ prophage carrying the T7 RNA polymerase gene and lacIq. Transformed plasmids containing T7 promoter driven expression are repressed until IPTG induction of T7 RNA polymerase from a lac promoter.	Lopez *et al*., (1999)
C41 (λDE3)	Derivative of *E. coli* BL21(λDE3) : F$^-$ *omp*T *hsd*S$_B$ (r$_B^-$ m$_B^-$) *gal dcm* (λDE3). Contains at least one uncharacterized mutation - prevents cell death associated with expression of toxic recombinant proteins.	Miroux & Walker (1996)
C43 (λDE3)	Derivative of C41 (λDE3) obtained using F$^-$ ATPase subunit gene, contains no plasmid.	Miroux & Walker (1996)

2.2.2 Preparing Chemically Competent Cells

The cell line was streaked on to an LB-agar plate using a sterile loop and a single colony was selected for overnight culture. 125 mL of Luria Broth in a 500 mL glass conical flask was inoculated with 1.25 mL of the overnight culture. 20 mM $MgSO_4$ was added to stimulate transformation efficiency. All buffers were filter-sterilized (F/S) and stored at 4 °C before using. The culture was grown at 37 °C, shaking at 800 RPM, until reaching OD 0.4-0.6 (making sure not to exceed $OD_{0.6}$). The cell suspension was transferred to four ice-cold, sterile centrifuge tubes (competent cells are very temperature sensitive and must be kept at 4°C at all times). The tubes were spun at

4,500 ×g for 10 minutes at 4 °C in rotor JA 25.5. The pellets were resuspended in 50 mL (or 0.4 × the original culture volume) of ice-cold TFB1 buffer (30 mM potassium acetate pH 5.8, 10 mM $CaCl_2$, 50 mM $MnCl_2$, 100 mM RbCl, 15% glycerol and was adjusted to pH 5.8 using F/S IM acetic acid) and all four suspensions were combined and left on ice for 5 minutes. The cells were spun again at 4,500 ×g at 4°C for 10 minutes and the pellet was resuspended in 5 mL (or 1/25 × original culture volume) of ice-cold, F/S TFB2 buffer (10 mM MOPS or PIPES pH 6.5, 75 mM $CaCl_2$,10 mM RbCl, 15% glycerol, adjusted to pH 6.5 using F/S 1M KOH). The cells were incubated on ice for 1 hour, before being pipetted at 4 °C in to 100 × 50 µL aliquots in 1.5 mL Eppendorf tubes. The tubes were flash frozen in liquid Nitrogen and stored at -80 °C. The cells remained fully competent for ~3 months.

2.2.3 Bacterial Transformation

An aliquot of chemically competent cells were thawed on ice for 15 minutes. The competent cells were inoculated with 100 ng plasmid DNA and left on ice for 30 minutes. The cells were heat shocked at 42 °C for 45 seconds and placed back on ice for 2.5 minutes. 300 µL SOC (Super Optimal broth with Catabolite repression) was added to the transformation and incubated at 37 °C, shaking for 1 hour. 100 µL was spread on to an LB-agar plate and incubated overnight at 37 °C.

2.2.4 Bacterial Electroporation

An electrical field is applied to the cells to increase the permeability of the membrane, allowing the DNA to be introduced into the cell, which was used to insert plasmid DNA into *P. putida* competent cells. 25 µL of *P. putida* competent cells were incubated with 100 ng DNA on ice for 30 minutes, in an electroporation cuvette before electroporation in a BioRad GenePulser at 250 V, 100 Ω, and 25 µF.

2.2.5 Bacterial Growth Media

LB

1 % (w/v) tryptone, 0.5 % (w/v) NaCl, 0.5 % (w/v) yeast extract.

2YT

1.6 % (w/v) tryptone, 1 % (w/v) yeast extract, 0.5 % (w/v) NaCl, adjusted to pH 7.0.

Auto Induction Media

Auto-inductive media was based on the an autoinduction method by Studier (2005), containing a combination of ZY media, NPS solution, 5052 solution and 1 mM $MgSO_4$. The ZY media 1 % (w/v) N-Z amine, 0.5 % (w/v) yeast extract. NPS solution was 25 mM ammonium sulphate, 50 mM potassium dihydrogen phosphate and disodium hydrogen phosphate, commonly made as a 20-fold (20 x) stock solution. 5052 solution was mixture of 0.5% (v/v) glycerol, 0.05% (w/v) glucose and 0.2% (w/v) α-lactose, commonly made as a 50-fold (50 x) stock solution.

LB-Agar plates

Comprised of LB media with 1.5 % (w/v) bacto-agar, heated to melt the agar, and cooled sufficiently to add antibiotic, before pouring 17 mL media in to each plate.

2.2.6 Preparation of Glycerol Stocks

3 mL LB + antibiotic was cultured overnight at 37 °C. 0.5 mL of the overnight culture, with 0.5 mL of sterilized 100 % (v/v) glycerol were mixed and flash frozen and stored at -80 °C.

2.3 Molecular Biology Techniques

2.3.1 Polymerase Chain Reaction

The polymerase chain reaction (PCR) was used predominantly to amplify genes for cloning in to expression vectors. Genes would commonly be screened across a variety of conditions (with and without $MgCl_2$ and DMSO) using High Fidelity (HF) Phusion

polymerase (Thermo Fisher Scientific), Phusion HF buffer, dNTPs, forward an reverse primers and template (complementary) DNA. The primers (oligos) were specific to the gene and contained a restriction site and template DNA were species specific. Four master mixes were made up with and without $MgCl_2$ and DMSO, adding the polymerase last to each master mix (**Table 2.2**). An Eppendorf Thermocycler was used for PCR, with the conditions outlined in **Table 2.3**.

Table 2.2 PCR Reaction Mixtures for HF Phusion Polymerase

	- $MgCl_2$ - DMSO µL	+ $MgCl_2$ µL	+ DMSO µL	+ $MgCl_2$ + DMSO µL
5 × Phusion HF buffer	24	24	24	24
10 mM dNTPs	2.4	2.4	2.4	2.4
10 µM Forward primer	6	6	6	6
10 µM Reverse Primer	6	6	6	6
50 mM $MgCl_2$	2.4	2.4	2.4	2.4
Template cDNA (5-50ng)	2.4	2.4	2.4	2.4
100% DMSO	-	-	6	6
Phusion DNA Polymerase	1.2	1.2	1.2	1.2
H_2O (up to 120 µl)	78	75.6	72	69

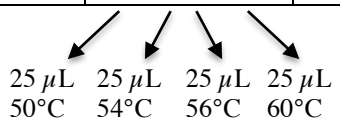

Table 2.3 The PCR program used for Phusion DNA Polymerase

Stage	Number of cycles	Temperature	Time
Initial Denaturation	1	98 °C	30 seconds
Primer Annealing →	25	98 °C	10 seconds
		50 - 60 °C[a]	30 seconds
		72 °C	30 seconds
Primer Extension	1	72 °C	10 minutes

[a] The annealing temperature was set to a gradient from 50 °C to 60 °C across the plate

PCR products were analysed by 0.8% or 1.0& agarose gel, depending on the size of the amplified gene. Upon successful amplification of the gene by PCR, the gene was either excised from the agarose gel and the Agarose removed using a Qiagen Gel Extraction Clean-Up Kit, or the PCR products were cleaned up using a Qiagen PCR Clean Up Kit. The DNA yield was quantified by Nanodrop.

2.3.2 DNA Quantification

Nanodrop technology was used to quantify DNA ND-1000 spectrophotometer (Thermo Scientific) using 1.0 μL samples.

2.3.3 Agarose DNA Electrophoresis

Agarose solution was prepared by dissolving 0.8 % or 1.0 % (w/v) of high-melting point agarose (Sigma-Aldrich) in to 1 x Tris-acetate-EDTA (TAE) buffer (40 mM Tris acetate, 1 mM EDTA), by heating in the microwave for 60 seconds. 1 μL of a 10 mg/ml stock of Ethidium bromide was mixed in to the molten agarose. Molten agarose was poured in to a gel cassette and left for 15 minutes to set, before being submerged in 1 x TAE buffer. Samples were supplemented with DNA loading dye and loaded in to the wells. Electrophoresis was conducted at 110 Volts for 35 minutes. Gels were analysed upon a trans-illuminator through a UV filter.

2.3.4 DNA Cloning

A summary of a typical DNA cloning protocol is summarised in the schematic below.

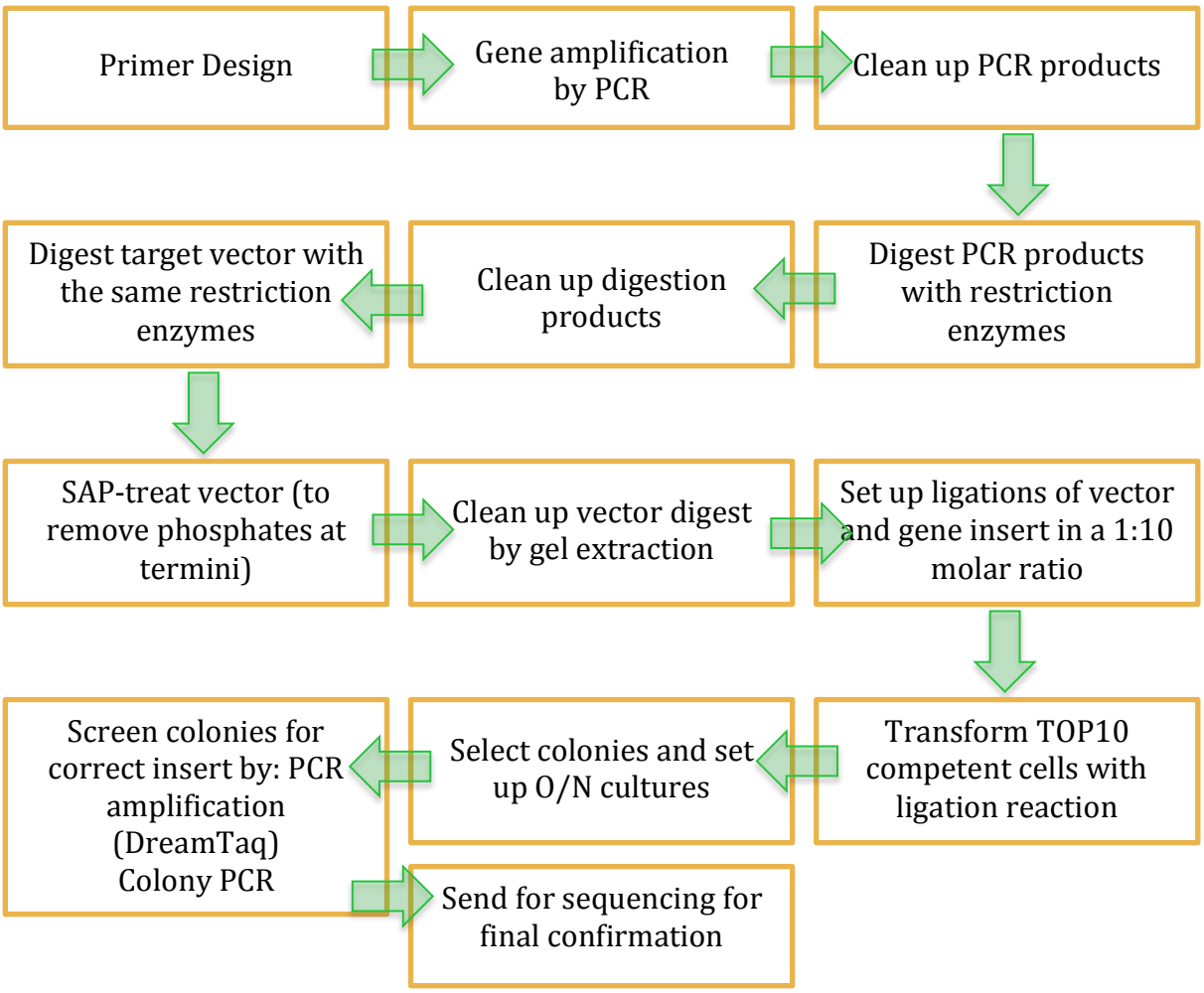

1 µg of PCR product DNA along with 1 µg of the destination vector was digested with the appropriate restriction enzymes, at the optimum temperature(s) for the restriction enzymes (usually 37 °C) for between 1 and 3 hours. The protocol provided with the specific restriction enzymes was followed. The vector (only) was treated with 1 µL of SAP (Shrimp Alkaline Phosphatase) for 30 minutes at 37 °C to remove the terminal phosphates from the digested vector ends and prevent them re-ligating back together. Digestion products were analysed by agarose gel and extracted from the gel and cleaned up using a Qiagen Gel-Extraction Kit and the yield was quantified by Nanodrop. A ligation reaction included a 1:10 molar ratio of vector : gene insert, with ATP, T4 DNA ligase and ligase buffer. Controls without vector were included. Ligation reactions were left overnight (3 hours minimum) at room temperature (20 °C).

Table 2.4 Typical Vector : Insert Ligation Reactions

	Negative Controls		
	Vector Only	Vector + Insert (No DNA Ligase)	Vector + Insert (With DNA Ligase)
Insert	-	-	3X μM
Vector	X μM	X μM	X μM
ATP	1 mM	1 mM	1 mM
Ligase	-	1 μL	1 μL
Ligase buffer	1x	1x	1x
water	Up to 25 μL	Up to 25 μL	Up to 25 μL

Aliquots of TOP10 competent cells were inoculated with 4 μL of each ligation reaction and transformed and plated onto LB-agar with the antibiotic selection of the plasmid vector being used for cloning. Colonies from the plate with vector, insert and DNA ligase were screened for potential positive clones.

2.3.4.1 Screening for Positive Clones

Screening methods for potential clones was done in one of three ways: conducting PCR on plasmid DNA extracted from the colonies, colony PCR (introducing the bacterial colony in to the PCR mixture as a DNA template, or by restriction digest. Colonies were selected from the vector+insert+DNA ligase LB-agar plate and amplified by growing in 3 mL LB + antibiotic for 5 hours minimum. The DNA was extracted from each culture using a DNA mini-prep kit (Qiagen). PCR could be performed on these plasmid preps. using one vector-specific primer and one gene-specific primer to ensure that the gene is present within the plasmid, and in the correct orientation. Alternatively, colonies from the vector+insert+DNA ligase LB-agar plate can be used as the DNA template for colony PCR by picking the colony with a tip-end and dipping it into PCR reaction mixtures. Another method for colony screening is doing a restriction digest of the extracted plasmid DNA potential clones, using one restriction enzyme that the enzyme was cloned into the vector with, and a vector-specific restriction site, often *XbaI* in pET vectors (Novogen), which is located upstream of the multiple cloning site (MCS). Potentially successful clones were sequenced by GATC Sequencing Services often using T7 primers (specific to pET vectors).

2.3.5 DNA Sequencing

80-100 ng.μL^{-1} plasmid DNA and 5 pmol.μL^{-1} primer (often vector specific T7 promoter or terminator of the pET vector or the primers used for the original PCR amplification of the target gene) were used for each sequencing reaction in a final volume of 10 µL. Reactions were submitted to GATC Biotech (Germany), and results were analysed using ApE Plasmid Editor (ApE) software.

2.3.6 Site-Directed Mutagenesis

Wildtype genes in their respective plasmid vectors (e.g. pET28::PaPBP1A) was used as the template for site-directed mutagenesis, following the protocol of the QuikChange II Site-Directed Mutagenesis Kit (Stratagene). Clones containing the correct mutation (a change of the catalytic active site residue *via* a single or double base change) were confirmed by DNA sequencing.

2.4 Recombinant Protein Expression in *E. coli*

2.4.1 Over-expression of *P. aeruginosa* PBP1A and *E. coli* PBP1A

*Ec*PBP1A was expressed in 6 x baffled flasks of 750 mL 2xYT media in each flask. C222222222222ultures were grown at 37 °C until they reached OD 0.6-0.7. Cultures were induced with 0.05 mM ITPG (Born *et al.*, 2006) and the temperature for expression reduced to 25 °C for 5 hours, or 18 °C overnight; both methods gave an equally high expression-level of viable, active *Ec*PBP1A. Cultures were pooled in to 1L centrifuge flasks and spun for 12 minutes at 4,000 x g at 4 °C in the Beckman JLA 8.1000 rotor. Cell pellets were weighed and resuspended in 3 mL resuspension buffer (25 mM Tris.HCl pH 7.5, 100 mM $MgCl_2$, 100 mM NaCl) per gram of cell pellet. Cells were lysed according to section 2.4.4.

2.4.2 Over-expression of *P. aeruginosa* PBP1B and *E. coli* PBP1B

The *E. coli* PBP1B gene was previously cloned into plasmid DML924 (conferring kanamycin resistance), which encodes a Hexa-Hig tag on the N-terminal end of the

protein. The construct was transformed into E. coli expression strain BL21 (DE3). An overnight culture was grown to inoculate 10 x 400 mL LB in 2.5 L baffled flasks. 50 μg/mL kanamycin and 0.2 % (final concentrations) glucose were added to select for the plasmid and encourage optimum expression, respectively. Cultures were grown at 37 °C until OD_{578} reached 0.7, upon which the cultures were induced to a final concentration of 1 mM IPTG. Cells were grown for a further 5 hours at 37 °C and then put on ice for 10 minutes before being centrifuged at 8,000 x g for 20 minutes.

2.4.3 *Ec*PBP1B and *Pa*PBP1B Expression Cell Line Trials

Alternative cell lines to BL21(DE3) were transformed and cultures of 200 mL were grown to OD_{600} 0.7. Upon reaching OD_{600} 0.7, the 200 mL culture was divided in to two, using 100 mL as a non-induced control and the other half was induced to 1 mM IPTG. The membrane fractions were harvested and run on two 10% SDS-PAGE gels. One gel was stained with Coomassie, the other gel was transferred to PDVF membrane and blotted with anti-His antibodies.

2.4.4 Large-Scale Bacterial Cell Lysis for the Preparation of Crude Cell Lysates

Bacterial cells were resuspended in 3 mL of resuspension buffer per gram of wet cell pellet weight and 2.5 mgs lysozyme per mL of cell suspension. 1 mg DNAaseI was added along with 1 mM PMSF and 1 μM of both leupeptin and pepstatin protease inhibitors. The resuspension was left to stir at 4 °C for 30 minutes before passing through a cell disrupter (Constant Systems Ltd). Cells were passed through the cell disrupter three times to complete the cell lysis process at 30,000 kpsi and 4 °C. Lysed cells were spun at 24,000 x g in the Beckman JA 25.50 rotor, for 40 minutes to pellet cell debris.

2.4.5 Harvesting the Membrane Fraction

The supernatant from the 24,000 x g spin containing cell cytosol was spun in a Beckman Coulter Optima L-90K Ultracentrifuge at 40,000 RPM using the Ti-45 (Titanium, max speed 45K RPM) rotor for 1 hour at 4 °C. The membrane pellet was scraped off the side of the centrifuge tube using a metal spatula and resuspended in to

resuspension buffer (without detergent) using a 1 mL Jencon glass homogenizer (cat# 361-039/P and 361-089).

2.4.6 Membrane Protein Solubilisation

The resuspended membrane pellet was supplemented with detergent (e.g. CHAPS, Triton-X-100 or DDM) to a suitable concentration for solubilisation, usually ~10xCMC. The suspension was left rocking/rolling at 4 °C for 4 hours to allow complete solubilisation. The length of solubilisation: the longer the better for more extraction of the desired protein, but longer than 4 hours can be detrimental to enzyme activity, personal communication, Dr. Andrew Quigley). The solubilised suspension was centrifuged at 40,000 RPM in the Ti-45 rotor for 1 hour at 4 °C to pellet any insoluble material. The supernatant was then incubated with loose resin, either Ni^{2+} bound chelating metal affinity resin, or TALON metal affinity resin (Co^{2+} metal ions (Clontech)).

2.5 Protein Purification

2.5.1 Purification of Class A PBPs

E. coli PBP1A was purified loosely based on the protocol in Born *et al.*, 2006, with minor optimisation. After solubilisation in detergent (e.g. TritonX-100 or CHAPS) and removal of unwanted insoluble material by centrifugation (section 2.4.6), the solubilised fraction was incubated with loose Ni^{2+}-bound chelating metal affinity resin for 1 hour on rollers at 4 °C. The slurry was poured in to an empty syringe barrel, used as a column. The resin was washed with 2x 40 mL of buffer with 5 mM imidazole. 5 mL aliquots of increasing imidazole concentration were made: 20 mM, 50 mM, 100 mM, 150 mM, 200 mM, 250 mM, 300 mM, 350 mM, 400 mM, 450 mM, 500 mM to elute the protein over a 50 mL gradient. Samples of each were run on 10% SDS-PAGE for analysis (section 2.6.1).

2.5.2 Immobilised-Metal-Affinity Chromatography (IMAC)

The protein has a hexa-His tag on its N-terminal, which readily binds to nickel metal

resin. The solubilized protein was incubated with the resin, rocking at 4 °C for 1 hour. The resin was transferred to the column and washed with 10 x 5 mL of extraction buffer + 15 mM imidizole, followed by elution with 3 x 5 mL of extraction buffer + 400 mM imidazole. The eluted fractions were dialysed multiple times before cleaving the his-tag with 2U / mL of thrombin. The protein was dialysed into a low-salt and low pH buffer (10 mM sodium acetate pH 5.0, 10 mM $MgCl_2$, 0.02% NaN_3, 10% glycerol, 100 mM NaCl) ready to for loading on to the Source S column on the AKTA. The jump in buffer pH from pH 7.5 to pH 5.0 is important relative to the pI (isoelectric point) of the protein, to ensure that the protein is negatively charged for binding to the Ni^{2+} beads.

2.5.3 Ion Exchange Chromatography: Source S Column

The protein was loaded onto the column and any contaminating proteins were washed away with 10 column volumes of Buffer A (10 mM sodium acetate pH 5.0, 10 mM $MgCl_2$, 0.02 % NaN_3, 10 % glycerol, 100 mM NaCl, 0.2 % TritonX-100). The protein was eluted at a flow rate of 1 mL / minute, over a 65 mL continuous gradient from 100 % Buffer A to 100 % Buffer B (10 mM sodium acetate pH 5.0, 10 mM $MgCl_2$, 0.02 % NaN_3, 10% glycerol, 2 M NaCl, 0.2 % TritonX-100). Eluted protein was dialysed into the appropriate buffer for long-term storage (10 mM soodium acetate pH 5.0, 10 mM $MgCl_2$, 0.02% NaN_3, 10% glycerol, 500 mM NaCl, 0.2 % TritonX-100) and stored at -80 °C in 50 µL aliquots.

2.6 Protein Analysis and Detection

2.6.1 SDS-PAGE

SDS-PAGE employs a multi-phasic buffer system with differing pH to cause separation according to molecular weight. The samples are loaded into very narrow starting zones, which along with the discontinuities, determines the subsequent sharpness of the separations and is responsible for the very high resolving power of the multi-phasic buffer system. The advantage of this system is that large volumes of dilute protein samples can be applied to the gel without loss of resolution of their component polypeptides. The pH of the Tris.HCl buffer used in the stacking gel has a different pH to the Tris.HCl buffer used in the resolving gel, which have been specifically selected

so that the proteins migrate at a pace between that of the leading Cl- ions and of the trailing glycinate ions. When the current is applied, a boundary is formed where the proteins collect in the stacking gel and then move according to molecular mass in the resolving gel. Lots of negatively charged SDS molecules bind to the hydrophobic regions of proteins, disrupting non-covalent bonds and cause unfolding. The intrinsic charge of the protein is masked, causing them to migrate to the cathode when the voltage is applied. Sample preparation involved measuring the protein concentration of each sample using Bio-Rad, to quantify against a standard curve, so as to set up samples with 25 μg of protein. If too much protein is loaded onto a gel, it can smear and individual bands are hard to define. For volumes of substances to make up the resolving and stacking gels, refer to tables in Appendix. Gels were run at 180 Volts for 50 minutes.

2.6.2 Western Blotting

Western blotting procedures have been optimised to reduce background and decrease experiment time, using the method outlined here.

SDS-PAGE, Transfer and Overnight Block

Proteins were resolved by SDS-PAGE (10% acrylamide for HMW proteins) or Native PAGE against either High Molecular Weight Calibration Standards (Amersham) or His-tagged protein markers (Benchmark or MagicMark XP, Invitrogen) and the resulting gel was washed in transfer buffer (Transfer Buffer (1L) 5.8 g Tris base, 2.9g glycine, 200 mL MeOH, 0.05% SDS (500 mgs) (for membrane proteins and those > 80 kDa). Polypeptides were transferred from the gel to a PVDF membrane (Hybond-P, GE Healthcare) at a constant voltage of 120V in transfer buffer for 90 minutes, using a BioRad electroblotting kit. Before transfer, the membrane was activated by placing in methanol for 5-10mins, washing with deionised water then adding to transfer buffer for 2mins. After transfer, membranes were blocked in 50mL of 10% Milk powder in TBS containing 0.1% Tween-20 (TBST-T) and rocked for 1 hour at room temperature before being left stationary (but rocked if possible) in the cold room O/N.

Antibody Incubations

Wash the milk away with 50mL of TBS-T for 15min. The TBS-T wash step was repeated twice more. Primary Incubation: 20mL of TBS-Tween containing 5% milk, add 20µL of anti-his IgG mouse monoclonal antibody (Roche - binds to either His terminus) or 8µl anti-His IgG mouse monoclonal (N-terminal preferential antibody – Sigma H1029), and leave to shake for one hour. Follow with three 20mL TBS-T wash steps of 15 mins each. Secondary Incubation: 20mL of TBS-T containing 5% milk, add 10µl of anti-mouse IgG conjugated to horseradish peroxidase derived from sheep (Sigma, A5906) was added and left to shake for two hours before three further TBS-T wash steps. For the final wash step, membranes were left to rock overnight at RT to reduce the background of unbound proteins.

Development

For developing – in the dark room, 5mL of western blotting reagent 1 (GE Healthcare) and 5mL of western blotting reagent 2 (GE Healthcare), or more recently – 2 mL of EZ-ECL Solution A and 2 mL Solution B were added to the membrane and allowed to develop for 2 minutes (preferably in the dark). The developed membrane was held by tweezers to drip excess developing solution onto a tissue, and placed is a cassette lined with cling-film. Exposure time to x-ray films (Super-RX NIF, Fujifilm) varied from 30 seconds and 5 minutes, but sometimes up to 30 minutes. Observed bands resulted from electrochemical luminescence (ECL) from proteins embedded in the membrane. Latterly, instead of developing using Fuji Film, a chemi-illuminescence detector was used to analyse the Western Blot PVDF Membrane.

2.6.3 Protein Concentration Determination

2.6.3.1 BioRad Assay

The BioRad assay was used to measure the protein concentration of soluble protein samples of unknown concentration and was carried out as described by the BioRad protocol. The concentrated BioRad reagent was diluted 1 in 5 with ddH_2O and 1 mL aliquoted in to plastic cuvettes. A standard curve was performed on each occasion,

using the sample volume of the protein sample of unknown concentration added as Bovine Serine Albumin (BSA), typically 1.5 µL. Each cuvette was inverted 3 times using parafilm as a cuvette 'lid', before measuring the absorbance at 595 nm. Protein samples were done in triplicate.

2.6.3.2 BCA Assay

A BCA (bicinchoninic acid) assay was used to measure the protein concentration of membrane protein samples of unknown concentration and was carried out as described by the Pierce protocol. BSA protein standards were made in 0.25 mg/mL increments from 0 to 2 mg/mL BSA. Reagents A and B were mixed at a 50:1 ratio, a volume sufficient for 9 x BSA standards plus the number of samples to test in triplicate). 1 mL of mixed BCA reagents was aliquoted into plastic cuvettes. 2 µL of each BSA standard was added to a cuvette, along with 2 µL protein sample of unknown concentration, always done in triplicate. Addition of protein samples was done accurately but with haste, as the colour change of the BCA reagents once mixed together, is time (and temperature) dependent. Parafilm was secured over the top off a cuvette and the cuvette was inverted three times to mix the protein sample with the reagent. Reactions were left to incubate at 37 °C in a static incubator for exactly 30 minutes. Absorbancies were measured against a blank (1 mL BCA A+B, + 2 µL water, i.e. 0 mg/mL BSA) at 562 nm using a using a Jenway 6306 UV-visible spectrophotometer. Protein concentrations were calculated based upon the standard curve. The working range for the assay is between 20 and 2000 µg/mL.

2.7 Compound Synthesis

2.7.1 UDP-Mur*N*Ac-Pentapeptide Synthesis

Method adapted from Lloyd *et al.* (2008). 2 mL reaction volumes were used containing 50 mM HEPES pH 7.5, 10 mM $MgCl_2$, 200 mM PEP, 50 mM KCl, 10 mM dithiothreitol, 10 mM UDP-Glc*N*Ac, 30 mM L-Ala, 30 mM D-Glu (or 100 mM D-Gln), 30 mM L-Lys, 30 mM D-Alanyl-D-Ala, 200 µM NADPH, 6 mM ATP, 25 mM isocitrate, 40 units isocitrate dehydrogenase (Sigma-Aldrich), 500 units of pyruvate kinase (Sigma-Aldrich), 300 µg MurA, 2000 µg MurB, 750 µg MurC, 1000 µg MurD,

1250 µg MurE and 1500 µg MurF. The synthesis was incubated at 37 °C overnight, before dilution with 5 mL sterile water, and filtration with a Vivaspin® centrifugal concentrator (10 kDa cut-off) to remove proteins. Non-canonical pentapeptides such as UDP-Mur*NA*c-L-Ala-γ-D-Glu-*meso*DAP-D-AzaTrp-D-Ala and UDP-Mur*NA*c-L-Ala-γ-D-Glu-*meso*DAP-D-Trp-D-Ala were synthesised in the same way as described here, with extra MurF, as the terminal dipeptides were synthesised prior to incorporation in to the pentapeptide by MurF.

2.7.2 UDP-Mur*N*Ac Pentapeptide Purification

20 mg of UDP-Mur*N*Ac pentapeptide (L-Ala-D-Glu-*meso*DAP-D-Ala-D-Ala) was desalted on the Source 30Q column with Buffer A 10 mM Sodium Bicarbonate pH 9.0, Buffer B 250 mM Sodium Bicarbonate. 2 mL fractions were collected. A Nessler's reagent test was conducted on the first and final fraction of the peak to test the amount of ammonium remaining in the eluted pentapeptide intermediate after the de-salting process. 500 µL of the sample to be tested was added to 500 µL of Nessler's reagent and the absorbance at A_{425nm} was measured after mixing. The obtained values were compared against a standard curve. Both fractions had the same absorbance reading and contained small traces of ammonium. Fractions of the major peak were pooled and the yield of purified pentapeptide was quantified (section 2.7.3) as 4.5 mgs. Purified pentapeptide can be converted in to LII, or can be labelled with a fluorophore prior to lipid synthesis.

2.7.3 Pentapeptide Quantification

The concentration of UDP-Mur*N*Ac-pentapeptide synthesised was calculated by measuring the absorbance of the solution at 260 nm using a Jenway 6306 UV-visible spectrophotometer, where the uracil moiety of the pentapeptide has an extinction coefficient of 10,000 $M^{-1}cm^{-1}$.

2.7.4 Labelling UDP-Mur*N*Ac-L-Ala-D-Glu-*meso*DAP-D-Ala-D-Ala with Fluorescamine

A 42-fold molar excess of fluorescamine (53 mgs) was dissolved in acetone (an equal volume to the pooled fractions of pentapeptide) and added to the pentapeptide for labeling at room temperature overnight with a magnetic stirrer in a round-bottomed flask, covered in foil. The acetone was removed fully by rotary evaporation and the reaction was neutralized with Tris.HCl pH 9.0. A 500 µL sample was injected onto a 1 mL Q-Sepharose column, and eluted over a 20 mL gradient from 10 mM to 1 M ammonium acetate pH 7.6 collecting 1 mL fractions. Each eluted peak was freeze-dried separately. The exact mass of UDP-Mur*NA*c-L-Ala-D-Glu-(N^{ε}-Fluorescamine)-*meso*DAP-D-Ala-D-Ala is 1472.43 and the molecular weight = 1473.24 Da.

2.7.5 Pentapeptide Dansylation: UDP-*N*-actylmuramyl-L-Ala-γ-D-Glu-(N^{ε}-dansyl)-*meso*DAP-D-Ala-D-Ala (Dansyl-labelled UDP-Mur*NA*c-pentapeptide)

A Source 30Q column (26 x 120 mm) on an AKTApurifier 10 was used to purify UDP-Mur*N*Ac-pentapeptide by anion exchange chromatography. Following purification, all ammonium acetate was removed before labelling with dansyl chloride by passing it through a Superdex Peptide column in sodium bicarbonate. The presence of any ammonium prevents access to the ε-amine group on the DAP of the pentapeptide and can discourage dansyl labelling. The removal of ammonium acetate is important to allow successful dansylation. After desalting, the pentapeptide was quantified and incubated for one hour in the dark with a 42 molar excess of dansyl chloride. The reaction was set up in a round-bottomed flask with a magnetic stirrer, in the dark, at room temperature, with dansyl chloride dissolved in an equal volume of acetone as pentapeptide. The dansyl group reacts instantaneously with the ε-amine group of the DAP. After one hour of incubation, the acetone was removed by rotary evaporation.

To separate the desired dansylated-pentapeptide from any unlabelled pentapeptide and unreacted dansyl chloride, the product was first centrifuged to remove any insoluble, precipitated material. The supernatant was purified by gel filtration on a Sephadex G25 column (80 × 3 cm), using a peristaltic pump and water as the solvent, at a flow-rate of 1 mL/min, collecting 5 mL fractions. The entire column and collection tubes were covered in foil to purify the labelled-pentapeptide in the dark. Labelled-pentapeptide eluted from the column first as it is the largest compound, closely followed by un-labelled pentapeptide. Unreacted dansyl chloride (dansic acid) eluted last as it is

smaller. The absorbance of the eluted fractions was measured at 340 nm, the excitation wavelength of the dansyl group. Fractions containing the labelled-pentapeptide were lyophilized over-night. The powder was dissolved in water to 1 mg/mL stock solution. Mass spectrometry was performed to confirm synthesis of the labelled compound.

2.7.6 Removal of the UDP Group from UDP-Pentapeptides

0.1 M HCl was added to the pentapeptide carefully until pH 1.0 was achieved and boiled at 99 °C for 30 minutes to destabilise the phosphodiester linkage between the UDP-group and the pentapeptide. The sample was neutralised to pH 7.5 with NaOH.

2.7.7 The Synthesis of Lipid II

The method of preparation was based upon that published (Breukink *et al*., 2003). To make LII, 4.8 μmol undecaprenyl phosphate (Larodan) was dried down under a stream of nitrogen gas before being resolubilised in a buffer with detergent. The buffer contained 50 mM HEPES (pH 7.6), 1 mM $MgCl_2$ and 1 % TritonX-100 (w/v). To this, 48 μmol UDP-Glc*N*Ac and 12 μmol UDP-Mur*N*Ac pentapeptide was added, for a final volume of 2 mL. The final component was *M. flavus* membrane vesicles (to a final membrane protein amount of 10.5 mg). This mixture was gently mixed at room temperature for 3 hours. Following incubation, the reaction was stopped with 3.5 mL 6 M pyridine acetate (pH 4.2) and the synthesised lipids extracted into 3.5 mL solvent (*n*-butanol). This was centrifuged at 4,500 g for 10 minutes and the top phase (*n*-butanol) extracted and mixed with an equal volume of water, before centrifugation, as before. The top phase was taken, the solvents evaporated and stored at -80 °C until purification.

2.7.8 The Purification of Lipid II

The synthesised lipids were purified by anion exchange, using a DEAE Sephacel column. A 20 mL glass pipette was used, with a glass wool plug at the bottom and filled with 3 mL of DEAE Sephacel resin. The resin was charged with 5 CV of 1 M ammonium acetate, then washed with 5 CV water. The running solvent was a mixture of chloroform, methanol and water (in the ratio 2:3:1), and the eluting solvent was the same but with ammonium bicarbonate added. The dried lipid sample was resuspended

in 6 mL of the running solvent. The resin was equilibrated with 10 CV of the running solvent and the resuspended lipids were loaded. The column was developed through 4 CV washes of the running solvent, with incremental increases in ammonium bicarbonate additive, from 0 mM - 300 mM in 50 mM steps, with a further 500 mM and 1000 mM wash. All of the wash and the loading flow-through samples were collected in glass vials and analysed by TLC (section 2.7.9). Samples containing the lipid of interest were combined and dried down by rotary evaporation and freeze-drying.

2.7.9 Thin Layer Chromatography

Samples of the LII purification elutions were analysed by TLC. 1.5 mL of eluted samples were dried down in a dessicator. The dried samples were resuspended in 20 µL of running solution. The running solvent was a mixture of chloroform, methanol, water and ammonia (in the ratio of 88:48:10:1). A TLC silica plate was prepared by pencil marking a line 1.5 cm from one end with spots 2 cm apart along its length. Lipid samples were carefully loaded in 2 µL aliquots and dried between loadings to maintain small spot sizes. The running solvent was added to a glass TLC tank to a depth of 1 cm and the dried TLC plate was added and developed at room temperature. The plate was removed when the solvent reached a few cm from the top and the plate was placed in an iodine vapour chamber until stained. Once stained, an image of the plate was promptly taken by camera or scanner as iodine staining is not permanent.

2.7.10 Lipid II Quantification

A 50 µL lipid samples and 50 µL chloroform/methanol/water 2:3:1 (v/v) were dried down and resuspended in 50 µL 50 mM HEPES, 10 mM $MgCl_2$, 30 mM KCl, 1.5 % (w/v) CHAPS, pH 7.6. One of the lipid samples and the blank were treated with: 50 µL 1 M HCl, boiled for 30 min, centrifuged at 3,000 x g for 5 min, and readjusted to pH 7.6. The inorganic phosphate hydrolysed from the lipids was quantified using a phosphate release assay. The phosphate release assay contained 50 mM HEPES, pH 7.6, 10 mM $MgCl_2$, 200 µM MESG, 1U PNP and 1 unit inorganic pyrophosphatase (IPP). The absorbance was monitored at 360 nm before addition of 10 µL lipid sample. The concentration of the lipid was calculated from the amount of phosphate released from the acid-hydrolysed lipid compared to the blank sample. The extinction coefficient of

the change in absorbance at A_{360nm} by 1 M P_i is 10,000 $M^{-1}cm^{-1}$ caused by the phosphorolysis of MESG.

2.7.11 Preparing Samples for Mass Spectrometry

50 µL samples were prepared for mass spectrometry, using 50 % acetonitrile and 50 % ddH_2O. Mass estimates were obtained by negative ion electrospray ionisation mass spectrometry (ESI-MS), either in the Chemistry Department facility or by Dr. Adrian Lloyd in Life Sciences.

2.8 Enzyme Activity Assays

2.8.1 Tris-Tricine Polyacrylamide Gel System

Assays of a 15 µL volume were set up to assay the transglycosylase activity of purified E. coli PBP1B. In most cases, 65 µM LII and 65 µM Dansylated LII were mixed together in a glass vile and the solvents (Chloroform and Methanol) in which the Lipid are dissolved were evaporated by N_2 gas. The dried LII wasresuspended in the appropriate volume of assay buffer to result in the total final concentration of 130 µM LII (65 µM Dansylated and 65 µM non-dansylated) in each 15 µL assay. The optimized assay buffer is 10 mM HEPES pH 7.5, 3 mM MgCl2, 150 mM NaCl, 0.18% TritonX-100. 2.3 mM Penicillin G was also added to inhibit any transpeptidase activity. 6 µM *E. coli* PBP1B was added to each assay and was the final component to be added before being gently mixed by pipetting. Reactions were left at 37 °C for 45 minutes before terminating the reaction at 60 °C for 10 minutes. Samples were centrifuged at 13,000 RPM for 5 minutes to pellet all protein in the assay. The supernatant was transferred to new tubes for avoid loading any protein on 14 to the gel. Loading buffer (100 mM Tris.HCl pH 8.8, 4% SDS, 40% glycerol) was added to each sample.

This gel system was first used and published by Schagger & von Jagow in 1987 and has more recently been used by Susanne Walker's lab (Barrett *et al*., 2007) and Thierry Vernet and Andre Zapun (Hellassa *et al.,* 2012). A 37.5 part acrylamide : 1 part bisacrylamide stock is used to achieve the correct final acrylamide percentages (9 % acrylamide, 2.6 % cross-linker) to separate the glycan lipid chains. No stacking gel is

required and the comb is inserted directing into the resolving gel. A blank sample is loaded into one of the lanes to monitor the electrophoresis progress, which consists of assay buffer, loading buffer and bromo-phenol blue. Bromophenol blue is not used in any of the assay samples as the dye can interfere with their separation and resolution. This gel system involves a dual buffer system, which is non-continuous. Anode buffer: 0.1 M Tris.HCl pH 8.8, Cathode buffer: 0.1 M Tris.HCl pH 8.25, 0.1 M Tricine, 0.1 % SDS. Gels are run at 110 Volts, 50 mAmps, for 1 hour. Gels are imaged under UV light and the dansylated LII is visible.

2.8.2 BOCILLIN Assay

Fluorescently labelled penicillin with BODIPY, commonly referred to as BOCILLIN FL can bind to the transpeptidase domain of PBPs. A 3 x molar ratio of BOCILLIN-FL to PBP was incubated at 37 °C in the dark for 1 hour. Protein loading dye was added to the sample, but they were not heat-denatured before analysis by SDS-PAGE. Results were visualised in the GelDoc (Syngene) using a short pass (SP) Y520 filter. Adjusting the histogram, to avoid capturing a saturated image, amended over-exposure and saturation. Densitometry could then we used to more quantitatively compare intensity and binding.

2.8.3 A Continuous Fluorescence Assay for Transglycosylase Activity

An assay was developed by Schwartz *et al.* in 2002, in which the transglycosylase activity of *E. coli* PBP1B is monitored continuously. This assay may also be suitable for other bifunctional PBPs. The principle behind the assay involves *N*-acetyl-Muramidase which breaks down polymers of LII that have been polymerized by PBP. The dansyl fluorophore attached to position 3 of the pentapeptide (*meso*DAP) in LII is released from a lipidic to an aqueous environment upon the breakdown of polymers into monomers by *N*-acetyl-Muramidase. This change in environment surrounding the fluorophore results in a decrease in fluorescence, indirectly representing the polymerisation of LII. The assay has been developed and adapted for use in a plate reader in 25 uL, to allow the potential for more high-throughput screening. All assays in the plate reader are carried out in 96-well, black, fluorescence compatible, NUNC plates, with excitation and emission of dansyl 340 and 520 nm. All assays were

conducted at 30 °C and specific buffers used are given in each case in the figure legend.

2.8.4 The Spectrophotometric Phosphate Release Assay for Transglycosylase Activity

This assay is a phosphate (P_i) release assay based on the dephosphorylation of the by-product of transglycosylation, undecaprenyl pyrophosphate (C_{55}-PP), by PgpB. In the presence of free inorganic phosphate, PNP (purine-nucleoside phosphorylase) converts MESG (absorbance maximum at 330 nm) to ribose-1-phosphate and 7-methyl-6-guanine (absorbance maximum at 355 nm). Inorganic phosphate consumption is proportional to the formation of 2-amino-6-mercapto-7-methylpurine, which has a peak absorbance wavelength of 355 nm. As there is minimal background absorbance at 355 nm from un-reacted substrate, the formation of reaction products can be followed by an increase at this wavelength. The concentration of LII input in to the polymerisation is directly proportional to the amount of undecaprenyl pyrophosphate (C_{55}-PP) formation (assuming polymerisation went to completion), which is proportional to the amount of free phosphate generated from dephosphorylation of C_{55}-PP by PgpB.

Discontinuous LII Polymerisation Assay

The polymerisation of Lipid II was set up in a 0.5 mL Eppendorf, to a final volume of 15 uL. The desired concentration of DAP/Lys LII (usually was dried down in a 0.5 mL Eppendorf with a gentle stream of N_2 gas. The LII was resuspended in 5 µL of 0.1% of DDM by vortex and a short spin in a microcentrifuge. 3 µL of 5x polymerisation assay buffer (100 mM Tris.HCl pH 7.6, 50 mM $MgCl_2$) is added to the LII substrate. The of *E. coli* PBP is added last, made up to 15 µL with *Ec*PgpB storage buffer. The polymerisation is placed in a PCR machine pre-set to 30 °C for up to 1 hour (or completion of polymerisation). Polymerisation is terminated by heating to 60 °C for 10 minutes, the heat-inactivated enzyme precipitates and is spun down in a microcentrifuge for 5 minutes. The soluble products in the supernatant (14 µL, including undecaprenyl pyrophosphate transglycosylation by-product) are transferred to a quartz cuvette containing the components for the continuous phosphate detection assay in the Spectrophotometer.

Continuous Inorganic Phosphate Detection Assay

Upon incorporation of a LII monomer in to a growing glycan chain through the enzymatic activity of a transglycosylase enzyme, the polyprenyl lipid tail (undecaprenyl pyrophosphate, UPP) is cleaved and released as a by-product. The outer-most phosphate on UPP can be cleaved by a phosphatase (e.g. PgpB) and quantified spectrophotometrically. A quartz cuvette comprised of 5 x assay buffer (100 mM Tris.HCl pH 7.6, 50 mM $MgCl_2$), 600 μM MESG, 0.4 Units PNP, up to 20 μL PBP, made up to 20 μL with *Ec*PgpB enzyme storage buffer (20 mM Tris.HCl pH 7.5, 1 mM $MgCl_2$, 2 mM BME, 0.5 M NaCl, 10 % glycerol, 0.5 mM (3 x CMC) DDM) and finally 14 μL of the discontinuous polymerisation. The absorbance was measured at A_{355nm} at 37 °C for 10-30 minutes. The spectrophotometric PNP/MESG coupling system used in this assay is illustrated in Figure 5.1.

2.8.5 Continuous Spectrophotometric Assay for D-Alanine Release

An assay used to discriminate between the two peaks involved D-amino acid oxidase, Horse Radish Peroxidase (HRP) and Amplex red. As this assay is selective for D-amino acids only, one peak should show activity and the other peak should not. The principle behind the assay is that in the presence of D-Amino Acid Oxidase (DAAO) enzyme, the D amino acid (D-azatryptophan) is deaminated, releasing the by-products ammonia and hydrogen peroxide. In the presence of HRP, hydrogen peroxide is reduced to oxygen, which breaks down Amplex red and causes a colour change, detected at a maximum of A_{555nm}. Assays were performed in a Cary 100 Spectrophotometer (Varian) at 37 °C.

2.8.6 The Continuous Transpeptidase Spectrophotometric Assay

To measure the transpeptidase activity of Penicillin-Binding Proteins, 50 mM BisTrisPropane pH 8.5, 20 mM MgCl2, 0.1% TritonX-100, 10 mM (or 50 uM) Amplex Red, 3.5 Units DAAO, 5.8 U HRP, 0.008 mgs *E. coli* LpoB, donor: 20 mM Lys-LII in 0.1% TritonX-100. A baseline reading was measured for a few minutes, before adding the PBP and finally the acceptor: 20 uM Mur*N*Ac pentapeptide. The assay was monitored at 555 nm, at 30degC, for 30-40 minutes.

2.8.7 MurF Assay for Dipeptide Incorporation

5 x assay buffer, 1 mM DTT, 0.2 mM NADH, 2 mM PEP, 1 mM ATP, 1 uL MurF, 1 uL, Pyruvate kinase lactate dehydrogenase, 1 uL UDP MurNAc tripeptide, 1 mM dipeptide, 1 mM ATP. 1mM of the Dazatryp dipeptide was sufficient to do kinetics with and do the synthesis with. *Sp*MurF was better for the azaTryp dipeptide. The assay was conducted by initiating the reaction with *Pa*MurF, ATP, and the dipeptide of interest for incorporation.

2.8.8 D-Ala-D-X Ligase (VanA) Assay

To determine whether the D-Ala-D-X ligase VanA, would incorporate D-tryptophan or D-azatryptophan in to the second subsite of the dipeptide formed, a continuous, coupled, spectrophotometric assay was used to test the axtivity of VanA (Daib, 1988). In the presence of ATP, VanA normally ligates D-Ala to D-Lactate. Upon the activity of VanA, ATP is hydrolysed forming ADP + P_i. In the presence of pyruvate kinase, PEP is converted to pyruvate, which is subsequently converted to lactate in the presence of lactate dehydrogenase. NADH is concurrently oxidised to NAD^+. This oxidation is observed as a reduction in absorbance at 340 nm.

2.9 Techniques for Protein Structure Analysis

2.9.1 Circular Dichroism Spectroscopy

Circular dichroism is a technique that can be used to determine protein secondary structure in solution and the extent of α-helicity, β-sheet and random coil. Circular dichroism is defined as the difference in absorption of left and right circularly polarized light (Correa & Ramos, 2009). When plane polarized light enters a chiral molecule it is resolved into two perpendicular vibrating waves that propagate at different velocities. Circular dichroism can be measured by the difference in absorbance of the material for circularly polarized light, ΔA, where $\Delta A = (A_L - A_R)$. This difference in absorption is easily converted to ellipticity units, θ, and typically spectra are generated by the CD spectropolarimeter as a function of θ (in millidegrees) against wavelength (nm). Millidegree units are converted into standard Mean Residue Ellipticity (MRE) units

(mdeg cm_2 $dmol_{-1}$), which incorporate mean residue weight, protein concentration in mg/mL, path length in cm and amino acid sequence length.

CD spectra were measured using a Jasco 815 spectropolarimeter at room temperature and using a 1.0 mm path-length quartz *circular* cuvette, roughly the size and shape of a £1 coin. All spectra were recorded at room temperature between 190-260 nm, using a data pitch of 0.2 nm, bandwidth of 2 nm, scanning speed of 100 nm/min, response time of 1 second, and either 16 or 32 accumulations. Specific protein concentrations buffers used are given in the text.

2.9.2 Protein Crystallisation

Sparse matrix screening was trialled with PBP1A proteins, including the commercially available MemStart and MemGold, in which conditions have been optimised for membrane proteins. Sitting drop crystal trays were set up with 100 µL precipitant per reservoir at 18 °C. 200 nL protein mixed with 200 nL precipitant using the Mosquito robot and trays checked after 24 and 48 hours initially.

Chapter 3

The Cloning, Expression and Purification of PBPs and their Associated Proteins

3.1 Introduction

The cloning, expression and purification of a vast array of Class A PBPs along with their associated proteins was pivotal to the success of this project. This chapter outlines the groundwork in put to achieve a wide plethora of proteins available to assay in the following chapters.

3.2 Experimental Aims

- Clone, express and purify Class A PBP genes along with the associated proteins for high-through-put expression
- Optimise protein expression levels
- Screen for the optimal detergent(s) for extraction and purification of membranous and membrane-associated proteins
- Purify the proteins to homogeneity / monodispersity
- Conduct initial X-ray crystallography trials of Class A PBPs

3.3 The Cloning, Expression and Purification of PBPs

A list of all the DNA constructs used in this body of work are described in **Table 3.1**.

Table 3.1 A Comprehensive Library of all PBP and PBP-associated DNA Constructs used Throughout this Project

Construct	Protein Fragment	Tag (Protease)	Restrict^{n} Sites	Anti biotic Select^{n}	Cloned by
***E. coli* PBP1A**					
pET28::*Ec pbp1a*	Full-length 1-850	N-term His (Thrombin)	*NdeI / NotI*	Kan	Amy O'Reilly
pET28::*Ec pbp1a* - E86Q	Full-length 1-850, with TG active site mutation E86Q	N-term His (Thrombin)	*NdeI / NotI*	Kan	Amy O'Reilly
pET28::*Ec pbp1a* - S473A	Full-length 1-850, with TP active site mutation S473A	N-term His (Thrombin)	*NdeI / NotI*	Kan	Amy O'Reilly
***E. coli* PBP1B**					
pET28(a)+:: *Ecpbp1b*	γ isoform: 'short'. Starts at M^{46} with an N-term extension of 6 amino acids: GSHMASM^{46}-N^{844}	N-term His (Thrombin)	*NheI / EcoRI*	Kan	pDML924 (Terrak *et al.*, 1999), Vollmer's group, Newcastle University, UK.
pET28(a)+:: *Ecpbp1b* - E233Q	with TG active site mutation E233Q	N-term His (Thrombin)	*NheI / EcoRI*	Kan	SDM of Newcastle PBP1B construct by Amy O'Reilly
pET28(a)+:: *Ecpbp1b* - S510A	with TP active site mutation S510A	N-term His (Thrombin)	*NheI / EcoRI*	Kan	SDM of Newcastle PBP1B construct by Amy O'Reilly
Vector::*Ec pbp1b* Δ106	*E. coli* PBP1B, missing everything before the UB2H domain begins at Y^{107}	??	??	??	Dr. David Roper, University of Warwick
***P. aeruginosa* PBP1A**					
pET28::*Pa pbp1a*	Full-length M^{1}-F^{822}	N-term His_6 (Thrombin)	*NdeI / NotI*	Kan	GenScript, *E. coli* codon-optimised
pET28::*Pa pbp1a* E86Q	Full-length M^{1}-F^{822} with TG active site mutation E86Q	N-term His_6 (Thrombin)	*NdeI / NotI*	Kan	SDM of Genscript construct by Amy O'Reilly
pET28::*Pa pbp1a* S461A	Full-length M^{1}-F^{822} with TG active site mutation S461A	N-term His_6 (Thrombin)	*NdeI / NotI*	Kan	SDM of Genscript construct by Amy O'Reilly
***P. aeruginosa* PBP1B**					
pET28:: *Pa pbp1b* Δ22	W^{23}-N^{774}	N-term His_6 (Thrombin)	*NdeI / NotI*	Kan	Amy O'Reilly
pET28:: *Pa pbp1b* Δ22 - E190Q	W^{23}-N^{774} with TG active site mutation E190Q	N-term His_6 (Thrombin)	*NdeI / NotI*	Kan	Amy O'Reilly

pET28:: *Pa pbp1b* Δ22 - S468A	W^{23}-N^{774} with TP active site mutation S468A	N-term His_6 (Thrombin)	*NdeI / NotI*	Kan	Amy O'Reilly
pIX1016::*Pa pbp1b* Δ22 *	W^{23}-N^{774} Plasmid for expression in *P. putida* cells	N-term His_6	*HindIII / XbaI*	gento mycin	Amy O'Reilly
Class B PBPs					
pSUMODave ::*Ecpbp2*	M^{1}-H^{633}, full-length	His SUMO (TEV)	*BamHI / XhoI*	Kan	Dr. Dean Rea, Roper Group, University of Warwick
pET52b::*Ec pbp3* Δ43	W^{44}-S^{588}, No TM domain	C-term His_{10} (Thrombin)	*BamHI / SacI*	Amp	Amy O'Reilly
pET52b::*Pa pbp3* - Δ34	A^{35}-G^{565}, No TM domain	C-term His_{10} (Thrombin)	*BamHI / SacI*	Amp	Amy O'Reilly
PBP-Associated Proteins					
pTrcHis6::*Ec pgpb*	M^{1}-S^{254}, Full length	C-term His_6	*NcoI / BglII*	Amp	Gift from Dr. T. Touzé, Université Paris-Sud
pAK147::*Ec cpob* Δ26 (pET21d)	Q^{27}-M^{263}, No TM domain	C-term His_6	*NcoI / XhoI*	Amp	Prof. Colin Kleanthous's group, University of Oxford
pProEx HTa ::*Pa ybgf*	M^{1}-R^{274}, full-length	N-term His_6 (TEV)	*NcoI / XhoI*	Amp	Genscript, *E. coli* codon-optimised
pET28b::*Ec ftsn*	M^{1}-G_{319}, full-length	C-term His_6 (Thrombin)	*NcoI / XhoI*	Kan	Dr. Dean Rea, Roper Group, University of Warwick
pET28d::*Ef* VanA	M^{1}-G^{343}, full length	N-term His_6 (Thrombin)	??	Kan	Dr. Sarah Baton, Roper Group, University of Warwick
pSUMODave ::*Ec lpoa* Δ27	G^{28}-S^{678}	His-SUMO (TEV)	*NcoI / XhoI*	Kan	Dr. Dean Rea, Roper Group, University of Warwick
pET28b::*Pa lpoa* Δ20	A^{21}-F^{604}, no TM domain	N-term His_6 (Thrombin)	*NdeI / NotI*	Kan	Amy O'Reilly
pProExHT::*Ec lpob* Δ21	G^{22}-Q^{213}	His (TEV)	*NcoI / XhoI*	Amp	Dr. Dean Rea, Roper Group, University of Warwick

* All constructs are for expression in *E. coli* except for pIX1016::*Pa*$PBP1B^{23\text{-}774}$, which expresses in *P. putida* cells.

3.3.1 The Cloning and Purification of *E. coli* PBP1A

The *Ec*PBP1A gene was amplified from *E. coli* chromosomal DNA by PCR **(Figure 3.1)**.

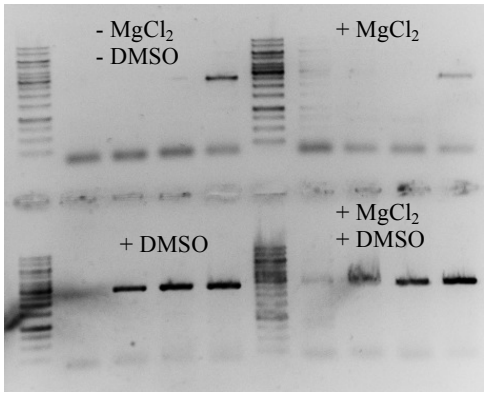

Figure 3.1 PCR Amplification of Full-length *E. coli* PBP1A. PCR products analysed by 1.0 % agarose gel. The four names in each section is an increase in annealing temperature from 50-60 °C. Expected size: 2.56 kb.

The PCR products were cleaned up and cloned in to the plasmid vector pET28 using the restriction digestion enzymes *NotI* and *NdeI* (Section 2.3.4). The pET28::*E. coli* PBP1A construct is the full length *E. coli* PBP1A protein with an N-terminal His_6-tag (93,636 kDa without the His_6-tag). This construct was expressed and purified according to section 2.3.4 and 2.5.1. After elution from Ni^{2+}-IMAC (**Figure 3.2a**), a second purification step by cation exchange using Sepharose S resin was employed to clean up the protein (**Figure 3.2b**).

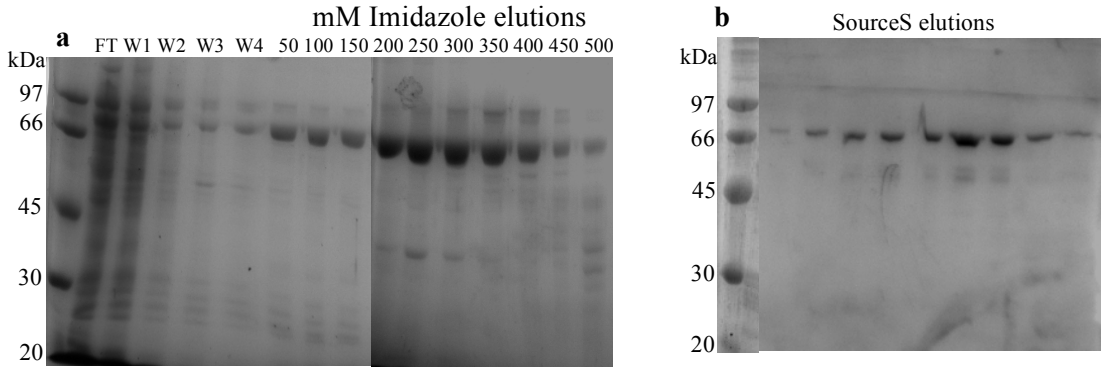

Figure 3.2 The Immobilised Metal Affinity Chromatography and Cation Exchange Purification of Full-length *E. coli* PBP1A. (a) 10% SDS-PAGE analysis of Ni^{2+}-IMAC elutions **(b)** 10% SDS-PAGE analysis of the subsequent Sepharose Q Ion Exchange purification. FT: Flow-through, W: wash

A second purification step was not always necessary after IMAC, but was employed on occasion if particularly clean protein was required, e.g. for X-ray crystallographic studies. 4 mg of pure protein per 750 mL of culture was routinely achieved.

3.3.2 The Purification of *E. coli* PBP1B

The pET28(a)+::*Ec*PBP1b construct was a kind gift from Waldemar Vollmer (Newcastle University, UK.) which is the γ-isoform, also known as 'short' (the α-isoform of *Ec*PBP1B is 46 amino acids longer than the γ-isoform). This construct starts at Met^{46} and has an N-terminal extension of 6 amino acids: GSHMAS M^{46}-N^{844} (89.48 kDa without the His_6-tag). This construct was expressed in BL21(λDE3) cells and purified according to sections 2.4.2 and 2.5.1 (**Figure 3.3**).

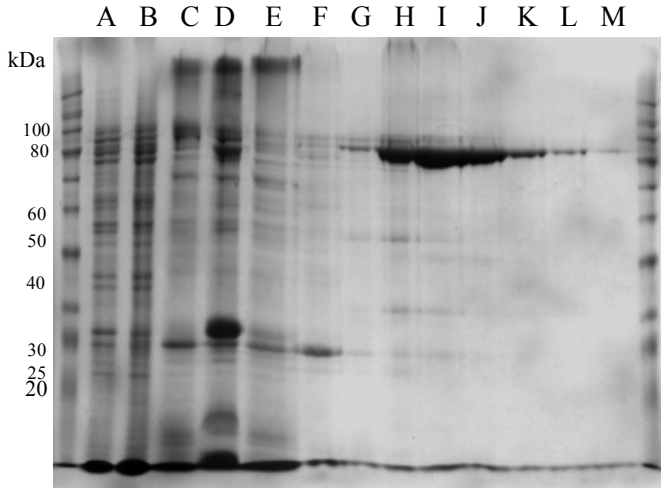

Figure 3.3 SDS-PAGE Analysis of the Purification of *E. coli* PBP1B M^{46}-N^{844}, by Ni^{2+} IMAC gravity flow column, at 4 °C. **A**: Crude extract (supernatant from 25,000g spin) **B**: Cytoplasm phase (supernatant from 40K RPM spin) **C**: After 1 hour solubilisation in TritonX-100 **D**: Soluble phase (supernatant after 44K RPM spin), incubated with Ni^{2+} resin) **E**: Flow-through **F**: Column wash **G**: 50 mM Elution **H**: 100 mM Elution **I**: 150 mM Elution **J**: 200 mM Elution **K**: 250 mM Elution **L**: 300 mM Elution **M**: 350 mM Elution.

In most cases, *E. coli* PBP1B was purified sufficiently enough after one pass through a Ni^{2+} column, as in Figure 3.3. The His_6-tag was cleaved by thrombin protease and purified by cation exchange using SourceS resin (Section 2.5.3). 3 mg of pure protein per 750 mL of culture was routinely achieved. A second purification step was rarely used, but if necessary, a pre-packed SourceS column would be used to clean up the protein further before cleavage of the His_6-tag with thrombin.

3.3.3 The Cloning and Purification of Full-length *P. aeruginosa* PBP1A

Pseudomonas aeruginosa PBP1a gene (gene locus PA5045) was amplified by PCR from genomic DNA (gDNA) using Phusion HF DNA polymerase under varying conditions (Section 2.3.1). The PCR products were a mixture of varying sizes, although the conditions with $MgCl_2$ only appeared to generate a PCR product of the correct size for *Pa*PBP1a (2.47 kb) (**Figure 3.4a**). Two fresh extractions of PA001 gDNA were purified from a mini-culture of *P. aeruginosa* PA001 using a Promega Wizard Genomic DNA Purification Kit and were tested as PCR template for *Pa*PBP1a amplification, using the PCR conditions with $MgCl_2$ (**Figure 3.4b**).

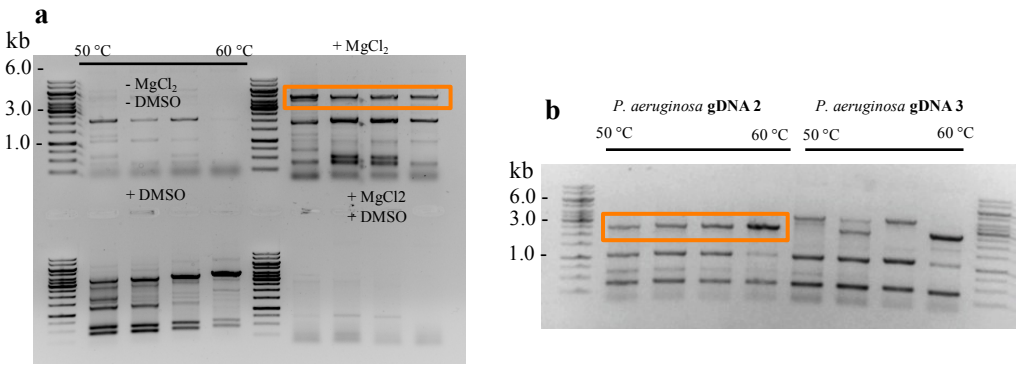

Figure 3.4 The Amplification of Full-length *P. aeruginosa* PBP1A by PCR. Analysed by 1.0 % agarose gel. **(a)** PCR in four different conditions, across an annealing temperature gradient (Section 2.3.1). **(b)** The most successful conditions from (a) were repeated with two new extracts of PA001 gDNA. *Pa*PBP1A gene = 2.47 kb).

The PCR products of *Pa*PBP1a were not clean and using fresh PA001 template did not alter the result. The four DNA bands highlighted in (a) were extracted with a scalpel and cleaned up using a Qiagen Gel Extraction Clean-Up Kit. A sample of the extracted PCR product was analysed on agarose gel to analyse its purity and size, before being cloned in to expression vector pET28b(+) using the restriction enzymes *NdeI* and *NotI*. After multiple attempts, the cloning of *Pa*PBP1a was unsuccessful and so full-length pET28b::*Pa*PBP1a was cloned by GenScript, using am *E. coli* codon-optimised synthetic gene. pET28b::*Pa*PBP1A was transformed in to the bacterial expression competent cells C43(λDE3) (Section 2.2.3) as this cell-line has been optimised for membrane protein expression and was the optimal cell line for *Pa*PBP1B after expression trials (section 2.4.3). *Pa*PBP1A was expressed according to Section 2.4.1 and purified by gravity flow IMAC **(Figure 3.5)** at 4 °C across a step-wise imidazole gradient.

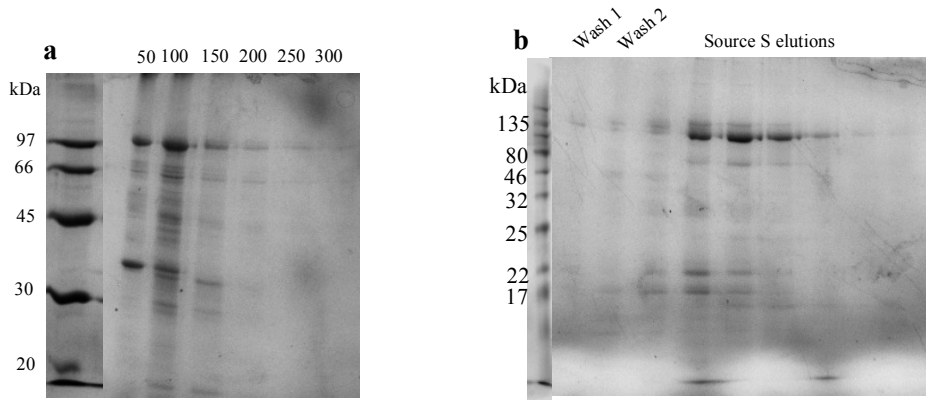

Figure 3.5 The Purification of pET28(b)::*Pa*PBP1A$^{1\text{-}822}$ by Ni^{2+} IMAC and SourceS Cation Exchange. (a) SDS-PAGE analysis of IMAC purification of *Pa*PBP1A, eluted with increasing concentrations of imidazole **(b)** After His_6-tag cleavage, the PBP was separated from it's His_6-tag and remaining Thrombin protease. *Pa*PBP1A = 91.2 kDa.

*Pa*PBP1A was purified to homogeneity in two steps of purification, before and after His_6-Tag cleavage. Purified *Pa*PBP1A was subsequently used in enzymatic assays in Chapters 4, 5 and 6 and X-ray crystallography trials later in this chapter.

3.3.4 Cloning *P. aeruginosa* PBP1B

The *Pa*PBP1B W^{23}-N^{774} gene was amplified by PCR using **(Figure 3.6a)** using the primers in Appendix 1. The amplified *Pa*PBP1B gene was cleaned up and it's purity analysed by agarose gel **(Figure 3.6b)**, alongside its destination vector. Upon cloning *Pa*PBP1b in to pET28b, the ligation reactions were transformed in to TOP10 competent cells (Section 2.2.3) and two colonies harboring the potential *Pa*PBP1b clone were cultured and the plasmid DNA extracted. Diagnostic PCR using Dream *Taq* DNA polymerase and T7 promoter and and reverse *Pa*PBP1B oligo amplified a gene product of the same size as *Pa pbp1b* (2256 bp) **(Figure 3.6c)**.

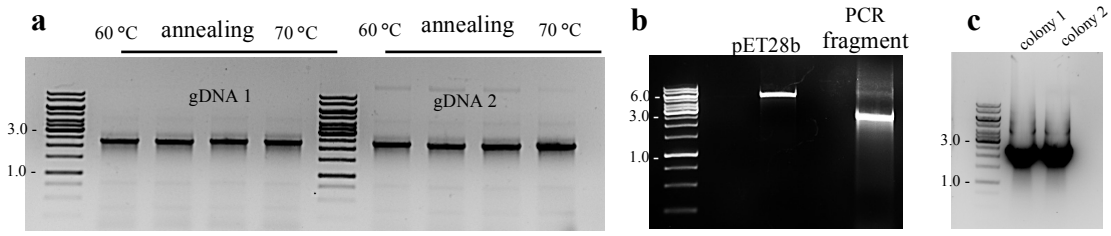

Figure 3.6 Amplification of *Pa*PBP1B W^{23}-N^{774} by PCR. (a) PCR using Accuprime *Taq* DNA polymerase (Invitrogen), with 4 μM $MgCl_2$ (including that in the PCR buffer) and 3 % DMSO, across a sliding temperature gradient from 60 - 70 °C during annealing. Two PA001 gDNA aliquots were used as template for amplification. The expected PCR fragment size = 2256 bp **(b)** The purified PCR product and destination vector pET28b analysed by 1.0 % agarose gel. **(c)** Diagnostic PCR of two colonies (TOP10 cells) potentially containing the pET28b::*Pa*PBP1b plasmid. Primers used for diagnostic PCR were the pET vector-specific T7 forward primer and the *Pa*PBP1B reverse primer initially used to amplify *Pa*PBP1B, the DNA polymerase used was Dream*Taq*.

*Pa*PBP1B W^{23}-N^{774} was successfully cloned into pET28b, which was tested for its optimum expression in a variety of cell lines, along with *Ec*PBP1B for direct comparison.

3.3.5 Expression Trials with *E. coli* PBP1B and *P. aeruginosa* PBP1B

Upon confirmation of the correct in-frame sequence, expression trials of *Ec*PBP1B and *Pa*PBP1B were done to identify the optimum bacterial cell line to express each protein (Section 2.4.3). Cells containing the expression plasmids were cultured with half being induced with IPTG and the other half remaining as an uninduced control. The isolated membrane fractions were analysed by SDS-PAGE and Western blot **(Figure 3.7).**

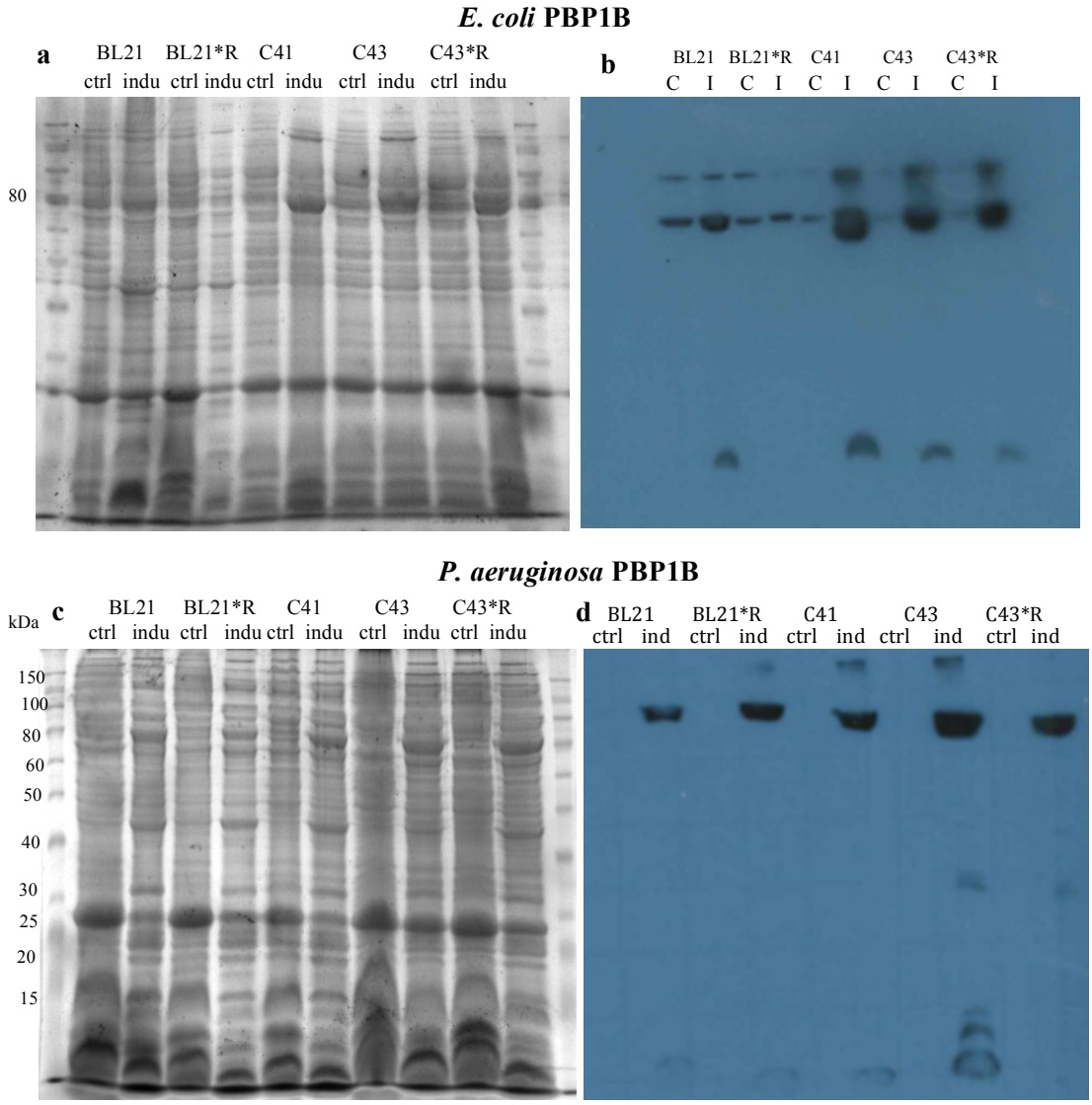

Figure 3.7 A Bacterial Cell-Line Expression Trial of *Pa*PBP1B and *Ec*PBP1B. The membrane fraction of IPTG-induced and non-induced cells were analysed by 10% SDS-PAGE and anti-His Western blot. Cells lines tested were BL21, BL21*R, C41, C43 and C43*R **(a)** *Ec*PBP1B membranes from each cell line analysed by 10% SDS-PAGE **(b)** *Ec*PBP1B membranes from each cell line analysed by anti-His Western blot **(c)** *Pa*PBP1B membranes from each cell line analysed by 10% SDS-PAGE **(d)** *Pa*PBP1B membranes from each cell line analysed by anti-His Western blot. C = non-induced control, I = induced to 1 mM IPTG upon reaching OD_{600} 0.7. *Ec*PBP1B = 89.48 kDa without the His_6-tag, *Pa*PBP1B = 83.05 kDa.

BL21(DE3) and BL21*R(DE3) cell lines did not express PBP1B as well as the BL21(DE3) derivative cell lines C41, C43 and C43*R (all DE3 lysogens). These cell lines are optimised for membrane protein expression (Miroux & Walker 1996). C43(DE3) was chosen for the expression of *Ec*PBP1B M^{46}-N^{844} and *Pa*PBP1B W^{23}-N^{774}. Upon selection of the optimum cell line, expressions at alternative temperatures and duration of expression were trialled **(Figure 3.8)**.

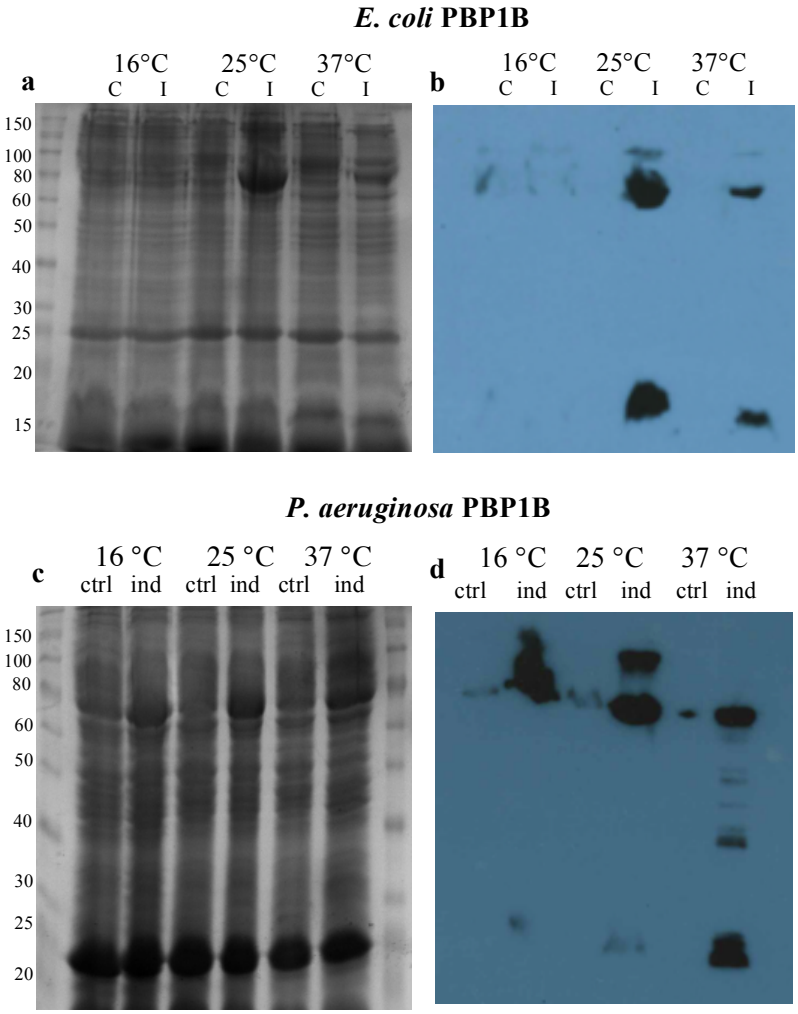

Figure 3.8 Expression Temperature Trials for *Ec*PBP1B and *Pa*PBP1B. The membrane fraction of IPTG-induced and non-induced cells were analysed by 10% SDS-PAGE and anti-His Western blot. Temperatures tested for optimum protein expression were 37 °C for 5 hours, 25 °C overnight and 16 °C overnight. **(a)** *Ec*PBP1B membranes from each cell line analysed by anti-His Western blot **(b)** *Ec*PBP1B membranes from each cell line analysed by anti-His Western blot **(c)** *Pa*PBP1B membranes from each cell line analysed by anti-His Western blot **(d)** *Pa*PBP1B membranes from each cell line analysed by anti-His Western blot. C = control, I = induced.

There was very little expression of either protein at 16 °C or 37 °C. Both *Ec*PBP1B and *Pa*PBP1B proteins were selected to be expressed for 18 hours overnight, at 25 °C to achieve optimal protein expression.

3.3.6 *P. aeruginosa* PBP1B Detergent Screen

A detergent screen of ionic, anionic and non-ionic detergents was conducted with *P. aeruginosa* PBP1B **(Figure 3.9)** to determine its solubility in different detergents and therefore which detergent would be preferable for maximum yield in further studies. The membrane fractions were isolated as in section 2.4.5, except on a smaller scale, using the benchtop Beckman T90K ultracentrifuge with the TLA 100.3 rotor and 2 mL samples instead of the large Ti45 rotor. Solubilisation was conducted as in section 2.4.6 at 5-fold the CMC of each detergent.

Figure 3.9 A Detergent Screen of *P. aeruginosa* PBP1B in a Variety of Ionic, Anionic and Non-Ionic Detergents. This screen highlights the extent to which each detergent solubilizes *Pa*PBP1B, visualised by anti-His Western blot. Soluble and insoluble fractions of *Pa*PBP1B are shown.

TritonX-100 had the best solubilizing ability by far and is the detergent most commonly used in the literature to extract and solubilise Class A PBPs as well as for use in PBP assays. If needed, the protein could be extracted in an alternative detergent that is more compatible with the technique intended for the specific use of the protein e.g. DM does solubilise *Pa*PBP1B to some extent and could be selected for crystallisation studies of the protein even though the amount of protein that is extracted by DM is not optimal compared to TritonX-100 so the yield of soluble protein extracted by DM is compromised relative to TritonX-100.

3.3.7 The Purification of *Pa*PBP1B

*Pa*PBP1B was expressed for 18 hours at 25 °C in C43(λDE3) cells and was extracted into four different detergents: CHAPS, TritonX-100, LDAO and DDM. All batches were purified by gravity flow Ni^{2+} IMAC at 4 °C (Section 2.5.2) (**Figure 3.10**). After cleavage of the His_6-tag by thrombin protease, a further purification step to remove the thrombin was by cation exchange using SourceS resin.

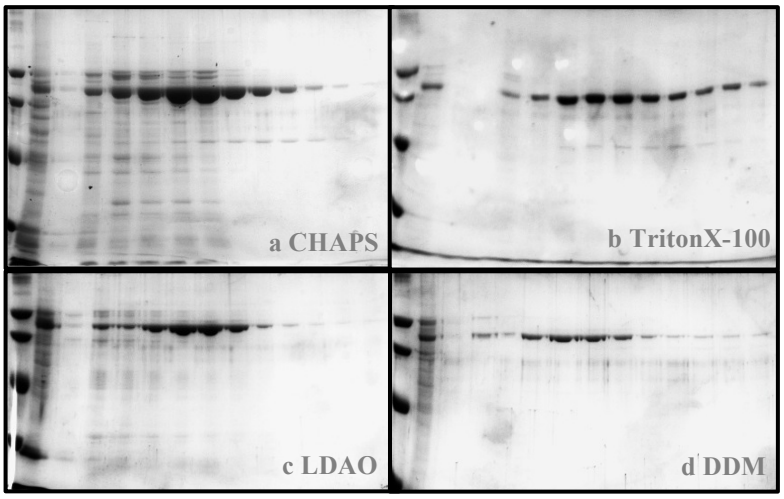

Figure 3.10 The Purification of pET28(b)::*Pa*PBP1B W^{23}-N^{774} in four detergents: CHAPS, TritonX-100, LDAO and DDM, by Co^{2+} IMAC. 10 % SDS-PAGE analysis of IMAC purification of *Pa*PBP1B, eluted with increasing concentrations of imidazole. *Pa*PBP1B W^{23}-N^{774} = 83.05 kDa once the His-tag has been cleaved.

*Pa*PBP1B was purified to homogeneity by IMAC followed by cation exchange. The ability of the *Pa*PBP1B transpeptidase domain to bind to fluorescent penicillin was a quick test to determine correct folding of the protein.

3.4 Initial Structural and Functional Characterisation of Purified *Pa*PBP1A and *Pa*PBP1B

3.4.1 Labelling *Pa*PBP1B with Fluorescent-Penicillin, BOCILLIN FL™

The binding of the *Pa*PBP1B transpeptidase domain to boron-dipyrromethene (BODIPY)-labelled penicillin (referred to as BOCILLIN FL™) was analysed to confirm correct folding of the transpeptidase domain (section 2.8.2). The proteins were incubated with a 3:1 molar ratio of BOCILLIN™ to protein, incubated for 1 hour at 37 °C, visualised by SDS-PAGE. BOCILLIN™ is acylated by the active site serine forming a covalent complex, which can be observed by fluorescence detection following SDS-PAGE **(Figure 3.11)**.

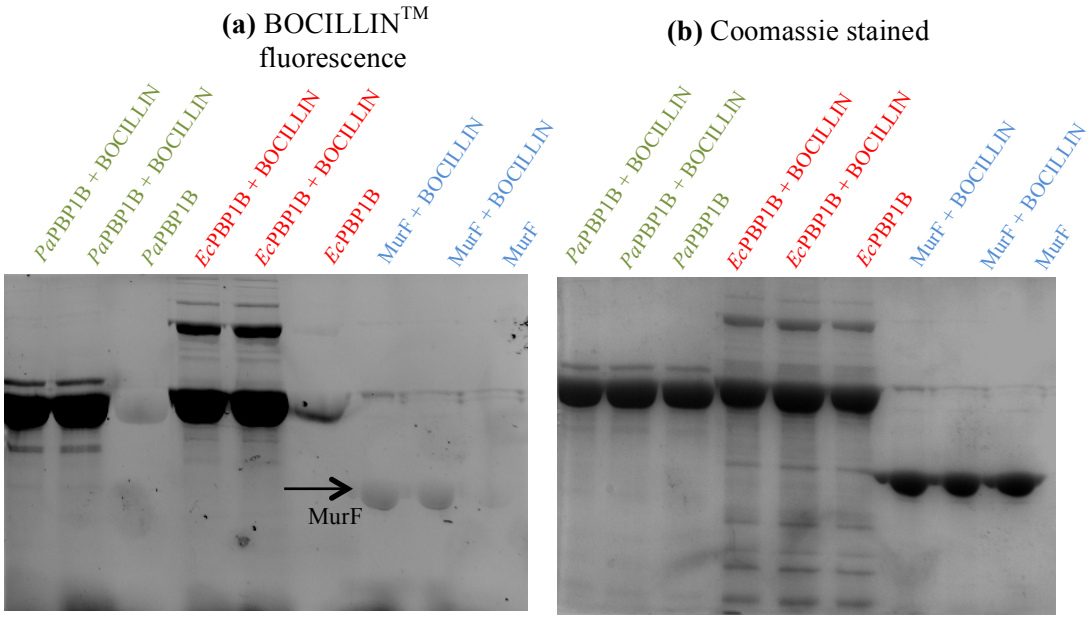

Figure 3.11 BOCILLIN™-FL Labelling of *Pa*PBP1B, *Ec*PBP1B and *Pa*MurF. (a) SDS-PAGE analysis of two PBPs (both purified in TritonX-100) and one negative-control protein MurF, ± BOCILLIN™-FL, imaged on a UV transilluminator in a Syngene G:Box using a ShortPass filter (suitable for detecting the λ_{Em} of BODIPY at 512 nm) and GeneSnap software to avoid a saturated image.

*Pa*PBP1B appeared to bind to BOCILLIN™-FL upon incubation together and *Pa*PBP1B does not indicate any fluorescence when not incubated with BOCILLIN™-FL. The same can be said for *Ec*PBP1B. The cytoplasmic ligase MurF, which does not have a transpeptidase domain, does not bind to BOCILLIN™-FL when incubated. The transpeptidase domains of *Pa*PBP1B and *Ec*PBP1B both appear to be folded correctly.

3.4.2 Circular Dichroism of *Pa*PBP1A and *Pa*PBP1B

As a pre-requisite to functional spectrophotometric studies as well as structural macromolecular X-ray crystallisation, *P. aeruginosa* Class A PBPs were analysed by Circular Dichroism (CD) (section 2.9.1) to ensure the proteins were properly folded, and to compare secondary structure characteristics of both proteins. CD provides information about molecular conformation and protein stability. In the instance of proteins, there are spectral signatures characteristic of α-helical, β-sheet and random coil secondary structures, and fitting software can determine the relative percentages of each in the sample. *Pa*PBP1A and *Pa*PBP1B were analysed by CD spectroscopy to test for a native protein fold **(Figure 3.12)**.

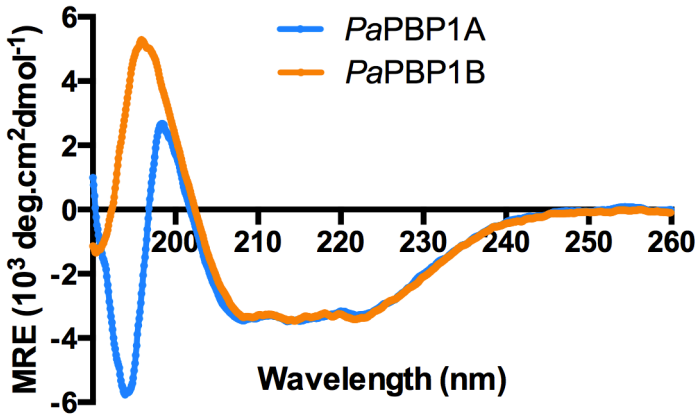

Figure 3.12 Circular Dichroism Analysis of *P. aeruginosa* PBP1A and 1B. Both proteins were solubilised in 1.5 mM CHAPS. Scans were made in the far UV range (190 - 260 nm) and all data was collected at 20 °C. Both PBPs were diluted in sodium phosphate buffer to a final PBP concentration of 0.1 mg/mL (1.1 µM and 1.2 µM respectively, in a 200 µL sample).

Examination of the CD spectra in CHAPS detergent shows weak peaks at around 208 nm and 222 nm, characteristic of a predominantly α-helical protein. Using the protein secondary structure prediction software PSIPred (Jones, 1999), the predicted α-helicity of *Pa*PBP1A was 53.7 and 61.2 % for *Pa*PBP1B derived from the protein sequences alone.

3.5 Further Investigation in the quest for active *Pa*PBP1B

3.5.1 The Cloning and Expression of Shorter, 'Soluble' PBP1B from *E. coli* and *P. aeruginosa*

Shorter protein fragments of *P. aeruginosa* and *E. coli* PBP1B were cloned that lacked the majority of the membrane-associated N-terminal region, with the aim to achieve a higher protein expression yield due to the protein being more soluble in nature and would not require detergents for extraction from the membrane. The *Ec*PBP1B protein fragment cloned and expressed was Y^{107}-N^{844} and the *Pa*PBP1B construct was Y^{65}-N^{774} with the initiating tyrosines being the first amino acid of the UB2H domain in PBP1B in both species. The PCR products of *Ec*PBP1B Y^{107}-N^{844} are in **Figure 3.13a**, with an expected size of 2214 bp. The chosen destination vector for PBP1B expression was pET22b as it carries an N-terminal pelB signal sequence for potential periplasmic localization. The majority of PBP1B resides in the bacterial periplasm, anchored to the

cytoplasmic membrane at its N-terminus. With the absence of N-terminal membrane associated regions in these designed constructs, the expressed protein may be free in the periplasmic space. Upon successful cloning in to plasmid pET22b, *Ec*PBP1B Y^{107}-N^{844} was expressed in BL21(λDE3) cells. The cells were lysed by sonication and spun down to pellet any insoluble material, leaving soluble proteins from the cytosol in the supernatant. A sample of both the pelleted insoluble material and the soluble supernatant were run on SDS-PAGE for analysis of the solubility of *Ec*PBP1B Y^{107}-N^{844} **(Figure 3.13b).** The same theory was applied to *Pa*PBP1B.

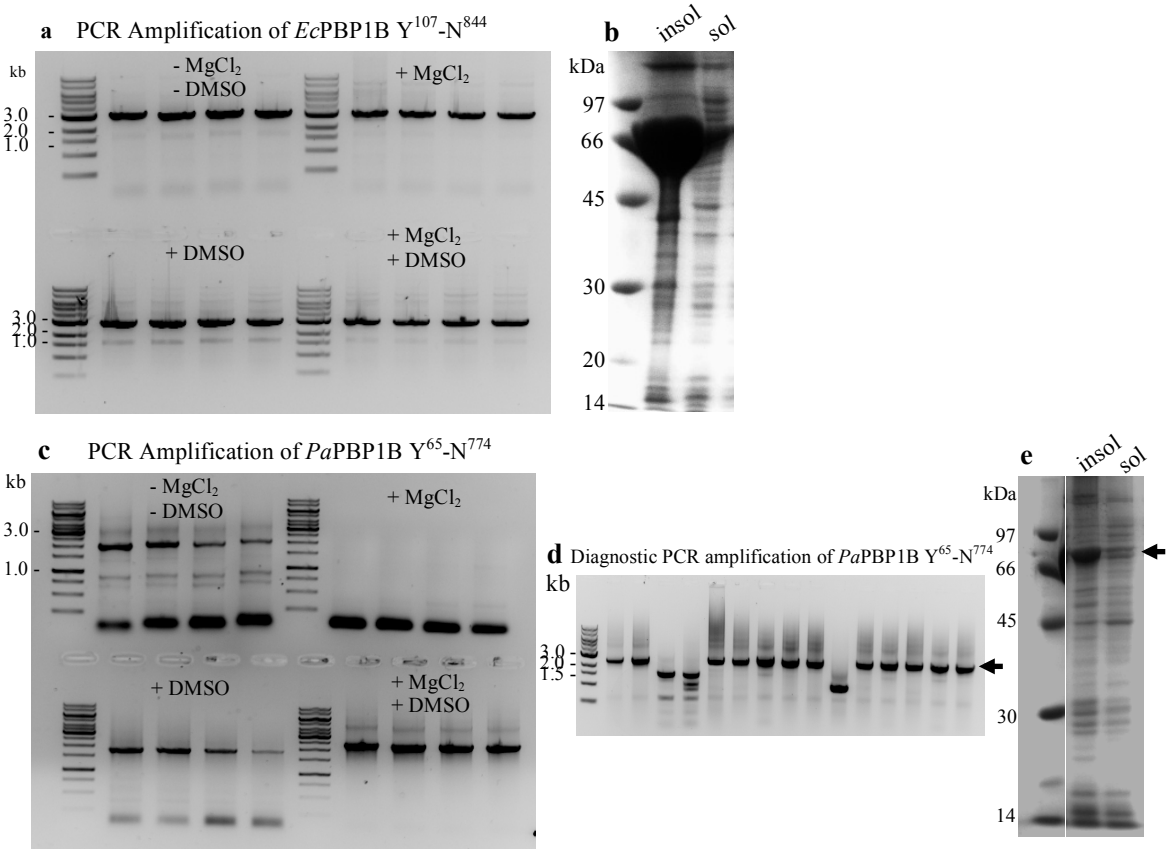

Figure 3.13 The PCR Amplification of *Ec*PBP1B Y^{107}-N^{844} and *Pa*PBP1B Y^{65}-N^{774} and Initial Solubility Expression Trial. PCR products were analysed by 1.0 % agarose gel and initial expression by 10 % SDS-PAGE. PCR of *Ec*PBP1B$^{107\text{-}844}$ **(a)** and *Pa*PBP1B$^{65\text{-}774}$ **(c)** was carried out as in section 2.3.1 using High Fidelity Phusion DNA polymerase in a range of conditions ± $MgCl_2$ and DMSO, across an annealing temperature gradient of 50-60 °C. *Ec*PBP1B gene size = 2214 kb and *Pa*PBP1b = 2256 kb. The PCR products were pooled, cloned into pET22b and expressed in BL21 (λDE3) cells. **(b)** and **(e)** The soluble and insoluble fractions of both *Ec*PBP1B$^{107\text{-}844}$ (82.0 kDa) and *Pa*PBP1B$^{65\text{-}774}$ (78.4 kDa) were analysed by 10% SDS-PAGE. **(d)** Diagnostic PCR of potential *Pa*PBP1B Y^{65}-N^{774} clones using the pET22b vector-specific T7 Forward primer, and the *Pa*1b reverse primer.

Both of these genes were successfully cloned in to pET22b and an expression analysis of the soluble versus insoluble phases revealed where the majority of the expressed proteins resided. Despite cleaving the N-terminal membrane-associated region, both proteins expressed predominantly in the insoluble phase. No further experiments were conducted with *Ec*PBP$^{107\text{-}844}$ as the M$^{46\text{-}844}$ construct showed average expression yields and already exhibited good enzymatic activity. It was unknown what affect cleaving the first 106 residues from the N-terminus would have on the activity of *Ec*PBP1B. However, the insoluble expression of *Pa*PBP1B Y$^{65\text{-}774}$ underwent a solubilisation experiment with TritonX-100 to see if *Pa*PBP1B could be extracted from the membrane (section 2.4.6) (**Figure 3.14a**). Triton-X100-solubilised *Pa*PBP1B Y^{65}-N^{774} was purified by IMAC (**Figure 3.14b**).

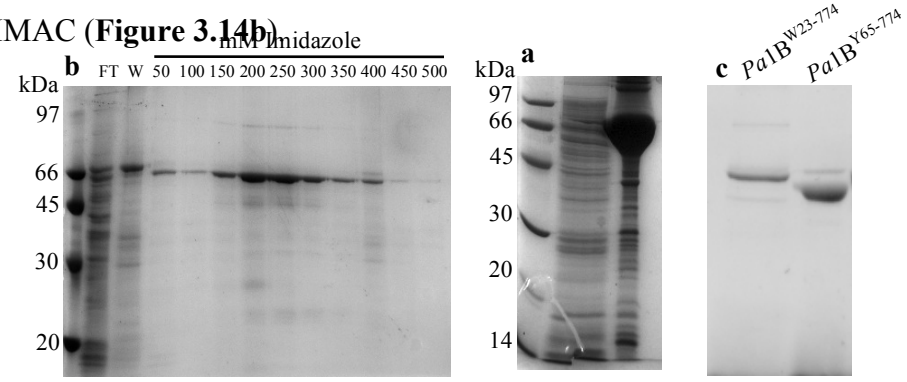

Figure 3.14 The Solubilisation and IMAC Purification of *Pa*PBP1B Y$^{65\text{-}774}$. (a) The solubilisation of *Pa*PBP1B Y$^{65\text{-}774}$ in 1% TritonX-100, with the insoluble and soluble fractions analysed by 10% SDS-PAGE **(b)** Ni^{2+} IMAC purification (gravity-slow column at 4 °C) of *Pa*PBP1B Y$^{65\text{-}774}$ analysed by 10% SDS-PAGE, FT: flowthrough, W: wash. **(c)** BOCILLIN^{TM} binding to the original *Pa*PBP1B W$^{23\text{-}774}$ and the shorter *Pa*PBP1B Y$^{65\text{-}774}$.

*Pa*PBP1B Y$^{65\text{-}774}$ was successfully extracted from the membrane with TritonX-100 and purified by IMAC. The transglycosylase activity of *Pa*PBP1B Y$^{65\text{-}774}$ was analysed by continuous fluorescence monitoring (Schwartz *et al.*, 2002), but was not active for transglycosylase activity. Incubating *Pa*PBP1B$^{65\text{-}774}$ with fluorescent penicillin (BOCILLIN^{TM}) indicated that the transpeptidase domain was folded correctly in an active conformation for both *Pa*PBP1B constructs.

3.5.2 Cloning *P. aeruginosa* PBP1B in to a *P. putida* Expression Construct and Homologous Protein Expression

Catalytic activity of *P. aeruginosa* PBP1B had not been observed with the constructs cloned and heterologously-expressed in *E. coli* cells and purified thus far. Therefore,

cloning the gene in to a *Pseudomonas*-compatible expression vector and expressing the protein homologously was trialled. The *Pa*PBP1B gene was amplified by PCR (section 2.3.1) (**Figure 3.15a**) and cloned in to low-copy number vector pIZ1016 with restriction sites *HindIII* and *XbaI*. Diagnostic PCR amplification of potential pIX1016::*Pa*PBP1B$^{23\text{-}774}$ clones revealed that 5 out of 12 colonies contained the *Pa*PBP1b gene (**Figure 3.15c**). These 5 clones were sequenced using vector-specific M13 forward primer and the reverse primer that was designed for original gene amplification. The gene was expressed in *P. putida* cells, the membrane fraction isolated and the over-expressed protein was extracted from the membrane with 0.2 % TritonX-100 and purified by IMAC.

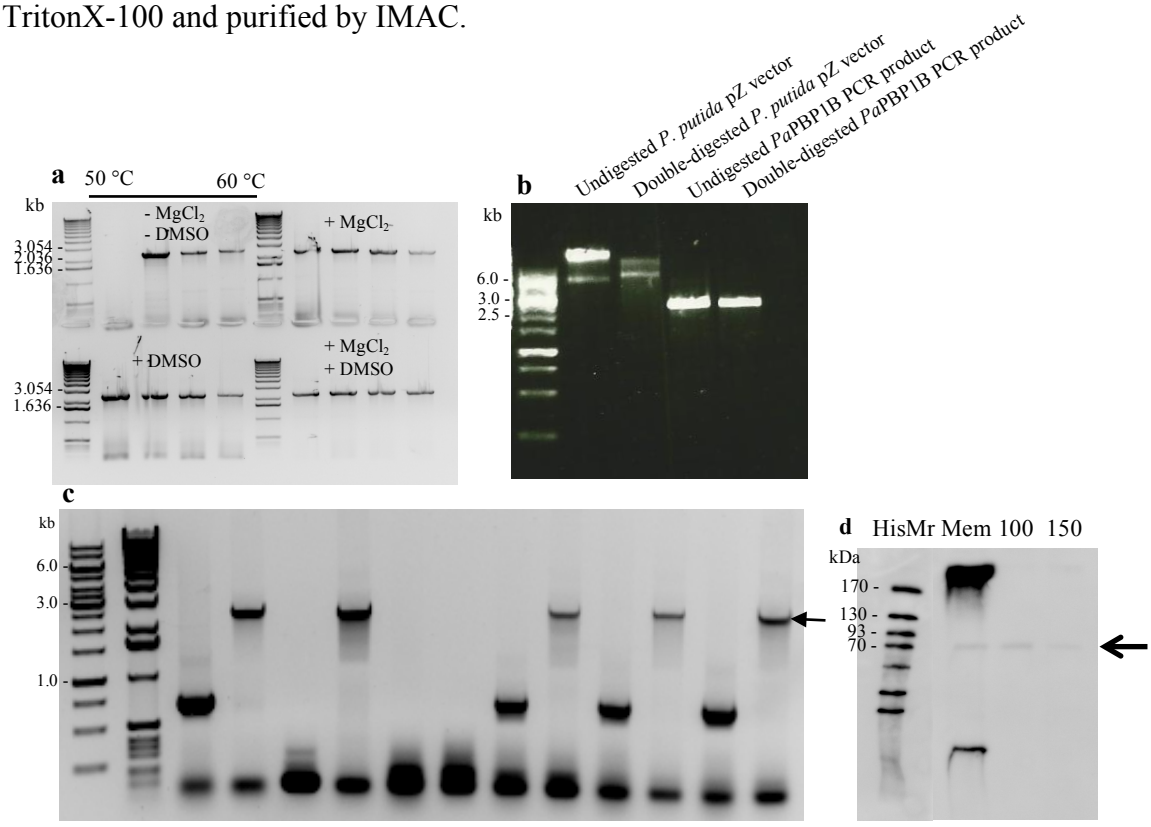

Figure 3.15 The Cloning of *Pa*PBP1B$^{23\text{-}774}$ in to the *P.Putida* Expression Vector pIZ1016 **(a)** PCR amplification of *Pa*PBP1B$^{23\text{-}774}$ using the wildtype pET28b *Pa*PBP1B construct as the template, in a combination of $MgCl_2$ and DMSO conditions, across an annealing temperature gradient from 50-60 °C **(b)** Restriction digestion of *Pa*PBP1B$^{23\text{-}774}$ PCR product and the pIZ1016 vector using *HindIII* and *XbaI* **(c)** Diagnostic PCR amplification of 12 potential pIZ1016::*Pa*PBP1B$^{23\text{-}774}$ clones, using M13 (forward) primer with the reverse primer that was designed for original gene amplification. **(d)** Anti-His Western blot of pIZ1016::*Pa*PBP1B$^{23\text{-}774}$ expression in a *P. putida* expression cell-line and IMAC purification, Mem = membrane fraction of *P. putida* cells over-expressing *Pa*PBP1B, 100, 150 are the mM imidazole elutions.

*Pa*PBP1B was successfully cloned in to a vector compatible with expression in *P. putida* cell-lines and was cultured in a large-scale expression, with protein expression

induced by the addition of arabinose. The level of *Pa*PBP1B expression was low, but pIZ1016 is a low-copy number plasmid. The protein was effectively extracted from *P. putida* membranes with TritonX-100 and purified by IMAC and visualised by anti-His Western blot (**Figure 3.15d)**. A final yield of 0.56 mg of protein was achieved which was tested for transglycosylase activity using a continuous fluorometric assay (Schwartz *et al.,* 2002), but no activity at all was detected.

All four Class A PBPs of interest (*E. coli* PBP1A, *E. coli* PBP1B, *P. aeruginosa* PBP1A and *P. aeruginosa* PBP1B) have been cloned and purified, summarised in **Figure 3.16** with all four amplified gene products and IMAC purification SDS-PAGE analysis.

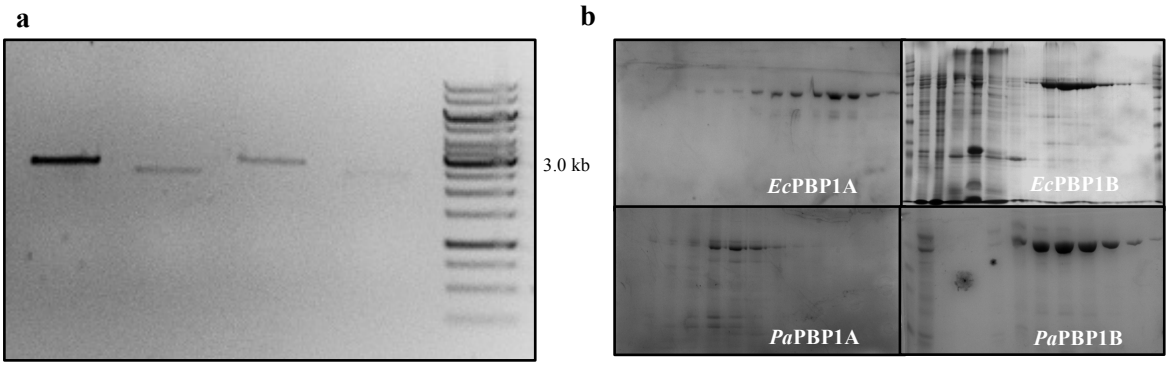

Figure 3.16 A Summary of the Cloning and Purification of all Four Class A PBPs: *Ec*PBP1A, *Ec*PBP1B, *Pa*PBP1A and *Pa*PBP1B. **(a)** The PCR amplified products of all four genes **(b)** The IMAC purification of all four proteins, analysed by 10 % SDS-PAGE.

3.6 Purification of PBP Catalytic Active Site Mutants

3.6.1 Site-Directed Mutagenesis and Purification of *E. coli* PBP1A and PBP1B Transglycosylase Active Site Mutants E86Q and E233Q Respectively

Primers were designed to alter the transglycosylase catalytic active site of *E. coli* PBP1A and PBP1B from glutamate to glutamine (Section 2.3.6). The primers used are in Appendix 1. Upon confirmation of successful site-directed mutagenesis by DNA sequencing (section 2.3.5), the mutated genes were expressed in C43(DE3) cells (sections 2.4.1 and 2.4.2 respectively) and the protein purified by IMAC (section 2.5.3) **(Figure 3.17)**.

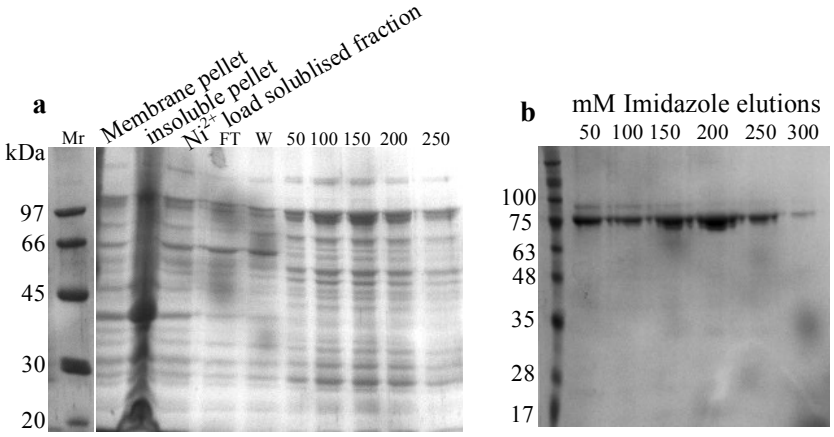

Figure 3.17 The Purification by IMAC of *E. coli* PBP1A and 1B Transglycosylase Mutants. Fractions analysed by 10% SDS-PAGE. **(a)** *E. coli* PBP1A transglycosylase active-site mutant E86Q purification by Ni^{2+} IMAC **(b)** *E. coli* PBP1B transglycosylase active-site mutant E233Q.

The transglycosylase active site mutants for the *E. coli* Class A PBPs were successfully engineered and purified. An experiment on how these catalytic active-site mutants expressed was conducted in the next section. These proteins analysed using a continuous fluorimetric transglycosylase assay in Chapters 4, 5 and 6 and compared against the wildtype function (section 4.7). The *Ec*PBP1A transglycosylase active-site mutant (E86Q) was also tested for transpeptidase (in)activity in section 6.9.2.6.

3.6.2 The Effect of Over-Expression of *E. coli* PBP Transglycosylase Catalytic Active Site Mutants on Cell Culture Growth

The impact of mutating the transglycosylase active site residue in *E. coli* PBPs upon the viability of the bacterial cell in cell culture was investigated. Meisel *et al.,* established that induction of overexpression of transglycosylase and transpeptidase deficient *Ec*PBP1B resulted in cell lysis (Meisel *et al.*, 2003). This analysis has been extended to a parallel comparison of the overexpression of both class A bifunctional enzymes: PBP1A and PBP1B with transglycosylase active site mutations. The transglycosylase catalytic active site residue glutamate of *Ec*PBP1A was mutated to the polar amino acid glutamine (E86Q) and the *Ec*PBP1B transglycosylase active site glutamate was also mutated to glutamine (E233Q). These *E. coli* PBP transglycosylase active site mutants were grown separately and in triplicate, with the mean value plotted in **(Figure 3.18)**, using the same protocol as wildtype protein expression. The cultures were grown overnight and the optical density (OD) of each culture was measured after 20 hours of growth (17.5 hours of protein expression).

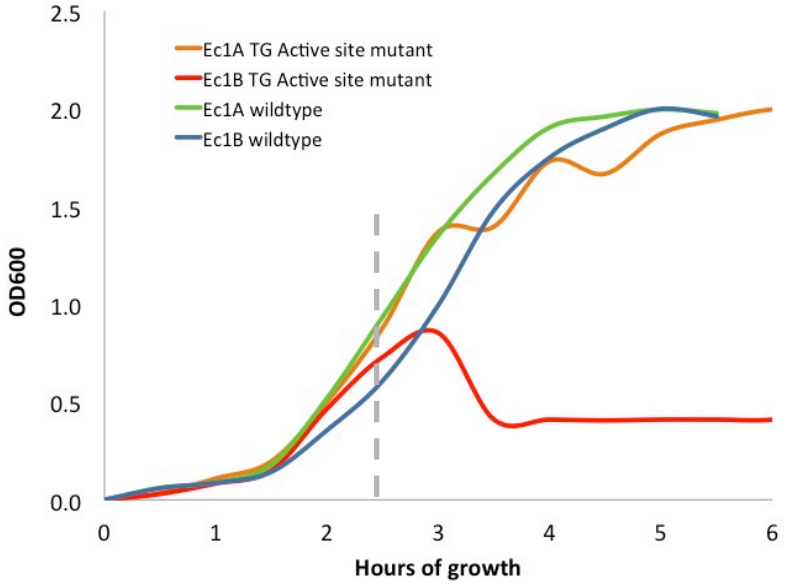

Figure 3.18 The Growth Curves of the Expression of the Transglycosylase Active Site Mutants *Ec*PBP1A and *Ec*PBP1B, independently. C43(DE3) cells were grown at 37 °C and induced with 0.5 mM IPTG at OD_{600}= 0.6-0.7 (grey dashed line). Upon induction the temperature was reduced for expression at 25 °C.

The lysis phenotype was found in *Ec*PBP1B only. Similar effects have been reported with a serine to cysteine (thiol) mutant of overexpressed class B, *E. coli* PBP3 (transpeptidase only) (Broome-Smith *et al.*, 1985). Upon the OD measurement of the cultures after 20 hours of growth, all cultures had remained constant since the previous measurement the night before, except for *E. coli* PBP1B transglycosylase active site mutant, whose density had increased. After induction of expression of the *Ec*PBP1B E233Q mutant, the density of the culture plummeted from OD_{600}=0.85 to 0.41 within 30 minutes and remained low for the next 3.5 hours. Upon measuring the culture after 17.5 hours of expression, the OD had returned to >2 absorbance units. The cell culture appeared to rescue and recover its phenotype and viability.

3.6.3 Site-Directed Mutagenesis and Purification of *E. coli* PBP1A and *E. coli* PBP1B Transpeptidase Active-Site Mutants S473A and S510A, respectively

The primers used to mutate the active-site serine of *E. coli* PBP1A and 1B are in Appendix 1. These mutated constructs containing the altered base-pairs were expressed in C43(DE3) and purified by IMAC (**Figure 3.19a**). The ability of the transpeptidase mutant to bind BOCILLIN^{TM} was compared to that of the wildtype protein (**Figure 13.19b** and **c**).

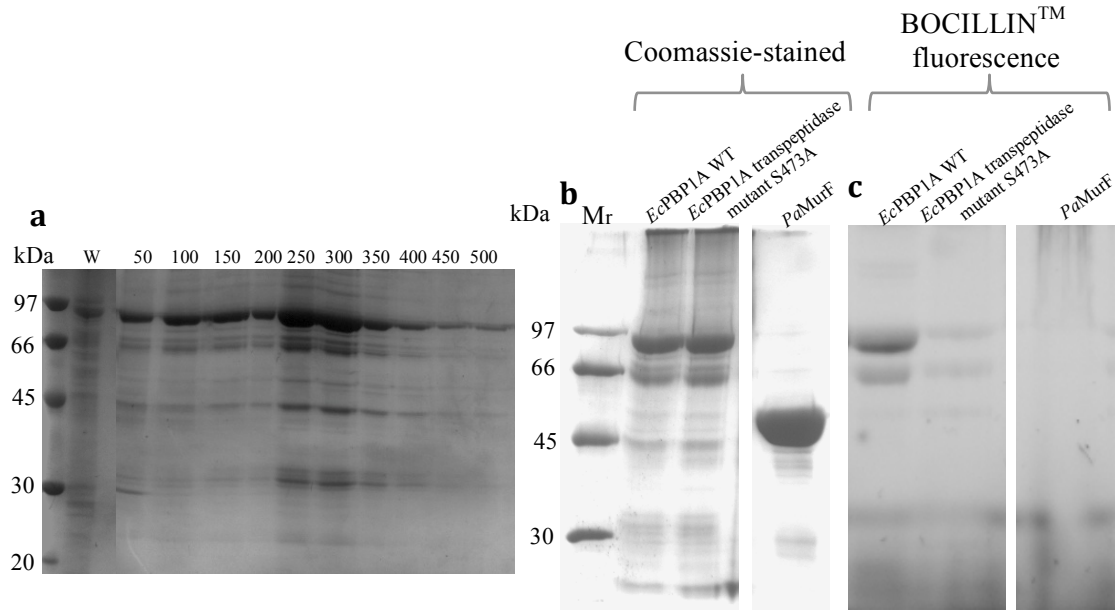

Figure 3.19 The Purification of *E. coli* PBP1A Active Site Mutant S473A and its Ability to Bind BOCILLIN™. (a) The purification of *Ec*PBP1A transpeptidase active site mutant, analysed by 10% SDS-PAGE **(b)** SDS-PAGE of wildtype and transpeptidase active site mutant *Ec*PBP1A incubated with BOCILLIN™ FL, stained with coomassie **(c)** BOCILLIN™ FL fluorescence of S473A mutant and *Ec*PBP1A wildtype. *Pa*MurF was included as a negative control, imaged on a UV transilluminator in a Syngene G:Box using a ShortPass filter (suitable for detecting the λ_{Em} of BODIPY at 512 nm) and GeneSnap software to avoid a saturated image.

*Ec*PBP1A S473A was successfully expressed and subsequently purified by IMAC. The wildtype transpeptidase domain bound to BOCILLIN, indicating a structurally native fold but the active site mutant did not bind to BOCILLIN, suggesting it was unable to bind to the alanine in the absence of the catalytic serine, as expected.

The transpeptidase active-site mutant of *Ec*PBP1B (S510A) was also confirmed by DNA sequencing, expressed, solubilised in TritonX-100 and purified by IMAC (**Figure 3.20a**). The purified protein was incubated with BOCILLIN™ to further confirm the absence of the active site serine in the transpeptidase domain (**Figure 3.20c**).

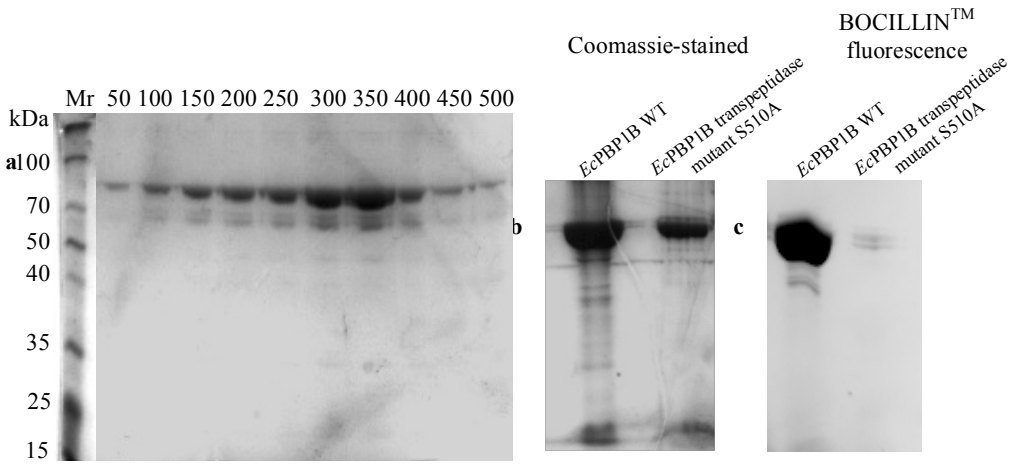

Figure 3.20 The Purification of *E. coli* PBP1B Transpeptidase Active-Site Mutant S510A and its Ability to Bind BOCILLIN™. (a) The purification of *Ec*PBP1B transpeptidase active site mutant by IMAC, analysed by 10% SDS-PAGE **(b)** SDS-PAGE of wildtype and transpeptidase active site mutant *Ec*PBP1A incubated with BOCILLIN™ FL, stained with coomassie. **(c)** BOCILLIN™ FL fluorescence of S510A mutant and *Ec*PBP1B wildtype, imaged on a UV transilluminator in a Syngene G:Box using a ShortPass filter (suitable for detecting the λ_{Em} of BODIPY at 512 nm) and GeneSnap software to avoid a saturated image.

The *Ec*PBP1B transpeptidase active-site mutant S510A was successfully genetically modified within the wildtype construct and the purified transpeptidase-inactive protein failed to bind to BOCILLIN™, as expected.

3.6.4 Site-Directed Mutagenesis and Purification of *P. aeruginosa* PBP1A Transglycosylase and Transpeptidase Active Site Mutants E86Q and S461A, respectively.

The transglycosylase and transpeptidase active-site mutants of *Pa*PBP1A: E86Q and S461A were engineered into the *Pa*PBP1A wildtype construct, confirmed by DNA sequencing, expressed, solubilised by TritonX-100 and purified by IMAC (**Figure 3.21**).

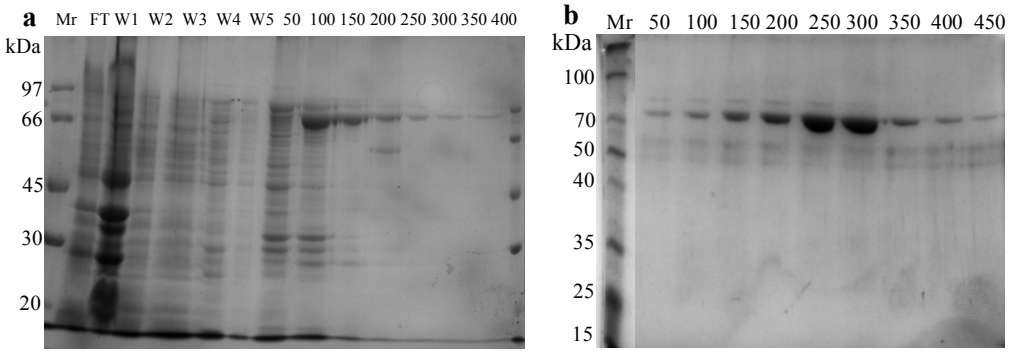

Figure 3.21 The Purification *P. aeruginosa* PBP1A Transglycosylase E86Q Mutant and Transpeptidase S461A Mutant. **(a)** The purification of *Pa*PBP1A transglycosylase active-site mutant by IMAC, analysed by 10% SDS-PAGE **(b)** The purification of *Pa*PBP1A transpeptidase active-site mutant by IMAC, analysed by 10% SDS-PAGE.

Both catalytic active-site mutants of *Pa*PBP1A were successfully expressed and purified. The functionality of these catalytically inactive *Pa*PBP1A active-site mutants (E86Q) and (S461A) were tested for transglycosylase activity in section 4.7 and transpeptidase activity in section 6.9.3.1.

3.7 The Cloning and Purification of PBP-Associated Proteins

3.7.1 Cloning and Purification of *P. aeruginosa* and *E. coli* PBP3

E. coli and *P. aeruginosa* PBP3 (FtsI) were cloned and purified for use in activity assays in the following chapters. PBP3 is a Class B monofunctional DD-transpeptidase and loss of PBP3 inhibits cell septation, causing cells to grow as elongated filaments. *Pa*PBP3 is essential for growth in *P. aeruginosa* (Chen *et al.,* 2017). Upon successful cloning of both PBP3 genes, constructs were expressed in BL21(DE3) cells, followed by IMAC purification **(Figure 3.22)**.

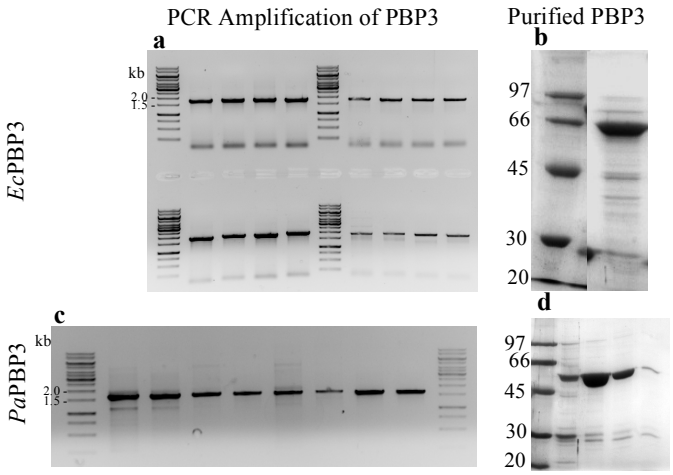

Figure 3.22 The PCR Amplification and Purification of *E. coli* PBP3 and *P. aeruginosa* PBP3. (a) PCR amplification of full-length *Ec*PBP3 (1.76 kb). PCR products were pooled, digested with *BamHI* and *SacI*, and cloned in to vector pET52b. **(b)** Purified *Ec*PBP3 (63.87 kDa) **(c)** PCR amplification of full-length *Pa*PBP3 (1.7 kb) **(d)** Purification of *Pa*PBP3 (61.10 kDa) by gravity-flow IMAC.

3.7.2 *E. coli* CpoB and *P. aeruginosa* YbgF

YbgF coordinates PBP1B and TolA and also modulates the activity of PBP1B *via* its interaction with LpoB, coordinating cell wall biosynthesis during division and the apparatus for constricting the outer membrane. A *E. coli* CpoB (formally YbgF) plasmid was a kind gift from Prof. Colin Kleanthous, University of Oxford. pAK147 full-length *Ec*CpoB with a C-terminal His_6 but lacking its signal peptide (1-26) was cultured and its protein purified according to Krachler *et al.*, 2010. Initially the insoluble and soluble phases of the cell extract were analysed to determine the location of *Ec*YbgF, before purifying by IMAC **(Figure 3.23)**.

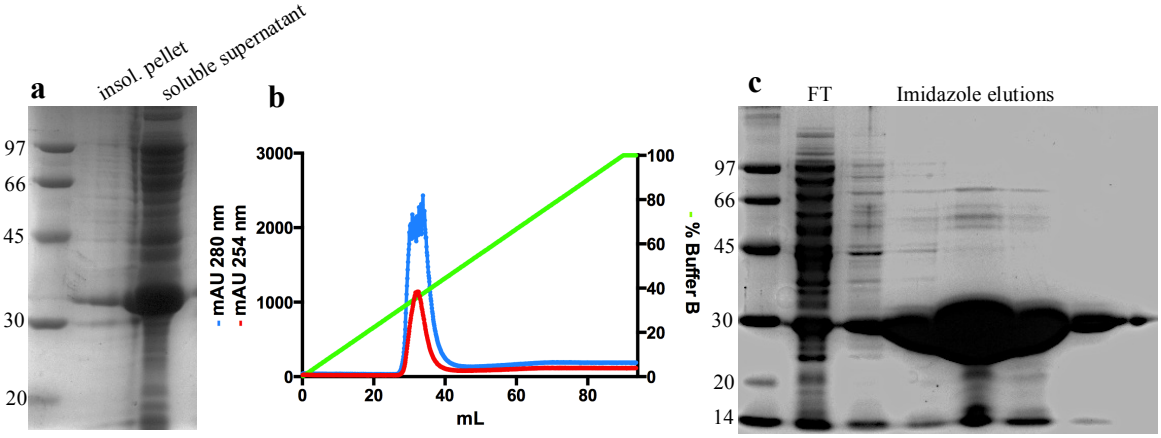

Figure 3.23 The Expression and Purification of *E. coli* CpoB (formally *Ec*YbgF). (a) Expression of *Ec*CpoB, analysing the insoluble and soluble fractions of the cell lysate **(b)** Chromatogram of the purification profile of *Ec*CpoB, purified by IMAC using a pre-packed 5 mL HisTrap column on an AKTA 10/100 system (GE Healthcare) in a cold cabinet at 4°C **(c)** 12 % SDS PAGE analysis of *Ec*CpoB$^{27\text{-}263}$ (25.448 kDa).

*Ec*CpoB expressed highly in the soluble phase of the bacterial cells and was easily purified by IMAC using an ÄKTA Purifier. The *P. aeruginosa* equivalent of *Ec*CpoB (*Pa*YbgF) was expressed and purified by gravity-flow IMAC (**Figure 3.24**).

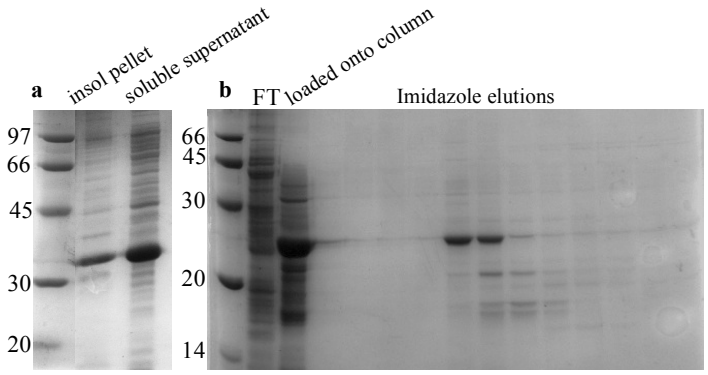

Figure 3.24 The Expression and Purification of full-length *P. aeruginosa* YbgF. (pProEx::*Pa*YbgF) **(a)** Expression of *Pa*YbgF, analysing the insoluble and soluble fractions of the cell lysate **(b)** 12 % SDS PAGE analysis of full-length *Pa*YbgF (29.10 kDa).

Both *E. coli* CpoB and *P. aeruginosa* were sufficiently expressed and purified for use in activity assays.

3.7.3 The Expression and Purification of *Enterococcus faecium* VanA

*Ef*VanA is a D-Ala-D-Lac ligase that requires ATP for activity and is known to make D-Ala-D-X dipeptides (Bugg *et al.*, 1991, which was required and used in a VanA-coupled assay in Chapter 6 (section 6.6.1). *Ef*VanA was expressed and purified according to the thesis of Dr. S. Batson (Batson, 2010) (described in section 2.8.8) with the results in **Figure 3.25**.

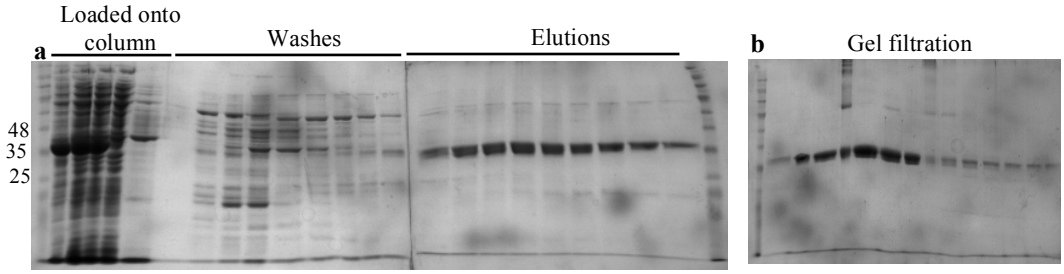

Figure 3.25 The Purification of *E. faeccium* VanA. **(a)** IMAC purification over a 5 mL HisTrap **(b)** Gel filtration of *Ef*VanA (37.44 kDa).

The specific activity of *Ef*VanA was calculated as 6.4 x 10^{-3} mol/min/mg.

3.7.4 The Expression and Purification of *E. coli* LpoA and LpoB

E. coli LpoA stimulates the transpeptidase activity of *E. coli* PBP1A and was over-expressed according to Jean *et al.,* 2014 (**Figure 3.26a**), from a construct cloned by Dr. Dean Rea at The University of Warwick (pSUMODave::*Ec*LpoA). *E. coli* LpoB was purified from a construct (pProEx::*Ec*LpoB) also cloned by Dr. Dean Rea and purified according to Paradis-Bleau *et al.*, 2010 (**Figure 3.26b**).

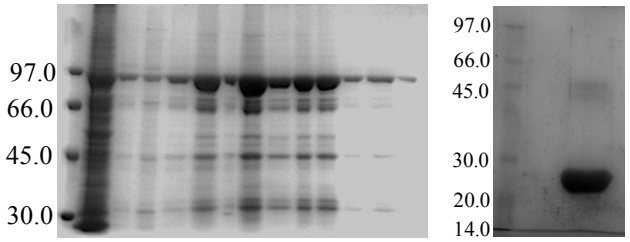

Figure 3.26 The Purification of *E.coli* LpoA and LpoB. The expected size of each was 72.8 kDa and 20.2 kDa respectively. **(a)** The purification analysis of IMAC elutions of *Ec*LpoA by 10 % SDS-PAGE **(b)** The purity analysis by 12 % SDS-PAGE of purified *Ec*LpoB.

E. coli LpoA was further purified by gel filtration and used to stimulate *Ec*PBP1A transpeptidase activity in Chapter 6. The orthologous protein in *P. aeruginosa*, *Pa*LpoA was also cloned and purified.

3.7.5 The Cloning and Purification of *P. aeruginosa* LpoA

*Pa*LpoA was amplified by PCR and cloned into pET28b using *NcoI* and *NotI*. The resulting expressed protein was purified by gravity-flow IMAC at 4 °C (**Figure 3.27**).

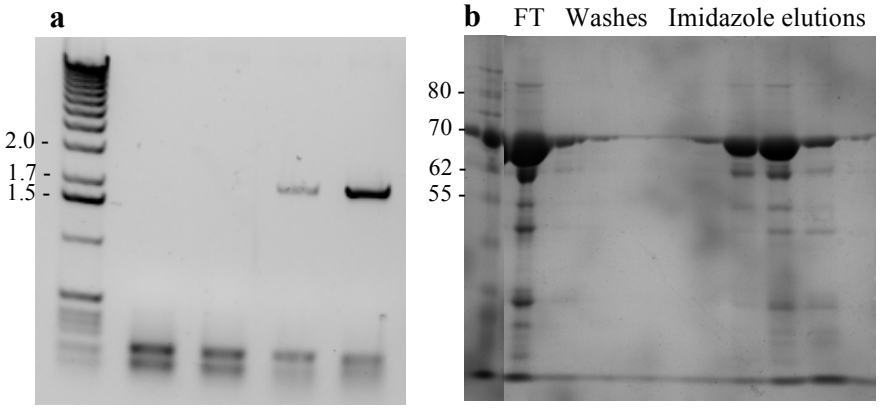

Figure 3.27 The PCR Amplification of the *PaLpoA* Gene and Purification of *Pa*LpoA Protein. **(a)** PCR amplification of the *PaLpoA* gene, using Q5 DNA polymerase, with four PCR aliquots across an annealing temperature gradient from 55-65 °C, gene size 1815 bp **(b)** Purification of *Pa*LpoA by Ni^{2+}-NTA IMAC (65.63 kDa).

*Pa*LpoA was tested for its ability to stimulate *Pa*PBP1A in section 6.9.3.

3.7.6 The Expression and Purification of *E. coli* FtsN

E. coli FtsN is an essential cell division protein that activates septal peptidoglycan synthesis and constriction of the cell and is a known binding-partner of *Ec*PBP1B. The pET28b::FtsN construct was cloned by Dr. Dean Rea and was purified according to Yang *et al*., 2004, **Figure 3.28**.

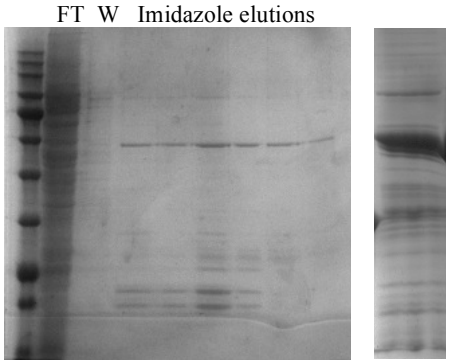

Figure 3.28 The Purification of *E. coli* FtsN. Purified by gravity-flow IMAC, analysed by 12 % SDS-PAGE (35.8 kDa)

3.8 PBP X-Ray Crystallography

3.8.1 Initial X-Ray Crystallography Screens of *E. coli* PBP1A, *P. aeruginosa* PBP1A and *P. aeruginosa* PBP1B

Crystallisation screens were set up in 96-well Greiner plates using a Mosquito robot. Commercially-available crystallisation matrix screens that have been designed to target membrane protein crystallisation were tested with the three PBPs. MemStart and MemGold (48 and 96 conditions, respectively) were tested using the sitting drop method of crystallography (section 2.9.2). *Ec*PBP1A, *Pa*PBP1A and *Pa*PBP1B were purified in LDAO and CHAPS, with CHAPS giving better results. A sitting drop of 200 nL of protein was deposited into the mother liquor (100 μL per well) and all crystals were grown at 18 °C. Protein concentrations were between 8.1 and 12.0 mg/mL and all affinity His-tags were cleaved prior to crystal trials. Crystal structures of PBPs already solved are discussed in the introduction sections 1.5.4 and 1.5.5. Trays were set up in the apo- and ligand-bound proteins and monitored every 24 hours for the first week,

then every 48 hours for the following 3 weeks. All crystals were formed by the end of week two. Trays of *E. coli* PBP1A in DDM, LDAO and CHAPS were set up with and without Moenomycin, using the screen MemGold and MemStart. Photos were taken of the apo-enzyme *Ec*PBP1A in CHAPS in MemGold (**Figure 3.29**).

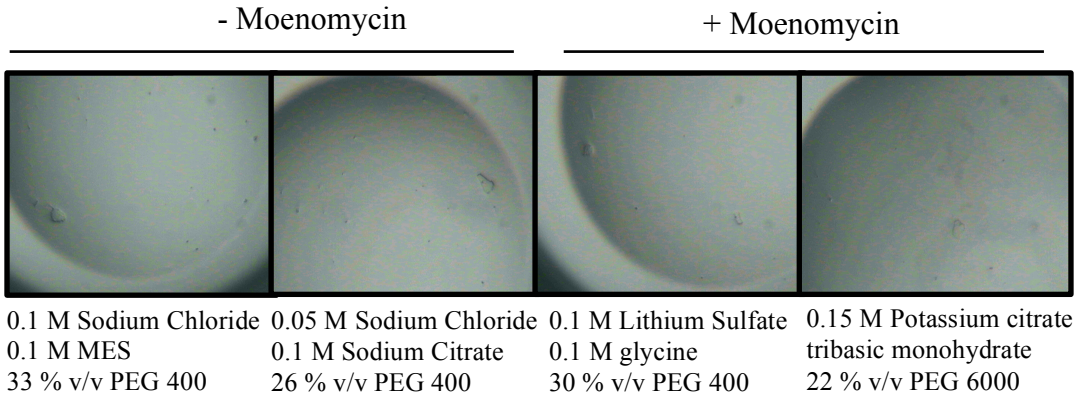

Figure 3.29 Crystallisation Screen of *E. coli* PBP1A, in its apo-enzyme form and co-crystallised with its ligand Moenomycin

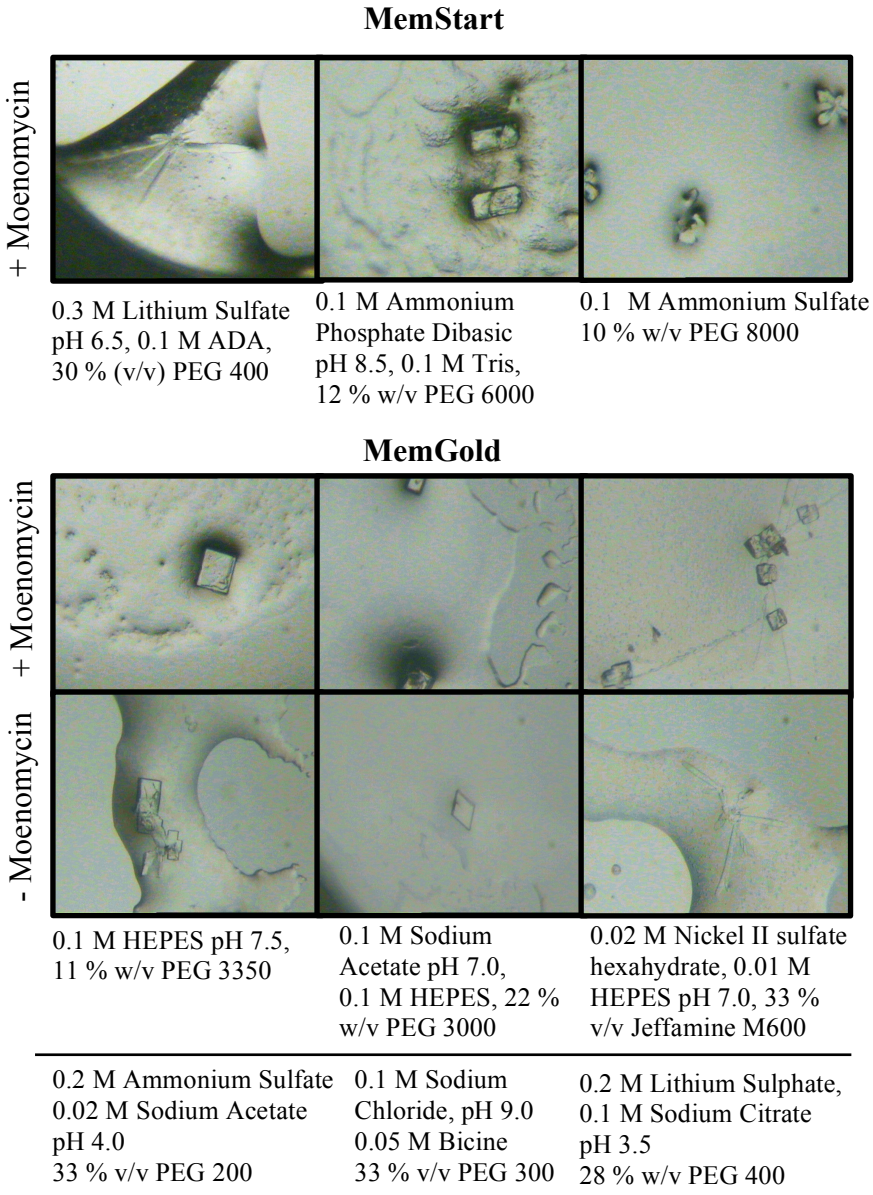

Figure 3.30 Crystallisation Screen of *P. aeruginosa* PBP1A, in its apo-enzyme form and co-crystallised with its ligand Moenomycin

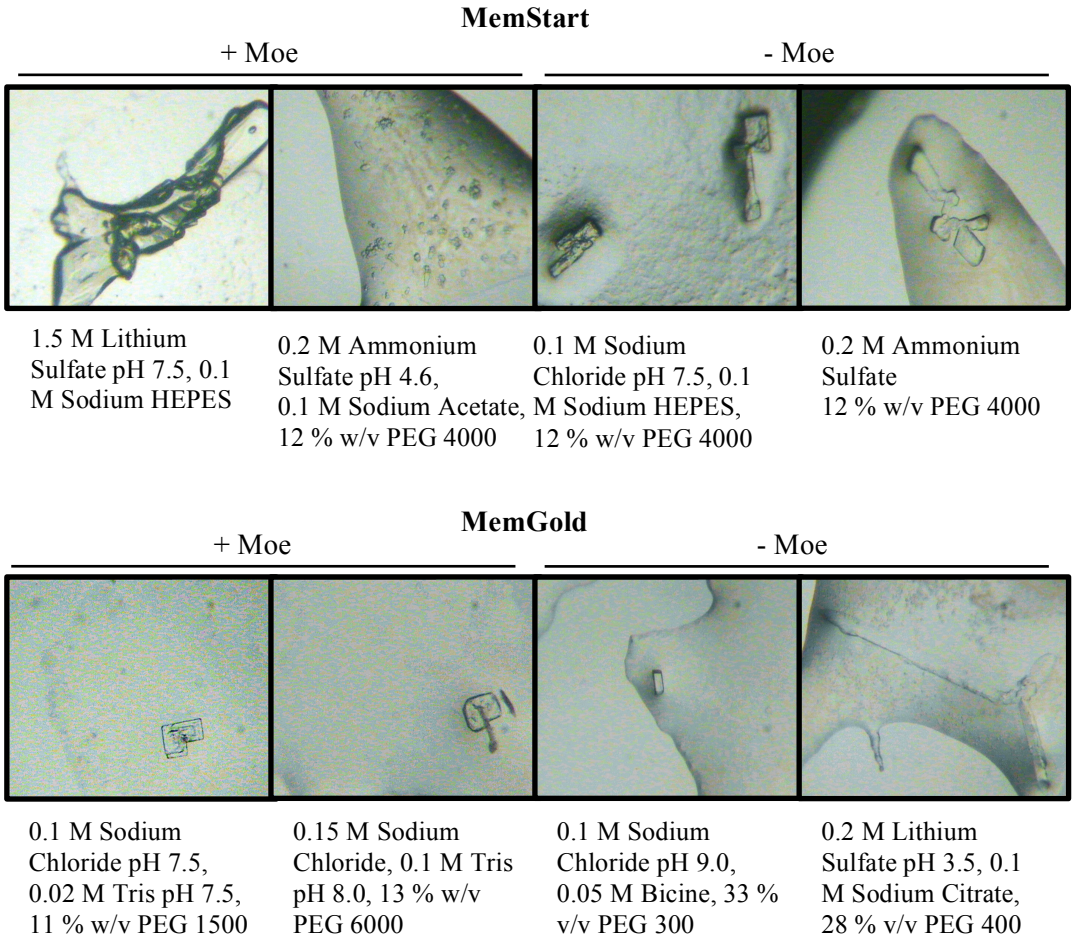

Figure 3.31 Crystallisation Screen of *P. aeruginosa* PBP1B, in its apo-enzyme form and co-crystallised with its ligand Moenomycin

It is unknown whether these initial crystals are true protein crystals or whether they are actually salt crystals or detergent crystals. In future crystal trials, it would be useful to check the monodispersity of the protein batch upon purification (e.g. by analysing its elution profile from a gel filtration column), before embarking on crystallisation studies. The homogeneous nature of the protein batch is of paramount importance to protein crystallography, particularly with the presence of detergent micelles with membrane proteins. One artefact of concentrating membrane proteins in VivaSpins is that it is not known how readily the detergent passes through the filter membrane and therefore whether the protein sample is concentrating uniformly with the detergent. It is possible that detergent could remain above the VivaSpin filter due to their 'sticky' and viscous nature thereby increasing the detergent concentration in the protein sample for crystallisation. The choice of detergent with respect to charge, micelle size and CMC is also critical for crystallisation and is protein-specific.

3.9 Discussion

3.9.1 The Lack of Activity of *Pa*PBP1B

The N-terminally shorter *Pa*PBP1B and *Ec*PBP1B proteins did not show much expression in the soluble phase of the 'soluble vs insoluble' expression trial (Figure 3.13 b and e). On reflection, it is highly likely that these proteins may have expressed in the periplasm, as this is where the majority of the PBP1B protein resides *in vivo*, with the N-terminal TM domain anchored to the cytoplasmic membrane in the full-length protein. Future studies could include the isolation of the periplasmic fraction of these expressions, so that proteins in the periplasm can be visualised separately from those in the cytoplasm. The 'proteome' in the periplasm will be smaller than that of the cytoplasm and it is very possible that the yield of these periplasmic proteins will be low relative to a cytoplasmic expressed protein. Isolating the periplasmic phase may reveal high-level expression of these shorter, potentially soluble PBP proteins. The *Pa*PBP1B $Y^{65\text{-}774}$ construct was designed to yield a soluble, high-level expressing protein. As the expressed products required extraction from the membrane with detergent, there is no advantage to this construct over the full-length *Pa*PBP1B cloned initially.

Bacterial cells expressing the *Pa*PBP1B protein with an N-terminal pelB signal sequence for localisation to the periplasm, could be isolated and extracted by osmotic shock to reveal the periplasm.

*Pa*PBP1B was expressed in *P. putida* but the purified protein yield was poor and did not exhibit any transglycosylase activity. Conditions need to be optimised for this enzyme, as each PBP is different and are notoriously difficult to show activity.

3.9.2 Over-Expression of the *Ec*PBP1B Transglycosylase Mutant

Over-expression of *E. coli* PBP1B transglycosylase active site mutant E233Q caused the optical density to fall upon induction by IPTG. One theory for this observation is that the high abundance of *Ec*PBP1B proteins in the cell sequester known associated proteins of *Ec*PBP1B, namely MltA (Vollmer *et al.,* 1999), PBP3 (Bertsche *et al*., 2006), FtsN (Muller *et al.,* 2007), LpoB (Typas *et al.,* 2010, Paradis-Bleau *et al.,* 2010)

and FtsW (Egan *et al.*, 2013), the latter of which is proposed to act as a LII flippase providing substrate for peptidoglycan formation. Removing essential components from protein complexes, disrupting vital protein-protein interactions (PPIs) that are required for coordination of cell wall biosynthesis with other processes.

3.9.3 PBP Crystallography Trials

Detergent-solubilised membrane proteins do not often form ordered crystal lattices (Newby *et al*., 2009). Changing the pI of the proteins changes the crystallisation conditions of the protein, for example a his_6-tag alters the pI of the protein, decreasing it by 0.5 Units, however a his_6-tag can aid crystallisation.
"X-ray crystallography is more of a religion than a science" Dr. Dom Bellini 2016.

3.10 Conclusions

A multitude of enzymes have been purified to homogeneity for use in this project, with certain proteins expressing better than others. Generally PBP1A expressed at a higher level than PBP1B. Although *Pa*PBP1B did not show any activity, the enzyme expressed very well and was easily purified to homogeneity, good enough to justify initial crystal trial experiments. *Pa*PBP1B was also cloned into a *P. putida* expression vector and expressed to a low level and purified.

3.11 Future Work

The circular dichroism of *Pa*PBP1A and PBP1B demonstrated natively-folded protein, and *in silico* prediction algorithms predicted ~50-60% α-helicity. Comparing the wildtype PBP CD spectrum with the catalytic active site mutants would be interesting to demonstrate any change is protein fold. It would also be interesting to investigate the thermo-stability of the PBPs using CD and compare to this to a parallel experiment using Thermoflour. Optimisation of crystallography conditions is needed for further structural studies of *Pa*PBP1A and *Pa*PBP1B.

The *Pa*5052 gene is the potential *P. aeruginosa* FtsN as it has genome synteny and predicted structural similarity. Cloning this gene would be interested to see if it exhibits

a function upon *Pa*PBP1B, similar that of *Ec*FtsN upon *Ec*PBP1B. Expressing the *Pa*PBP1B UB2H domain of *Pa*PBP1B would also be of interest, in the quest to find an *E. coli* LpoB homologue in *P. aeruginosa*. Also, as *Ec*PBP2 stimulates PBP1A in a similar way to LpoA, it is possible that a similar situation exists in *P. aeruginosa*, cloning *Pa*PBP2 would be needed for this.

The *Pa*PBP1B construct used in this project was W23-N744. Testing the activity of the full-length protein may help in generating an active construct of this protein. Over-expressing the current *Pa*PBP1B W23-N744 construct in *E. coli* membranes and assaying the activity of *Pa*PBP1B in a membranous environment would be interesting, as other proteins present *in vivo* that are usually removed upon purification may be aiding the activity of *Pa*PBP1B.

Chapter 4
The Kinetic Analysis of the Transglycosylation Activity of *E. coli* PBP1A and *P. aeruginosa* PBP1A

4.1 Current Transglycosylase Assays in the Literature

The kinetic activity of PBPs has been challenging due to the difficulty in obtaining and synthesising relevant and native substrates. This is compounded by the nature of PBPs and their integral association with the cell membrane. PBPs are stabilised *in vitro* using synthetic detergents that aim to mimic the cell membrane. Defining the amount of detergent to use to maintain PBP integrity and activity while still creating a native environment in which to assay the function of the PBP is one of the more challenging aspects of this project. The improved knowledge of synthesising lipid-linked intermediates has aided the study of transglycosylation (Schwartz *et al*., 2001, van Nieuwenhze *et al*., 2002, Breukink *et al*., 2003,). The mechanism of transglycosylation is illustrated in Figure 1.4, with the substrates and products involved in the mechanism being as follows:

$$(\text{Glc}\mathit{N}\text{Ac-Mur}\mathit{N}\text{Ac})_n\text{-U}_n\text{-P-P} + \text{Lipid II} \rightarrow (\text{Glc}\mathit{N}\text{Ac-Mur}\mathit{N}\text{Ac})_{n+1} + \text{U}_n\text{-P-P}.$$

A myriad of assays aiming to detect and monitor transglycosylase activity have been developed over the last 20 years, summarised below.

4.1.1 Thin Layer Chromatography Assays

Thin layer chromatography was one of the earliest methods of separating out and visualising the products of transglycosylation (van Heijenoort *et al.,* 1978, Di Guilmi *et al.*, 2003). The labelled lipid II was incubated with a transglycosylase and the reaction products distinguished by thin layer chromatography (TLC). The lipid II substrate can be labelled either radioactively with ^{14}C on the L-alanine at position 1 of the pentapeptide or the Glc*NA*c sugar ring (van Heijenoort *et al.,* 1978), or alternatively the ε-amino group on the *meso*DAP residue in the pentapeptide can be labelled with a fluorescent moiety including dansyl (Schwartz *et al.*, 2002), NBD (van Dam *et al.*, 2007) and fluorescamine (Schwartz *et al*., 2001). After polymerisation, the polymerised products were run on TLC. Any material that remained at the origin (immobile

polymeric fragments) was digested with lysozyme before being separated by TLC and compared with monomer and dimer peptidoglycan fragments of known structure (van Heijenoort *et al.,* 1978). TLC is not the only method of separating multi-length glycan polymers, polyacrylamide gel-based systems have also been employed to show processivity and activity.

4.1.2 SDS-PAGE Analysis of Transglycosylation Products

A polyacrylamide gel system (Tricine-sodium dodecyl sulfate-polyacrylamide) originally designed to separate large proteins of 1-100 kDa (Schägger & von Jagow, 1987), has been exploited and adapted for the analysis of transglycosylation reaction products (Barrett *et al.*, 2007, Helassa *et al.*, 2012). The monomer substrate is radio- or fluorescently-labelled prior to polymerisation to enable detection. This technique was used to analyse the distribution of transglycosylase products following time-dependent incubations of *E. coli* PBP1B and *A. aeolicus* PBP1A with heptaprenyl-[^{14}C]-Lipid II (Barrett *et al*., 2012, Yuan *et al*., 2007). The sensitivity of this assay is questionable and is qualitative rather than quantitative, however, it is a useful technique for overall visualisation of polymerisation results. The length of glycan chains in *E. coli* peptidoglycan is 10-40 disaccharide units (Vollmer, 2008) with chain lengths detected *via* this polyacrylamide separation technique ranging from the monomer Lipid II, through Lipid IV, detecting glycan chain lengths of approximately 30 and 50 disaccharide units with *E. coli* PBP1A and *E. coli* PBP1B (Helassa *et al.*, 2012). By general agreement, transglycosylases are processive rather than dispersive, catalysing multiple rounds of polymerisation without releasing the elongating glycan polymer (Yuan *et al*., 2007). Long glycan chains were detected without the accumulation of short chains, concurrent with the processive model of transglycosylation (Barrett *et al*., 2007).

4.1.3 HPLC Analysis of Transglycosylation Products

The analysis and separation of polymerised products has also been conducted using high-pressure liquid chromatography - HPLC. Radio-labelled LII as well as fluorescently-labelled LII have both been used for this technique and can be polymerised (Bertsche *et al.*, 2005 & Biboy *et al.,* 2013). Fluorescently labelling the LII

can be done prior to polymerisation (Heaslet *et al.,* 2009) or post-polymerisation (Schwartz *et al.*, 2001), before HPLC analysis. The advantage to labelling post-reaction is that the fluorophore does not interfere transglycosylation progress.

4.1.4 High-Through Put (HTP) Screening Assays Based on Moenomycin Displacement

High-through-put assays have used the displacement of moenomycin from the transglycosylase active site, as a screen for potential inhibitors (Cheng *et al.*, 2008, Gampe *et al.*, 2011). Cheng et al designed a highly sensitive fluorescence anisotropy assay using a fluorescein-labelled moenomycin. Fluorescence anisotropy properties decreased when competitively-binding compounds displaced the fluorescein-labelled moenomycin (Cheng *et al*., 2008). Gampe *et al.* developed a fluorescence polarisation assay, based upon displacement of a fluorescently-labelled minimal pharmacophore of moenomycin in an effort to identify low micromolar inhibitor binding. Although both of these assays by-pass the need for LII substrates, they rely upon chemically modified derivatives of the moenomycin pharmacophore (Gampe *et al*., 2011).

4.1.5 Continuous Fluorescence Assays

The first continuous, coupled assay of transglycosylase activity reported was based upon the increased quantum yield of fluorescence signal from a dansyl fluorophore when in a hydrophobic micellar environment (Schwartz *et al* 2002). The lipid II substrate is labelled with a fluorescent dansyl moiety attached to the ε-amino group of the *meso*DAP residue in the pentapeptide stem. The polymerised products are hydrolysed by the presence of muramidase, which cleaves the glycosidic bond between Glc*NA*c and Mur*NA*c sugars. Upon product digestion by muramidase, polymerisation is visualised by a decrease in fluorescence due to a shift from a lipidic to a soluble environment. This assay has been used extensively in this chapter, and is described further below.

A novel FRET assay was developed to elucidate transglycosylase activity (Huang *et al.,* 2013) using LII analogues, including the pentapeptide chain being labelled with NBD. Structures of the hit compounds identified using this assay are in Table 1.3. Liu and

Wong also employed a nitrophenol LII analogue to characterise the transglycosylase function of *S. pneumoniae* PBP1b spectrophotometrically (Liu & Wong, 2006). The continuous fluorometric assay developed by Schwartz *et al.,* using dansyl-labelled (dansylated) LII (Schwartz *et al.*, 2002) forms the basis for the analysis of transglycosylase activity in Class A PBPs in this chapter. The advantages of this assay are that it is continuous, it is easy to set up, it is quantitative, it can be monitored in real time and is high-throughput.

4.2 Experimental Aims

- To use *E. coli* PBP1B as a model enzyme for the study of transglycosylation
- Develop the continuous, fluorescence transglycosylation assay in to a high-throughput plate reader format
- Optimise the transglycosylase assay for *E. coli* PBP1A and *P. aeruginosa* PBP1A, including ionic strength, detergent and pH.
- Kinetically characterise the Class A PBPs, defining the K_m and V_{max} for different substrates
- Synthesise transglycosylase active-site mutants for the transglycosylase domain of the three Class A PBPs and test their transglycosylase activity
- Characterise the effect of LpoA, LpoB, PBP2 and PBP3 on transglycosylation activity of *E. coli* PBP1B, *E. coli* PBP1A and *P. aeruginosa* PBP1A

4.3 *E. coli* PBP1B as a Control Enzyme for the Study of Transglycosylation by Class A Transglycosylase Enzymes

4.3.1 A Continuous Fluorescence Assay for Transglycosylase Activity

The assay developed by Schwartz *et al.* in 2002 in which the transglycosylase activity of *E. coli* PBP1B (*Ec*PBP1B) was monitored continuously has been replicated and adapted for use for a variety of transglycosylases in the literature (Sung *et al.*, 2009, Offant *et al.,* 2010, Huang *et al.,* 2012) and for other Class A PBPs in this thesis. The LII used for the substrate was fluorescently labelled by dansylation of the ε-amino group of the third position amino acid in the stem peptide. Upon successful synthesis of

UDP-Mur*N*Ac-L-Ala-D-Glu-*meso*DAP-D-Ala-D-Ala, a dansylation reaction was conducted to label the ε-amino group on the third-position DAP, before converting in to a lipid. The fluorescence signal followed in this continuous assay is the shift in spectral intensity of the dansyl moiety, at its emission optimum of 520 nm, due to its release from a lipidic to an aqueous environment upon the hydrolysis of polymers into monomers by *N*-acetyl-muramidase (**Figure 4.1**). This change in environment for the fluorophore causes a decrease in fluorescence, indirectly representing the polymerisation of LII.

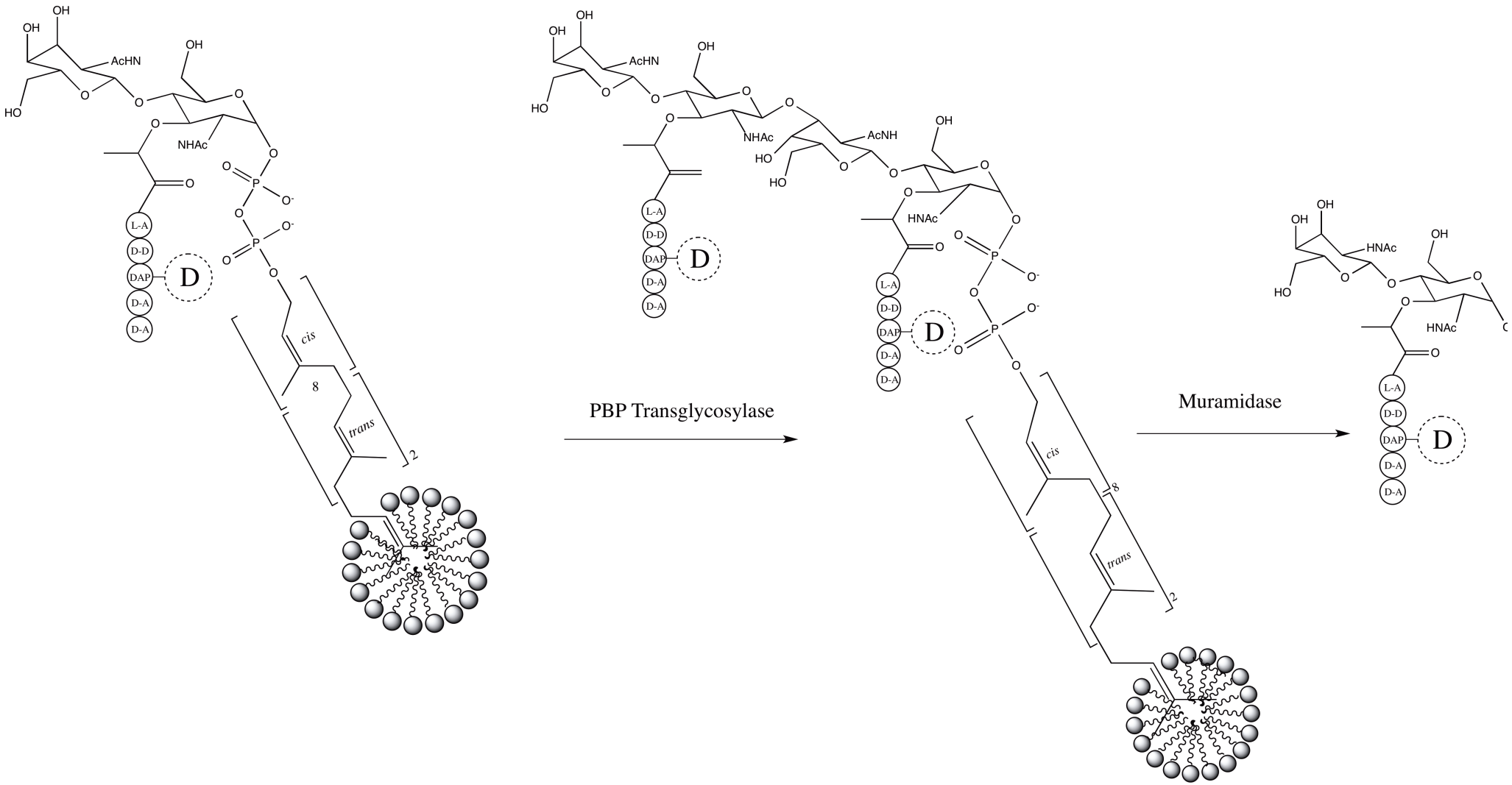

Figure 4.1 The Continuous Fluorometric Assay for the Detection of Glycan Chain Polymerisation (Adapted from Schwartz *et al.,* 2002). The monomer lipid II was used, with the fluorescent reporter, Dansyl, represented as 'D'. *N*-acetyl-muramidase, mutanolysin, derived from a *Streptomycete* was used to hydrolyse the polymers and release the dansyl fluorophore from its lipidic environment. This change in environment alters the fluorometric properties of the dansyl fluorophore, reported as a decrease in fluorescence emission at 520 nm. The decrease in fluorescence continuously (indirectly) monitors the polymerisation of the monomer lipid II into glycan strands.

4.3.2 Assay Scale-Up: From Fluorimeter to Plate Reader

This fluorescence assay was initially recreated using the same enzyme as previously tried and tested in by Schwartz *et al*, *Ec*PBP1B. Development began using a steady-state fluorimeter with a Xenon light source and R1527 photomultiplier tube, with assays being conducted at a volume of 200 µL in a quartz cuvette. The natural progression was to transfer this assay in to a plate reader format, for high-throughput purposes to reduce the assay volume, consumption of dansylated LII and cost of reagents. The difference between the output from the fluorimeter compared to the plate reader is minimal (**Figure 4.2**).

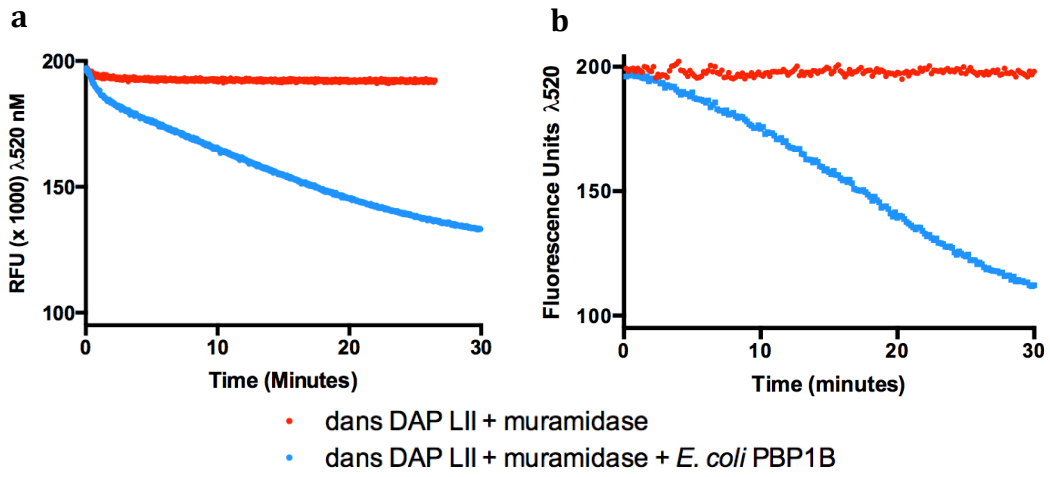

Figure 4.2 The Continuous Fluorometric Transglycosylation Assay in a Fluorimeter Compared to a Plate-Reader. The comparison between **(a)** a continuous fluorescence transglycosylation assay in a 200 uL assay volume in a quartz cuvette in the fluorimeter and **(b)** the same assay in a volume of 25 uL in a well of a 96-well plate. Both assays copied exactly the reaction conditions given in Schwartz *et al*., 2002. 50 mM HEPES, pH 7.5, 0.085% decyl PEG, 10 mM $MgCl_2$, 10% DMSO, 0.1 µg muramidase, 10 µM dans-DAP-LII, 50 nM *Ec*PBP1B.

The continuous assay is reproducible in both a fluorimeter and plate-reader format, so all subsequent assays were conducted using a Clariostar plate reader, with a reaction volume of 25 µL, using a 96-small-well plate (section 2.8.3). The transfer of this assay to a plate-reader was also published at this time (Helassa *et al.*, 2012). A 'proof of principle' assay was conducted in the plate reader, with controls (Moenomycin is a potent inhibitor of transglycosylation and so was used as a negative control), illustrated in **Figure 4.3**.

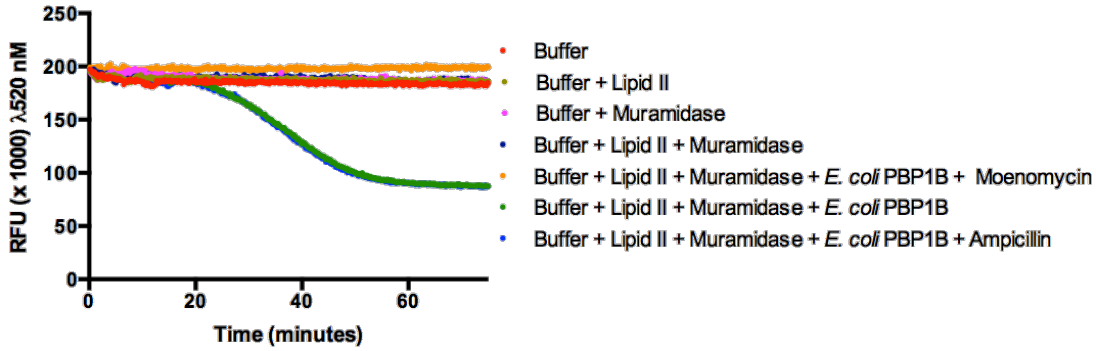

Figure 4.3 The Continuous Fluorometric Transglycosylase Assay - Proof of Principle assay with Positive and Negative Controls. 50 nM *Ec*PBP1B, 10 µM dans-DAP-LII. (**a**) Assay buffer (50 mM HEPES, pH 7.5, 0.085% decyl PEG, 10 mM $MgCl_2$, 10% DMSO) alone (**b**) buffer + 10 µM LII (**c**) buffer + 0.1 µg muramidase (**d**) buffer + LII + muramidase (**e**) buffer + LII + muramidase + 50 nM *Ec*PBP1B + 50 µM Moenomycin (transglycosylation inhibitor) (**f**) buffer + LII + muramidase + *E. coli* PBP1B (**g**) buffer + LII + muramidase + *Ec*PBP1B + 250 µM ampicillin (transpeptidation inhibitor).

The assay was initiated with the *Ec*PBP1B enzyme in all cases in Figure 4.3, also, initiating the reaction with the substrate dansylated LII was tested to ensure that the reagent used to initiate polymerisation was independent of how the assay proceeded (data not shown).

Figure 4.3 is a proof of principle experiment showing that LII substrate is only polymerised in the presence of the LII polymerase *Ec*PBP1B, with the exception when *Ec*PBP1B is in the presence of MoenomycinA, the potent transglycosylase inhibitor. The presence of ampicillin, which binds to the transpeptidase domain of the PBP, had no affect on the transglycosylase activity of *Ec*PBP1B. A valid alternative to using *N*-acetyl muramidase to break the glycosidic bonds in the glycan sugar backbone is hen egg white lysozyme. A comparison assay between the use of *N*-acetyl muramidase and lysozyme to hydrolyse the polymers was conducted, concluding that there is no difference between the efficiency of polymer breakdown or assay progression (data not shown).

It has been well documented that the Class A PBP transglycosylases *Ec*PBP1A (Barrett *et al.*, 2007) and PBP1B (Schwartz *et al.*, 2002) exhibit an initial polymerisation lag phase. *In vitro*, upon initiation of a transglycosylase reaction, glycan chains do not exist and the enzyme has to perform *de novo* polymerisation of LII forming a short polymeric glycan strand. *In vivo*, however, transglycosylases are 'primed' by a pre-existing polymerised precursor, providing a scaffold for elongation (Schwartz *et al.*, 2002).

This fluorescence continuous assay can be successfully replicated with the model enzyme *Ec*PBP1B and in a plate reader format. Subsequently, further Class A PBPs (*Ec*PBP1A, *Pa*PBP1A and *Pa*PBP1B) were tested for transglycosylase activity using the same assay and initially the same assay conditions as those used for *E. coli* PBP1B. However the assay conditions needed to be optimised for *Ec*PBP1A and *Pa*PBP1A including the optimum detergent for activity, the optimum pH and ionic strength.

4.4 The Kinetic Characterisation of Transglycosylation for the Model Enzyme *E. coli* PBP1B

4.4.1 Dependence of *E. coli* PBP1B Transglycosylase Activity on Enzyme Concentration

The dependence of *Ec*PBP1B concentration on the initial rate of glycan chain polymerisation was tested to determine if there is a linear relationship between enzyme concentration and initial reaction rate. With EcPBP1B exhibiting a polymerisation lag, the initial rate of reaction was taken from the beginning of the linear phase of the reaction, usually 30 seconds after reaction initiation. The initial rate was measured over a time interval of 30 seconds, after the initial 30 second lag. A substrate concentration of 10 μM dans-DAP-LII was used to ensure that the initial velocity measured was independent of substrate concentration and that the initial rate of reaction (V_0) was dependent on *Ec*PBP1B enzyme concentration. The LII substrate used for all of these assays was dansylated on the pentapeptide as a means of detection. Enzyme dependence was conducted with two substrates of LII, with a variation in their prenyl chain length: dansylated-DAP LII C_{55} and dansylated-DAP LII C_{35} (**Figure 4.4**). C_{55} LII is the native carbon chain length, with C_{35} (a heptaprenyl lipid chain) being a variant with a shorter lipidic carbon tail and is a more soluble substrate due to its shorter lipid chain. A prenyl chain length of more than 20 carbon atoms is critical for the transglycosylase processivity of (Perlstein *et al.,* 2010). Transglycosylases in *E. coli* membranes have a preference for C_{35} over their native C_{55} substrate *in vitro*, as the shorter lipid chain minimises the possibility of aggregation as observed with the undecaprenyl pyrophosphate in LII-C_{55} (Ye *et al.,* 2001).

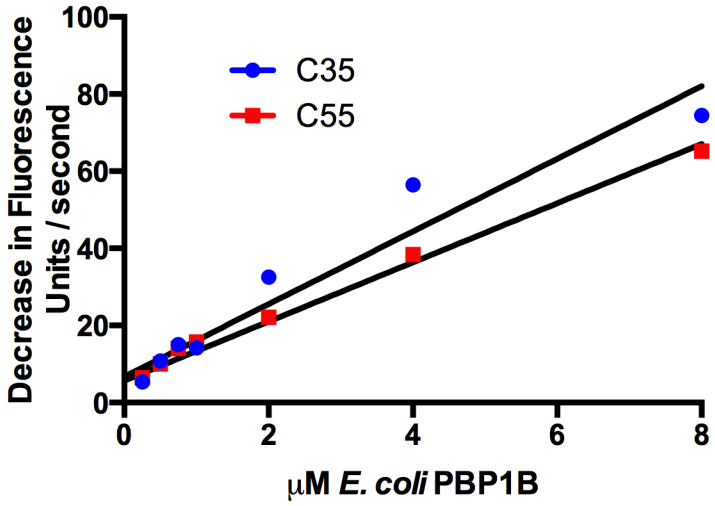

Figure 4.4 Dependence of *E. coli* PBP1B Transglycosylase Activity on Enzyme Concentration. • Dans-DAP-LII C_{55} and • dans-DAP-LII C_{35}. The substrate concentration used in both cases was 10 μM LII. *Ec*PBP1B was purified in TritonX-100 and 50 mM HEPES, pH 7.5, 10 mM $MgCl_2$, 10% DMSO, 0.1 μg muramidase, 10 μM Dans-DAP-LII. 25 μL reaction volume in a well of a 96-well plate.

*Ec*PBP1B has a linear relationship between enzyme concentration and initial reaction velocity, with both dans-DAP-LII C_{55} and dans-DAP-LII C_{35} substrates. This plot indicates that the amount of product formed is dependent upon enzyme concentration.

4.4.2 Michaelis-Menten Kinetic Constants

The Michaelis Menten model demonstrates a measure of how well a substrate complexes with its enzyme (binding affinity). The Michaelis Mention equation relates reaction rate to substrate concentration [S]. V_{max} is the maximum rate achieved at saturating enzyme concentration. K_m is the Michaelis Menten constant defined as the substrate concentration at which the reaction rate is half V_{max}. Scheme (1) is the rate equation from which the parameters K_m, V_{max}, K_{cat} and v_0 are derived.

Scheme (1) $$[E] + [S] \underset{K_2 \; - [S]}{\overset{K_1 \; + [S]}{\rightleftharpoons}} [ES] \xrightarrow{K_{cat}} [E] + [P]$$

K_m, K_{cat} and the initial velocity V_0, can all be found from a solution to the parent equation, by plotting experimental data on a Time vs [S] graph. Scheme 1 is based on a single substrate turnover with the assumption of steady-state kinetics and a single enzyme binding site. K_m and V_{max} can be inferred from a graph, which can be used to determine the V_0 parameter.

Equation (4.1)

$$v_0 = \frac{V_{max}[S]}{K_m + [S]}$$

K_m can be calculated by:

Equation (4.2)

$$K_m = \frac{K_{cat} + K_2}{K_1}$$

V_{max} can be calculated by:

Equation (4.3)

$$V_{max} = K_{cat}[E_T]$$

4.4.3 The Kinetic Profile of *E. coli* PBP1B with dansDAP-LII C_{35} and C_{55} Polyprenyl Chain Lengths

The dependence of *Ec*PBP1B transglycosylase initial velocity on its substrate dans-DAP-LII with C_{35} and C_{55} prenyl tails was characterised (**Figure 4.5**).

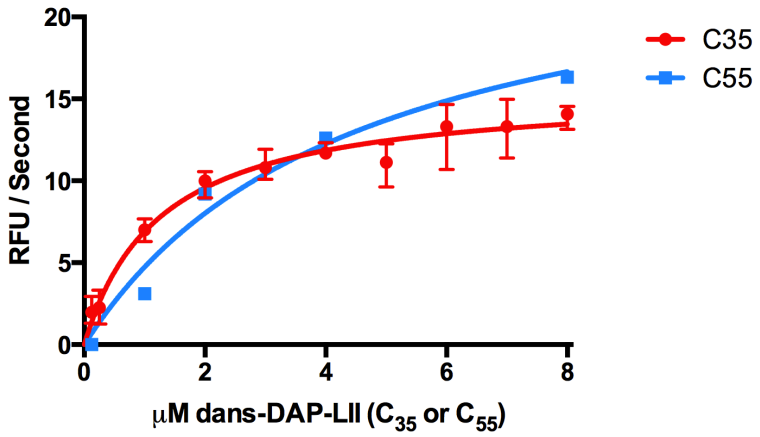

Figure 4.5 The Initial Rate of Transglycosylation in *Ec*PBP1B with Increasing dans-DAP-LII Substrate Concentration, using two substrates with different polyprenyl chain lengths. 50 nM *Ec*PBP1B used. Reaction conditions: 50 mM HEPES pH 7.5, 10 mM $MgCl_2$, 10% DMSO, 0.1 μg muramidase, 10 μM dans-DAP-LII. Both data sets were fitted to the Michaelis-Menten equation, Equation 4.1 using GraphPad Prism 6.

There is a hyperbolic relationship between the initial enzyme velocity (v_0) and the substrate concentration, enabling the data to be fitted to the Michaelis-Menten equation (Equation 4.1) to determine K_m and v_{max} by non-linear regression. The kinetic parameters for *Ec*PBP1B with both dans-DAP-LII C_{35} and dans-DAP-LII C_{55} (calculated using GraphPad Prism 6) are presented in **Table 4.1**.

Table 4.1 A Summary of the V_{max} and K_m data derived from the Michaelis-Menten equation for the two substrates dans-DAP-LII C_{35} and dans-DAP-LII C_{55}. The data was fitted to Equation 4.1 by non-linear regression, enabling kinetic constants to be derived.

Substrate	v_{max} (RFU / sec)	K_m (µM)	V_{max}/K_m (RFU/sec/µM)	R^2
Dans-DAP-LII C_{35}	15.3 ± 0.72	1.25 ± 0.23	12.2 ± 2.32	0.93
Dans-DAP-LII C_{55}	26.1 ± 5.10	4.49 ± 1.79	5.81 ± 2.58	0.97

The K_m for *Ec*PBP1B with dans-DAP-LII C_{35} was lower than for the C_{55} substrate equivalent, suggesting that *Ec*PBP1B has a higher affinity for the C_{35} substrate over the C_{55} substrate, also observed by Suzanne Walker and colleagues in Ye *et al*., 2001.

4.5 Buffer Optimisation Screening with *E. coli* PBP1A and *P. aeruginosa* PBP1A and PBP1B

The assay buffer conditions used in Schwartz *et al,*, 2002 were used as a starting point, however the percentage of DMSO was thought of as extremely high and was reduced from that published (25 %) to 10 % as this high DMSO concentration may interfere with protein-protein interactions. DMSO was subsequently shown to prevent the interaction between *E. coli* PBP1B and *E. coli* LpoB (Dr. A. J. Egan PhD Thesis, The University of Newcastle, 2014). In order to further characterise the transglycosylase activity of both *E. coli* and *P. aeruginosa* PBPs, the impact of pH, ionic strength and detergent choice on the activity of these enzymes was assessed and optimised in the following sections.

4.5.1 Optimal Detergent(s) for Transglycosylase Activity of *E. coli* and *P. aeruginosa* PBP1A

*Pa*PBP1A and *Ec*PBP1A were extracted and purified into four different detergents: CHAPS, DDM, LDAO and TritonX-100 according to (sections 2.4.6 and 2.5.1, e.g. Figure 3.10), to test which detergent(s) the enzymes would be active and stable in (**Figure 4.6**). Three of these detergents are non-ionic and CHAPS is zwitterionic. The percentage and concentration of each detergent used for both extraction and purification is summarised in **Appendix 1**.

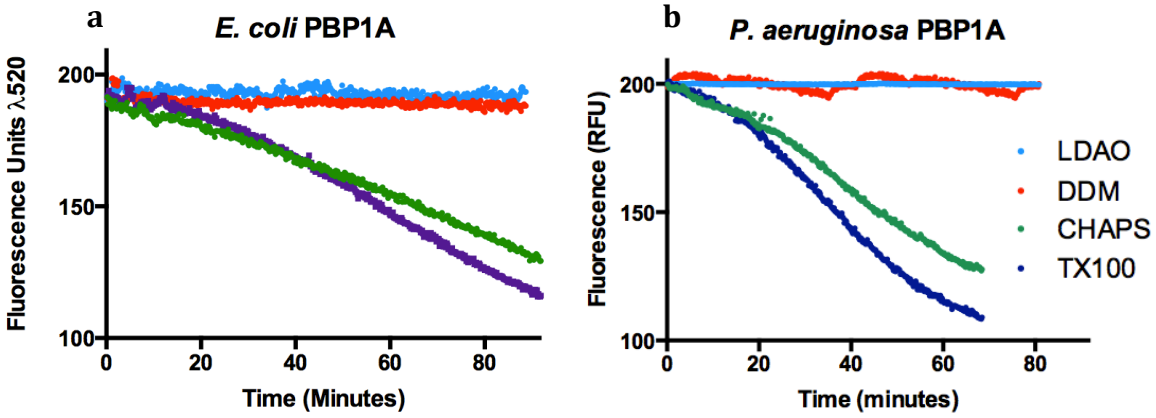

Figure 4.6 The Transglycosylase Activity of *Pa*PBP1A and *Ec*PBP1A in LDAO, DDM, CHAPS and TritonX-100 (a) *Pa*PBP1A **(b)** *Ec*PBP1A. Each detergent was present at 3xCMC final concentration in the assay. Reaction conditions: 50 mM HEPES, pH 7.5, 10 mM $MgCl_2$, 10% DMSO, 0.1 µg muramidase, 10 µM Dans-DAP-LII, 100 nM PBP1A.

*Pa*PBP1A and *Ec*PBP1A were both active in the detergents CHAPS and TritonX-100, but neither were active in LDAO or DDM. TritonX-100 was used for the remaining continuous assays, unless stated otherwise, as it is much cheaper than CHAPS and the two detergents showed little difference in PBP activity.

An alternative protocol for getting *Ec*PBP1A and *Pa*PBP1A into each of the four detergents. The CHAPS-purified PBP1A proteins were reconstituted in to another detergent of choice. The CHAPS-purified PBP1A proteins were used because of the properties of CHAPS and its extremely high CMC (0.49 %) and so samples can easily be diluted below the CMC. The PaPBP1A and EcPBP1A (CHAPS) enzymes were diluted sufficiently to reduce the concentrations of CHAPS to below its CMC, substituting the lipidic environment for the new detergent in the storage buffer. Although the PBPs were originally extracted and purified in CHAPS, they were subsequently exchanged into TritonX-100, DDM or LDAO. The same results as above were seen, where both *Ec*PBP1A and *Pa*PBP1A were active when exchanged to TritonX-100 and when conserved in CHAPS, but were inactive when exchanged in to DDM or LDAO.

4.5.2 Testing Optimal Detergent(s) for *P. aeruginosa* PBP1B Activity

*Pa*PBP1B did not show transglycosylase activity in the conditions that *Ec*PBP1A, *Ec*PBP1B, and *Pa*PBP1A had all shown activity. The enzyme was also extracted and

purified separately in to each of the four detergents (CHAPS, DDM, LDAO and DPC) to test transglycosylase activity in each environment (**Figure 4.7**).

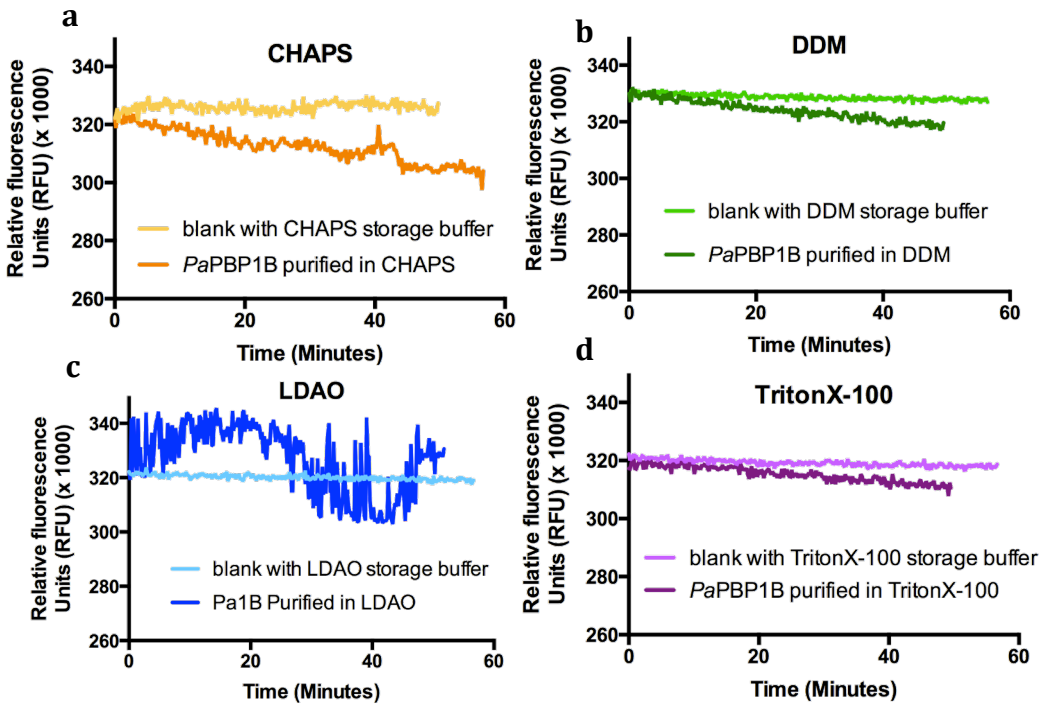

Figure 4.7 The Transglycosylase Activity of *P. aeruginosa* PBP1B after Extraction and Purification in to CHAPS, DDM, TritonX-100 and LDAO. (a) CHAPS **(b)** DDM **(c)** Triton-X100 and **(d)** LDAO. Reaction conditions: 50 mM HEPES, pH 7.5,10 mM $MgCl_2$, 10% DMSO, 0.1 µg muramidase, 10 µM dans-DAP-LII, 1 µM *Pa*PBP1B.

The only detergent in which *Pa*PBP1B exhibited significant changes in fluorescence, compared with the control in the zwitterionic detergent, CHAPS (a), but much lower activity than *Ec*PBP1A or *Pa*PBP1A. *Pa*PBP1B did not show enough activity to be able to continue any kinetic studies including determining its K_m with LII. Optimising the activity of *Pa*PBP1B will need further analysis as part of future work.

4.5.3 The Optimisation of pH for Transglycosylase Activity

pH can have substantial affects on the activity of an enzyme: protein structure, ionization state of the catalytically active amino acid and the behaviour of the substrate. The catalytic residue of transglycosylation is Glu86 in both *E. coli* and *P. aeruginosa* PBP1A, whose side chain is negatively charged and has a pK_a value between 4-7 depending on surrounding environment, which is deprotonated at pH 6-9. Before testing PBP1A activity, the effect of pH on the emission maximum of the dansyl group was

assessed. The λ_{max} of dans-LII remained unchanged at different pH. To test the effect of pH on the PBP1As, the initial velocity of transglycosylation was tested from pH 6.5 to 9.5 (**Figure 4.8**).

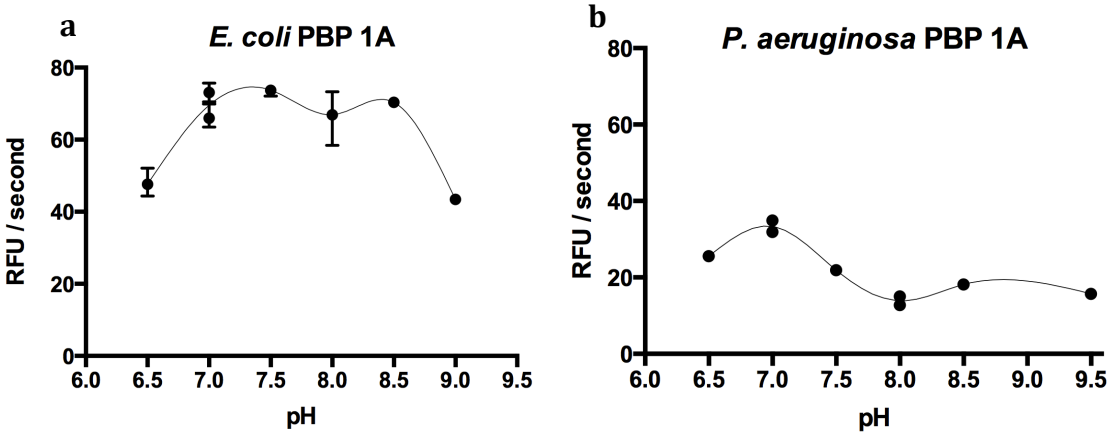

Figure 4.8 The Dependence of *E. coli* and *P. aeruginosa* PBP1A Transglycosylase Activity on pH. **(a)** The optimum pH for *Ec*PBP1A and **(b)** *Pa*PBP1A. The initial rate of transglycosylation was measured at different pH, using the continuous fluorometric transglycosylation assay. 50 mM buffer pH 6.5-9.5, 10 mM $MgCl_2$, 10% DMSO, 0.1 µg muramidase, 10 µM dans-DAP LII C_{55}, 100 nM PBP1A. The buffering agent used at pH 6.5 = CAPS, pH 7.0 = MOPS, pH 7.0 HEPES, pH 7.5 = HEPES, pH 8.0 = Tricine, pH 8.0 = BisTrisPropane (BTP), pH 8.5 = BTP, pH 9.0 = CHES, pH 9.5 = CHES.

*Ec*PBP1A has a pH maximum in HEPES at pH 7.5, with its transglycosylase activity varying in Tricine and BTP at pH 8.0. The conditions published in Schwartz *et al.,* for the optimal assay conditions for *Ec*PBP1B transglycosylase activity also concluded HEPES pH 7.5 (Schwartz *et al*., 2002). The 'shoulder' to the pH profile curve between pH 6.0 and 7.0 in (a) *Ec*PBP1A is significant and is probably due to loss of transglycosylase activity as the Glu86 residue is protonated. This suggests that the pK_a of this catalytic Glu86 residue in *Ec*PBP1A is in the range of pH 6.5-7.0.

With *Pa*PBP1A, there is no major change in activity over pH 6.5-9.5 but the pH optimum is 7.0 in HEPES. All subsequent transglycosylase assays were conducted in HEPES pH 7.5 for *Ec*PBP1A, and at pH 7.0 for *Pa*PBP1A.

4.5.4 The Optimisation of NaCl Concentration for Transglycosylase Activity

The concentration of sodium chloride and therefore the ionic strength in the assay could affect the activity of these Class A PBPs (**Figure 4.9**), as it has been shown that the

presence of NaCl has an inhibitory impact on the activity of *Ec*PBP1B (Adrian Lloyd, personal communication).

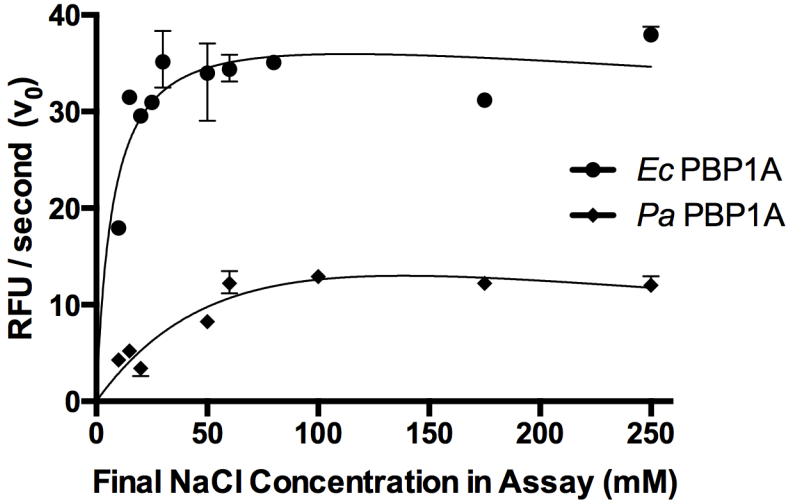

Figure 4.9 The Transglycosylase Activity of *E. coli* and *P. aeruginosa* PBP1A at Increasing Ionic (NaCl) Concentration, from 0-250 mM NaCl. Assays were conducted in 50 mM HEPES pH 7.0 for *Pa*PBP1A, pH 7.5 for *Ec*PBP1A, 10 mM $MgCl_2$, 10 % DMSO, 0.1 µg muramidase, 10 µM dans-DAP LII C_{55}, 0.5 µM PBP1A.

The activity of these two PBPs was enhanced with increasing NaCl concentration, up to a maximum of 60 mM NaCl. Beyond this concentration, no additional PBP activity was observed. In all subsequent transglycosylation assays, a total NaCl concentration of 60 mM was used. The data in Figure 4.9 was fitted to the Michaelis Menten Equation 4.1.

4.6 The Kinetic Characterisation of Transglycosylation of *E. coli* PBP1A and *P. aeruginosa* PBP1A and PBP1B

4.6.1 Dependence of *E. coli* PBP1A and *P. aeruginosa* PBP1A Transglycosylase Activity on Enzyme Concentration

As observed for *Ec*PBP1B, a linear relationship between enzyme concentration and initial velocity was confirmed. It was observed that at a lower LII concentration (3 µM), linearity was only observed at > 0.6 µM enzyme **Figure 4.10 (a)**, whereas when a higher LII concentration of 10 µM was used, a more typically linear relationship was seen **Figure 4.10 (b)**.

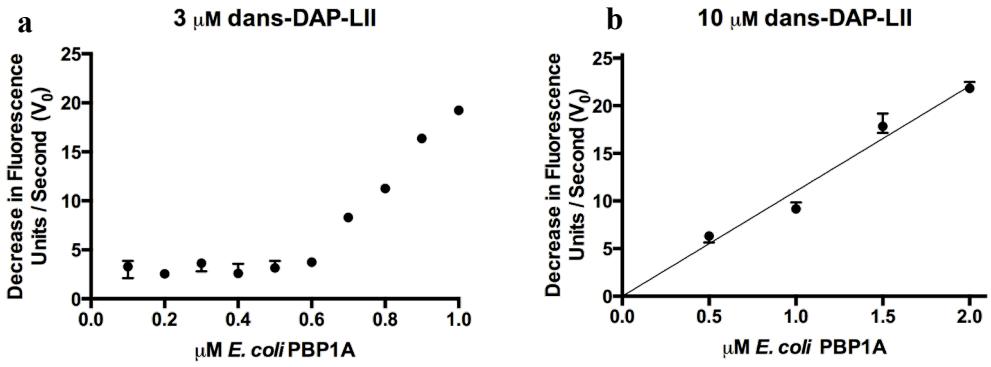

Figure 4.10 The Dependence of Initial Rate of Transglycosylation on *E. coli* PBP1A Concentration at 3 and 10 μM dans-DAP-LII. The relationship between the initial reaction rate of transglycosylation, and *Ec*PBP1A concentration. (**a**) 3 μM dans-DAP LII C_{55} and (**b**) 10 μM dans-DAP LII C_{55}. Reaction conditions: 50 mM HEPES pH 7.5, 10 mM $MgCl_2$, 60 mM NaCl, 10 % DMSO, 0.1 μg muramidase, *Ec*PBP1A was delivered to the assay in 0.02 % (v/v) TritonX-100.

The plot obtained when using a lower substrate concentration suggests that as the *Ec*PBP1A enzyme concentration in the assay increases to above 0.5 μM, a distinct change in enzyme activity occurred. This could indicate that the *Ec*PBP1A dimerises > 0.5 μM and the enzyme becomes more stable in a dimeric form. This difference in behaviour of the enzyme at different concentrations suggests either that substrate binding to the enzyme promotes an active conformation of *Ec*PBP1A or it could suggest that as *Ec*PBP1A dimerises upon reaching a threshold enzyme concentration and this in itself increases the turnover of the enzyme. In addition, it is highly possible that at these low concentrations of enzyme, the amount of detergent in the assay buffer reduces the frequency at which the PBP encounters and collides with its LII substrate, shielded by excess detergent. A further experiment reducing the amount of detergent to the absolute minimal amount would be ideal. *Ec*PBP1B in Figure 4.4 shows a linear relationship between enzyme concentration and initial reaction rate, which obeys classical Michaelis Menten kinetics more so than *Ec*PBP1A in Figure 4.10.

The dependence of the initial rates of transglycosylation for *Pa*PBP1A at two different substrate concentrations are compared below (**Figure 4.11**).

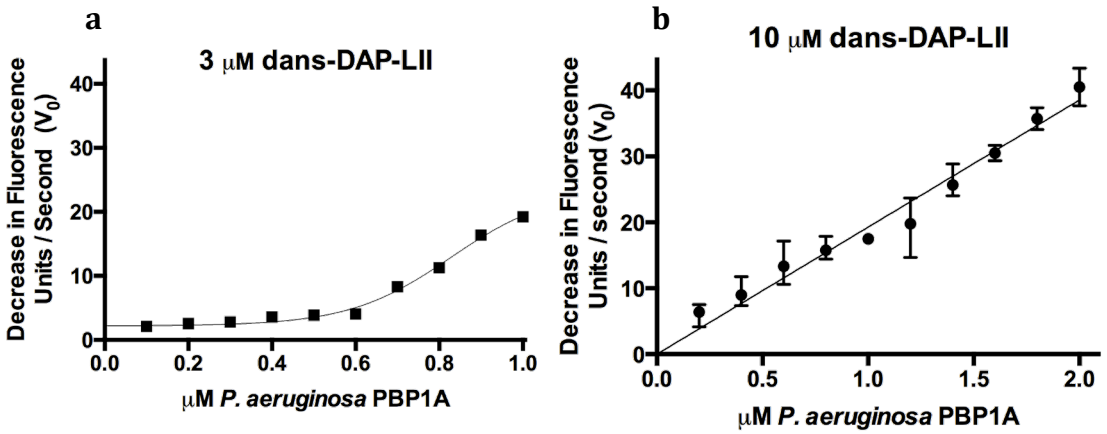

Figure 4.11 The Dependence of Initial Rate of Transglycosylation on *P. aeruginosa* PBP1A Concentration at 3 and 10 μM dans-DAP-LII. **(a)** 3 μM dans-DAP LII C_{55} and (**b**) 10 μM dans-DAP LII C_{55}. Reaction conditions: 50 mM HEPES pH 7.5 for *E. coli*, pH 7.0 for *P. aeruginosa*, 10 mM $MgCl_2$, 60 mM NaCl, 10% DMSO, 0.1 μg muramidase, 3-10 μM dans-DAP-LII C_{55}, *Pa*PBP1A was delivered to the assay in 0.02 % (v/v) TritonX-100.

The curve shown when using a lower substrate concentration shows that as the *Pa*PBP1A enzyme concentration in the assay increases to above 0.6 μM, the initial rate of reaction increases rapidly. The observed behaviour of *Pa*PBP1A is similar that seen for *Ec*PBP1A in Figure 4.10.

4.6.2 The Kinetic Profile of *E. coli* PBP1A and *P. aeruginosa* PBP1A

4.6.2.1 The Kinetic Profile of *E. coli* PBP1A and *P. aeruginosa* PBP1A with dansDAP-Lipid II C_{55} and C_{35}

The kinetic characterisation of *E. coli* and *P. aeruginosa* PBP1A was determined with dans-DAP-LII C_{55}, dans-DAP-LII C_{35} and dans-Lys-LII C_{55}. The affinity of the transglycosylase domain of two Class A PBPs (*E. coli* and *P. aeruginosa* PBP1A) for a variety of LII substrates was tested in the continuous fluorometric assay. All substrates investigated were labelled with a dansyl group for fluorescence detection and all assays were conducted as in (section 2.8.3).

It has been established that there is a linear relationship between *E. coli* PBP1A and *P. aeruginosa* PBP1A concentration and the initial transglycosylation rate. PBP1A concentrations used for *E. coli* and *P. aeruginosa* were selected where the relationship between v_0 and enzyme concentration is linear. The ability of these PBP1A enzymes to

utilise a variety of transglycosylase substrates from assessed, defining the V_{max} and K_m values for each enzyme and LII substrate combination. K_{cat} could not be calculated as the consumption of LII substrate could not be determined from change in fluorescence alone. The kinetic profiles of *Ec*PBP1A and *Pa*PBP1A with two LII substrates: dans-DAP-LII C_{55} and dans-DAP-LII C_{35} is displayed in **Figure 4.12**.

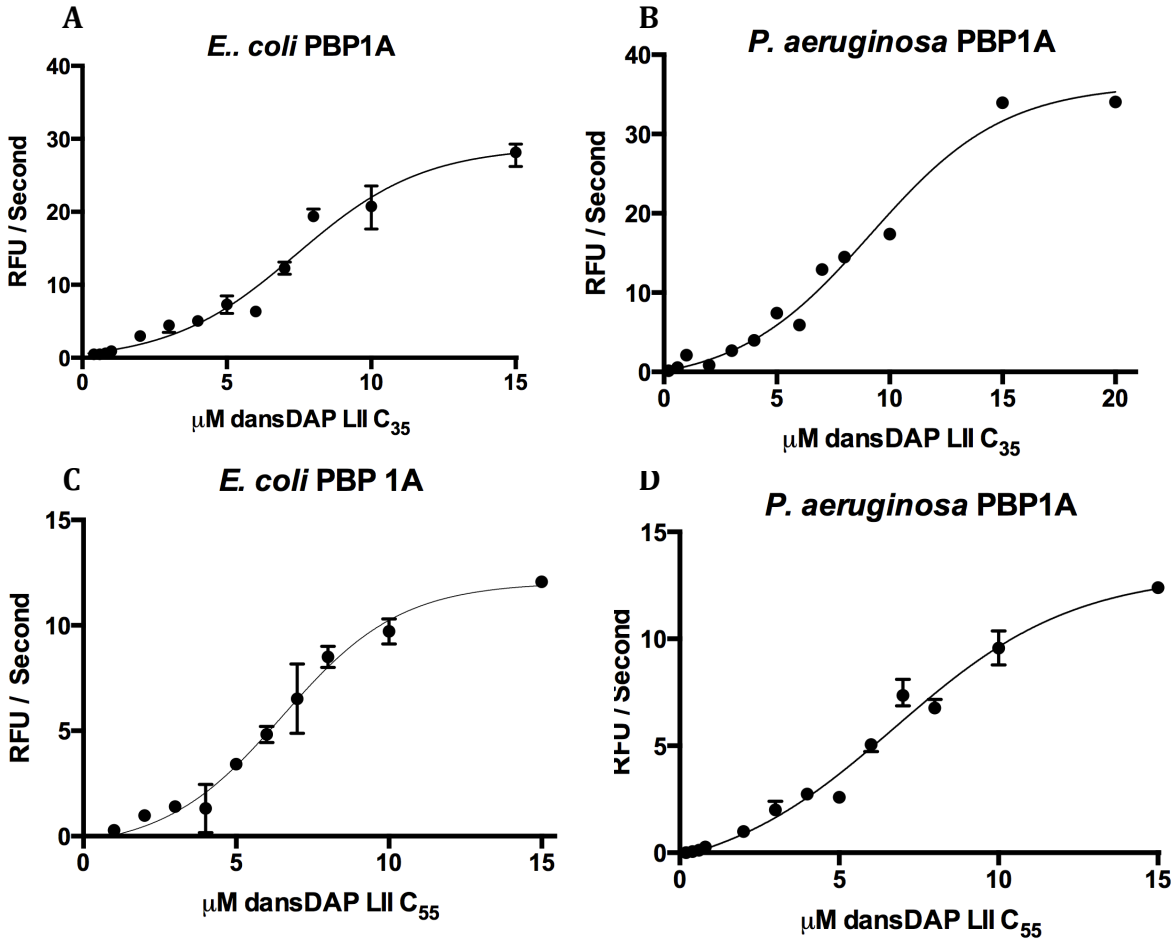

Figure 4.12 The Dependency of *E. coli* and *P. aeruginosa* PBP1A upon LII Substrate Concentration (dans-DAP-LII C_{55} and dans-DAP-LII C_{35}). The data was fitted to both the 'dual substrate' equation and the Hill Equation (section 4.5.2.2), with K_m and V_{max} derived values summarised in Tables 4.2-4.5. **(a)** *Ec*PBP1A with dans-DAP-LII C_{35} **(b)** *Pa*PBP1A with dans-DAP-LII C_{35} **(c)** *Ec*PBP1A with dans-DAP-LII C_{55} **(d)** *Pa*PBP1A with dans-DAP-LII C_{55}. Reaction conditions: 50 mM HEPES pH 7.5 for *E. coli*, pH 7.0 for *P. aeruginosa*, 10 mM $MgCl_2$, 60 mM NaCl, 10% DMSO (v/v), 0.1 μg muramidase, 0-15 μM dans-DAP-LII, 0.75 μM PBP1A was delivered to the assay in 0.02 % (v/v) TritonX-100. Each value represents the mean ± standard deviation of 3 reactions.

The resulting kinetic profiles are sigmoidal rather than the usual hyperbolic curves exhibited in traditional Michaelis-Menten kinetics. The sigmoidal shape reflects low enzyme activity at low substrate concentrations, with a rapid increase in enzyme activity

at higher substrate concentrations until V_{max} is achieved. An acceleration in v_0 is seen from 5 μM LII substrate onwards, suggesting that there is a minimum concentration of LII required (as well as PBP1A ≥ 0.5 μM) for an initial rate to be observed. Therefore this initial lag-phase observed in Figure 4.12 is in part related to the low LII concentration. This sigmoidal shape could also suggest that there are two different substrates throughout glycan chain polymerisation: (1) The LII monomers being incorporated into the growing glycan chain and (2) the polymerized glycan strand waiting to accept a nascent LII monomer. The binding of one substrate to the enzyme affects the affinity to which the other substrate can interact.

The poor fit of this data to the Michaelis Menten equation (Equation 4.1) indicates that this particular equation is an inappropriate model to fit the data to. Biochemical reactions with a single substrate often follow Michaelis Menten kinetics, however, Class A PBPs do not necessarily follow traditional Michaelis Menten kinetics as they can be described as having two substrates: a transglycosylase donor and acceptor substrate, which are both LII substrates. Alternative models were sought to fit this PBP1A kinetic data to, which considered two substrates separately for the transglycosylase domain during transglycosylation. The first substrate was the transglycosylase donor and the second substrate being the transglycosylase acceptor, defining values for two Km constants: Km_a and Km_b.

4.6.2.2 The Dual-Substrate Kinetic Equation and the Hill Equation

In vitro, transglycosylases perform *de novo* synthesis of glycan chains and require two LII substrate molecules to bind in to the active site (Scheme 2).

(Scheme 2) $[E] + [S] \underset{}{\overset{K_{m1}}{\rightleftharpoons}} [ES] \underset{- [S]}{\overset{K_{m2} + [S]}{\rightleftharpoons}} [ES_2] \xrightarrow{K_{cat}} [E] + [P]$

A kinetic equation that considers two substrates, can be derived from Scheme 2 (assuming that rapid equilibrium kinetics exist, K_{m1} and K_{m2} are equilibrium constants and that the substrate(s) remain unchanged over the initial rate measurements, which are based on the formation of Lipid IV from two molecules of LII. **Equation 4.4** considers both LII substrates, introducing a K_m for both the transglycosylase donor and acceptor. The derivation of Equation 4.4 is in **Appendix 2**.

$$\text{Equation (4.4)} \qquad v_0 = \frac{V_{max}[S]^2}{K_{mA}K_{mB} + K_{mB}[S] + [S]^2}$$

Under initial conditions, a single turnover of the PBP1A transglycosylase domain involves two moles of the same substrate per mol of enzyme. The dual-substrate equation considers a donor and an acceptor substrate that are both the same thing, generating K_m values for the acceptor and donor substrates separately. Under initial rate conditions, the majority of catalysis is likely to be the formation of Lipid IV: LII monomer + LII monomer. Over time, the donor substrate increases in length, constantly altering the donor substrate with the catalytic cycle.

The kinetic data for *E. coli* PBP1B with dansDAP-LII-C_{35} and C_{55} in Figure 4.5 was fitted to the dual-substrate equation (Equation 4.4) in addition to the Michaelis Menten equation, however a poor fit to the dual equation was observed for *E. coli* PBP1B, therefore this model does not represent the data as closely as the Michaelis Menten equation. The PBP1A data was fitted to this 'dual-substrate' equation (Equation 4.4) and the extracted kinetic constants for each enzyme and LII substrate combination is summarised in **Tables 4.2** to **4.5**.

The other equation sought to fit the kinetic data to was the Hill equation for cooperativity (**Equation 4.5**), where the binding of substrate molecule to one monomer of enzyme changes the affinity of another monomer (the enzyme must be dimer or tetramer).

$$\text{Equation (4.5)} \qquad v_0 = \frac{v_{max}[S]^h}{S_{0.5} + [S]^h}$$

The Hill coefficient (h) is used as a measure of cooperativity and a h value of >1.0 indicates positive cooperativity where the binding of one substrate molecule can induce structural or electronic changes that result in altered affinities for the vacant sites (Segel *et al.*, 1993). The sigmoidal shape of the curves that fit the Hill equation exhibit, indicate that there are two different substrates throughout glycan chain polymerisation: (1) The LII monomers being incorporated into the growing glycan chain and (2) the polymerized glycan strand waiting to accept a nascent LII monomer. The binding of one substrate to the enzyme affects the affinity to which the other substrate can interact.

4.6.2.3 The Kinetic Profile of *E. coli* PBP1A and *P. aeruginosa* PBP1A with dansLys-Lipid II C_{55}

The kinetic profile of *E. coli* and *P. aeruginosa* PBP1a with dansLys-LII C_{55} was conducted for comparison with that of dansDAP-LII-C_{55}. The K_m for the native substrate for Gram-positive rather than Gram-negative PBPs was determined for *E. coli* and *P. aeruginosa* PBP1a in **Figure 4.13**. The data was fitted to both the 'dual-substrate' equation and the Hill Equation, with K_m and V_{max} derived values summarised in Tables 4.2-4.5. The derived kinetic constants are summarised in **Tables 4.2-4.5**.

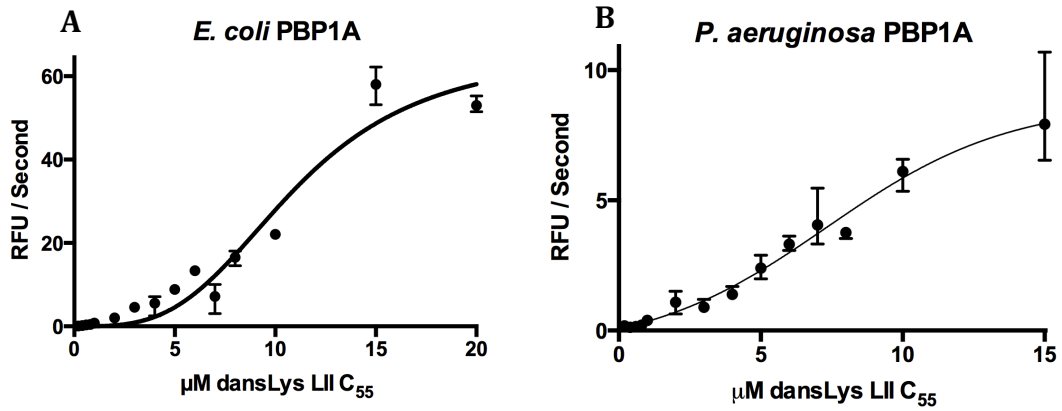

Figure 4.13 The Dependency of *E. coli* and *P. aeruginosa* PBP1A upon dansLys-LII C_{55} Substrate Concentration. The data was fitted to both the 'dual-substrate' equation and the Hill Equation, with K_m and V_{max} derived values summarised in Tables 4.2-4.5. Values represent mean ± standard deviation of 3 reactions. The curve illustrated in this figure is the data fitted to the dual-substrate equation **(a)** *Ec*PBP1A and **(b)** *Pa*PBP1A with the non-canonical substrate dansLys-LII. Reaction conditions: 50 mM HEPES pH 7.5 for *E. coli*, pH 7.0 for *P. aeruginosa*, 10 mM $MgCl_2$, 60 mM NaCl, 10% DMSO (v/v), 0.1 μg muramidase, 0-20 μM dansLys-LII C_{55}, 0.75 μM PBP1A was delivered to the assay in 0.02 % (v/v) TritonX-100, n = 3.

The sigmoidal kinetic profile suggests again that there are two substrates in this polymerisation, with monomer LII molecules being joined to other LII molecules initially, and subsequently glycan strands becoming the substrate for elongation with additional LII moieties. For *Ec*PBP1A with dansLysLII (Figure 4.13a), the data was fitted to the dual-substrate equation (Eq. 4.4) with an R^2 value of 0.87 but Prism identified the fit as 'ambiguous'. However, when the data was fitted to the Hill equation (Eq 4.5) the R^2 value was 0.94 and was deemed to be a more appropriate fit by GraphPad Prism (Table 4.2 and 4.3). *P. aeruginosa* PBP1A with dansLys-LII fitted to both equations but the fit to the Hill equation was optimal (Table 4.4 and 4.5). V_{max}/Km

and $V_{max}/S_{0.5}$ were calculated measures of catalytic efficiency and suggest that dansLII-C_{35} is a preferred substrate over dansLII-C_{55}, confirming the published finding that the shorter lipid chain minimises the possibility of aggregation as observed with the undecaprenyl pyrophosphate in LII-C_{55} *in vitro* (Ye *et al.,* 2001).

Table 4.2 The Kinetic Parameters for *E. coli* PBP1A Transglycosylase Activity Fitted to the Dual-Substrate Equation. Data in Figures 4.12 and 4.13 was fitted to Equation 4.4.

LII substrate	V_{max} (RFU/sec)	K_m (μM)	V_{max} / K_m (RFU/sec/μM)	R^2
dansDAP LII C_{55}	17.48 ± 8.02	Ambiguous fit	N/D	-
dansDAP LII C_{35}	22.85 ± 10.52	1: 9.92 ± 2.96 2: 10.67 ± 3.37	1: 2.30 2: 2.14	0.96
dansLys LII C_{55}	Ambiguous fit	N/D	N/D	-

Table 4.3 The Kinetic Parameters for *E. coli* PBP1A Transglycosylase Activity Fitted to the Hill Cooperativity Equation. Data in Figures 4.12 and 4.13 was fitted to Equation 4.5.

LII Substrate	V_{max} (RFU/sec)	$S_{0.5}$ (μM)	V_{max} / $S_{0.5}$ (RFU/sec/μM)	Hill Coefficient	R^2
dansDAP LII C_{55}	13.12 ± 0.97	6.97 ± 0.44	1.88 ± 0.18	3.19 ± 0.44	0.97
dansDAP LII C_{35}	38.66 ± 5.59	9.41 ± 1.40	4.11 ± 0.85	2.25 ± 0.32	0.96
dansLys LII C_{55}	66.21 ± 6.58	11.00 ± 0.99	6.02 ± 0.81	3.29 ± 0.50	0.94

Table 4.4 The Kinetic Parameters for *P. aeruginosa* PBP1A Transglycosylase Activity Fitted to the Dual-Substrate Equation. Data in Figures 4.12 and 4.13 was fitted to Equation 4.4.

LII substrate	V_{max} (RFU/sec)	K_m (μM)	V_{max} / K_m (RFU/sec/μM)	R^2
dansDAP LII C_{55}	17.47 ± 4.66	Ambiguous fit	N/D	
dansDAP LII C_{35}	25.57 ± 4.72	1: 13.46 ± 2.40 2: 11.86 ± 2.23	1:1.90 2: 2.16	0.97
dansLys LII C_{55}	15.63 ± 1.60	1: 7.64 ± 1.31 2: 13.02 ± 2.89	1: 2.05 2: 1.20	0.92

Table 4.5 The Kinetic Parameters for *P. aeruginosa* PBP1A Transglycosylase Activity Fitted to the Hill Cooperativity Equation. Data in Figures 4.12 and 4.13 was fitted to Equation 4.5.

LII Substrate	V_{max} (RFU/sec)	$S_{0.5}$ (μM)	V_{max}/$S_{0.5}$ (RFU/sec/ μM)	Hill Coefficient	R^2
dansDAP LII C_{55}	16.48 ± 1.67	8.81 ± 0.97	1.87 ± 0.28	2.13 ± 0.22	0.98
dansDAP LII C_{35}	43.27 ± 3.90	10.60 ± 1.02	4.08 ± 0.54	2.48 ± 0.29	0.97
dansLys LII C_{55}	14.00 ± 5.12	12.60 ± 5.46	1.11 + 0.63	1.70 ± 0.36	0.92

The determined K_m values of *Ec*PBP1B transglycosylase domain for dansDAP-LII-C_{35} vs. dansDAP-LII-C_{55} are 1.1 μM vs 4.5 μM, respectively, demonstrating a higher affinity towards the shorter (C_{35}) prenyl chain lipid.

Kinetic constants were determined for PBP1A from *E. coli* and *P. aeruginosa*, extracted by fitting the data to two equations (dual-substrate and Hill equations). The affinity for dansDAP-LII-C_{35} and slightly lower than that of dansDAP-LII-C_{55}, with less deviation between the two compared to the difference in K_m values between these substrates obtained for *Ec*PBP1B. The $S_{0.5}$ value (substrate concentration at half maximal rate) for *Ec*PBP1A with dansDAP-LII-C_{55} was determined as 6.97 ± 0.44 μM when fitted to the Hill equation, compared to 9.41 ± 1.40 μM for dansDAP-LII-C_{35} indicating that *E. coli* PBP1A has a slight preference for LII with a C_{55}-prenyl chain compared to LII with a C_{35}-prenyl chain.

Comparing the affinity of *E. coli* PBP1A for DAP vs Lys-LII demonstrated a preference for DAP-LII, which was expected as *meso*DAP is the native substrate for Gram-negative PBPs. The $S_{0.5}$ values (determined by data fitting to the Hill equation) for *Ec*PBP1A and dansDAP-LII was 6.97 ± 0.44 μM compared with 11.00 ± 0.99 μM for dansLys-LII.

As for *P. aeruginosa* PBP1A, the results in Table 4.4 and 4.5 echo that of *Ec*PBP1A with a preference for dansDAP-LII-C_{35}. The $S_{0.5}$ values obtained by fitting the data to the Hill equation were 8.81 ± 0.97 and 10.60 ± 1.02, respectively, suggesting a small preference for the native C_{55} substrate. There was very little difference in the $S_{0.5}$ values between dansLys-LII-C_{55} and dansDAP-LII-C_{55}.

4.7 The Activity of Transglycosylase Active Site Mutants

The three Class A PBPs that have thus far exhibited transglycosylase activity were mutated at their transglycosylase active site. The transglycosylase active-site mutants of *E. coli* PBP1A (E86Q), PBP1B (E233Q) and *P. aeruginosa* PBP1A (E86Q) were genetically engineered by site-directed mutagenesis, and the proteins were purified according to section 2.5.1. The transglycosylase activity of these catalytic active-site mutants were analysed using the continuous fluorometric assay (**Figure 4.14**).

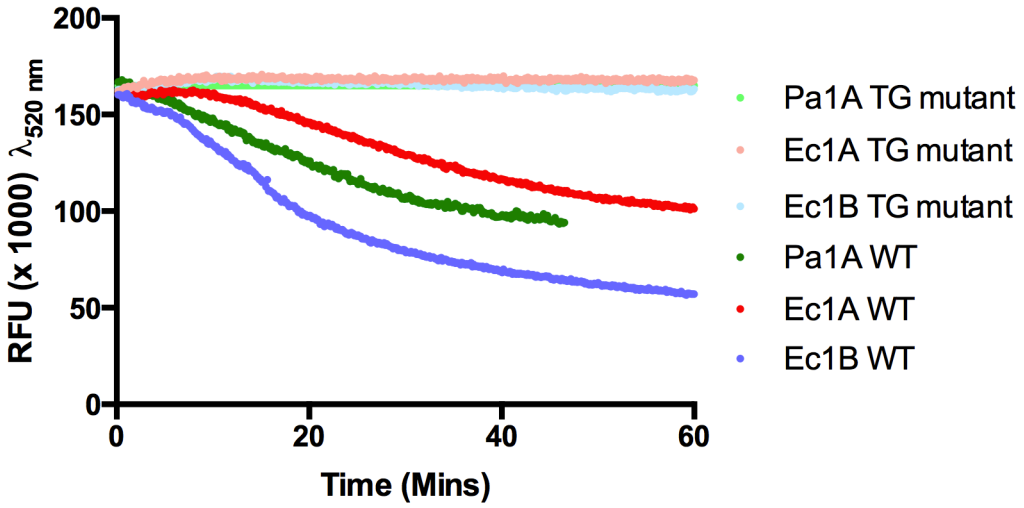

Figure 4.14 The Transglycosylase Activity of PBP Transglycosylase Active-Site Mutants. *Ec*PBP1A (E86Q), *Ec*PBP1B (E233Q) and *Pa*PBP1A (E86Q). Transglycosylase mutants are in pastel colours, wildtype PBP activities are in bold colours.

All the wildtype PBPs exhibited their expected transglycosylase activity and the proteins with the mutated (glutamate to glutamine) transglycosylase active site did not demonstrate any ability to polymerise LII, further confirming the necessity of the glutamate for transglycosylase activity.

4.8 The Effect of PBP-Associated Proteins on Transglycosylase Activity

Recently there have been advancements in the knowledge of PB-associated proteins and how these proteins interact with, and stimulate PBP activity. The outer-membrane proteins LpoA and LpoB regulate peptidoglycan synthesis (Typas *et al.,* 2010, Paradis-Bleau *et al.*, 2010). It was published that *Ec*LpoA stimulates the transpeptidase activity of *Ec*PBP1A, and *Ec*LpoB stimulates both the transpeptidase and transglycosylase activities of *Ec*PBP1B. This theory was tested with *Ec*PBP1A and *Pa*PBP1A.

4.8.1 The Effect of *E. coli* LpoA, LpoB and *P. aeruginosa* LpoA upon the Transglycosylase Activity of PBP1A

As *Ec*LpoB stimulates *Ec*PBP1B transpeptidase activity and *Ec*LpoA stimulates both *Ec*PBP1A transpeptidase and transglycosylase activities, the affect of *Pa*LpoA on the transglycosylase activity of *Pa*PBP1A was investigated and compared to that of *E. coli* (**Figure 4.15**). It is possible that the transglycosylase function of *Pa*PBP1A is stimulated as a consequence of transpeptidase stimulation *via* LpoA binding to the ODD domain.

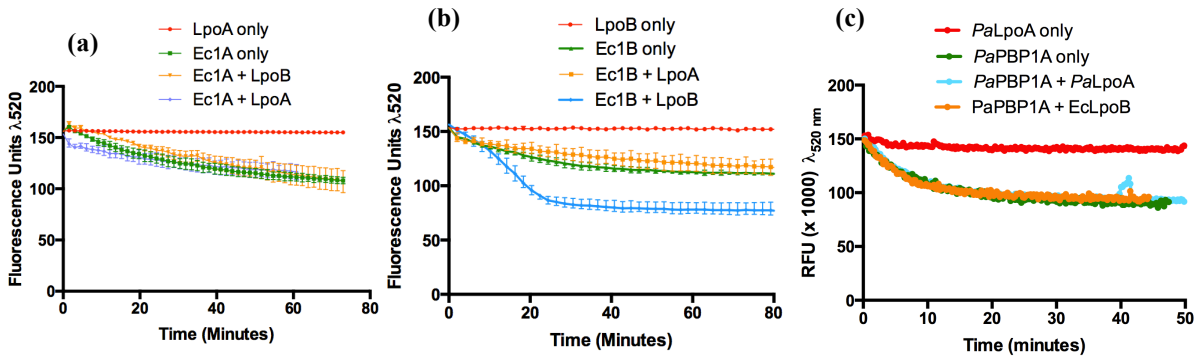

Figure 4.15 The Effect of PaLpoA upon the Transglycosylase Activity of *Pa*PBP1A (c), alongside **(a)** the affect of *Ec*LpoA on *Ec*PBP1A transglycosylase activity and **(b)** *Ec*LpoB on *Ec*PBP1B transglycosylase Activity. Reaction conditions: 50 mM HEPES pH 7.5, 10 mM $MgCl_2$, 60 mM NaCl, 10% DMSO, 0.1 µg muramidase, 10 µM dansDAP-LII C_{55}, 0.5 µM *Ec/Pa* PBP1A was used in each assay, 1.5 µM *Ec*LpoA, 1.5 µM *Ec*LpoB, 1.5 µM *Pa*LpoA.

*Ec*LpoA stimulates the transpeptidase domain of *Ec*PBP1A, but has no affect on transglycosylase activity (Lupoli *et al.*, 2014), equally, *Pa*LpoA does not show any stimulation of the transglycosylase activity of *Pa*PBP1A. The effect of *Pa*LpoA upon the transpeptidase activity of *Pa*PBP1A is discussed in section 6.9.3. A dose-response curve of *Ec*PBP1B to increasing concentrations of both *Ec*LpoA and LpoB is illustrated in **Figure 4.16**.

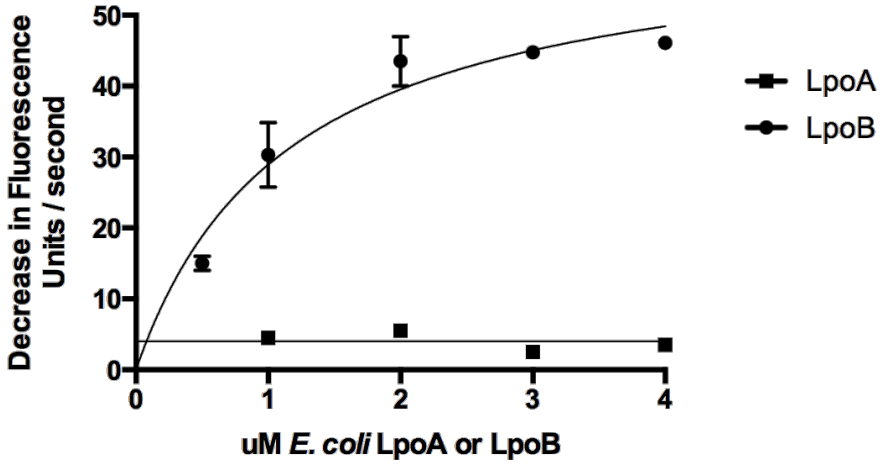

Figure 4.16 A Dose-Response of *Ec*PBP1B Transglycosylase Activity to *Ec*LpoB and *Ec*PBP1A Transglycosylase Activity to *Ec*LpoA. A titration of *Ec*LpoA and LpoB outer lipoproteins with their cognate PBPs. Reaction conditions: 50 mM HEPES pH 7.5, 10 mM $MgCl_2$, 60 mM NaCl, 10% DMSO, 0.1 µg muramidase, 10 µM dans-DAP-LII C_{55}, 0.5 µM PBP1B used in each assay.

*Ec*PBP1B transglycosylase activity is stimulated with increasing concentrations of *Ec*LpoB, however, *Ec*PBP1A transglycosylase activity is not stimulated by the presence of *Ec*LpoA. In Chapter 6, the transpeptidase activity of *Pa*PBP1A, *Ec*PBP1A and *Ec*PBP1B are stimulated by the presence of *Pa*LpoA, *Ec*LpoA and *Ec*LpoB respectively.

4.8.2 The Effect of *E. coli* PBP2 and FtsN on the Transglycosylase Activity of Class A PBPs

The monofunctional *Ec*PBP2 was shown to stimulate the transglycosylase activity of *Ec*PBP1A, and *E. coli* FtsN stimulates transglycosylase activity in *Ec*PBP1B (Bertsche *et al.*, 2005). This was extended to *P. aeruginosa* to see if *Ec*PBP2 and/or *Ec*FtsN had an effect on the transglycosylase activity of *Pa* Class A PBPs (**Figure 4.17**). *E. coli* PBP3 was shown to have no effect on the transglycosylase activity of *Ec*PBP1B (Egan PhD Thesis, 2014), to which it interacts and PBP3 does not interact with *Ec*PBP1A, so no PBPs were chosen to be tested with PBP3. The amount of TritonX-100 in the assay buffer was adjusted to compensate for the addition of TritonX-100 in the storage buffers of the PBP-associated proteins, to ensure a consistent final TritonX-100 concentration in each reaction, of 0.2 %.

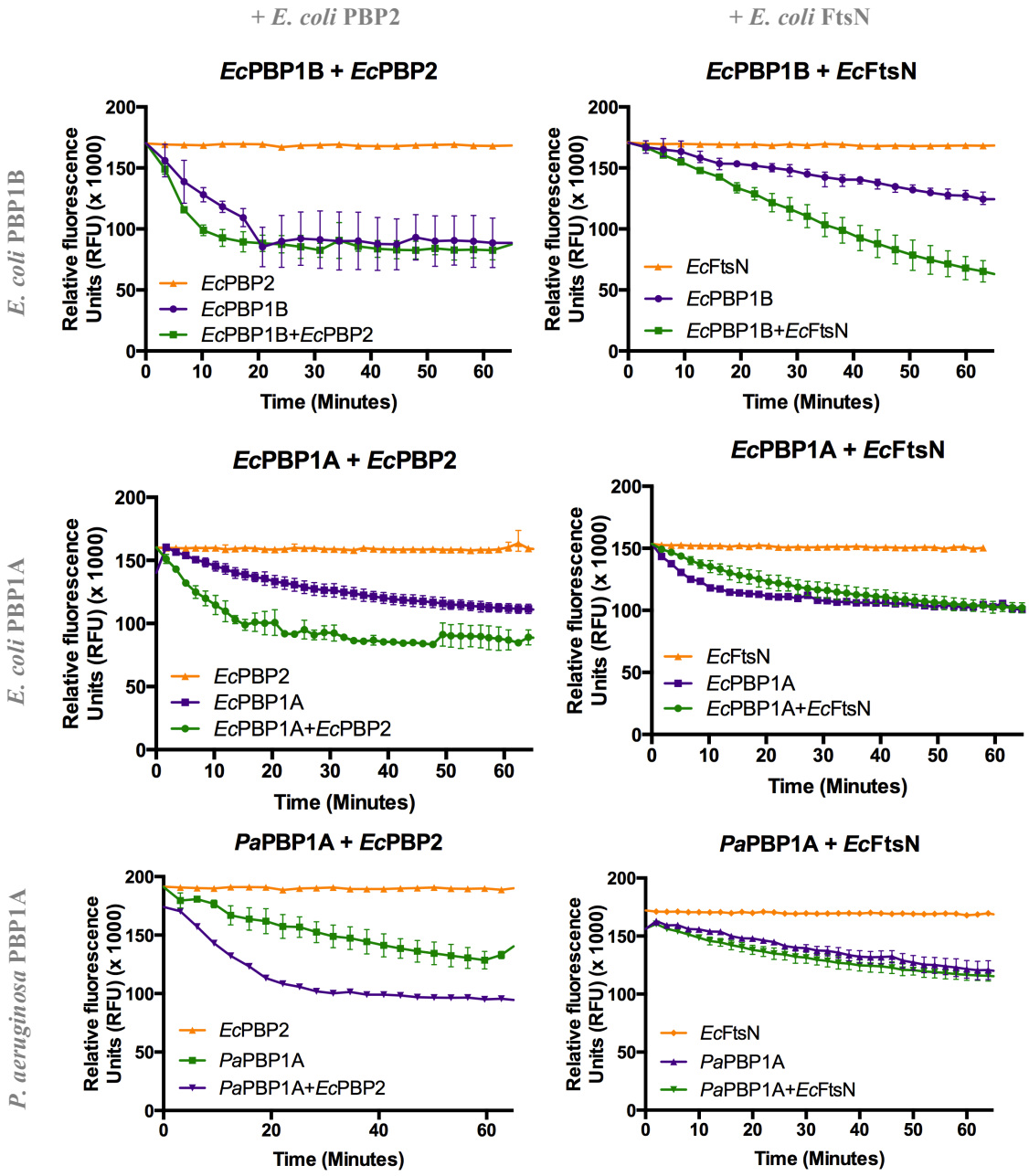

Figure 4.17 The Effect of *E. coli* FtsN and PBP2 on PBP1A and PBP1B. Graphs labelled with specific proteins accordingly. Reaction conditions: 0.5 µM *Ec*PBP2, 0.5 µM *Ec*PBP3, 0.5 µM PBP. 50 mM HEPES pH 7.5, 10 mM $MgCl_2$, 60 mM NaCl, 10% DMSO, 0.1 µg muramidase, 10 µM dansDAP-LII-C_{55}.

The affect of *Ec*PBP2 and *Ec*FtsN on the transglycosylase activities of *Ec*PBP1B were assayed for comparison with that of both *Ec*PBP1A and *Pa*PBP1A (Figure 4.17). The presence of *E. coli* PBP2 with *Ec*PBP1B in a transglycosylase assay demonstrated little enhancement in the initial reaction rate of transglycosylation, with the amount of LII consumed plateauing to the same amount. In the presence of *Ec*FtsN, however, a 2-3-fold enhancement of transglycosylation by *Ec*PBP1B was observed. For *E. coli* PBP1A,

the presence of *Ec*PBP2 showed a 2-3-fold enhancement in transglycosylation activity but no enhancement in activity in the presence of FtsN. As for *P. aeruginosa* PBP1A, *Pa*PBP1A transglycosylase activity was slightly increased by as much as 10-20% in the presence of *E. coli* PBP2, and *Pa*PBP1A transglycosylase activity was not stimulated by *E. coli* FtsN. What is interesting is that *Ec*PBP2 also had a slight stimulatory affect on its non-cognate PBP, *Ec*PBP1B, at least upon the initial rate of transglycosylation.

4.9 Discussion

4.9.1 Plate Reader versus Fluorimeter for Transglycosylase Activity Measurement

Using the plate reader to measure the fluorescence output of the continuous transglycosylase reaction rather than doing individual assays in a cuvette in a fluorimeter is beneficial for high-throughput screening and reduces material requirements. However, as a 96-well plate has a lower path length compared to the 1 cm path length of a cuvette, the background noise and light scattering increases in a plate well compared to a cuvette. The increase in assay noise from using a shorter assay path length is highlighted when analogous results from a 1 cm path length cuvette assay in a fluorimeter are compared with that from a much shorter path length in a plate reader. The advantage of reduction in assay volume from 200 µL in a cuvette to 25 µL in a well outweighs any issue with background noise, due to the more high-through-put nature of a 96-well plate, and the cost saving on the LII substrate. The major disadvantage of the plate reader is that the assay initiator, e.g. PBP enzyme is added externally by a multi-channel pipette, and readings are taken when the 96-well plate is back inside the equipment. This misses the very initial rate of the reaction, and could be avoided if dispensers were used to add the enzyme to each well, removing the need to remove the plate from the reader. This is suitable if there is enough PBP enzyme to prime the dispenser lines beforehand and not run out of reagents half way through. Using dispensers places a higher demand on the use of enzyme, but if this can be afforded, it is preferable as it allows the easier capture of the initial rate of reaction.

The linear regression curve should pass through the origin, as in the absence of enzyme the rate should also be zero. A suggestion for why the curve does not pass through the

origin could be an artifact of the assay technique itself. The assay is initiated in a 96-well plate using a multi-channel pipette and upon initiation to plate is automatically returned to the plate reader machine and measurements are resumed. The very initial reaction rate is missed between final reagent addition and the first fluorescence measurement, which could justify why initial rates above zero are being observed at the initial fluorescence measurement, 'time zero'. As all transglycosylation assays have been conducted in a uniform manner through this body of work, all assays are directly comparable to each other.

The transfer of the spectrophotometric phosphate release assay in to a plate reader format would speed up the testing of the range of reaction conditions and would save reagents. The assay is very low-throughput at present in a cuvette. With more time, a plate reader format for this assay would be pursued.

4.9.2 Different Substrates Exhibit Different Levels of Fluorescence in the Continuous Assay

The kinetic profile of each PBP was characterised with a range of substrates, including dans-DAP-LII C_{35} and dans-DAP-LII C_{55} and the Lysine equivalents. The proportion of dansylation of C_{35} LII and C_{55} LII could be different to each other, as the length of the polyprenyl chain could interfere with the successful dansylation of the pentapeptide stem. The different levels of fluorescence between the different substrates need to be taken in to account in future studies.

4.9.3 Defining the Optimum pH of the Transglycosylase Activity of PBPs

Upon testing the pH optimum of *Pa*PBP1A and *Ec*PBP1A, a biphasic profile was observed for *P. aeruginosa* PBP1A, which could indicate different orientations of either the PBP or the LII in detergent, exposing different regions. However it is more likely that it is due to experimental setup. The relationship between pH and activity could be affected by the buffer salt used. In the event that this experiment was repeated, the same buffer salt would be tested across a small range of pH, to rule out any effect of the individual buffer salts on PBP activity.

4.9.4 The Effect of Detergent on Substrate Fluorescence in the Continuous Assay

Different detergents may have varying impacts on the efficiency of fluorescence of the dansylated-LII substrate in the continuous reaction. It is not known how each detergent specifically affects the levels of fluorescence and the emission spectra of the dansyl moiety, but this should be considered and taken in to account in future studies.

4.9.5 *P. aeruginosa* PBP1A and *E. coli* PBP1A Transglycosylase Kinetics

The dependency of initial reaction rate upon substrate concentration was investigated using the continuous fluorometric assay for transglycosylation, generating kinetic constants for *E. coli* PBP1A and *P. aeruginosa* PBP1A. The data was initially fitted to the traditional Michaelis-Menten equation with little success as the fits were so poor. The dual-substrate equation (Equation 4.4) which takes each kinetic cycle and binding of two LII substrates, was a better fit than the Michaelis-Menten equation, but the Hill equation of cooperativity was the optimal fit for these kinetics. The Hill equation is a modified Michaelis-Menten equation that takes cooperativity of substrate binding in to consideration. Therefore it can be concluded that the transglycosylation kinetics of *E. coli* and *P. aeruginosa* PBP1A assumes cooperativity. The Hill coefficients (h) for both proteins with all three substrates was > 1.0, indicating positive cooperativity (Table 4.3 and 4.5). All coefficients were between 1.7 - 3.29 and these Hill values can be used to estimate the number of binding sites involved in cooperativity (Segel *et al.*, 1993). The $S_{0.5}$ values show that the LII substrates had a marginally higher affinity for *E. coli* PBP1A over *P. aeruginosa* PBP1A. Although it could be argued that it is possible that *P. aeruginosa* PBP1A had fewer functional active sites than the *E. coli* PBP1A batch, and that the specific activity of the transglycosylase domain differs between the two proteins, as this was not assayed.

The fact you do not see this behavior in the presence of 10 μM DAP-LII might indicate that substrate binding promotes the active conformation of the *E. coli* PBP1A (whether this is due to dimerization or whatever else that might cause this). If dimerization is the cause of this it suggests that the substrate decreases the Kd for subunit association. Of course, if there is a reciprocal relationship in that dimerization increases the turnover of

the enzyme, this in itself might be enough to explain the non-Michaelis-Menten kinetics observed.

For some transglycosylases, it has been suggested that the formation of the Lipid IV intermediate is the rate-limiting step of processive polymerisation (Wang *et al.,* 2011). The binding of Lipid IV causes a rearrangement / reassortment of the active site of the enzyme, which upon completion gives an enhanced catalytic capability and promotes a faster reaction rate. This hypothesis could account for the initial lag phase observed in the assays of a range of transglycosylases *in vitro* (Schwartz *et al.*, 2002, Barrett *et al*., 2005, Chen *et al*., 2003, Wang *et al*., 2011). It has been shown that *Ec*PBP1A and *Ec*PBP1B (as well as *S. aureus* PBP2 and MGT) all lose their initial lag phase when pre-incubated with (a chemically blocked galactose adduct form of) Lipid IV (Wang *et al*., 2011).

4.10 Conclusions

All three Class A bifunctional enzymes showed transglycosylase activity using the continuous fluorometric assay, although *Pa*PBP1B did not show full activity in any detergent tested, but potentially showed some activity in the detergent CHAPS and further investigation is needed with this enzyme. The two other enzymes were active in both TritonX-100 and CHAPS. The pH screen returned a pH optimal of pH 7.5 for *Ec*PBP1A, and 7.0 for *Pa*PBP1A.

All three enzymes showed activity with different substrates, with varying carbon tail lengths as well as with both dansDAP-LII and the Gram-positive Lysine variant of LII. Kinetic data for *Ec*PBP1A and *Pa*PBP1A did not fit Michaelis-Menten kinetics and fitted more readily to the Hill equation of cooperativity, additionally, they both exhibit similar kinetic behaviour when investigating their dependence on enzyme concentration.

As expected, the transglycosylation activity of *Ec*PBP1B was stimulated in the presence of *E. coli* FtsN and *Ec*PBP1A was stimulated in the presence of *E. coli* PBP2. As there was no DNA construct readily available for *Pa*PBP2, the purified *Ec*PBP2 protein was tested for its ability to enhance the transglycosylase activity of *Pa*PBP1A, which

showed a small stimulation (10-20 %) in transglycosylase activity. *E. coli* PBP2 enhanced the transglycosylase activity of *Ec*PBP1A by 2-3 fold, but not *Pa*PBP1A. Cloning *Pa*PBP2 would be of interest to assess the stimulatory affect of PBP2 upon PBP1A transglycosylase activity in *P. aeruginosa*.

4.11 Future Work

4.11.1 Optimising the Detergent for Transglycosylation Activity

The detergents tested in this chapter for transglycosylase activity optimisation were all non-ionic (electrically neutral) detergents. The ExCy range of detergents demonstrated the best transglycosylation activity out of the non-ionic detergents tested. Other detergent families including anionic, cationic and amphoteric detergents could be tested for their suitability to aid transglycosylase activity. Detergents create detergent micelles; alternatively, membrane mimetics maintain protein solubility and stability by encasing the protein in a lipid bilayer. n-dodecyl phosphocholine (DPC) is an example of a membrane mimetic, commonly used for high-resolution NMR structures. Nanodiscs are another technique employed in structural characterisation studies. They are much smaller than detergents and have a much smaller curvature, hence they reduce light scattering in biophysical structural techniques. Styrene Maleic Acid co-polymer Lipid Particles (SMALPs) are a type of lipid bilayer nanodisc being used for activity and structural studies of membrane proteins (Dafforn *et al.*, 2010).

4.11.2 Further Investigation of *Pa*PBP1B Activity

The investigation of *Pa*PBP1B activity should be pursued further to identify the conditions under which *Pa*PBP1B is active. This could include the buffer conditions used or another detergent entirely. The zwitterionic detergent CHAPS was the detergent that potentially showed some activity of *Pa*PBP1B, so exploring zwitterionic detergents further would be useful for investigating *Pa*PBP1B activity.

*Pa*PBP1B was tested for extraction and purification in to Styrene Maleic Acid co-polymer Lipid Particles (SMALPs), but the over-expressed protein was not successfully extracted by the nanodisc. This method could be tried again, using a larger culture

growth and expression of *Pa*PBP1B. The cloning of a range of different constructs would be advised, with a His_6 tag at the N- and the C-terminus, separately.

4.11.3 The Lack of an LpoB Protein in *Pseudomonas aeruginosa.*

*Pa*PBP1B did not show transglycosylase activity to the same extent as *Ec*PBP1A or *Pa*PBP1A. It is possible that this protein requires a longer substrate as a primer for polymerisation to proceed. *Pa*PBP1B did not show enough activity to be able to continue any kinetic studies including determining its K_m with LII. Optimising the activity of *Pa*PBP1B will need further analysis as part of future work. Determining whether *E. coli* LpoB is capable of stimulating the transglycosylase activity of *Pa*PBP1B would also be of interest. If *Ec*LpoB were to positively enhance the transglycosylase activity of *Pa*PBP1B, it may indicate the presence of an equivalent LpoB protein in most *Pseudomonas spp*.

Chapter 5
A Discontinuous Spectrophotometric Assay for The Detection of Transglycosylase-Dependent Undecaprenyl Pyrophosphate Production

5.1 Transglycosylation Generates the By-Product Undecaprenyl Pyrophosphate (C_{55}-PP)

Structural modification of LII can interfere with activity of the enzyme and bring into question whether modified substrate analogues are appropriate for obtaining a realistic representation of the native enzyme activity

In peptidoglycan polymerisation, transglycosylation forms a linear polymer from the monomer LII, in the presence of a transglycosylase enzyme (PBP). Each LII monomer harbors an undecaprenyl chain that anchors it to the bacterial membrane. Undecaprenyl phosphate (C_{55}-P) is a lipid carrier that allows the transport of hydrophilic oligosaccharide precursors (e.g. LII) across the cytoplasmic membrane (Manat *et al.*, 2014) towards the periplasm where elongation of the glycan chain takes place.

C_{55}-P has an important role in bacterial cells as a lipid carrier, required for the synthesis of bacterial cell wall components including teichoic acids, lipopolysaccharides and peptidoglycan. It is synthesised by the sequential addition of eight isoprene units on to farnesyl pyrophosphate catalysed by undecaprenyl pyrophosphate synthase (UppS), forming undecaprenyl pyrophosphate (C_{55}-PP), before being dephosphorylated to C_{55}-P (Touzé & Mengin-Lecreulx, 2008).

During transglycosylation, upon the LII monomer being incorporated into a growing glycan chain, the C_{55}-PP is cleaved off and recycled. The outer-most phosphate of C_{55}-PP can be removed by an undecaprenyl pyrophosphate phosphatase (e.g. PgpB), which can be detected by the chromogenic nucleoside MESG in the presence of PNP (purine nucleoside pyrophosphatase) (Webb, 1992) and quantified spectrophotometrically (**Figure 5.1**).

5.2 Undecaprenyl Pyrophosphate Phosphatases Dephosphorylate C_{55}-PP

In *E. coli,* four undecaprenyl pyrophosphate phosphatases are involved in the dephosphorylation of C_{55}-PP to C_{55}-P + P_i: UppP (formally BacA), YbjG, YeiU and PgpB, with the latter three being members of the type 2 phosphatidic acid phosphatase (PAP2) family of enzymes (El Ghachi, 2004). These three enzymes have conserved, glutamate-rich sequence motifs located on the periplasmic face of the cytoplasmic membrane (Stukey 1997, Chang 2014) and they all contribute to the total C_{55}-PP phosphatase activity in *E. coli* (El Ghachi, 2005). UppP has been suggested to generate 75% of the total cellular C_{55}-PP phosphatase activity, whereas the other enzymes may account for the remaining 25% phosphatase activity (El Ghachi, 2004, El Ghachi 2005). All four of these proteins are integral membrane proteins, with PgpB (phosphatidylglycerophospate phosphatase B) and UppP being the most heavily studied (Touze 2008, Tatar 2014, Bickford 2013). The X-ray crystal structure of *Ec*PgpB was solved in 2014 (Fan *et al.,* 2014) and was shown to have six transmembrane domains and a large periplasmic loop. Over-expression of PgpB or UppP *in vivo* results in bacitracin resistance and increased levels of undecaprenyl pyrophosphate phosphatase activity (Siewert 1967). Bacitracin is a dodecapeptide antibiotic that blocks C_{55}-P formation by binding tightly with C_{55}-PP and preventing its dephosphorylation (Toscano, 1982).

5.3 Phosphate Release as a Means of Quantifying Lipid II Turnover

An assay was devised by Webb in 1992, exploiting the difference in absorbance between the nucleoside MESG (a guanosine analogue called 7-methyl-6-thioguanosine) and it's purine base product 7-methyl-6-guanine, when in the presence of inorganic phosphate and PNP (purine nucleoside pyrophosphorylase). (**Figure 5.1**) The absorbance maximum of the base product is shifted to 355 nm compared to 330 nm of the former nucleoside (Webb, 1992). The change in absorbance is directly related to the change in inorganic phosphate concentration and so can be used to directly quantify phosphate release. The phosphatase activity of *Ec*PgpB can be examined by measuring the kinetics of inorganic phosphate release by coupling two enzymatic reactions: the chromogenic nucleoside MESG in the presence of PNP. This concept was developed by Dr. Adrian Lloyd at The University

of Warwick to exploit the production of the by-product C_{55}-PP with each addition of LII to the glycan polymer and the subsequent inorganic phosphate release. A spectrophotometric assay was developed for the detection of inorganic phosphate release from transglycosylation.

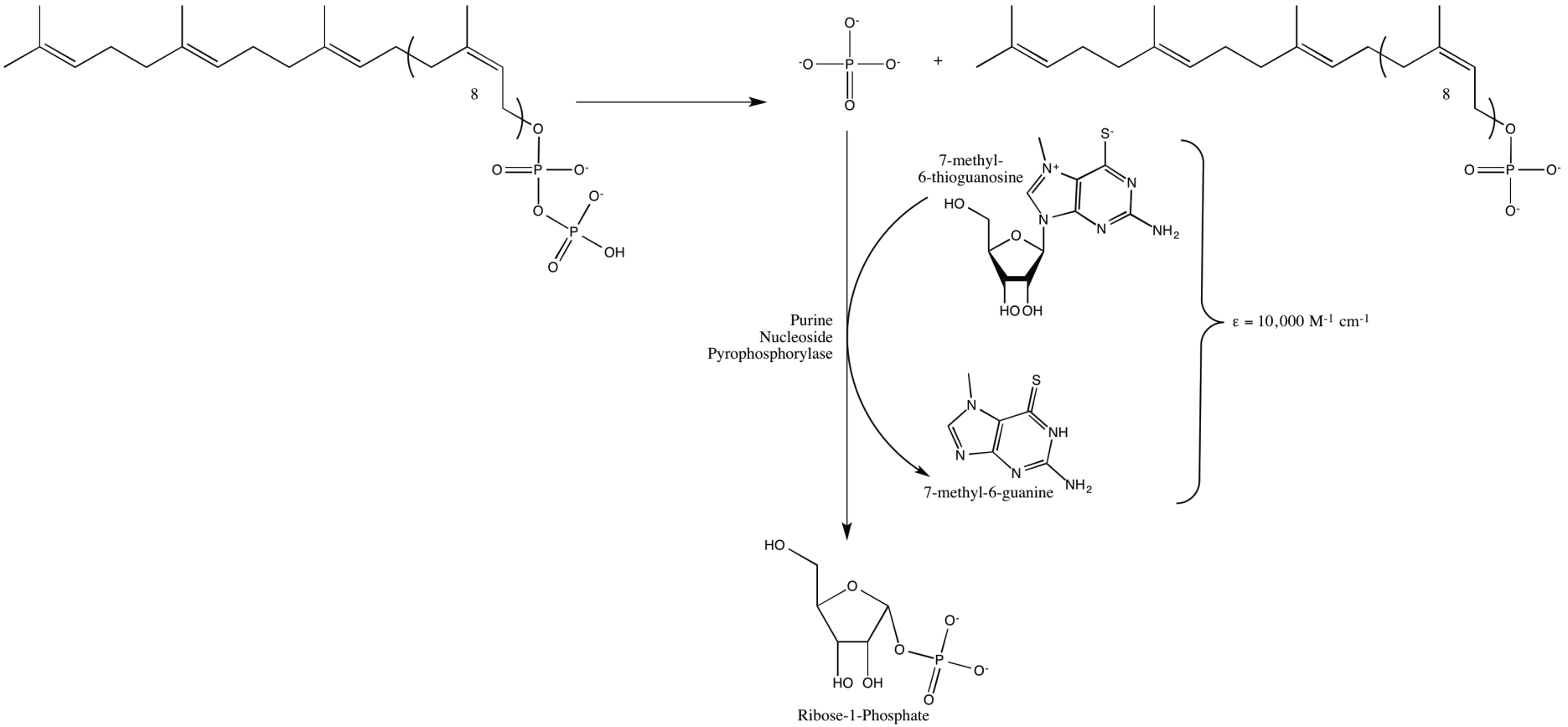

Figure 5.1 A Schematic of the Coupled System for Inorganic Phosphate Detection. A phosphatase (e.g. PgpB) removes the terminal phosphate from the transglycosylation by-product undecaprenyl pyrophosphate (C_{55}-PP). In the presence of this free inorganic phosphate and purine nucleoside pyrophosphorylase (PNP), a guanosine analogue 7-methyl-6-thioguanosine is converted to its base product 7-methyl-6-guanine. This base product has a shifted absorbance maximum of 355 nm, allowing the direct spectrophotometric quantification of the concentration of inorganic phosphate. Ribose-1-phosphate is generated as a result.

5.3.1 Advantages of this Discontinuous Assay for Transglycosylation Detection

The major advantage to this assay compared to the continuous fluorometric assay described earlier in this Chapter, is that there is no modification to the substrate. With the substrate being in its native form, this assay is the first transglycosylation assay with no LII substrate modification and is the most comparable reflection of natural peptidoglycan synthesis *in vivo*. The main undecaprenyl pyrophosphate phosphatase used for these studies was *Ec*PgpB as Touzé *et al.,* kinetically characterised the phosphate-specific activity of this enzyme *in vitro*. The phosphatase *Ec*UppP was also trialed but the construct failed to show any activity.

5.3.2 Disadvantages of this Discontinuous Assay for Transglycosylation Detection

The disadvantage of this assay is that it is discontinuous. The assay method involves the incubation of PBP with non-labelled LII. Transglycosylation is ceased by heating and any precipitated material (aggregated PBP enzyme) is removed by centrifugation. The soluble transglycosylation products (including by-product undecaprenyl pyrophosphate) are added to the coupled, continuous assay in a cuvette for quantification spectrophotometrically of the total phosphate released by *Ec*PgpB. Another disadvantage is that MESG has a narrow pH window in which its absorbance maximum is at 355 nm, pH 7.6, which overlaps with physiological pH for *Ec*PgpB activity. The absorbance spectrum of MESG changes as a function of pH. In the pH range 6.5-8.5, there is a UV absorbance difference between the phosphorylase substrate and product - this feature is exploited in this assay, to quantify phosphate.

5.4 Experimental Aims

- To develop a spectrophotometric assay for the detection of transglycosylase activity
- To express and purify *E. coli* PgpB
- To establish optimal assay conditions and to kinetically characterise the transglycosylase activity of *E. coli* PBP1A and *P. aeruginosa* PBP1A, using the spectrophotometric assay

5.5 The Expression and Purification of *E. coli* PgpB

The pTrc::*E. coli* PgpB construct was a gift from Dr. Touzé (The University Paris Sud) with a His_6-tag on the C-terminus, an IPTG-inducible promoter and ampicillin resistance. The plasmid was over-expressed exactly according to Touzé *et al* 2008, in C43(DE3) cells, using 750 mL 2YT media in 2L baffled glass flasks x 4. The protein was extracted and solubilised in 0.04 % DDM and purified by IMAC (**Figure 5.2 a**). A sample of four fractions from the major peak in (**a**) were run on SDS-PAGE to assess the protein purity at elution from IMAC (**Figure 5.2 b**). Purified *Ec*PgpB in DDM was characterised by CD (**Figure 5.2 c**), in 10 mM sodium phosphate buffer pH 7.3.

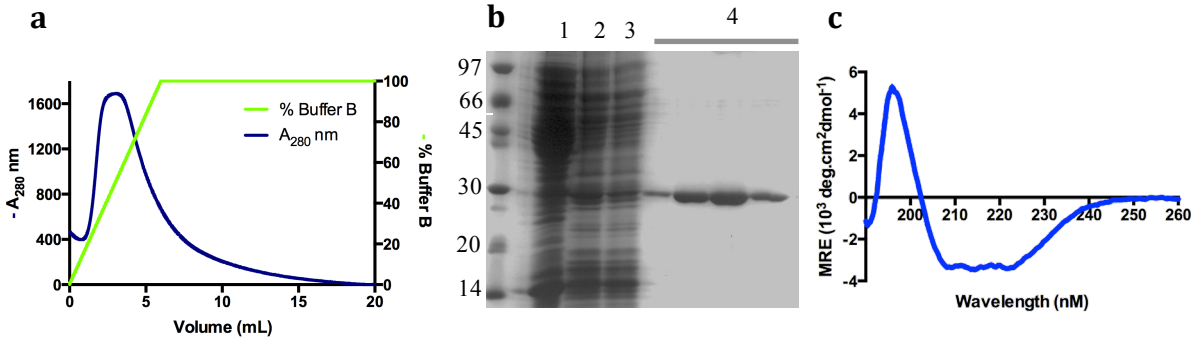

Figure 5.2 The Purification of *E. coli* PgpB with initial Biophysical Characterisation by Circular Dichroism (CD). (a) *Ec*PgpB IMAC purification chromatogram, using a 5 mL Nickel Fast Flow column on an ÄKTA Purifier **(b)** 12% SDS-PAGE coomassie-stained gel: 1 = flow through, 2 = 10 mM Imidazole wash, 3 = 20 mM Imidazole wash, 4 = four eluted fractions within the major peak in (a), with the molecular weight of 30.3 kDa. **(c)** CD spectrum of 5 µM C-His_6-*Ec*PgpB in 10 mM sodium phosphate buffer pH 7.3, containing 0.5 mM DDM.

The expression of *Ec*PgpB yielded ~2 mgs of pure protein per 750 mL cell culture. The over-expressed protein was extracted and solubilized efficiently with 3 x CMC (0.5 mM) of the non-ionic detergent n-Dodecyl-β-D-maltoside (DDM), yielding sufficient quantities of correctly folded, active protein. TritonX-100 and CHAPS detergents were also tested for compatibility with *Ec*PgpB and results were similar to DDM (**Figure 5.11**). Examination of the CD spectrum of *Ec*PgpB shows weak minima peaks at 208 nm and 222 nm, indicating a predominantly α-helical protein. Using the fitting software DichroWeb, CDSSTR (Whitmore & Wallace, 2004) an α-helicity percentage of 56% was confirmed, 41 % β-strand and 3 % β-turn/random coil. The secondary structure prediction software PSIPred (Jones, 1999) returned 61.8 % α-helicity, 35 % β-strand and 3.2 % β-turn/random coil from the protein sequence alone.

5.6 The Development of a Spectrophotometric Assay for the Detection of Transglycosylase Activity

5.6.1 Phosphate Dose-Response Curve with the MESG-PNP Coupling System

To determine the suitability of this assay system to measure the rate of inorganic phosphate (P_i) production, the coupled MESG system was used to determine the linearity of response for measuring a range of P_i concentrations (**Figure 5.3**) to determine to total change in absorbance given a specific input concentration of P_i. The phosphate (P_i) detection system used is illustrated in Figure 5.1.

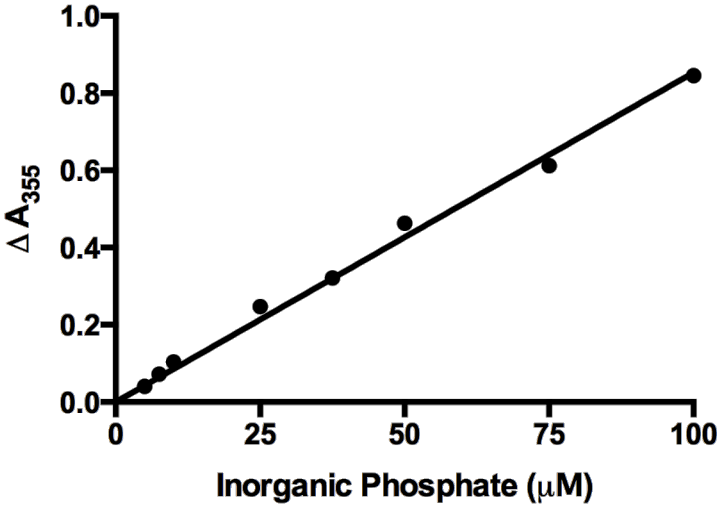

Figure 5.3 Correlating phosphate addition to the total change in absorbance of MESG at 355 nm. Assay conditions were 20 mM Tris.HCI pH 7.6, 0.4 Units of PNP and 600 μM MESG to ensure that MESG was not rate-limiting in the assay. The amount of *Ec*PgpB (200 nM) was chosen such that the reaction was complete within 10 minutes.

The change in absorbance at 355 nm due to the phosphorylase-catalyzed reaction of MESG as a function of inorganic phosphate concentration shows a linear relationship. Therefore this coupling system is suitable for measuring phosphate release, and has been shown to be sensitive to detecting phosphate as low as 2 μM phosphate (Webb 1992).

5.6.2 Initial Rate Dependence on *E. coli* PgpB Concentration

To study the relationship between increasing *Ec*PgpB enzyme concentration on the initial reaction rate, assays were conducted with increasing concentrations of *Ec*PgpB from zero to 1 μM (**Figure 5.4**). The UPP substrate concentration was present in excess at 1.8 mM to ensure the reaction was independent of substrate concentration. These reactions were conducted using synthesised UPP (Warwick BaCWaN Facility), rather than from LII.

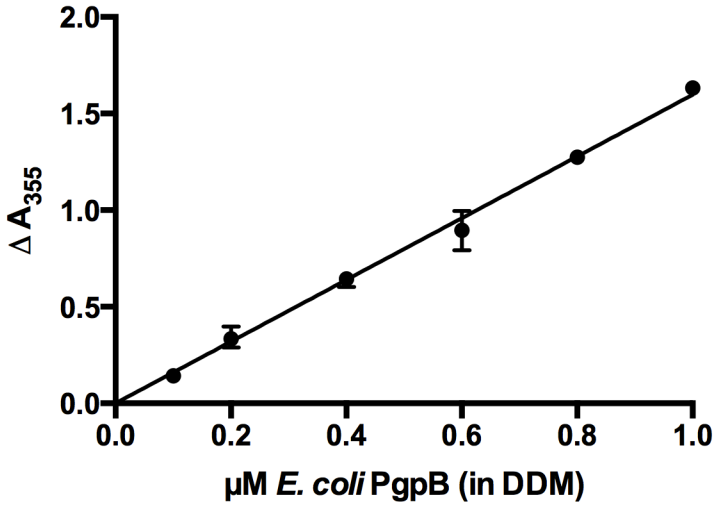

Figure 5.4 The Dependence of the Initial rate of Reaction upon the *Ec*PgpB Enzyme Concentration. *Ec*PgpB was present in the assay at a final concentration of 0.5 mM DDM (3 x CMC) of DDM. The substrate (C_{55}-PP) concentration was present in excess at 1.8 mM.

The initial rate of reaction is proportional to the concentration of *Ec*PgpB, is independent of substrate concentration and follows the characteristics of a zero-order reaction. A variety of different substrates have been identified for *Ec*PgpB with C_{55}-PP being the native substrate and the rest, including diacylglycerol (DGPP) being non-native substrates.

5.6.3 Comparison Between Substrates of *E. coli* PgpB

*Ec*PgpB has wide substrate specificity; Touzé *et al*. tested *Ec*PgpB activity with a variety of substrates with and without different phospholipids. *Ec*PgpB can dephosphorylate diacylglycerol pyrophosphate (DGPP), Phosphatidic acid (PA), phosphatidylglycerol phosphate (PGP) and LysoPA (Funk 1992, Dillon 1996), in addition to its native substrate C_{55}-PP. However, C_{55}-PP is dephosphorylated with much

lower efficiency compared to DGPP (**Figure 5.5**) and farnesyl pyrophosphate (C_{15}-PP) (Touzé *et al.,* 2008). DGPP is a phospholipid whereas C_{55}-PP is an isoprenoid and their only structural feature in common is the pyrophosphate head group. *Ec*PgpB activity *in vitro* is enhanced by phospholipid presence, which potentially helps with conformation of the long C_{55} carbon chain interactions with the membrane (Touzé, 2008). The phospholipid PE (phosphatidylethanolamine) has recently been shown to inhibit *Ec*PgpB activity *in vitro*, and the crystal structure of *Ec*PgpB bound to PE was solved in 2016 (Tong *et al.*, 2016).

The presumed *in vivo* substrate for *Ec*PgpB (C_{55}-PP) and a non-native substrate DGPP were compared for activity with *Ec*PgpB. The *Ec*PgpB concentration used was 200 nM. *Ec*PBP1A was used for the majority of the analysis of *E*cPgpB from here, as much analysis has previously been done on the transglycosylase activity of *E*cPBP1B (Schwartz, 2002).

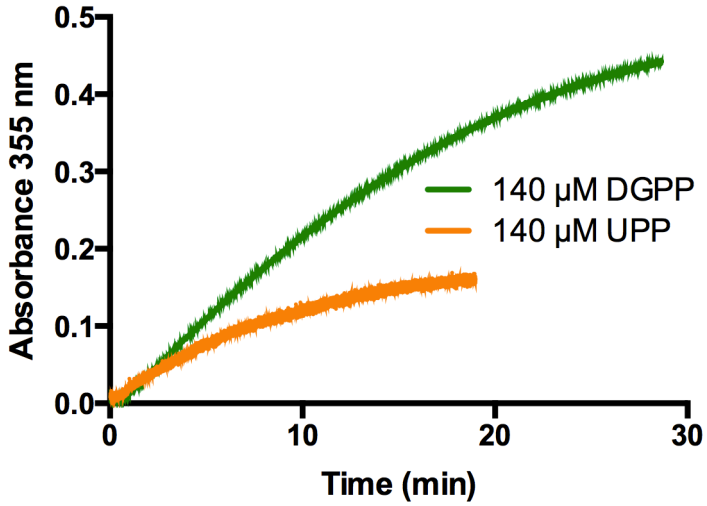

Figure 5.5 A Direct Comparison of Substrate Preference of *E. coli* PgpB, between the native substrate undecaprenyl pyrophosphate (C_{55}-PP/UPP) and the non-native substrate diacyl glycerol pyrophosphate (DGPP). The initial rate of reaction for C_{55}-PP was 0.104, and 0.290 for DGPP. 140 µM of each substrate was used and both were resuspended in to 5 µL of a 0.1% DDM solution (equivalent to 0.05 mM DDM in a 200 µL assay), the [DDM] in the assay was maintained at 3xCMC (0.5 mM). [*Ec*PgpB] concentration = 200 nM. Continuous reaction conditions were 20 mM Tris.HCl pH 7.6, 10 mM $MgCl_2$., 0.4U PNP, 600 µM.

The native substrate C_{55}-PP was turned over much slower than the non-native substrate DGPP, with the initial rate with DGPP being 3-fold-faster than that of C_{55}-PP ($_0$ of 0.29 compared to that of 0.10). An initial lag was not seen with DGPP but was evident with C_{55}-PP, even though C_{55}-PP is the native *in vivo* substrate and DGPP is not. This result

was expected, as *Ec*PgpB has a low specificity towards lipid pyrophosphate substrates compared to phospholipids such as DGPP, and PgpB has been shown to not be the sole pyrophosphate phosphatase *in vivo*. It is thought that multiple phosphatases contribute to the pyrophosphate pyrophosphatase activity, including YbjG and YeiU.

5.6.3.1 Kinetics of Dependence of *E. coli* PgpB on Undecaprenyl Pyrophosphate (C_{55}-PP) and Diacylglycerol Pyrophosphate (DGPP)

The phosphatase activity of *Ec*PgpB was kinetically characterised with its native substrate C_{55}-PP and the non-native substrate DGPP (**Figure 5.6**). The initial velocity of the reaction (v_0) was measured at a variety of substrate concentrations from up to 1 mM substrate. A fixed concentration of 200 nM *Ec*PgpB was used.

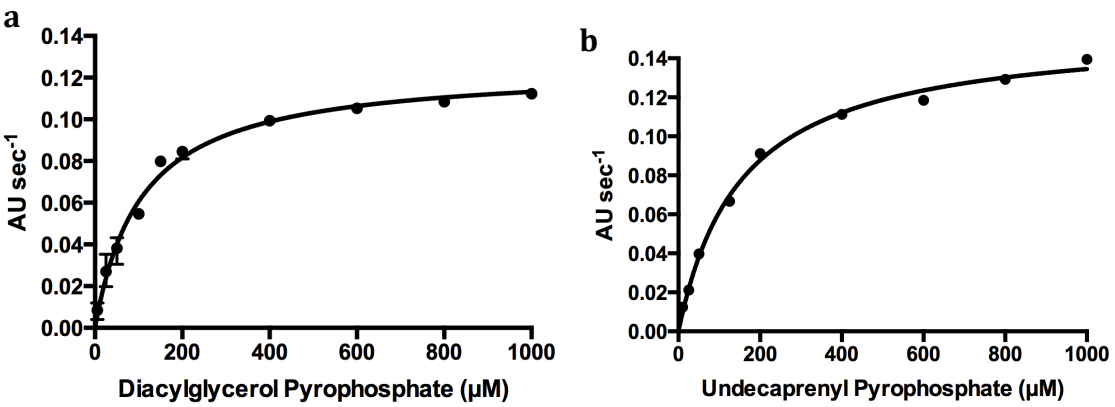

Figure 5.6 Kinetics of Dependence of *E. coli* PgpB Phosphatase Activity with (a) its natural substrate undecaprenyl pyrophosphate C_{55}-PP and (b) the non-native substrate DGPP. A fixed concentration of 200 nM *Ec*PgpB was used. DGPP assays were performed in duplicate and C_{55}-PP assays were conducted once only at each substrate concentration due to the precious, expensive and elusive nature of this substrate. 200 nM *Ec*PgpB was used in reaction conditions: 20 mM Tris.HCl pH 7.6, 10 mM $MgCl_2$.

There is a hyperbolic relationship between the initial enzyme velocity (v_0) and the substrate concentration, enabling the data to be fitted to the Michaelis-Menten equation (Equation 4.1) to determine K_{cat} and K_m by non-linear regression. The kinetic parameters for *Ec*PgpB with both C_{55}-PP and DGPP (calculated using GraphPad Prism), are presented in **Table 5.1**.

Table 5.1 A Summary of the V_{max} and K_m data derived from the Michaelis-Menten equation for the two substrates C_{55}-PP and DGPP. The data was fitted to Equation 4.1 by non-linear regression, enabling kinetic constants to be derived. The lower table lists the equivalent data published by Touzé *et al*. (2008).

Substrate	V_{max} ($AU.s^{-1}$)	K_m (μM)	K_{cat} (s^{-1})	K_{cat}/K_m ($\mu M^{-1}.s^{-1}$)	R^2
C_{55}-PP	0.155	153 ± 12.0	7.76 ± 0.18	0.05 ± 0.004	0.99
DGPP	0.125	106 ± 8.8	6.26 ± 0.18	0.06 ± 0.005	0.98

Substrate	Published K_m (μM)	Published K_{cat} (s^{-1})	Published K_{cat}/K_m ($\mu M^{-1}.s^{-1}$)
C_{55}-PP	530 ± 90	9.0 ± 0.7	0.017 ± 0.003
DGPP	84 ± 14	280 ± 20	3.5 ± 0.7

As the substrate concentration increased, the reaction velocity increased until it began to plateau at ~400 μM for DGPP and later for C_{55}-PP. Increasing either substrate concentration from 400 μM to 1000 μM made little difference to the reaction velocity. The V_{max} values for the two substrates are very similar but the K_m data differ significantly. The K_m for C_{55}-PP is 1.5-fold that of DGPP, further indicating that *Ec*PgpB has a higher affinity for the DGPP substrate over C_{55}-PP, despite it being a non-native substrate. Previously reported K_m for *Ec*PgpB with C_{55}-PP was 300 μM (Fan *et al* 2014). The K_m value extracted for UPP/C_{55}-PP was 153 ± 12.0, which is 3.5-fold lower than the published value of 530 ± 90. The K_m value derived previously at The University of Warwick was 192 ± 17.2 (Abrahams, 2011). The K_{cat}/K_m values derived from fitting the data to the Michaelis-Menten equation assess the catalytic efficiency of *E. coli* PgpB, with the values extracted similar for both DGPP (6.26 ± 0.18) and UPP (7.76 ± 0.18).

5.6.4 A Time-Dependent Profile for *E. coli* PBP1A Transglycosylation

The reaction conditions for both the discontinuous polymerisation and continuous assay were devised from the literature and the method protocol was adapted from a previous PhD student, Katherine Abrahams (Abrahams, 2011). Conditions required for successful transglycosylation in the previous assay in this chapter included 20 mM Tris.HCl pH 7.6 as the buffering agent, 10 mM $MgCl_2$ was required for

transglycosylase catalytic site activity and a non-ionic detergent required to solubilise the LII substrate. DDM was selected, as *Ec*PgpB was shown to be active in this detergent, and was successful in showing the activity of *S. aureus* monofunctional glycosyl-transferase (MGT). Conditions for the continuous assay were kept constant to the discontinuous polymerisation, maintaining a maximum DDM concentration of 3xCMC. An excess of detergent micelles devoid of substrate creates a crowded environment of 'empty' micelles which could interfere with PgpB activity. High concentrations of detergent have been documented to detrimentally affect the activity of PgpB (Touzé *et al.*, 2008) and *Ec*PBP1B (Schwartz *et al*., 2002).

The length of time needed for the completion of transglycosylation was determined to ensure that the quantity of LII put in to the polymerisation, is equal to the amount of undecaprenyl pyrophosphate produced and also proportional to the amount of free inorganic phosphate generated by PgpB. The time required to polymerise LII to completion was determined by setting up a series of polymerisation reactions with an excess of DAP-LII (1.8 mM) and ceasing polymerisation at increasing time intervals (**Figure 5.7**). *Ec*PBP1A in TritonX-100 was used as the transglycosylase to polymerise the LII.

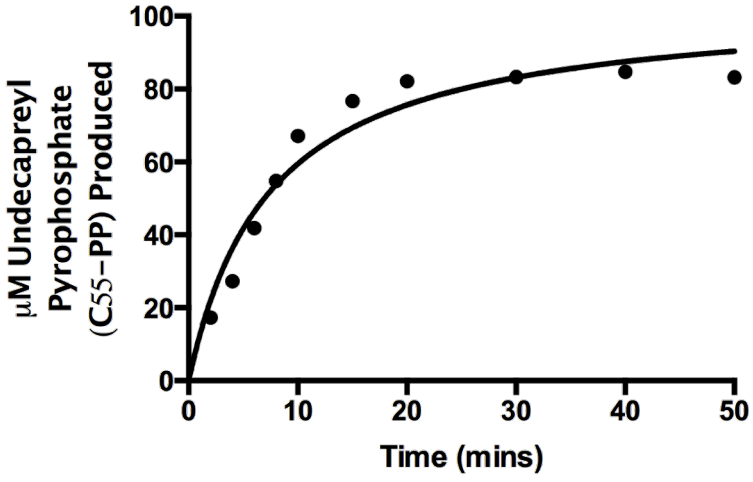

Figure 5.7 Time-dependence of Undecaprenyl Pyrophosphate Generation in the Transglycosylation Polymerisation Reaction. The average of two replicates plotted. The V_{max} calculated using the Michaelis-Menten equation in Prism GraphPad was 103.8 ± 6.29. An excess of 1.8 mM DAP-LII was used in each polymerisation assay, 200 nM *Ec*PgpB was used in reaction conditions: 20 mM Tris.HCl pH 7.6, 10 mM $MgCl_2$.

The majority of the LII had been consumed within 20 minutes of polymerisation at 30 °C, as not much more undecaprenyl pyrophosphate was produced after this time point.

The V_{max} has been calculated as 104 ± 6.29 µM.min^{-1}, indicating that the polymerisation has not quite reached completion after 50 minutes, but the amount of C_{55}-PP generated were the same after 20, 30 40 and 50 minutes of polymerisation.

5.6.5 Comparing the Substrate Preferences of three Class A Bifunctional PBPs

Each of the three PBPs (*Ec*PBP1A, *Ec*PBP1B and *Pa*PBP1A) were incubated with both Lys- and DAP-LII for 20 minutes and one hour before quantifying the amount of phosphate released *via* the continuous-coupled assay (**Figure 5.8**), a no-enzyme negative control was also run after leaving polymerisation for one hour.

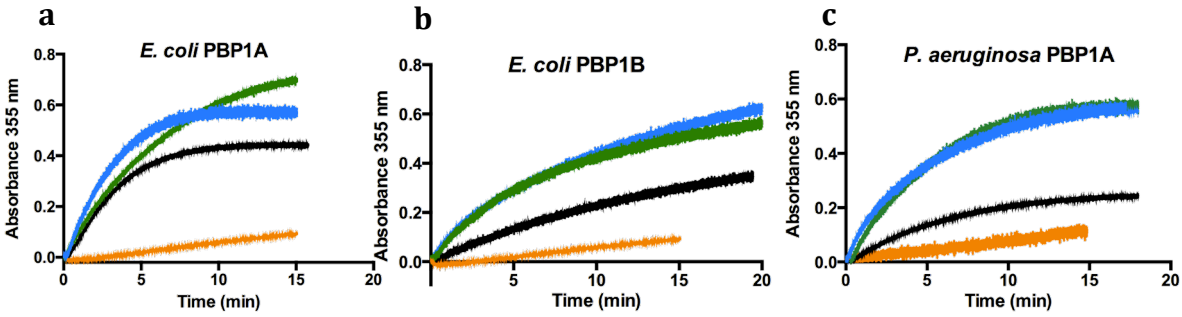

Figure 5.8 Comparing the Substrate Preference of *Ec*PBP1A, *Ec*PBP1B and *Pa*PBP1A with both Lys- and DAP-LII. (**a**) 5 µM *Ec*PBP1A (**b**) 5 µM *Ec*PBP1B (**c**) 5 µM *Pa*PBP1A. – – 1 hour Lys-LII polymerisation, — 20 minute Lys-LII polymerisation, — 20 minute DAP-LII polymerisation, — no PBP enzyme negative control (polymerisation incubation for 1 hour). 80 µM LII used. A LII polymerisation assay was conducted at 30 °C for both 20 minutes and 60 minutes before the PBP was heat-inactivated at 60 °C. The amount of C_{55}-PP produced by transglycosylation was measured *via* the release of the terminal inorganic phosphate and quantification of the free phosphate released. 200 nM *Ec*PgpB was used in each assay and 200 µM DAP- or Lys-LII substrate was used in reaction conditions: 20 mM Tris.HCl pH 7.6, 10 mM $MgCl_2$.

Both DAP- and Lys-LII generate the same undecaprenyl pyrophosphate by-product (C_{55}-PP) upon transglycosylation. DAP-LII was shown to be the preferred substrate by approximately 3-fold for all three PBP enzymes, as all of the DAP-LII had been turned-over after just 20 minutes of polymerisation in the presence of PBP. The change in A_{355} nm after 20 minutes indicated that all the DAP-LII had been consumed; therefore there was no need to leave the polymerisation for longer than 20 minutes. In contrast, the Lys-LII did not show full consumption of substrate after 20 minutes, and so was left for 1 hour to ensure completion of polymerisation before testing the total amount of phosphate released. The negative control without PBP present did not show a positive result for free inorganic phosphate. Upon the total consumption of all the 200 µM

substrate polymerised, the amount of phosphate released for DAP- and Lys-LII was comparable, but DAP-LII generated the C_{55}-PP faster than Lys-LII.

Concluding that DAP-LII is used more favourably over Lysine-LII, a range of DAP-LII concentrations were polymerised and assayed via phosphate release. The kinetic profile of *Ec*PgpB with undecaprenyl pyrophosphate (C_{55}-PP) generated from DAP-LII, by three Gram-negative Class A bifunctional PBPs was characterised below.

5.6.6 The Kinetic Profile of *E. coli* PgpB with C_{55}-PP and Three Class A PBPs

The amount of phosphate released was measured from increasing concentrations of DAP-LII. The DAP-LII was initially polymerised by a PBP, and the undecaprenyl pyrophosphate generated from each completed polymerisation was quantified continuously. The concentration of DAP-LII polymerised initially is proportional to the amount of C_{55}-PP generated. The C_{55}-PP is turned over by *Ec*PgpB and the terminal phosphate released, enters in to the MESG coupling system and all free phosphate is quantified (**Figure 5.9**).

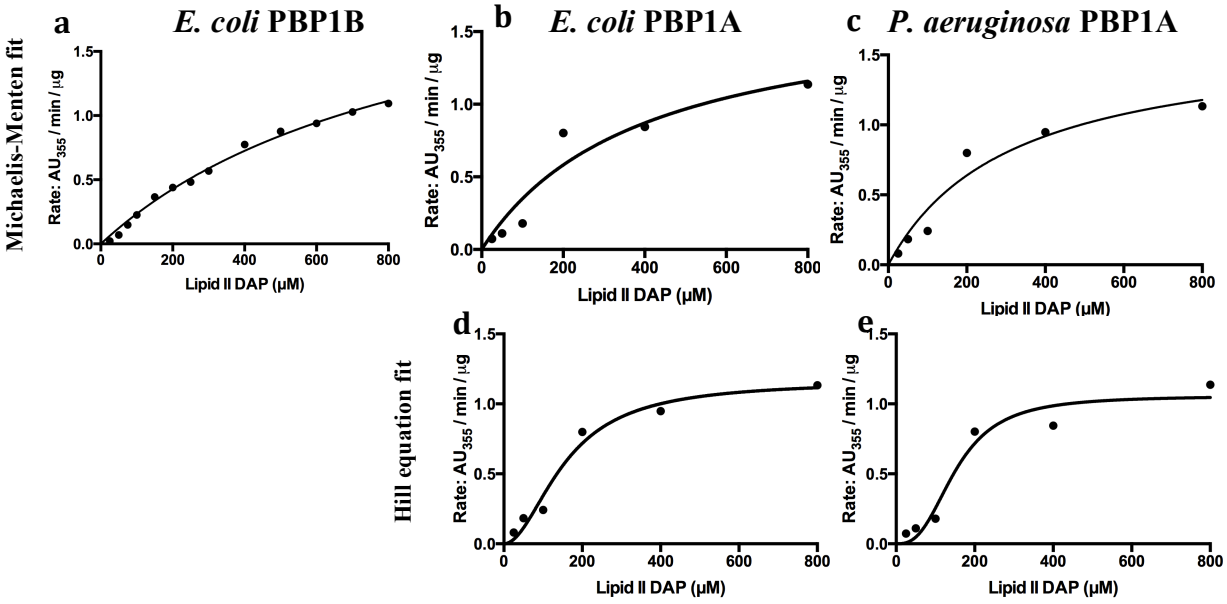

Figure 5.9 The Kinetic Profile of *E. coli* PgpB with DAP-LII generated undecaprenyl pyrophosphate (C_{55}-PP) from 3 different Class A PBPs. (**a**) *Ec*PBP1B, (**b**) and (**d**) *Ec*PBP1A (**c**) and (**e**) *P. aeruginosa* PBP1A. *Ec* and *Pa* PBP1A data was fitted to the Hill equation in addition to the Michaelis-Menten equation, as a sigmoidal relationship was observed. Increasing concentrations of DAP-LII were incubated with PBP for one hour (completion). The amount of phosphate released was quantified as change in absorbance at 355 nm. 200 nM *Ec*PgpB was used in reaction conditions: 20 mM Tris.HCl pH 7.6, 10 mM $MgCl_2$. The final change in absorbance at 355 nm is when all free inorganic phosphate has been turned-over by the MESG-coupling system.

P. aeruginosa PBP1A had the highest K_m of the three PBPs and so turned over DAP-LII at a slower rate than the other two PBPs. The kinetic parameters of *Ec*PgpB-dependent P_i release are presented in **Table 5.2**, fitted to the Michaelis-Menten equation (Equation 4.1). The data was also fitted to the Hill equation (Equation 4.5), as the data indicates a sigmoidal approach to V_{max} (**Table 5.3**).

Table 5.2 The Kinetic Constants for each PBP, with data fitted to the Michaelis-Menten equation (Equation 4.1). LII was polymerised with each PBP, with subsequent P_i hydrolysis from undecaprenyl pyrophosphate by *Ec*PgpB.

PBP	V_{max} (AU/min/µg)	K_m (µM)	V_{max}/K_m	R^2
***E. coli* PBP1A**	1.73 ± 0.44	395 ± 111	4.38×10^{-3}	0.93
***E. coli* PBP1B**	2.41 ± 0.22	926 ± 122	2.60×10^{-3}	0.96
***P. aeruginosa* PBP1A**	1.64 ± 0.28	313 ± 122	5.24×10^{-3}	0.99

Table 5.3 The Kinetic Constants for each PBP, with data fitted to the Hill equation (Equation 4.5). LII was polymerised with each PBP, with subsequent P_i hydrolysis from undecaprenyl pyrophosphate by *Ec*PgpB.

PBP	V_{max} (AU/min/µg)	K_m (µM)	V_{max}/K_m	R^2
***E. coli* PBP1A**	1.16 ± 0.11	156 ± 27.8	7.46×10^{-3}	0.98
***P. aeruginosa* PBP1A**	1.06 ± 0.11	152 ± 26.2	8.48×10^{-3}	0.96

Little is known kinetically about *P. aeruginosa* PBPs as there is very little published compared to *E. coli* PBPs. *Ec*PBP1B did not reach V_{max}, therefore the K_m value extracted for this enzyme using the Michaelis-Menten equation is large, 926 ± 122 µM. The K_m values extracted from the Michaelis-Menten fitting are much higher than previously defined in Chapter 4, using the continuous fluorescence assay for monitoring transglycosylation. The K_m data derived by fitting to the Hill equation defines lower K_m values that more closely resemble those defined by the continuous fluorescence assay, although the K_m values in Table 5.3 are still 10-fold those defined by the continuous assay. The substrate measured in the fluorescence continuous assay is not identical as it is dansylated and the substrate used in the PgpB assay is native LII. However, the PgpB assay is a stopped assay and the fluorescence assay is continuous and so the derived kinetic values are likely to be more reliable.

5.6.7 Testing Transglycosylase and Transpeptidase Active Site Mutant Activity Using the Discontinuous Coupled Spectrophotometric Assay

Transglycosylase (TG) and transpeptidase (TP) active site mutants were synthesised by site-directed mutagenesis (section 2.3.6). Active-site residues mutated are as follows: *Ec*PBP1A = E86Q and S473A, *Ec*PBP1B = E233Q and S510A, *Pa*PBP1A = E86Q and S461A and *Pa*PBP1B = E190Q and S469A. The *Pa*PBP1B active-site mutants were successfully mutated confirmed by DNA sequencing, however, these mutants were never expressed as an active wildtype *Pa*PBP1B protein could not be obtained as a positive control to compare against these active-site mutants. The activity of all other mutant PBPs: *Ec*PBP1A, *Ec*PBP1B and *Pa*PBP1A were tested against their wildtype in the discontinuous DAP-LII polymerisation assay, with the (**Figure 5.10**).

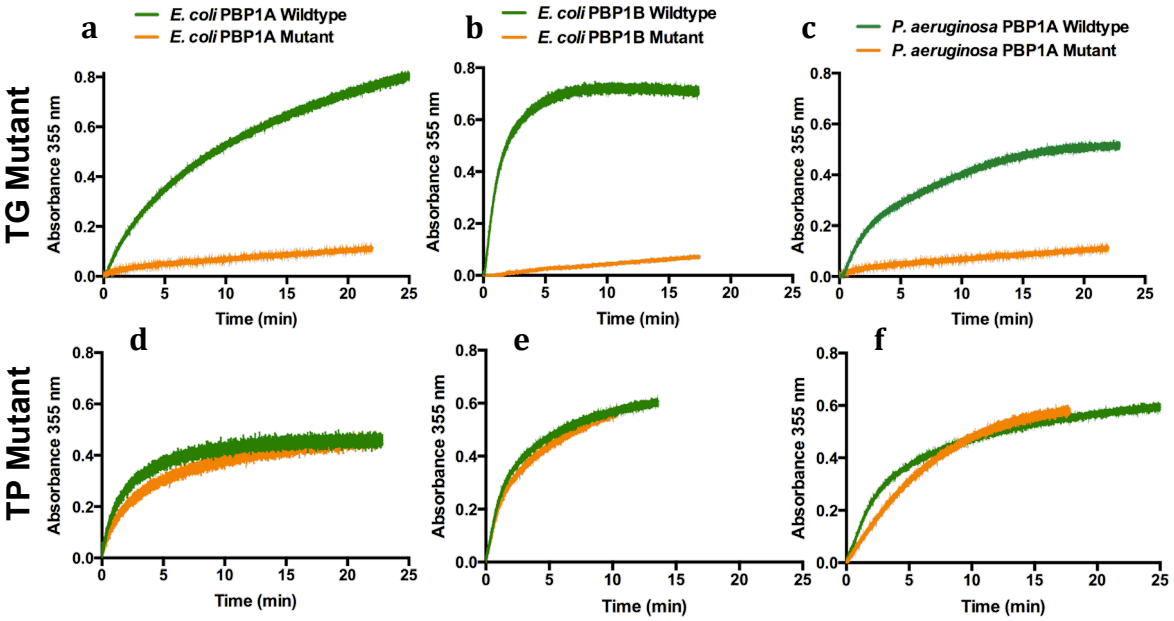

Figure 5.10 The activity of both transglycosylase and transpeptidase wildtype and active site mutants were tested using *Ec*PgpB. (**a-c**) TG active site mutant for each PBP (**d-f**) TP active site mutant for each PBP (**a+d**) *Ec*PBP1A (**b+e**) *Ec*PBP1B (**c+f**) *Pa*PBP1A, — Wildtype PBP — active site mutant. 200 nM *Ec*PgpB was used in each assay and 200 µM DAP-LII substrate was used in reaction conditions: 20 mM Tris.HCl pH 7.6, 10 mM $MgCl_2$.

The transpeptidase active site mutant (**d-f**) had no affect on the measurement of phosphate released from undecaprenyl pyrophosphate, the assays with the TP active site mutant were comparable to the wildtype. Assays containing the TG active site mutant (**a-c**) didn't show any phosphate presence and therefore no transglycosylase activity.

The drive behind optimising this assay for transglycosylase activity was to ultimately develop the assay in to one that assayed both transglycosylase and transpeptidase activity simultaneously, giving alternative read-outs for both activity. The major factor preventing such a development is the kinetics of the *Ec*PgpB enzyme and how slowly it turns over phosphate in the current conditions. In the continuous transglycosylase assay using fluorescently-labelled-LII, the principle detergent used to solubilise the LII substrate is decyl PEG. Adrian Lloyd used this range of detergents to optimise a transpeptidase assay and suggested trying this detergent and a range of similar detergents as a means of increasing the kinetic activity of *Ec*PgpB and potentially the availability and presentation of the undecaprenyl pyrophosphate to *Ec*PgpB and the coupling system.

5.6.8 Detergent Screening of *E. coli* PgpB Activity

5.6.8.1 The Activity of *E. coli* PgpB when purified in TritonX-100, CHAPS and DDM

*Ec*PgpB was purified in both DDM and TritonX-100 (Section 5.5) with its activity analysed after extraction and solubilisation in these three detergents (**Figure 5.11**). *Ec*PgpB was extracted and purified in each detergent (0.03 % DDM, 0.5% TritonX-100 and 1 % CHAPS.

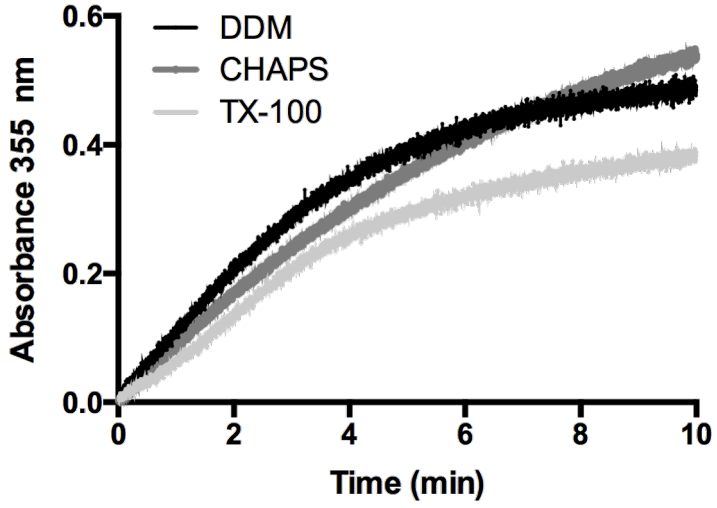

Figure 5.11 The activity of *E. coli* PgpB when extracted and purified in DDM, TritonX-100 and CHAPS. DAP-LII was used at 200 µM in the discontinuous polymerisation with 200 nM *Ec*PgpB and 200 µM DAP-LII substrate and 8 µM *Ec*PBP1A was used in reaction conditions: 20 mM Tris.HCl pH 7.6, 10 mM $MgCl_2$.

*Ec*PgpB was active in all three non-ionic detergents: DDM, TritonX-100, and CHAPS. The initial rate of reaction differed slightly with each detergent, with *Ec*PgpB in DDM being the fastest, and *Ec*PgpB in TritonX-100 being the slowest. In theory, all three preparations should release the same amount of phosphate from the undecaprenyl pyrophosphate from transglycosylation, as the same amount of LII was in the polymerisation, assuming that *Ec*PBP1A went to completion in all assays. *Ec*PgpB in CHAPS releases the most phosphate as the ΔA_{355} is greatest in this detergent, but the three detergents differ only marginally.

5.6.8.2 *E.coli* PgpB Activity in Ethylene Glycol Alkyl Ether Detergents

Ethylene glycol alkyl ether detergents are non-ionic surfactants with worm-like micelles. The micelles are analogous to real polymers but importantly different in that they can break and recombine like equilibrium polymers (Shirari *et al* 2006). Their micellar size is not fixed but fluctuates around an equilibrium volume (Miyake, *et al* 2008). These series of detergents have a range of poly(Ethylene glycol) units and ethers, denoted as (ExCy) (**Table 5.4**).

Table 5.4 A Summary of the Ethylene Glycol Ether Detergents Tested for Suitability for *Ec*PgpB Activity

Decyl PEG Name	Abbreviation	MW (g/mol)	CMC (mM)
Tetraethylene glycol monododecyl ether	E_4C_{12}	334.49	0.069[a]
Pentaethylene glycol monodecyl ether	E_5C_{10}	406.60	0.07[b]
Hexaethylene glycol monododecyl ether	E_6C_{12}	450.65	0.087[b]
Octaethyleneglycol monodecyl ether	E_8C_{10}	538.75	0.11[b]

a Fragento *et al*, 1996, Langmuir **12** pp477
b Sigma Aldrich Website

*Ec*PgpB activity was tested with five of the ExCy detergents (**Figure 5.12**). The discontinuous assay was carried out as in section 2.8.4. The continuous assay was conducted by using assay buffer containing the ExCy detergent, conducting the continuous assay in a final concentration of 3xCMC of each ExCy detergent. The *Ec*PgpB used was extracted and purified in CHAPS and when added to continuous

assay, the micellar concentration of the ExCy detergent present in the continuous assay buffer is at 3x its critical micellar concentration, but the CHAPS that the *Ec*PgpB is delivered drops below its CMC. Therefore the *Ec*PgpB enzyme is likely to switch from a CHAPS detergent micelle to a ExCy detergent micelle to maintain stability and solubility. *Ec*PgpB could not be purified in these ExCy detergents individually because the detergents are extremely expensive and it is unknown whether they would work as a detergent for extraction and purification.

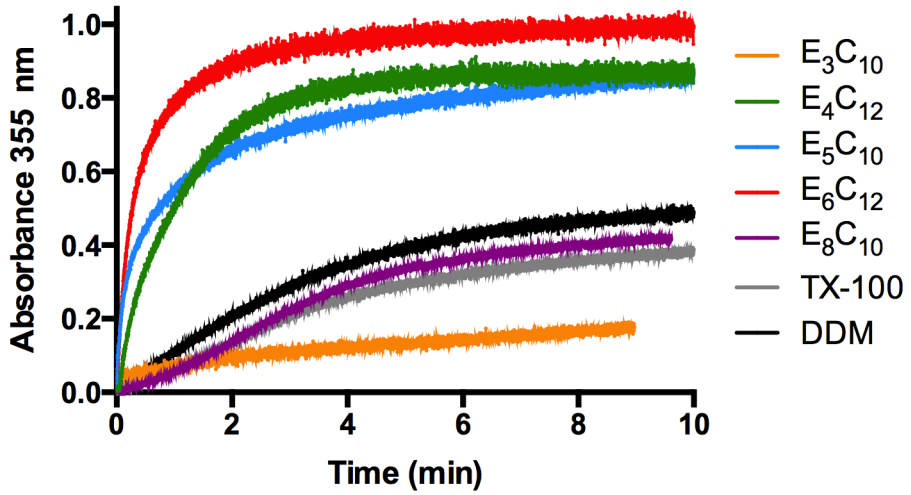

Figure 5.12 *E. coli* PgpB activity tested in the presence of the non-ionic ethylene glycol alkyl ether detergents E_4C_{12}, E_5C_{10}, E_6C_{12} and E_8C_{10}. *Ec*PgpB was delivered to the continuous assay in CHAPS, but as the CHAPS became diluted it dropped below its CMC and the *Ec*PgpB switched to the E_xC_y detergent in the continuous assay buffer. The discontinuous assay was carried out the same in all cases, with only the E_xC_y detergent in the assay buffer in the continuous assay differing. 200 µM DAP-LII substrate was used in the polymerisation, with 200 nM *Ec*PgpB in the continuous assay, in reaction conditions 20 mM Tris.HCl pH 7.6, 10 mM $MgCl_2$.

The ethylene glycol ether detergent with the shortest and the longest ethylene glycol chain showed the least *Ec*PgpB activity. When handling the detergents, it became apparent that the detergents with shorter ethylene glycol chain (E_3, E_4), the more viscous the detergent was. E_3C_{10} exhibited the lowest *Ec*PgpB activity with E_4C_{12}, E_5C_{10} and E_6C_{12} all demonstrating very good activity for *Ec*PgpB. E_6C_{12} has the fastest initial rate, and reaches a higher absorbance of all the detergents and so dephosphorylated more C_{55}-PP molecules than the other detergents.

5.6.9 *E. coli* PgpB Activity ± $MgCl_2$, in a Variety of Non-ionic Detergents

The activity of *Ec*PgpB was tested in the presence and absence of magnesium chloride ($MgCl_2$) in each detergent: DDM, TritonX-100, E_3C_{10}, E_4C_{12}, E_5C_{10} and E_8C_{10} (**Figure 5.13**). In each case, the discontinuous assay was carried out as in section 2.8.4, with the polymerisation and continuous assay buffers altered to ensure the conditions were consistent with 3xCMC of each detergent and the correct concentration of $MgCl_2$. The *Ec*PgpB was purified in CHAPS, with the detergent being tested, present in each assay buffer. The concentration of CHAPS is diluted below its CMC, and the detergent present stabilises and maintains the solubility of *Ec*PgpB.

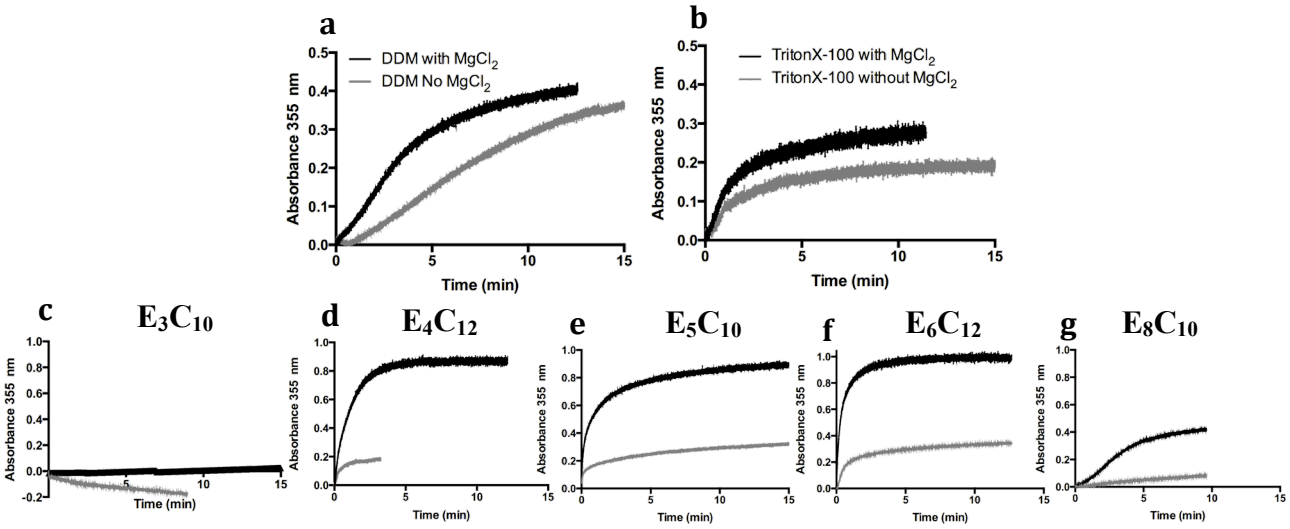

Figure 5.13 The Activity of *E. coli* PgpB with and without Magnesium Chloride ($MgCl_2$) in a Range of Detergents: (**a**) DDM (**b**) TritonX-100 (**c**) E_3C_{10} (**d**) E_4C_{12} (**e**) E_5C_{10} (**f**) E_6C_{12} (**g**) E_3C_{10}. — Assay contains $MgCl_2$, — No $MgCl_2$ added to assay, only the $MgCl_2$ delivered to the assay in the *Ec*PgpB enzyme storage buffer, which is diluted 40-fold in the volume of the continuous assay and equates to a final $MgCl_2$ concentration of 25 μM.

In every case, the presence of > 25 μM $MgCl_2$ enhanced the activity of *Ec*PgpB, irrespective of the detergent that *Ec*PgpB was in. When the assay was conducted in the ethylene glycol alkyl ether series of detergents, the presence of $MgCl_2$ was amplified compared to in DDM or TritonX-100. The absence of $MgCl_2$ (only the 25 μM donated from the *Ec*PgpB storage buffer) had less of an effect on the activity of *Ec*PgpB in the assays with DDM and TritonX-100 compared to the ExCy detergents. In the assays in the ExCy detergent series, the concentration of $MgCl_2$ had a much greater effect on the activity of *Ec*PgpB. In addition, two divalent cations ($MgCl_2$ or $CaCl_2$) per active site of

UppS (Undecaprenyl Pyrophosphate Synthase) are shown to be absolutely required for UppS activity (Chang 2014).

5.7 Discussion

Traditionally transglycosylation has been monitored with radiolabelled or fluorescentl-labelled substrates (Offant *et al*., 2010; Schwartz *et al*., 2002; Terrak & Nguyen-Disteche, 2006). This assay has the advantage of using only natural substrates and quantifying transglycosylation discontinuously, however, the length of polymers cannot be determined, except for by mass spectrometry.

5.7.1 Comparing the Continuous Fluorescence Assay with the Phosphate Release Spectrophotometric Assay

The main advantage of the fluorometric assay is that it is continuous, with transglycosylation progression visualised in real-time. This assay is in contrast to the spectrophotometric assay, in which transglycosylation is discontinuous and is stopped after completion. The main disadvantage of the fluorometric assay is that it misses the initial rate of reaction, less so if dispensers are used to initiate the reaction, if enough reagents are available for dispenser priming. Another disadvantage of the continuous transglycosylase assay is that it is hard to quantify exactly how much LII substrate has been turned over at any given time, even upon reaction completion it may not be the case that all LII has been used up. With some further studies and standardized assays conducted, it could be possible to translate the change in relative fluorescence units into the volume of LII consumed.

The main advantage of the spectrophotometric assay is that the substrate used is non-labelled and so is as close to native as possible and is the only assay known to use native substrate. The main disadvantages being that is it not a continuous assay, and it is much less high-through put at present compared to the continuous assay as the spectrophotometric assay is done in a 200 µL cuvette whereas the continuous assay has been translated in to a plate reader format.

5.7.2 Ceasing Transglycosylation Polymerisation

Ceasing transglycosylation in the LII polymerisation assay was done by heating to 60 °C for 10 minutes, which was successful at stopping polymerisation, as the PBP was visibly aggregated after this procedure. However, it is possible that heating the reaction products to 60 °C could destabilize the undecaprenyl pyrophosphate released during polymerisation and hence affect the true quantification of glycan chain polymerisation. A simple test could be conducted involving heating undecaprenyl pyrophosphate to different temperatures and analysing the phosphate released after exposure to each temperature. Also, by heating the reaction, transglycosylation does not halt instantaneously. With *E. coli* PgpB showing dependence upon divalent cations quenching with EDTA is possible. EDTA could be added to LII polymerisation to sequester the $MgCl_2$, which this would halt transglycosylation, although this would not be a realistic solution, as EDTA would also affect the activity of *Ec*PgpB in the subsequent continuous reaction. Quenching with EDTA was also shown to not be 100 % effective at ceasing PgpB activity, retaining a small degree of activity (Abrahams, 2011).

5.7.3 *E. coli* PgpB Activity in Different Detergents

Upon determining the *Ec*PgpB activity in different detergents, the ability of the MESG-PNP coupling system to turn over free phosphate in the presence of each detergent should have been investigated initially to demonstrate that the detergent didn't interfere with the coupling system. See section 5.9.3 for associated future work.

5.8 Conclusions

The dose-response plot of increasing concentrations of inorganic phosphate demonstrated that the MESG-PNP coupling system was appropriate for accurately measuring phosphate release and showed a linear response between phosphate and absorbance (Figure 5.3). The initial rate of reaction was also linear relative to *Ec*PgpB concentration (Figure 5.4). PgpB gave a K_m value of 154 ± 12.0 μM for its native substrate UPP, and 106 ± 8.7 μM for the non-native substrate DGPP. The published K_m values by Touze *et al.*, are 530 ± 90 μM for UPP and 80 ± 14 μM for DGPP. The

affinity that *Ec*PgpB has for its native substrate was found to be 3.5-fold greater than previously published and similar to that published for DGPP (Table 5.2).

*Ec*PgpB is expressed and purified according to Touzé *et al*, 2008 in DDM is well folded and shows activity in this environment. Alternative detergents were tested for activity, including TritonX-100 and CHAPS, which showed similar activity to *Ec*PgpB in DDM (CD was not carried out on *Ec*PgpB in these additional detergents).
The MESG-PNP coupling system showed a linear dose-response curve for the phosphate concentration, suggesting a stable system for phosphate detection and the rate of the continuous reaction was shown to be linear to *Ec*PgpB concentration. DGPP was shown to be a better substrate for *Ec*PgpB than it's native substrate undecaprenyl pyrophosphate, with a lower K_m and faster initial rate of reaction. DAP LII was also used more favourably by the PBPs compared to Lys-LII, as the rate of DAP-LII consumption was faster than that of Lys-LII. This is also backed-up from results using the continuous transglycosylase assay. All three Class A enzymes showed activity using this assay method, with *Pa*PBP1A having the lowest K_m of the three PBPs and so turned over DAP-LII the slowest. Transglycosylase active-site mutants were proven to be non-functional in both transglycosylase assays in this chapter, while the TP active-site mutants did not inhibit transglycosylase activity.

5.9 Future Work

5.9.1 The PgpB Assay has the Potential to Monitor Transglycosylation Continuously

This discontinuous assay for transglycosylation has the potential to be continuous, with transglycosylation occurring concurrently with PgpB cleaving the phosphate, followed by phosphate detection by the coupling system. The kinetic rate of the pyrophosphatase will need stimulation in order for a phosphate release rate to be detected. The addition of cytoplasmic membrane phospholipids such as cardiolipin and phosphatidyl glycerol has been shown to enhance the activity of E. coli PgpB by 5.4-fold (Touze *et al.,* 2008), which could be incorporated in to a continuous format, providing such phospholipids

5.9.2 The Stability and Activity of PgpB in Different Detergents

As the kinetic speed of *E. coli* PgpB is a limiting factor in this assay thus far, the stability of this enzyme should be tested and optimised. Circular dichroism would indicate sufficient folding of the enzyme, but also, a thermoflour assay that measures changes in thermal shift and quantifies the change in thermal denaturation temperature of a protein, is ideal for measuring the stability of proteins in different detergents.

5.9.3 Scrutinise the Kinetic Capability of *E. coli* PgpB in a Wider Range of Detergents

EcPgpB was successfully used to indirectly visualise transglycosylation, but speeding up its enzymatic ability is necessary for the assay to be developed into a continuous format. *Ec*PgpB could be extracted and purified in to one of the series of Ethylene Glycol Alkyl Ether detergents, in which PgpB exhibited good activity, however, this would be very expensive as a lot of detergent is required to extract and purify a protein. Other phosphatases such as BacA should be trialled as an alternative to PgpB.

5.9.4 Investigate Alternative Undecaprenyl Pyrophosphate Phosphatases to PgpB

As UppP (formally BacA) is now thought to generate 75% of the undecaprenyl pyrophosphate in a bacterial cell, the spectrophotometric, phosphate-release assay could be tried with UppP as an alternative to PgpB. UppP has been suggested to generate 75% of the total cellular C_{55}-PP phosphatase activity, whereas the other enzymes may account for the remaining 25% phosphatase activity (El Ghachi, 2004, El Ghachi 2005).

5.9.5 The PgpB Assay and Bacitracin

The PgpB assay could be conducted in the presence of bacitracin, which binds to undecaprenyl pyrophosphate, and showed increased levels of undecaprenyl pyrophosphate phosphatase activity *in vivo* (El Ghachi *et al*., 2005). Modification of bacitracin with a fluorophore reporter could allow indirect monitoring of transglycosylation (Manat *et al.*, 2014).

Chapter 6
The Study of Transpeptidation in Class A Penicillin Binding Proteins from *E. coli* and *P. aeruginosa*

The precise catalytic mechanism of transpeptidation by PBPs is yet to be fully understood and assay methods are limited. The synthesis of transpeptidase donor and acceptor compounds in this chapter will aid in understanding specific requirements for these molecules and their function in transpeptidation. Efforts in developing compounds towards a FRET assay in this chapter aim to further observe the process of transpeptidation in real time, providing further enzymatic and mechanistic insights.

6.1 Defining Transpeptidase Donors and Acceptors

The mechanism of transpeptidation is an attractive target for antibiotics as it occurs on the outer face of the cytoplasmic membrane of the bacterium, and is a lethal target. If this system is disrupted and peptidoglycan formation is prevented, e.g. by the action of penicillin, the bacterial cell wall will lyse under osmotic pressure. Transpeptidation forms the cross-links between two adjacent pentapeptide strands to form a pentapeptide bridge and a mesh-like structure of high tensile strength to resist osmotic stresses. In transpeptidation, there is a donor substrate and an acceptor substrate (**Figures 6.1** and Figure 1.6). The donor substrate forms an acyl-enzyme complex with the PBP (section 1.45) and is often part of an elongating glycan chain. The acceptor substrate is part of an adjacent glycan strand (Lupoli *et al.*, 2011).

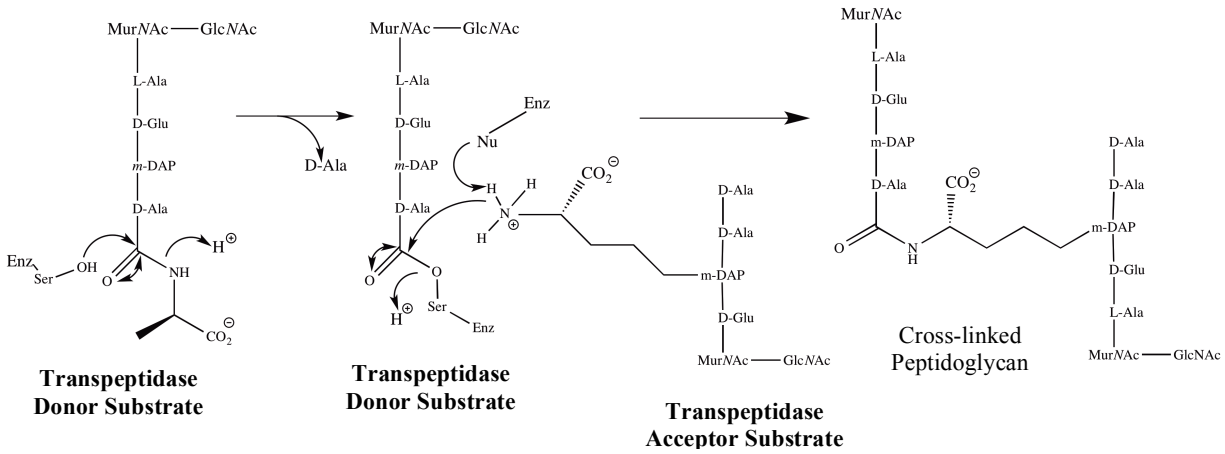

Figure 6.1 Transpeptidase Donor and Acceptor Compounds. In the mechanism of transpeptidation (section 1.4.5), the active site serine of the PBP forms a covalent bond with the carbonyl of the penultimate D-alanine of the donor strand. This releases the C-terminal D-alanine from the pentapeptide stem forming a PBP-seryl Mur*N*Ac-Glc*N*Ac tetrapeptidyl species. The ε-amino group of the diaminopimelyl moiety of the acceptor displaces the PBP, forming a peptide bond constituting a 3-4 cross-link formed between the fourth D-alanine on the donor strand and the third *meso*DAP residue on the acceptor strand.

In order to monitor transpeptidation specifically, the requirements of a transpeptidase donor assay substrate are that it is able to polymerise LII, with the second requirement that it is not able to cross-link to any adjacent glycan strand. Most Gram-negative bacteria cross-link to the *meso*DAP residue on the acceptor strand, so labelling the reactive ε-amine of the *meso*DAP residue with a dansyl or fluorescamine fluorophore prevents the substrate from being a transpeptidase acceptor, but not in principle, a donor.

In the transpeptidase acceptor molecule, the *meso*DAP residue at position three of the peptide stem cross-links to the fourth residue of the transpeptidase donor. Natural peptide acceptors have been shown to contain reactive amine D-amino acids (Lupoli *et al*., 2011). In the case of *meso*DAP, there are two stereocentres with differing configuration: L and D. In peptidoglycan, the L-stereocentre is incorporated into the peptide backbone and is not involved in DD-transpeptidase cross-linking, whereas the D-stereocentre cross-links to the fourth amino acid of the donor strand (Pillai *et al.*, 2006).

6.2 Transpeptidase Assays in the Literature

DD-Transpeptidase activity is challenging to measure and characterise, as the products are not easily distinguished from uncross-linked peptidoglycan, because they have similar chromatographic properties (Jha & de Sousa, 2006). The transpeptidase domain of PBPs functions as both a DD-transpeptidase as well as a DD-carboxypeptidase, both of which result in the release of D-alanine, but nearly all assays available do not distinguish between the two functions. Efforts towards the development of transpeptidase assays in the past have included making peptide thioester substrates as a means for showing transpeptidation (Grandchamps *et al.*, 1995). However, these thioester substrates were not entirely representative of native *in vivo* peptidoglycan and had low affinity. Additionally, the thiolester linkage was reactive towards non-enzymatic hydrolysis, making PBP assays with these substrates relatively insensitive (Adams *et al.*, 1991).

The drive to search for potential transpeptidase inhibitors resulted in assays being developed that relied on how well the inhibitor compound out-competed the β-lactam for transpeptidase active-site binding. A scintillation Proximity Assay (SPA) was developed to screen for potential transglycosylase and transpeptidase inhibitors, assaying the transpeptidase in an *E. coli* membrane environment (Kumar *et al.*, 2014). Using Wheat Germ Aglutinin (WGA)-SPA beads, the cross-linked products were distinguished from the uncross-linked substrate as well as uncross-linked LII. This two-step assay first treated the membranes with a concentration of vancomycin that inhibited transglycosylation, but not MraY or MurG, to accumulate LII in the *E. coli* membranes. The second step of this assay involved the addition of D-Ala-D-Ala to counter the presence of the vancomycin and trigger transpeptidation. The results were captured by scintillation counts.

Assays that have used native substrates used methods including chromatography and spectrophotometry, mostly to detect amino acid exchange. The products of peptidoglycan synthesis can, after enzymatic digestion, be separated by HPLC and analysed quantitatively using mass spectrometry to detect and confirm the presence of cross-linked material, the extent of cross-linking as well as the relative abundance of the various muropeptides (Vinatier *et al.*, 2009). Vollmer and colleagues developed an

assay using radio-labelled LII as the substrate for polymerisation by *E. coli* PBP1A (Born *et al.*, 2006) and *E. coli* PBP1B (Bertsche *et al.*, 2005), then subsequently digesting the polymerised products with cellosyl ready for analysis by HPLC. Synthesised peptidoglycan products have also been analysed by LC-MS without the need for radioactivity (Lebar *et al*., 2014). The disadvantage of all of these assays thus far, is that they are all stopped assays with none of them showing any kinetic activity in real-time (with the exception of the thiol ester substrate assays, which suffer from intrinsic instability of the substrate within the assay).

6.2.1 The Exchange Reaction

The exchange reaction is the most recent attempt at characterising the two steps of transpeptidation. The first step of transpeptidation is donor activation resulting in the release of the terminal D-alanine and the esterification of the remaining tetrapeptide to the transpeptidase active site of the PBP. The second step of the exchange reaction involves the attack by D-alanine (or for the purposes of assay, an alternative D-amino acyl species) of the PBP-tetrapeptide intermediate to reform the pentapeptide of the donor strand. In this instance, the reaction overall is a transpeptidation event, but by reversal of the initial acylation of the PBP with its donor substrate. To study the suitability of peptidoglycan donor chains as a substrate for the second step of transpeptidation (linking with the acceptor), Lupoli *et al.*, trialled a variety of L and D amino acids (alanine, glycine, tryptophan, phenylalanine and tyrosine) as potential participants in the exchange reaction (**Figure 6.2**).

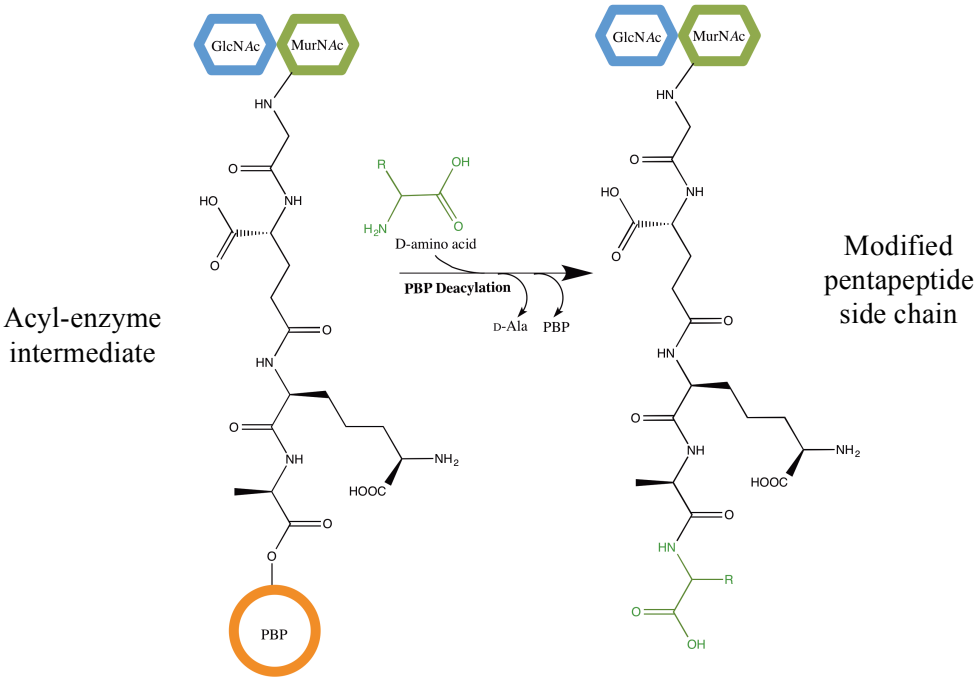

Figure 6.2 The D-Amino Acid Exchange Reaction

The D-amino acid acted as the nucleophile and exchanged the terminal D-alanine with the added amino acid. Only the D-amino acids were incorporated (exchanged) in to the fifth position of the donor strand. This exchange reaction has been exploited to label the peptide with fluorescent D-amino acids (Kuru *et al.*, 2012).

6.3 Experimental Aims

- To develop novel donor and acceptor substrates for the study of transpeptidation via a FRET assay
- To synthesise UDP-Mur*N*Ac-L-Ala-γ-D-Gln-*meso*DAP-D-Ala-D-Ala labelled with Fluorescamine
- To characterise the synthesised compounds as potential transpeptidase donors and acceptors
- To characterise the transpeptidase activity of *P. aeruginosa* and *E. coli* Class A PBPs, via a continuous spectrophotometric assay
- To monitor the continuous, *in vitro* detection of the transpeptidase activity of *E. coli* PBP1A, followed by optimising the assay conditions.

- To analyse the ability of transglycosylase and transpeptidase active site mutants to perform transpeptidation
- To test the transpeptidase function of *P. aeruginosa* PBP1A under the conditions defined for *E. coli* PBP1A.

6.4 The Development of a FRET Assay Allowing the Kinetic Characterisation of Class A PBPs

Developing a novel transpeptidation assay will extend our understanding of the transpeptidase mechanism through kinetic analysis of PBPs which itself could be used to identify potential inhibitors.

Compared to transpeptidation assays involving radioactivity, using fluorescence as a reporter for reaction progression is more convenient and can be visualised in real-time. Fluorescent labels appended to the pentapeptide stem in LII and have successfully been used as reporters in continuous assays for transglycosylation (Schwartz *et al.*, 2001, Mohammadi, *et al.*, 2011). The convenience of using fluorescence over radioactivity and the ability to already incorporate fluorophores in to peptidoglycan precursors, together with the opportunity to selectively label the transpeptidase donor and acceptor are sound justification for the choice to use FRET to study transpeptidation.

6.4.1 Definition of FRET

Förster Resonance Energy Transfer (FRET) involves donors and acceptors of energy, which is transferred through space from a donor fluorophore to an acceptor fluorophore. FRET can be used to measure the relative amount of donor and acceptor fluorophore complexes, protein-protein interactions, protein-ligand interactions, or protein-protein inter-distances, usually by labelling the proteins with fluorophores.

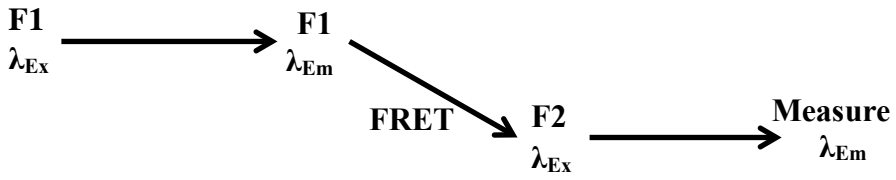

6.4.2 The Förster Radius (R_0)

The Förster distance (radius, R_0) is the critical distance at which 50% of internal quenching occurs. Each pair of fluorophores has their own R_0 length (in Ångstroms). The bigger the R_0 value, the larger the distance over which that emission can be transferred to the FRET acceptor, but the efficiency of transfer is reduced. It can be useful to increase the R_0 to accommodate for the long undecaprenyl chain in LII, which is approximately 50Å (Huang *et al.*, 2013). The Förster radius can be determined from the optical properties of the fluorophores used (Roy *et al*. 2008).

6.4.3 The Pros and Cons of FRET

FRET can be a convenient alternative to radioactivity assays as they continuous, quantitative, high throughput and can be used to determine kinetic constants such as inhibition constant (K_i). FRET can be a highly sensitive method that can be used to measure distance or changes in distance *in vitro* and *in vivo*. However, some drawbacks to the technique include the requirement for a low background to have a sensitive signal-to-background ratio for real-time enzymatic assays. FRET-pair labelling also needs to be bright, with the donor fluorophore completely saturated by the acceptor fluorophore. Occasionally, free fluorophores can mask energy transfer and fluorescence can be quenched. Additionally, modification of the substrate can either eliminate its ability to support the enzyme activity or significantly modifies the kinetics of the enzyme relative to that displayed by native substrates. Fluorescence is also relative, rather than absolute.

6.5 Designing the Transpeptidase Donor and Acceptor Compounds for FRET

In the specific case of this assay, the terms ‘transpeptidase acceptor’ and ‘transpeptidase donor’ are used to describe the substrates involved in the transpeptidase reaction. In addition to this terminology, donor and acceptor are also used in the FRET literature to indicate which fluorophore donates or accepts the fluorescence energy, i.e. donor fluorophore and acceptor fluorophore. In this FRET assay, **the transpeptidase donor is labelled with the FRET acceptor fluorophore and the transpeptidase acceptor harbours the FRET donor fluorophore.**

Considerations when designing the transpeptidase FRET assay included determining the requirements for a donor molecule and for acceptor molecules. For a molecule to be a donor only, the epsilon amino group on the third amino acid in the peptide stem must not be capable of nucleophilic attack thereby also acting as an acceptor molecule. There are three methods of ensuring that a peptidoglycan precursor acts as a transpeptidation donor only:

1. Labelling the *meso*DAP residue with a fluorophore attached to its ε-amine group shields the D-stereocentre of the DAP residue. Blocking this functional group prevents acceptor capability and ensures donor-only capability. Dans-LII has this property of only being able to serve as an acyl donor in the transpeptidase reaction. The large dansyl group attached to position 3 prevents the non-proteinaceous *meso*-DAP from acting as an acyl-acceptor.
2. Another requirement of the transpeptidase donor is that it must be able to be polymerised in to a linear glycan strand, as a polymeric fragment of peptidoglycan, i.e linear glycan strands without any chance of cross-linking with each other are required for transpeptidation to occur.

Acceptor molecules need only be a single amino acid with the amine nucleophile in the D-configuration. L-amino acids are discriminated against (Lupoli *et al,*, 2011, Lebar *et al.,* 2014).

6.5.1 Criteria for a Successful FRET System

1) The optimum fluorescence emission of the donor molecule must overlap with the excitation wavelength of the acceptor (Willard *et al.*, 2001).

An overlap between the emission spectra of the donor fluorophore and the absorption spectrum of the acceptor fluorophore is necessary for energy transfer to occur. FRET efficiency (the degree to which energy is transferred), is related to the overlap between the respective spectra of the fluorophores, and is highly dependent on the distance between them (dynamic range). At the middle of the dynamic range, half of the energy would be transferred from donor to acceptor.

2) The distance between the two fluorophores, defined as the Förster Radius (R_0) is optimal between 20-80Å, depending on the nature of the pairing (Corry *et al.*, 2005).

There is a spectral overlap integral between the donor fluorophore emission spectrum and the acceptor fluorophore absorbance spectrum, which can be calculated. Using the calculated spectral overlap integral, the Förster radius for a specific fluorophore pair can then be calculated if the quantum yield of the donor in the absence of the acceptor is known, the dipole orientation factor, the refractive index of the solvent system and Avogadro's number. FRET efficiencies (obtained by experimentation) can be used to estimate the separation distance between the two fluorophores.

6.5.2 Selecting the Optimum Fluorophores for Transpeptidase Donors and Acceptors

6.5.2.1 Potential FRET Donor Fluorophores

The intensity of emission of a fluorophore is determined primarily by its extinction coefficient and quantum yield, which are both dependent on the environment of the fluorophore. Fluorophores that could potentially be compatible with being incorporated in to the transpeptidase acceptor molecule are listed in **Table 6.1**.

Table 6.1 Potential Fluorescent Amino Acids that can be Incorporated in to the Pentapeptide Stem of the Transpeptidase Acceptor Molecule (Molecular Probes website).

	Absorbance		**Fluorescence**		
FRET Donor Fluorophore	**Ex λ (nm)**	**Extinction Coefficient***	**Em λ (nm)**	**Quantum Yield** (Φ_f)**	**Molecular weight (g/mol)**
D-Tryptophan	280	5,690	348	0.20	204.23
D-7-Azatryptophan	300	5,080	390	0.03	205.21
Tyrosine	274	1,400	303	0.14	181.19
Phenylalanine	257	200	282	0.04	165.19

*All extinction coefficients reported at the absorption maximum of the fluorophore
** All quantum yields given are for an aqueous environment

D-Azatryptophan and D-tryptophan have very similar extinction coefficients but D-azatryptophan has a much lower quantum yield comparatively. All potential fluorophores have similar spectral maxima because they are all α-amino acids. These properties were considered when matching this FRET donor fluorophore with an acceptor fluorophore See **Figure 6.3** for the selected FRET acceptor fluorophores.

6.5.2.2 Potential FRET Acceptor Fluorophores

A variety of fluorophores were considered as FRET acceptor fluorophores including dansyl, Fluorescamine, Fluorescein, NBD, Rhodamine II, Biotin, and BODIPY^{TM}. Which all have varying quantum yields, extinction coefficients and fluorophore size. The selected fluorophores are required to be able to label the DAP residue on the transpeptidase donor molecule. The fluorophore selected would be a FRET acceptor fluorophore, but would be labelling the transpeptidase donor molecule.

There is a large variety in the molecular weights of the fluorophores, with BODIPY^{TM} being this largest. The 'bulkiness' of the fluorophore needs to be considered so that it does not interfere with the natural transpeptidase mechanism. The excitation wavelength of this FRET acceptor fluorophore has to overlap significantly with the emission wavelength of the selected FRET donor fluorophore. After extensive research in to a variety of different fluorophore pairings, two sets of fluorophore pairs were chosen for this FRET assay.

Dansyl chloride has traditionally been used to label the *meso*DAP residue on the pentapeptide stem, for tracking transglycosylation processivity (Schwart *et al.,* 2002; Liu *et al*., 2010). The excitation wavelength (λ_{Ex}) of dansyl is 340 nm and the emission wavelength (λ_{Em}) of D-tryptophan is also 340 nm (Figure 6.3). Therefore the dansyl label on the pentapeptide stem can be the FRET acceptor fluorophore and a D-tryptophan residue can be incorporated in to the pentapeptide stem of the transpeptidase acceptor. The considerations with using D-tryptophan as a fluorophore are that it is sensitive to solvent polarity as a fluorophore (Vivian & Callis, 2001), which is also the case for dansyl. Also, in the presence of a proteinaceous enzyme in an assay environment, any aromatic amino acids in the enzyme would also be excited at 280 nm and potentially interfere with FRET and contribute to background noise. An alternative

to D-tryptophan is D-7-azatryptophan, whose excitation spectrum is red shifted by 20 nm but has the disadvantage that its quantum yield is lower. D-7-Azatryptophan can be incorporated in to the pentapeptide stem to serve as a FRET donor fluorophore. The cognate acceptor fluorophore is fluorescamine. The emission maximum of D-7-azatryptophan is 360-390 nm, overlapping with the excitation maximum of fluorescamine.

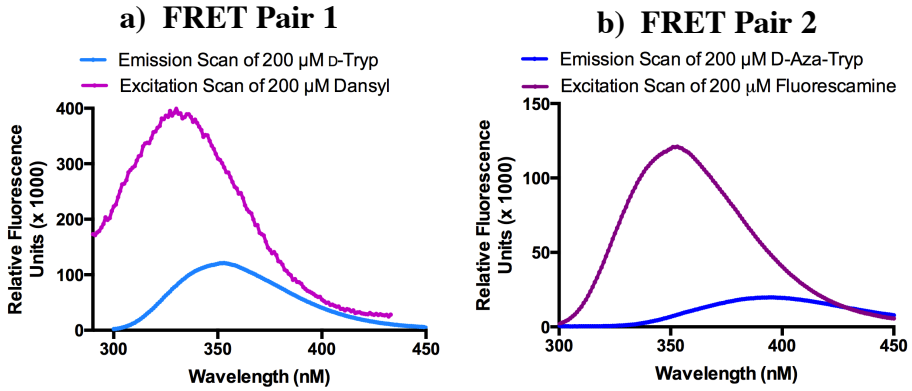

(a) FRET Pair 1		λ_{Ex} (nm)	λ_{Em} (nm)	Extinction Coefficient	Quantum Yield (Φ_f)
Donor Fluorophore	D-Tryptophan	280	340	5,690	**0.20**
Acceptor Fluorophore	Dansyl	340	520	4,550	0.70
(b) FRET Pair 2					
Donor Fluorophore	D-7-Azatryptophan	295	360	5,080	0.03
Acceptor Fluorophore	Fluorescamine	390	470	26,000	0.23

Figure 6.3 Potential FRET Fluorophore Pairs and their Fluorometric Properties (a) The emission spectrum of the FRET donor fluorophore (D-tryptophan) overlaps sufficiently with the excitation maximum of the acceptor fluorophore (Dansyl). **(b)** The emission spectrum of the FRET donor fluorophore (D-azatryptophan) overlaps sufficiently with the excitation maximum of the acceptor fluorophore (Fluorescamine).

Other factors in addition to overlapping spectra were considered when selecting fluorophores, such as quantum yield (brightness of fluorescence), the Förster distance between the two fluorophores, along with the size and shape of the fluorophore. The ability of the fluorophore to incorporate naturally in to the peptidoglycan precursor without disrupting transpeptidation is of paramount importance, which is another justification for selecting amino acids as FRET donor fluorophores, as amino acids are present in the pentapeptide stem of all peptidoglycan precursors naturally. A summary of the selected FRET fluorophore pairs is in **Figure 6.5**.

6.5.2.3 Considering R_0: The Förster Distance Between Rwo FRET Pairs

The Förster radius (R_0) for a specific FRET pair is the distance at which half the energy in transferred from the donor fluorophore to the acceptor fluorophore. For any specific dye pair, only a small measurable range of distances around R_0 can be accurately quantified. Using the extinction coefficient of fluorescamine and the quantum yield of D-azatryptophan, the R_0 for this FRET pair was calculated to be 25.74 Å according to the Förster equation. The R_0 for D-tryptophan and dansyl was calculated as 26.14 Å.

6.5.2.4 The Selected Fluorescent Compounds to be Synthesised

In the proposed FRET assay, the transpeptidase donor is labelled with the FRET acceptor fluorophore and the transpeptidase acceptor harbours the FRET donor fluorophore, clarified in **Figure 6.4**.

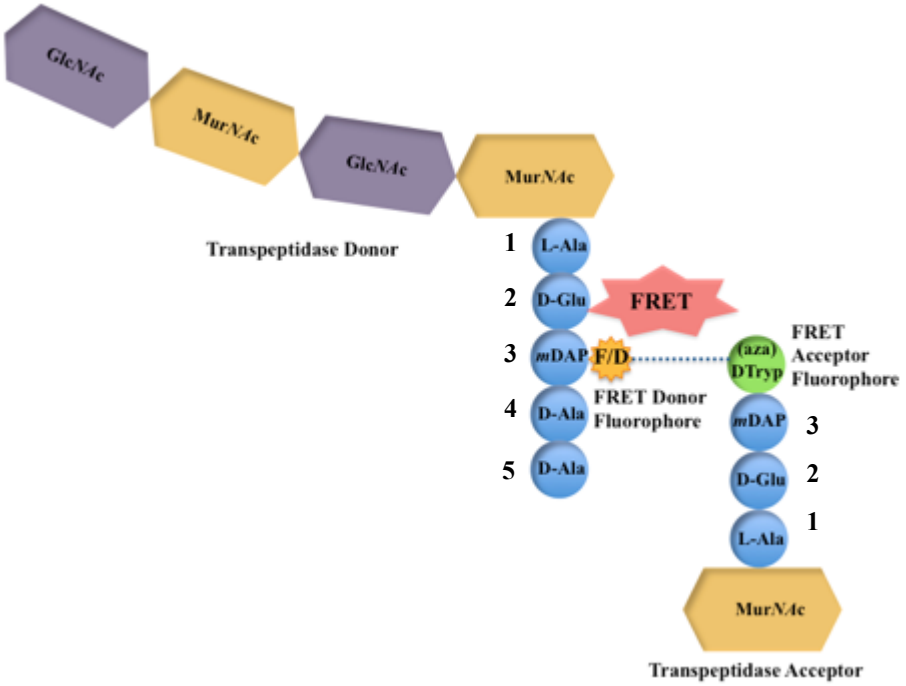

Figure 6.4 A Schematic of the Concept Behind the Proposed FRET Assay Mechanism. Energy transfer should occur when the third position ε-amino group of the diaminopimelyl moiety of the transpeptidase acceptor forms a cross-link with the carbonyl of the forth position D-alanyl residue of the transpeptidase polymeric donor. The transpeptidase donor is Dansyl- or Fluorescamine-labelled DAP-LII (F/D in figure), with the FRET acceptor fluorophore being the dansyl or fluorescamine label. The transpeptidase acceptor is Mur*NA*c-L-Ala-D-Glu-*meso*DAP-D-Trp-D-Ala or Mur*NA*c-L-Ala-D-Glu-*meso*DAP-D-Azatrp-D-Ala, with the D-trp or D-azatrp at the fourth position being the FRET donor fluorophore.

The chemical structures of the four compounds synthesised are in **Figure 6.5**.

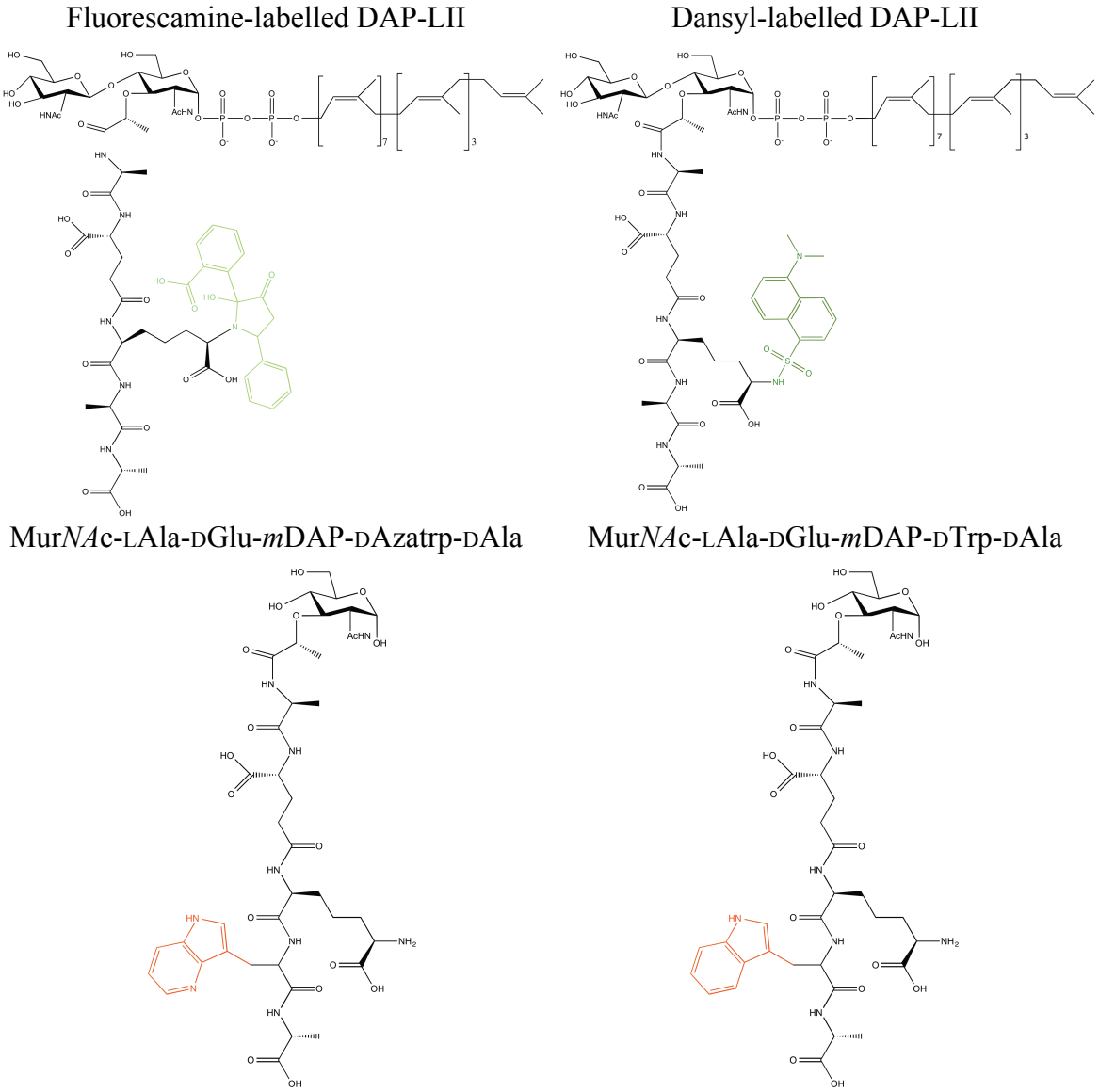

Figure 6.5 The Structures of the Four Compounds Chemi-Enzymatically Synthesised to Function as FRET Donors and Acceptors as well as Transpeptidase Acceptors and Donors.

These substrates were designed so that the fluorophore causes the least interference to the transpeptidase function and flexibility of the compound. The FRET donor fluorophores are amino acids that are thought to be able to be tolerated in to the native peptide stem on a transpeptidase acceptor (Lebar *et al.*, 2014, Lupoli *et al.*, 2011, Schouten *et al.*, 2006). The FRET acceptor fluorophores were attached to the ε-amino group on the *meso*DAP residue in the pentapeptide stem.

6.5.3 The Fluorescent Properties of the Selected Fluorophores

The emission maxima for each fluorophore were tested under different pH conditions (**Figure 6.6**).

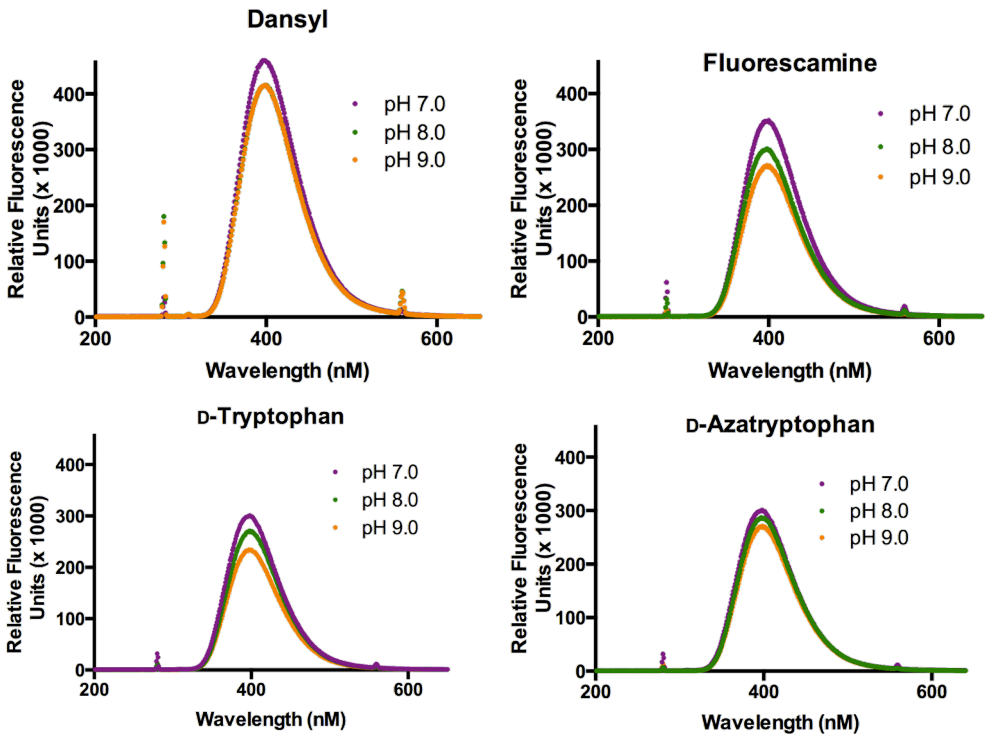

Figure 6.6 The Emission Maxima of the Four Fluorophores Dansyl, Fluorescamine, D-Tryptophan and D-Azatryptophan were tested between pH 7.0 and 9.0.

Each of the fluorophores have the same emission maximum under different pH conditions, although the fluorescence efficiency (quantum yield) differs slightly (insignificantly) under different pH conditions, with each fluorophore having a slightly lower quantum yield at pH 7.0 compared to pH 9.0. Assays were conducted at pH 8.5 as this is the optimum pH for the transpeptidase activity of *E. coli* PBP1B (Adrian Lloyd, personal communication).

6.6 Synthesis of the Transpeptidase Acceptor Compounds

6.6.1 Synthesis of Mur*NA*c-L-Ala-D-Glu-*meso*DAP-D-Azatrp-D-Ala

Introducing an alternative acceptor in the form of D-tryptophan was recently shown with *E. coli* PBP1A (Lupoli *et al.*, 2011). The more intrinsically fluorescent molecule, D-azatryptophan is used as a potential acceptor in the transpeptidase reaction in this FRET assay. Incorporating a non-canonical amino acid in to the pentapeptide stem at the fourth position involved synthesising the UDP-Mur*NA*c-L-Ala-D-Glu-*meso*DAP and subsequently exploiting the promiscuity of the ATP-dependent Mur ligase MurF, which naturally attaches the D-Ala-D-Ala dipeptide on to the UDP-Mur*NA*c-Tripeptide. MurF (from the Gram-negative species *P. aeruginosa*) was tested to see if its specificity could be exploited to incorporate the unusual dipeptide at the terminus of the tripeptide.

There are two ways in which D-azatryptophan could be incorporated into the pentapeptide: either as a residue previously ligated to D-Ala, forming a dipeptide substrate prior to incorporation in to the peptide stem by MurF, or by the utility of D-alanyl-D-alanine ligase (Ddl) where two D-Ala residues are ligated together by Ddl A or B. However, DdlA/B is D-Ala specific (Healey *et al.* 2000) and would be unlikely to ligate D-azatryptophan to D-Ala. VanA and VanB are alternative ligases to DdlB, both of which ligate D-Lac to D-Ala, and VanC is a D-Ala-D-Ser ligase. D-Ala-D-X ligases all use zwitterionic D-Ala and proceed in a two-step reaction. Initially, a phosphoryl intermediate is formed proceeded by nucleophilic attack of this intermediate by the second substrate. VanA is a D-Ala-D-Lac ligase that requires ATP for activity and is known to make D-Ala-D-X dipeptides (Bugg *et al.*, 1991). A continuous spectrophotometric ADP-coupled release assay, for the enzymatic analysis of VanA was published (Daib *et al.,* 1988). The substrate specificity of VanA was tested to see if it was more promiscuous than DdlB and would attach D-Ala to D-azatryptophan (**Figure 6.7**).

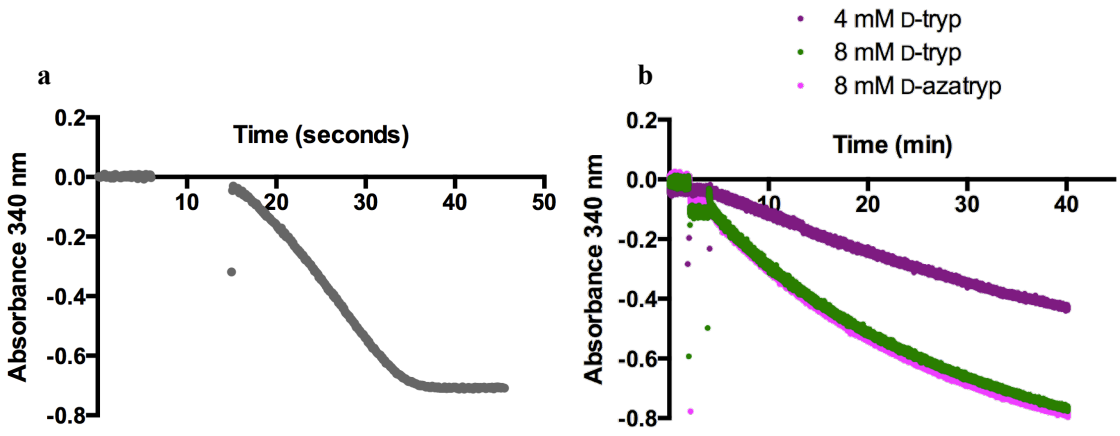

Figure 6.7 The Ligation of D-Tryptophan and D-Azatryptophan on to D-Ala by the D-Ala-D-Lac ligase *E. coli* VanA. (a) The addition of 4 mM D-Lactate as a positive control for the D-Ala-D-Lac ligase VanA **(b)** Testing the ability of VanA to ligate D-Ala to D-Trp (4mM or 8mM) or D-Azatrp (8 mM). Assay conditions: 10 mM HEPES pH 7.5, 10 mM $MgCl_2$, 10 mM KCl, 0.15 mM NADH, 2 mM PEP, 7.5 Units pyruvate kinase, 9 Units lactate dehydrogenase, 5 mM ATP, 0.1 mM D-Ala and either 4 mM or 8 mM D-Trp of D-Azatrp. A low concentration of D-Ala was used along with a very high concentration of the D-tryptophan and D-azatryptophan, to promote incorporation of the unusual amino acid in to the second site of the dipeptide. Monitored at 340 nm as the pyridine ring of NADH absorbs light at this wavelength but the aromatic ring of NAD^+ does not.

VanA successfully ligated D-Trp to D-Ala as well as D-Azatryptophan to D-Ala. MurF may also incorporate these unusual dipeptides in the pentapeptide stem, resulting in D-trp or D-azatrp at the fifth position. However, for the purposes of this FRET assay, D-trp and D-azatrp are needed at the forth position in the pentapeptide, so this is not a suitable methods for incorporating the non-canical residues into the pentapeptide stem. Alternatives to VanA are VanC, VanC2 or Lmdl, but in all cases the non-D-Ala amino acid is second in the dipeptide sequence, resulting in the terminal amino acid in the pentapeptide stem deviating from the canonical D-Ala. D-Azatryptophan would need to be first in the dipeptide in order for it to reside at position four in the pentapeptide after incorporation by MurF, VanA ligase does not allow for this. The substrate specificity of MurF may be flexible enough to incorporate a D-azatrp-D-Ala dipeptide. The dipeptide (-R-D-Azatrp-D-Ala-OH) was synthesised separately by ActivoTech and used to test the promiscuity of *Pa*MurF with respect to ligation of D-azatrp-D-Ala to the C-terminal DAP carboxyl of UDP-Mur*NA*c-L-Ala-D-Glu-*meso*DAP.

Both *Pseudomonas aeruginosa* (*Pa*) and *S. pneumoniae* (*Sp*) MurF were tested in a continuous coupled spectrophotometric assay (**Figure 6.8a**). ADP released upon the successful ligation of the dipeptide to the tripeptide is phosphorylated by pyruvate

kinase, with PEP regenerating the ATP consumed by MurF. The pyruvate formed from pyruvate kinase is reduced to lactate with the concurrent oxidation of NADH to NAD^+ + H^+ by lactate dehydrogenase. The oxidation of NADH is observed as a decrease in absorbance at 340 nm, due to fewer pyridine rings from NADH, as NADH is oxidised. This coupled assay was utilised to see whether MurF could incorporate the unusual dipeptide D-azatrp-D-Ala (**Figure 6.8 b-c**), which was necessary to confirm before setting up a pentapeptide synthesis reaction.

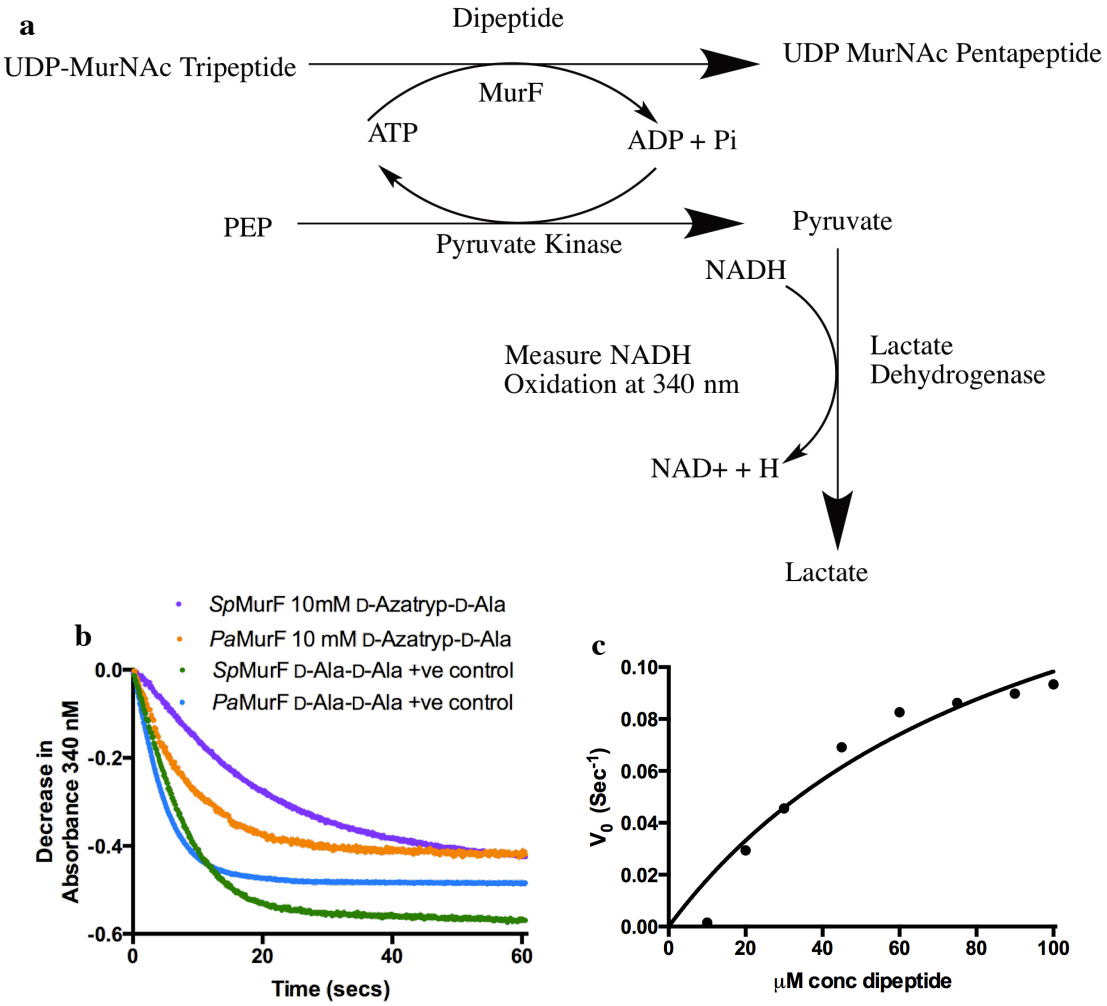

Figure 6.8 The Incorporation of Non-Canonical Dipeptides (D-Azatryp-D-Ala) at the C-Terminus of the Pentapeptide Stem, using MurF. (a) A schematic of the continuous, coupled spectrophotometric assay used to test the substrate specificity of MurF with respect to ligation of the non-canonical dipeptide -R-D-Azatrp-D-Ala-OH to form UDP-Mur*N*Ac-L-Ala-D-Glu-*meso*DAP-D-Azatrp-D-Ala. **(b)** The incorporation of the non-canonical dipeptide D-Azatrp-D-Ala, using both *P. aeruginosa* MurF and *S. pneumoniae* MurF. The native D-Ala-D-Ala dipeptide was the positive control, incorporated using both *Pa* and *Sp*MurF. 1 mM of dipeptide was used in each assay and 1 µM MurF **(c)** The dependence of *Pa*MurF initial velocity on D-Azatrp-D-Ala, data fitted to Equation 4.1 by non-linear regression.

Both Gram-negative (*Pa*) and Gram-positive (*Sp*) MurF successfully attached the unusual dipeptide on to the tripeptide. The affinity of *Pa*MurF for the dipeptide D-Azatrp-D-Ala was calculated as a K_m of 96 µM ± 14. To exploit the observation that *Pa*MurF could utilise D-Azatrp-D-Ala, a pentapeptide synthesis reaction of UDP-Mur*NA*c-L-Ala-D-Glu-*meso*DAP-D-Azatrp-D-Ala was set up (section 2.7.1) and the products were subsequently purified on an anion exchange Source 30Q column, upon a gradient from 10 mM to 1 M ammonium acetate (**Figure 6.9**).

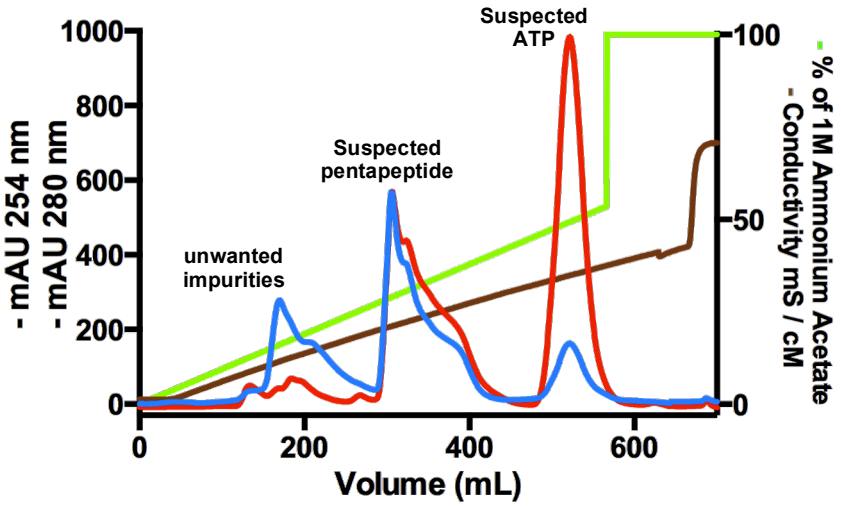

Figure 6.9 Purification of the potential transpeptidase acceptor UDP-Mur*NA*c-L-Ala-D-Glu-*meso*DAP-D-Azatrp-D-Ala on a Source 30Q column with an ammonium acetate gradient from 10 mM to 1 M.

The first peak to be eluted was suspected to be unwanted impurities, with the second peak being more likely to contain the desired organic compound with its prominent absorbance at A_{254} nm, due to the presence of the UDP group. This elution pattern is common from previous experience with purification of UDP-Mur*N*Ac-DAP pentapeptide, suggesting that the second peak was likely to be the desired compound. The third peak displays the typical profile of ATP, i.e. a A_{254} : A_{280} ratio of 6:1. The fractions in the second peak suspected to be the UDP-pentapeptide were pooled and lyophilised to remove the ammonium acetate.

To confirm the presence of pentapeptide in this second peak a coupled, enzymatic assay was used. Here, the terminal D-Ala was released from the pentapeptide by the enzyme *E. coli* DacB, a low molecular weight penicillin-binding protein with DD-carboxypeptidase activity, D-alanine was then oxidised by D-amino acid oxidase (DAAO), generating hydrogen peroxide which was detected by horse radish peroxidase-

catalysed reaction with the chromogen Amplex Red, to generate the red dye resorufin with an intense absorbance at 555 nm ($\varepsilon = 55{,}000 M^{-1}.cm^{-1}$). This coupled assay confirmed the presence of the C-terminal D-amino acid residue of the suspected pentapeptide. Fractions in the other peaks were also tested for the presence of pentapeptide, with peaks 1 and 3 testing negative for the presence of pentapeptide (**Figure 6.10**).

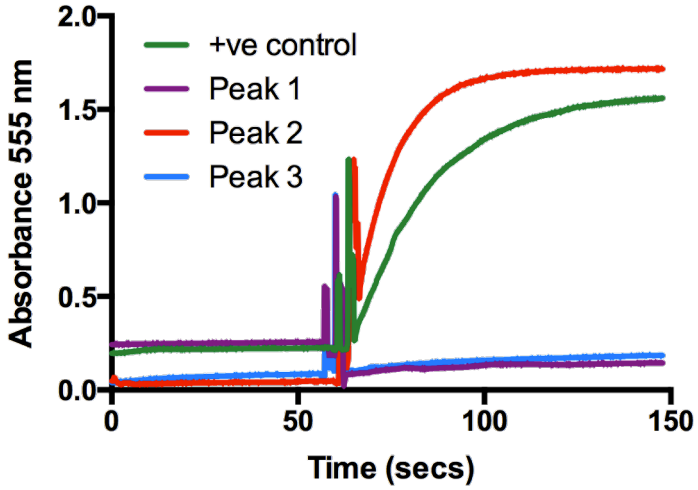

Figure 6.10 Determining the presence of pentapeptide by release of the terminal D-Ala residue from UDP-Mur*NA*c-L-Ala-D-Glu-*meso*DAP-D-Azatrp-D-Ala. Elution peaks in Figure 6.9 were analysed for pentapeptide presence. The positive control used was UDP-Mur*NA*c-L-Ala-D-Glu-*meso*DAP-D-Ala-D-Ala.

The second peak from the pentapeptide purification in Figure 6.9 was confirmed enzymatically to be pentapeptide; therefore it could be concluded that MurF incorporated D-Azatrp-D-Ala in to UDP-Mur*NA*c-L-Ala-D-Glu-*meso*DAP-D-Azatrp-D-Ala. This product was then assessed for purity using a MonoQ analytical column developed with a gradient of 10 mM – 1 M Ammonium Acetate (**Figure 6.11**).

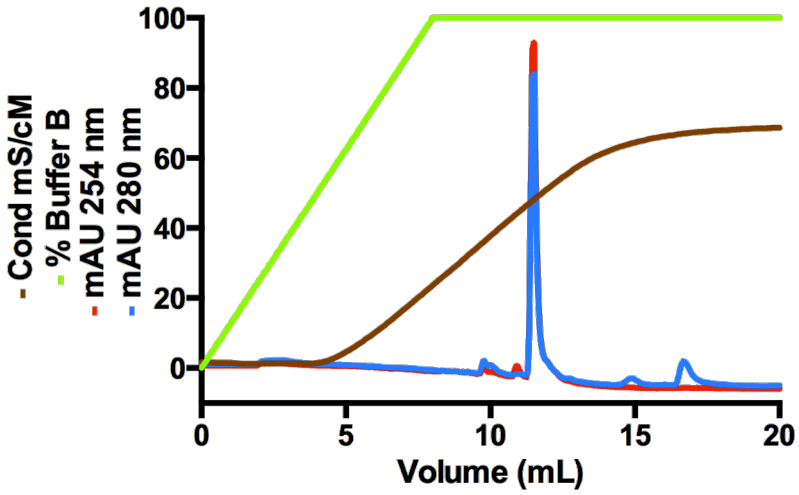

Figure 6.11 MonoQ analysis of UDP-Mur*NA*c-L-Ala-D-Glu-*meso*DAP-D-Azatrp-D-Ala to assess the purity of the pentapeptide.

The pentapeptide was subjected to mass spectrometry, which confirmed identity as UDP-Mur*NA*c-L-Ala-D-Glu-*meso*DAP-D-Azatrp-D-Ala (**Figure 6.12)**. The exact mass (m) of the compound was calculated as 1308.34 Daltons. The expected mass-to-charge (m/z) values of the singly, doubly and triply charged ions under nanospray-time-of-flight (TOF) M/S conditions were (m-1)/1 = 1308.34, (m-2)/2 = 653.17, (m-3)/3 = 435.11.

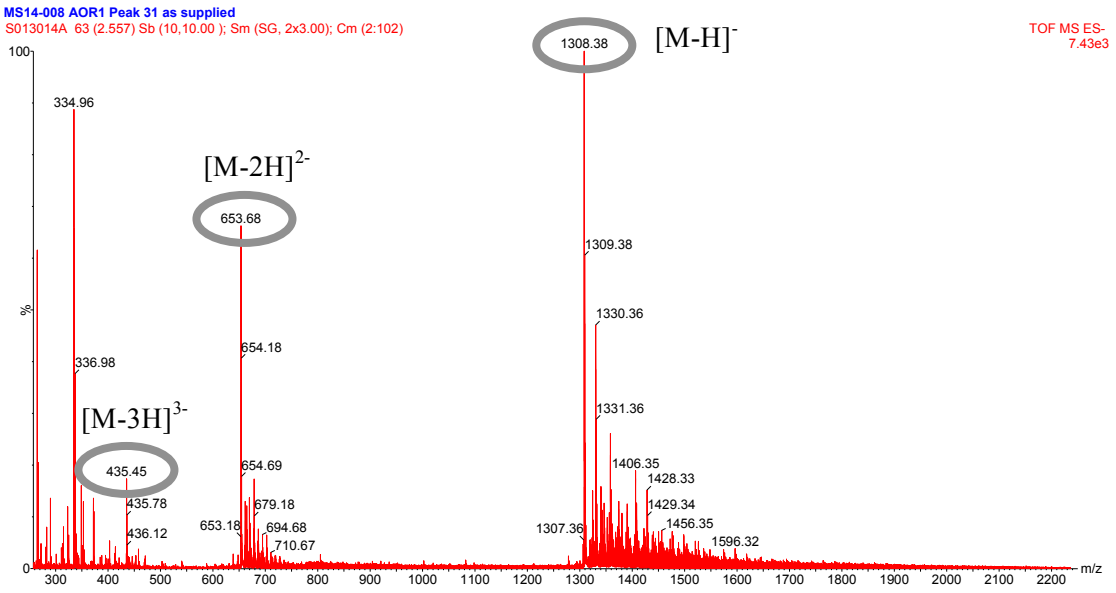

Figure 6.12 The mass spectrometry results of UDP-Mur*NA*c-L-Ala-D-Glu-*meso*DAP-D-Azatrp-D-Ala. Observed: 1308.38, expected: 1308.34, observed: 653.68, expected: 653.17, observed: 435.45, expected: 435.11.

Half of the purified UDP-Mur*NA*c-L-Ala-D-Glu-*meso*DAP-D-Azatrp-D-Ala was stored at -20 °C and the rest was further modified to remove its UDP group by acid hydrolysis, as native transpeptidase acceptors do not have a UDP group. The acid hydrolysed sample was purified to remove the hydrolysed UDP group, by anion exchange on a Source 30Q column, over an ammonium acetate gradient (data not shown). The final pentapeptide product (Mur*NA*c-L-Ala-D-Glu-*meso*DAP-D-Azatrp-D-Ala was lyophilised to remove the ammonium acetate before analysing its function as a transpeptidase acceptor. A final yield of 2.4 mgs was calculated (section 2.7.3).

6.6.2 Synthesis of Mur*NA*c-L-Ala-D-Glu-*meso*DAP-D-Trp-D-Ala

To establish the feasibility of synthesis of a second, non-canonical UDP-Mur*NA*c pentapeptide with the amino acid D-tryptophan at the fourth position of the

pentapeptide, the ability of *Pa*MurF to incorporate the dipeptide D-tryptophanyl-D-alanine in place of D-alanyl-D-alanine was evaluated. Using the spectrophotometric-coupled assay in Figure 6.8 the ability of *Pa*MurF to incorporation of D-Trp-D-Ala into the pentapeptide stem and the affinity of this enzyme for this substrate was evaluated (**Figure 6.13)**.

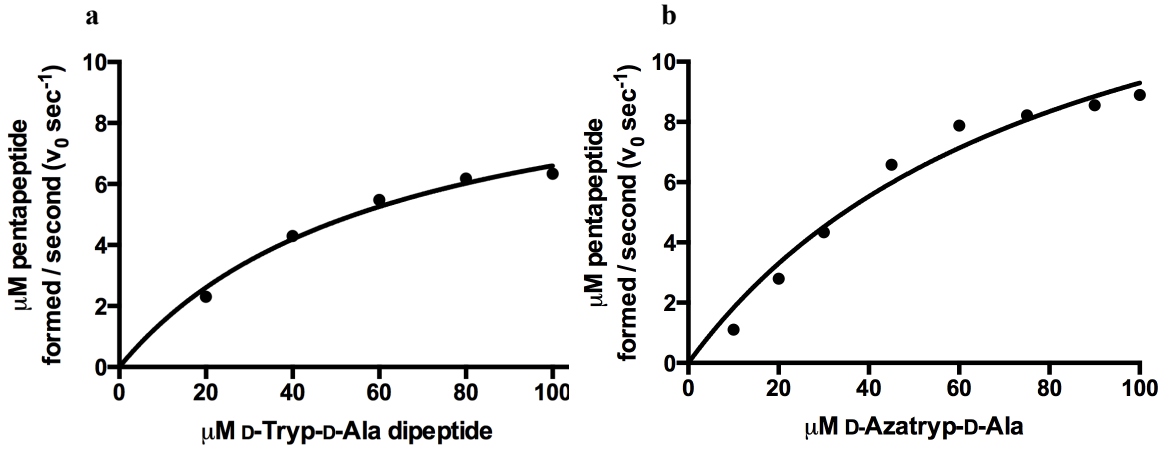

Figure 6.13 The Incorporation of the Dipeptide D-Trp-D-Ala into the pentapeptide stem, using *Pa*MurF. (a) D-Trp-D-Ala attachment to the tripeptide **(b)** D-Ala-D-Ala attachment to the tripeptide.

D-Trp-D-Ala was confirmed as a substrate for *Pa*MurF and can be enzymatically incorporated into the tripeptide. The K_m of MurF for D-Ala-D-Ala was determined using PRISM 6, as 20 μM ± 5. Comparing the K_m values determined for *Pa*MurF with three dipeptides are: D-Trp-D-Ala: 62 ± 13, D-Ala-D-Ala: 20 μM ± 5 and D-Azatrp-D-Ala 96 μM ± 14. D-Ala-D-Ala had the best affinity for *Pa*MurF as expected as it is the native substrate, with D-Trp-D-Ala being a substrate with a lower affinity for MurF and D-Azatrp-D-Ala being the least efficient substrate. An enzymatic synthesis reaction with D-Trp-D-Ala was conducted to synthesise the potential transpeptidase acceptor UDP-Mur*NA*c-L-Ala-D-Glu-*meso*DAP-D-Trp-D-Ala (Section 2.7.1). The synthesis reaction products were purified by anion exchange using a Source 30Q column and an ammonium acetate gradient from 10 mM to 1 M (**Figure 6.14**).

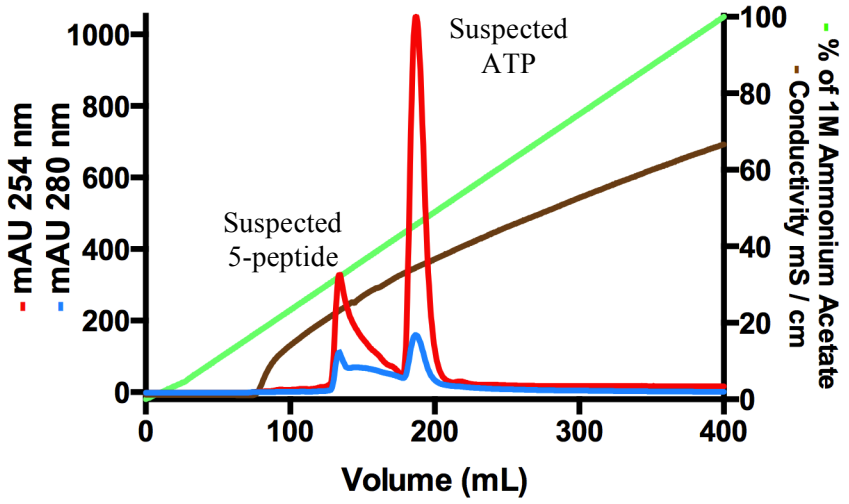

Figure 6.14 The purification of the reaction products of the enzymatic synthesis of UDP-Mur*NA*c-L-Ala-D-Glu-*meso*DAP-D-Trp-D-Ala, by anion exchange Source 30Q.

The first peak eluted from the Source 30Q column in Figure 6.14 was suspected to be the desired pentapeptide, with the second peak being ATP. Fractions from both peaks were tested individually for the presence of pentapeptide using DacB and DAAO, via D-Alanine release (**Figure 6.15**).

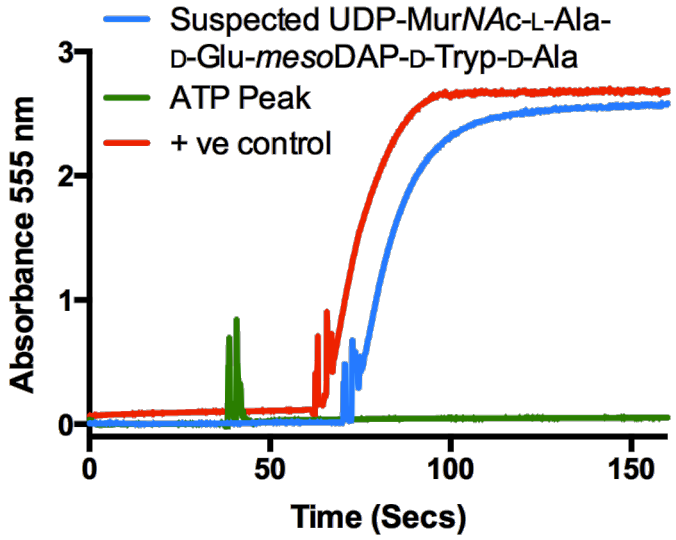

Figure 6.15 Determining the presence or absence of UDP-Mur*NA*c-L-Ala-D-Glu-*meso*DAP-D-Trp-D-Ala in peaks from its elution profile from Source30Q Purification. A spectrophotometric, coupled assay testing for the presence of pentapeptide was used to identify the peaks from purification. Both peaks from Figure 6.14 were tested for pentapeptide presence. The positive control used was 1 µM UDP-Mur*NA*c-L-Ala-D-Glu-*meso*DAP-D-Ala-D-Ala.

The first peak was positive for the presence of UDP-Mur*NA*c-L-Ala-D-Glu-*meso*DAP-D-Trp-D-Ala. Fractions positive for the presence of pentapeptide were pooled and lyophilised to remove the ammonium acetate. Each fraction positive for pentapeptide presence was analysed separately on a 1 mL analytical MonoQ column to check its

purity. The pure fractions were pooled and the final purity of the combined fractions was again analysed by MonoQ (**Figure 6.16**).

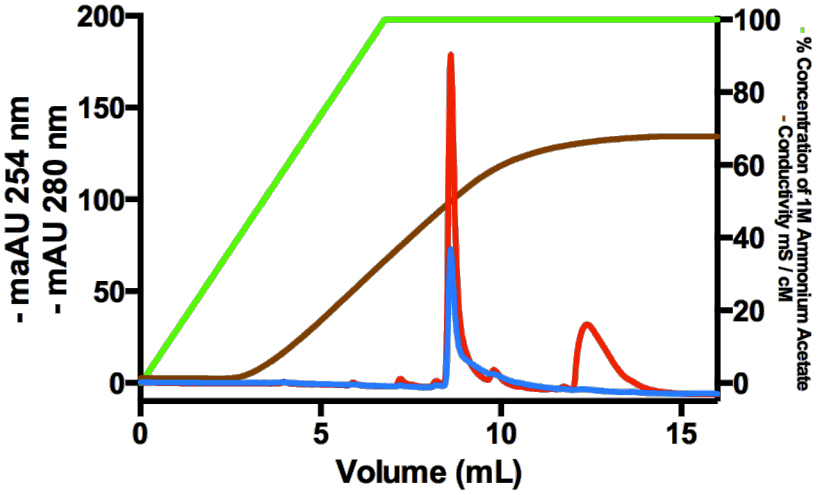

Figure 6.16 Analysis of the purity of UDP-Mur*NA*c-L-Ala-D-Glu-*meso*DAP-D-Trp-D-Ala. MonoQ analysis of UDP-Mur*NA*c-L-Ala-D-Glu-*meso*DAP-D-Trp-D-Ala purity of the lyophilised compound purified by Source 30Q (Figure 6.14).

The final yield of UDP-Mur*NA*c-L-Ala-D-Glu-*meso*DAP-D-Trp-D-Ala was quantified (section 2.7.3) as 1.6 mgs and analysed by mass spectroscopy (**Figure 6.17**).

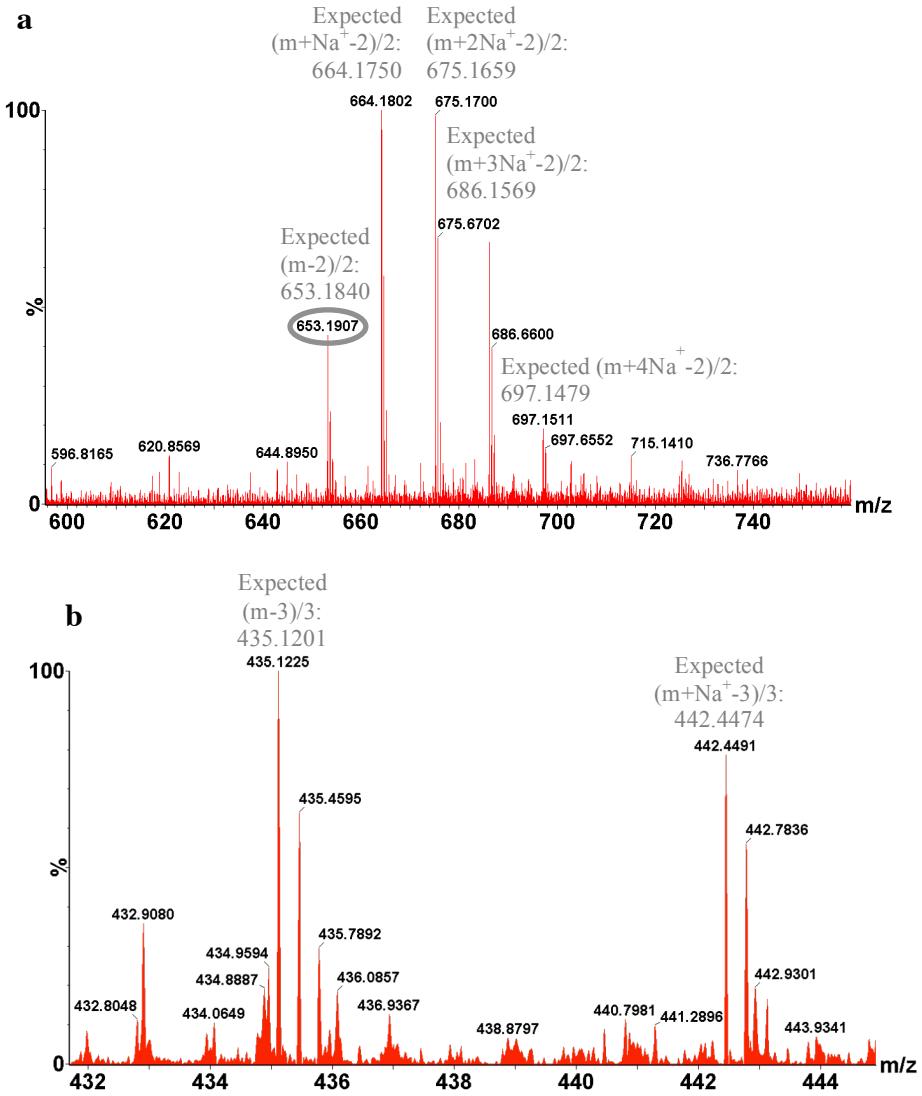

Figure 6.17 Negative Ion Nanospray mass spectroscopy analysis of UDP-Mur*NA*c-L-Ala-D-Glu-*meso*DAP-D-Trp-D-Ala. Exact Mass = 1308.38 Daltons, expected singly charged ion = 1307.38 Da, singly charged ion not observed. **(a)** The doubly-charged species. Expected doubly charged ion = 653.19, observed = 653.1907 **(b)** The triply-charged species: expected triply-charged ion = 435.127, observed = 435.1225).

The doubly charged species was present along with the triply charged species. With confirmation of the double and triple-charged species of the pentapeptide in the mass spectrometer, it can be surmised that the desired compound UDP-Mur*NA*c-L-Ala-D-Glu-*meso*DAP-D-Trp-D-Ala has been synthesised. The final yield of this compound was determined in mgs and the ability of this derivative pentapeptide to serve as a transpeptidase acceptor was subsequently tested along with the other transpeptidase donor and acceptor compounds. Thus, the two acceptor compounds have been synthesised: UDP-Mur*NA*c-L-Ala-D-Glu-*meso*DAP-D-Azatrp-D-Ala and UDP-

Mur*NA*c-L-Ala-D-Glu-*meso*DAP-D-Trp-D-Ala. The transpeptidase donor compounds are synthesised in section 6.7.

6.7 Synthesis of the Transpeptidase Donor Compounds

6.7.1 Synthesis of Dansylated (*meso*DAP) Lipid II

Dansylated LII has the unique property of only being able to serve as an acyl donor in the transpeptidase reaction. The large dansyl group attached to position 3 prevents the non-proteinaceous *meso*DAP from acting as an acyl-acceptor. UDP-Mur*NA*c-L-Ala-D-Glu-*meso*DAP-D-Ala-D-Ala was synthesised and desalted as described in section 2.7.3 to prepare the compound for labelling with dansyl chloride. A 42-molar excess of dansyl chloride added to the pentapeptide. The reaction was left over night in the dark. The reacted products were purified by anion exchange on a source 30Q column (**Figure 6.18 a**). The major peak from this purification was run on MonoQ for test for sample purity (**Figure 6.18 b**).

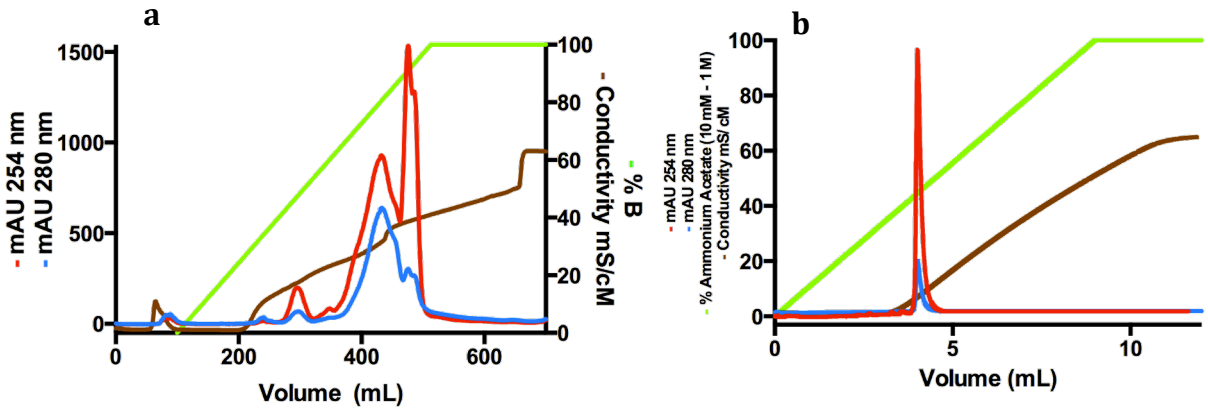

Figure 6.18 The Purification of dansDAP-LII (a) Anion Exchange by Source 30Q of UDP-Mur*NA*c-L-Ala-D-Glu-*meso*DAP-D-Ala-D-Ala) **(b)** MonoQ analysis of dansylated DAP LII.

The dansylated pentapeptides eluted from the column in the second peak, with any un-labelled material eluting earlier. Fractions from the second peak were lyophilised and a sample was analysed on a small analytical MonoQ column and demonstrates a single narrow peak. This sample was analysed by mass spectrometry and confirmed as dansylated-pentapeptide. The pentapeptide was synthesised in to a lipid (section 2.7.7), purified and analysed by TLC before using. The total yield of Fluorescamine-labelled DAP-LII was quantified as 1.86 mgs.

6.7.2 Synthesis of Fluorescamine-labelled Lipid II (C_{55}-PP-Mur*NA*c-GlcN*A*c-L-Ala-D-Glu-(N^{ε}-Fluorescamine)-*meso*DAP-D-Ala-D-Ala

Initially, UDP-Mur*NA*c-L-Ala-D-Glu-*meso*DAP-D-Ala-D-Ala was synthesised and subsequently purified. To remove any residual ammonium acetate carried over from the purification of this precursor, which might prevent its modification with fluorescamine, and to provide a suitable medium within which the ε-amino group of the DAP of the pentapeptide could be acetylated, the pentapeptide was desalted by gel filtration (Superdex Peptide 10/300 GL) in to 0.25 M sodium bicarbonate pH 9.0 prior to labelling with the fluorophore, fluorescamine. Fractions from the major peak were pooled and introduced to the Fluorescamine fluorophore in a labelling reaction. The properties of Fluorescamine as a fluorophore are described next.

6.7.2.1 Fluorescamine as a Primary-Amine Labelling Fluorophore

Fluorescamine (4-phenylspiro [furan-2(3H),1-phthalan]-3,3-dione) a heterocyclic dione, is a selective fluorophore that reacts with primary amines to form a highly fluorescent product. It has excellent fluorescent enhancement and long fluorescent lifetimes (hundreds of nanoseconds) (Berezin & Achilefu, 2010). The scheme of amine-fluorescamine reaction is shown in **Figure 6.19**.

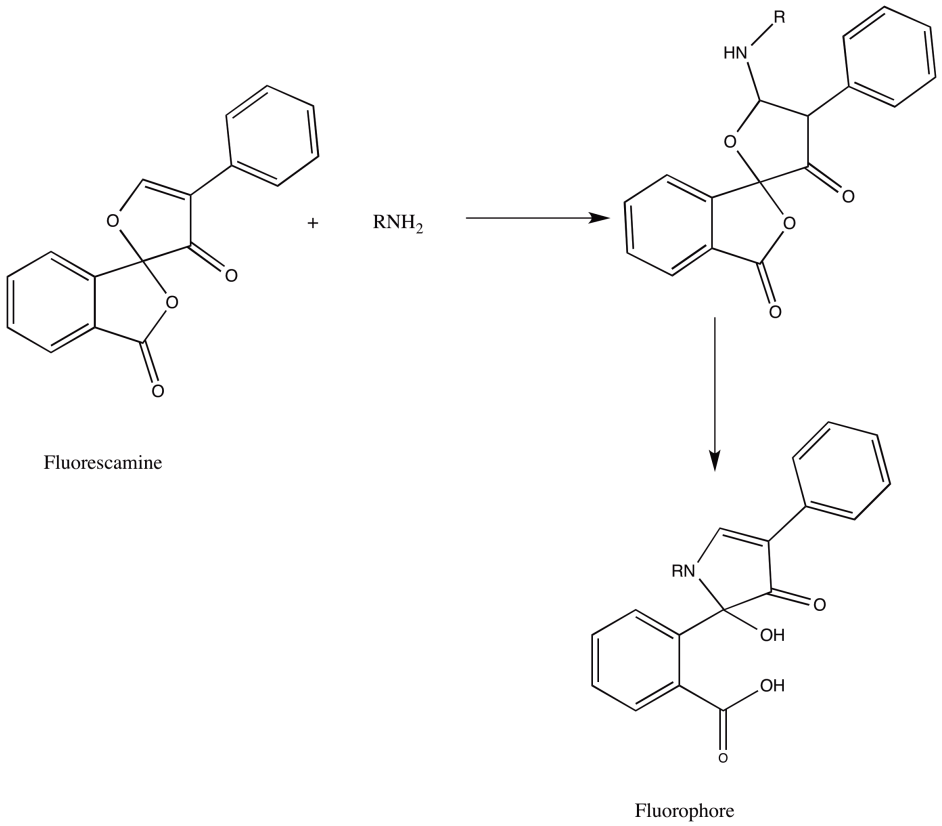

Figure 6.19 A Schematic of Fluorescamine as a Fluorophore. The reaction of the chiral, non-fluorescent fluorescamine with a chiral amine begins by nucleophilic addition of the amine nitrogen to the C=C double bond of fluorescamine, resulting in the breakage of a C-O bond and loss of the chiral centre of fluorescamine (to yield the dione). Closing the 5-membered ring by a second nucleophilic attack of the amine nitrogen on the benzoyl ketone forms a fluorescent product with two chiral centres (De Bernardo *et al.*, 1974).

Fluorescamine is a non-fluorescent compound that reacts with primary amines at room temperature to yield a highly fluorescent product. The excess of reagent is destroyed by water to form a non-fluorescent hydrolysis product (Stein *et al.*, 1974). The reaction of fluorescamine with primary amines is strongly pH dependent and the fluorescence is developed only in alkaline media (pH of 8.0-9.5), which disappears completely in acidic media (Stockhert *et al.,* 2008). The derivatives of amines-fluorescamine are formed immediately and are stable for at least 1 day. The extent of the reaction between fluorescamine and primary amines and the fluorescent intensities of the resulting fluorophores, depend on pH, solvent composition, reagent concentration and the accessibility of the amine being labelled (Udenfriend *et al.*, 1972).

In previously successful dansylation labelling reactions, a 42-fold molar excess of dansyl chloride was used relative to the UDP Mur*NA*c pentapeptide target. For the Fluorescamine-labelling reaction, two ratios of fluorescamine were trialled: UDP

Mur*NA*c (DAP) pentapeptide 2:1 and 42:1, both in 50% acetonitrile. The two reactions were left overnight and subsequently terminated with a 10-fold molar excess of Tris (free base) relative to fluorescamine. As Tris is a free amine, it reacted with the 'free-unreacted' fluorescamine.

Fluorescamine is not fluorescent when not attached to an amine (Chen *et al.*, 1978) and usually does not require separation of the product from unreacted, excess fluorescamine. Although to ensure purity, the sample was run down a Sepharose Q column, with an extra detection wavelength set to 390 nm, the excitation of fluorescamine (**Figure 6.20a**). The major peak from purification was tested enzymatically for the presence of pentapeptide, using the DD-carboxypeptidase DacB (**Figure 6.20b)**.

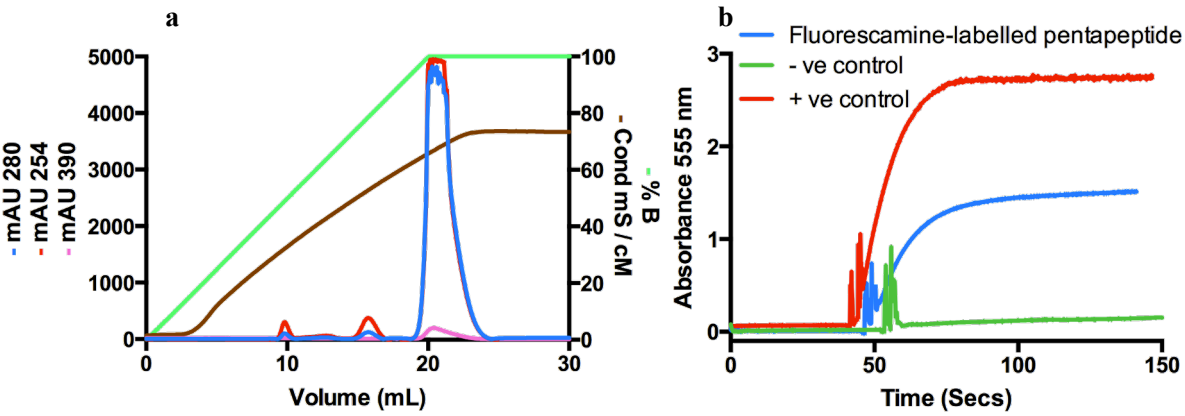

Figure 6.20 The Purification of Fluorescamine-labelled DAP-Pentapeptide and enzymatic analysis of the elution products (a) The pentapeptide was purified using SepharoseQ resin. The absorbance at λ_{390} nm is the excitation wavelength of fluorescamine. **(b)** Determining the presence or absence of pentapeptide using the DD-carboxypeptidase DacB which removes the C-terminal D-Ala from the pentapeptide. A sample from the major peak from SepharoseQ purification was tested for pentapeptide presence (blue). The positive control (red) was the native pentapeptide UDP-Mur*NA*c-L-Ala-D-Glu-*meso*DAP-D-Ala-D-Ala, the negative control (green) was a sample from one of the minor peaks in (a).

Fluorescamine is present in the major peak in (a), confirmed spectrophotometrically using DacB. The suspected fluorescamine-labelled pentapeptide was sent for mass spectral analysis (**Figure 6.21**). Unlabelled pentapeptide (UDP-Mur*NA*c-L-Ala-D-GLu-*meso*DAP-D-Ala-D-Ala) has the exact mass of 1193.33 Da, whereas the fluorescamine-labelled compound should have an exact mass of 1471.41 Da.

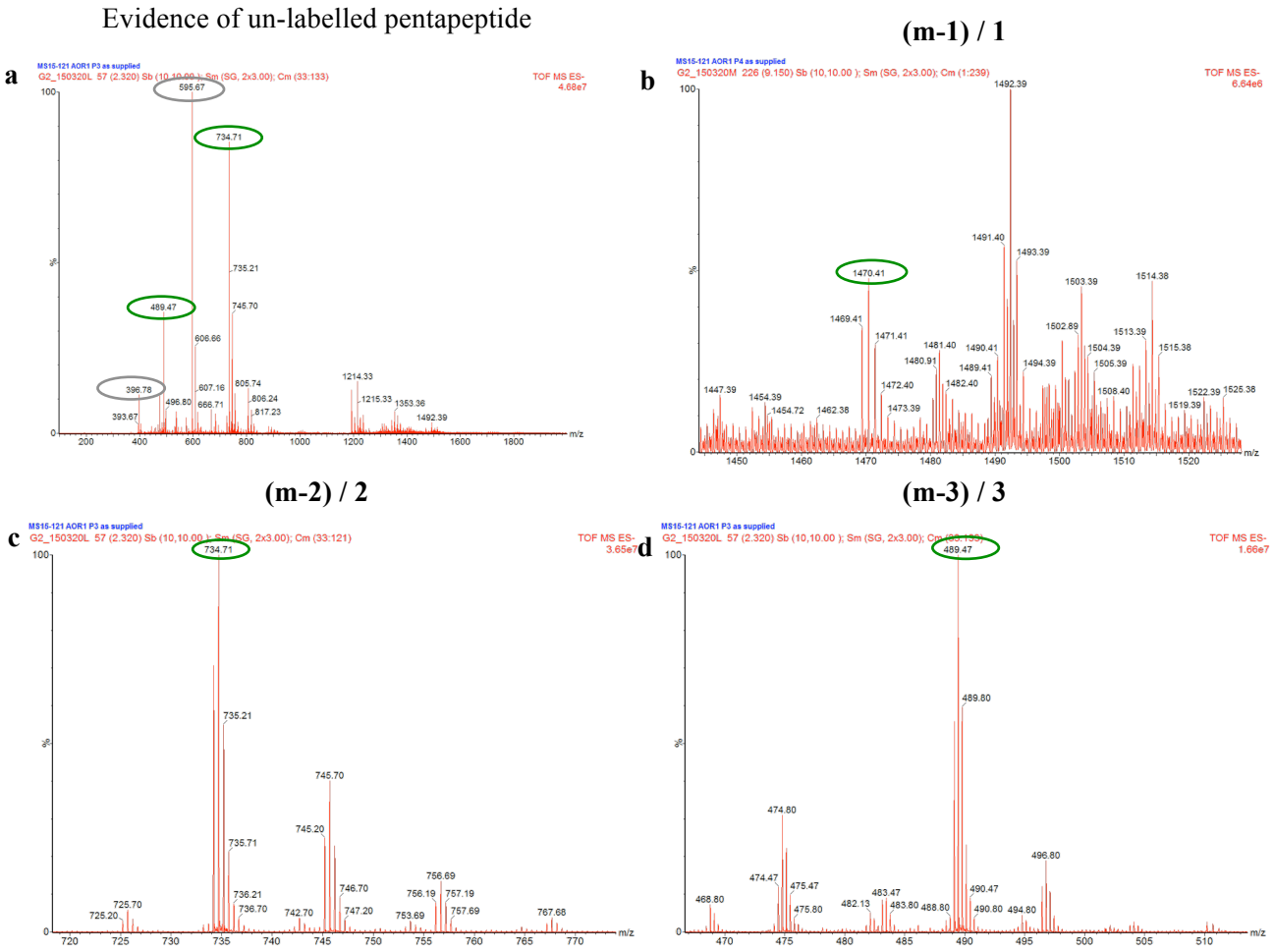

Figure 6.21 Mass Spectral Analysis of Purified Fluorescamine-Labelled UDP-Mur*NA*c-L-Ala-D-Glu-*meso*DAP-D-Ala-D-Ala (negative-ion). Fluorescamine-labelled pentapeptide has an exacted mass of 1471.41 Da. The singly charged species has an expected mass of (m-1)/1 = 1470.41 Da, observed: 1470.41, the doubly charged species has an expected mass of (m-2)/2 = 734.71 Da, observed: 734.71, the triply charged species has an expected mass of (m-3)/3 = 489.47 Da, observed: 489.47. The Fluorescamine-labelled pentapeptide species are circled in green. The singly charged species is shown in **(b)**, the doubly charged species in **(a)** and **(c)** and the triply-charged species is in **(d)**. Unlabelled UDP-Mur*NA*c-L-Ala-D-Glu-*meso*DAP-D-Ala-D-Ala has an exact mass of 1193.33 Da and are present in the sample, highlighted in grey. The singly charged species has an expected mass of (m-1)/1 = 1192.33 Da, species not observed, the doubly charged species has an expected mass of (m-2)/2 = 595.67 Da, observed: 595.67 Da, the triply charged species has an expected mass of (m-3)/3 = 396.78 Da and an observed mass of 396.78. The doubly and triply-charged species are in (a).

Mass spectral analysis indicates that there is fluorescamine-labelled pentapeptide in the sample, with some unlabelled pentapeptide as well. The singly charged ion was visible for the labelled pentapeptide, but not for the un-labelled species. The doubly and triply-charged species for both labelled and unlabelled were visible. A lipid synthesis reaction was set up with the Fluorescamine-labelled pentapeptide, with the intention that the majority of the pentapeptides in the final lipid would be labelled with Fluorescamine.

The lipid synthesis (section 2.7.7) was subsequently purified using DEAE resin with a mobile phase of Chloroform : Methanol : Water in the ratio 2:3:1. LII species were eluted isocratically, by incorporating increasing concentrations of ammonium bicarbonate into the water component of the mobile phase. The eluted fractions were analysed by thin layer chromatography (TLC) (**Figure 6.22**, section 2.7.9).

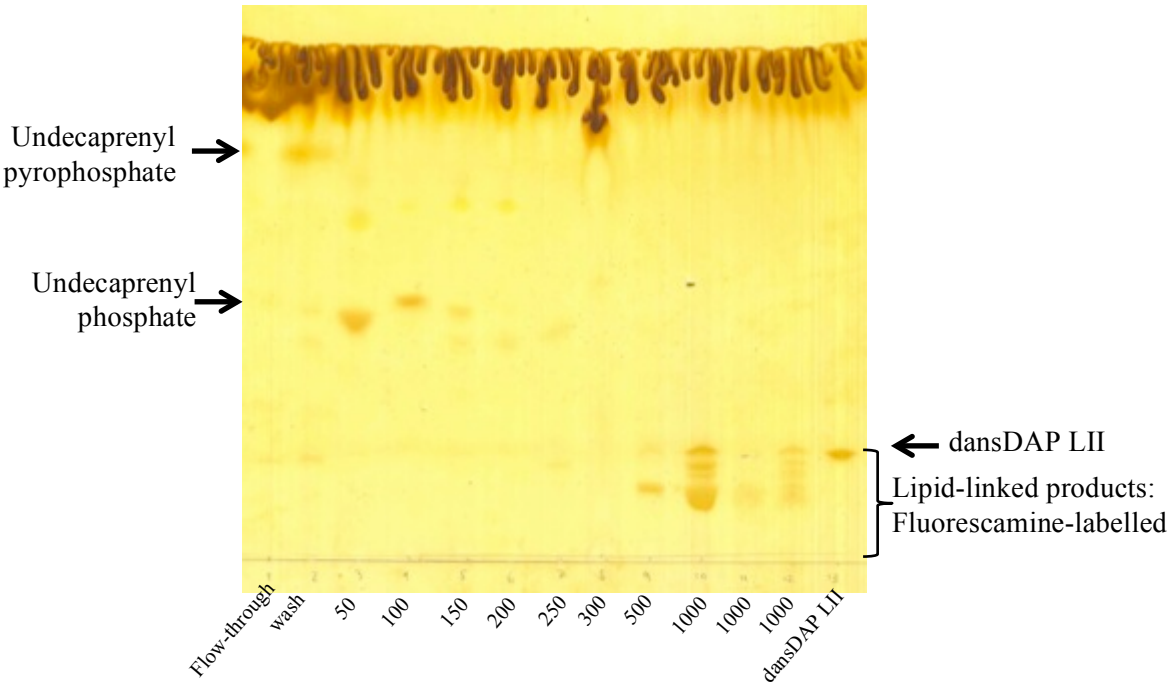

Figure 6.22 Thin Layer Chromatography of eluted fractions of purified Fluorescamine-labelled LII. A sample of dansDAP-LII was run in the final lane to compare the relative migration of the Fluorescamine-labelled species relative to the dansDAP-LII.

The chloroform : methanol 500 mM ammonium bicarbonate (2:3:1) and the chloroform methanol: 1M ammonium bicarbonate (2:3:1) 1M washes appeared to contain the lipid, with multiple bands present. Either the lipid has broken down and these were degradation products and/ or the sample contains impurities such as DAP-LII derived from the proportion of UDP-Mur*N*Ac-pentapeptide that had not originally reacted with fluorescamine. The chloroform : methanol 500 mM ammonium bicarbonate (2:3:1) and the chloroform : methanol: 1M ammonium bicarbonate (2:3:1) 1M washes were lyophilised and quantified using a phosphate release assay. The chloroform : methanol 1M ammonium bicarbonate tested negative in the phosphate release assay, however, the chloroform : methanol 500 mM ammonium bicarbonate (2:3:1) elution contained acid-labile phosphate at a concentration indicating the sample contained 332.74 µM LII species. An absorbance spectrum of both elutions is in **Figure 6.23** to test the presence of the Fluorescamine label on the pentapeptide.

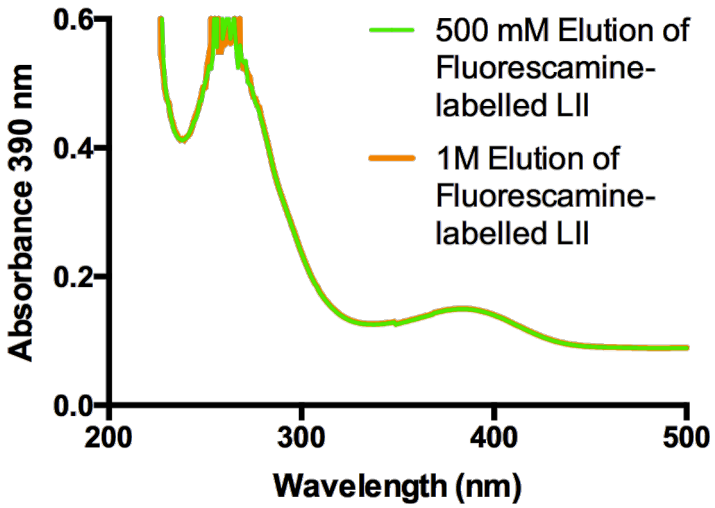

Figure 6.23 An Absorbance Scan of Fluorescamine-Labelled DAP-LII between 200 and 800 nm. The expected absorption maximum of Fluorescamine is 390 nm.

The pronounced absorbance at 260 nm is commonly observed in Fluorescamine spectra (Jameson & Reinhart, 2012) and the peak at 390 nm is the Fluorescamine moiety. Samples of both ammonium bicarbonate concentrations at which lipid species eluted were sent for mass spectral analysis, but only non-labelled DAP-LII was detected in both samples. It is known from previous research (Tim Bugg Personal Communication, Bagga, 2004), that Lipid I/II compounds labelled with fluorophores are very hard to analyse by electrospray mass spectrometry. Judged by the spectral properties of the purified lipids that absorbed at wavelengths indicative of the presence of a fluorescamine group, labelling DAP-LII with Fluorescamine was successful (also see Fluorescamine-DAP-LII polymerisation in a continuous fluorometric transglycosylase assay **(Figure 6.24)**.

6.7.2.2 Enzymatic Characterisation of Fluorescamine DAP-LII as a substrate for *E. coli* PBP1B transglycosylation

To confirm the functionality and identify of the putative fluorescamine-DAP-LII, the ability of this modified lipid to behave as a transpeptidase donor in the continuous fluorometric transglycosylase assay was assessed. The positive detection of DAP-LII species with the spectral signal indicative of a fluorescamine modification, albeit without a positive identification of fluorescamine-labelled DAP-LII by mass spectrometry required another means of confirmation of the formation of this potential substrate. Therefore, the ability of the Fluorescamine-labelled DAP-LII to polymerise in

to a linear glycan strand by a transglycosylase was evaluated using *E. coli* PBP1B, and with varying concentrations of Fluorescamine-LII (**Figure 6.24**).

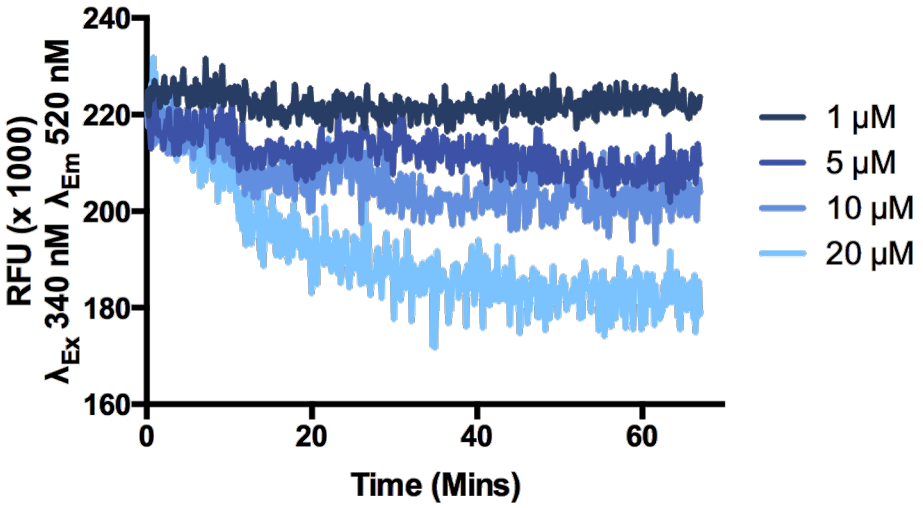

Figure 6.24 The polymerisation of Fluorescamine-labelled DAP-LII by *E. coli* PBP1B. Transglycosylase polymerisation was monitored using the continuous fluorometric assay (Schwartz *et al.,* 2002), modified and adapted to monitor the spectral maxima of fluorescamine λ_{Ex} 390 nm and λ_{Em} 470 nm.

Indicated in the fall in fluorescence at λ_{Em} 470 upon transition of the fluorescamine label from a micellar to an aqueous environment, coupled to muramidase, Fluorescamine-DAP-LII was shown to be capable of polymerisation in to linear glycan chains in a concentration-dependent manner catalysed by *Ec*PBP1B. *Ec*PBP1B transpeptidation activity is predicted upon active transglycosylation to generate a polymeric transpeptidase donor (Bertsche *et al*., 2005). The demonstration that the preparation of Fluorescamine-DAP-LII was polymerisable enabled investigation of this substrate as a potential transpeptidase donor in a FRET assay, where it was to be used as a FRET acceptor.

6.8 Analysis of the Activity of the Synthesised Compounds, as Functional Transpeptidase Acceptors and Donors

Upon the synthesis of a complete set of FRET pairs, the compounds were tested for activity in their expected functions. Therefore, the synthesised transpeptidase donors (Dansyl and Fluorescamine-labelled LII - FRET acceptors) were assayed for their ability to be polymerised by a transglycosylase. Also, the transpeptidase acceptors were tested for potential acceptor capability using a continuous coupled, spectrophotometric

assay, developed to monitor, quantify and visualise transpeptidase activity in real-time (section 2.8.5). This assay was developed by Dr. Adrian Lloyd in August 2014, which has been used in this thesis to test whether these synthesised compounds act as transpeptidase donors or acceptors, as well as testing the purified PBPs for their ability to function as transpeptidases. *Ec*PBP1B was used as the enzymatic LII polymerase (transglycosylase) throughout the characterisation of these four compounds, as it has been used as the model enzyme for the majority of studies in this thesis and the wider field.

6.8.1 Activity of the Synthesised Compounds as Functional Transpeptidase Acceptors, using L-Lysine-LII as the Transpeptidase Donor

The transpeptidase acceptor that most closely resembles that found natively *in vivo* (Mur*NA*c-L-Ala-D-Glu-*meso*DAP-D-Ala-D-Ala) (section 2.7.6) was initially used with LII with L-lysine at the third position in the pentapeptide stem (Lys-LII) as the transpeptidase donor. Lys-LII can only act as a transpeptidase donor and not a transpeptidase acceptor because the lysine does not, unlike *meso*DAP (the natural residue replaced by lysine in Lys-LII) possess an ε-carbon amino and carboxyl group in the D-stereoisomeric configuration (Lupoli *et al.*, 2014). Conversely, one of the requirements of a Gram-negative transpeptidase for its acceptor is that it must have a D-stereocentre at the third position of the peptide stem, as in D,L-DAP (Lupoli *et al.*, 2011).

All steady-state kinetic assays were conducted in a dual beam format with Lys-LII in one cuvette but not the other, which enables any background rate to be taken into consideration. The presence and absence of Lys-LII is the distinguishing feature between the duplicates. The reference cuvette lacking the transpeptidase donor Lys-LII was substituted with the solvent that Lys-LII was resuspended in, usually Hexa-ethylene glycol, monododecyl ether (E_6C_{12}). *Ec*PBP1B was added to both cuvettes and its absorbance monitored until a stable baseline was reached before adding the acceptor to both cuvettes, initiating the reactions. Incubation of the donor-only Lys-LII with the PBP initially, accounted for any DD-carboxypeptidase activity before the addition of the acceptor, which allows subsequent transpeptidase activity to be kinetically tracked.

The transpeptidase activity of *Ec*PBP1B with initially established using substrates that have exclusive activity as only either a transpeptidase donor or acceptor. Lys-LII was used as the transpeptidase donor and Mur*NA*c pentapeptide DAP (L-Ala-D-Glu-*meso*DAP-D-Ala-D-Ala) as the transpeptidase acceptor, analysed for their ability to support *Ec*PBP1B transpeptidase activity (**Figure 6.25**). This combination of transpeptidase donor and acceptor were expected to work together. Gram-negative *Ec*PBP1B naturally uses DAP-LII *in vivo*, but is known to also accept Lys-LII *in vitro*.

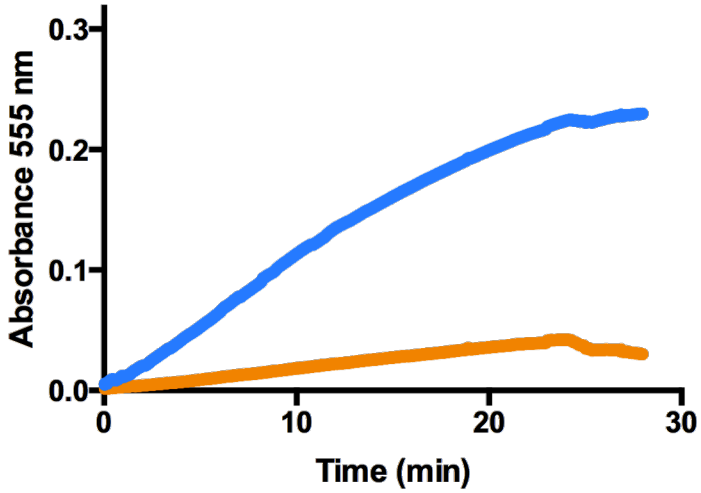

Figure 6.25 Analysing the Capability of Lys-LII to act as a Transpeptidase Donor with Mur*NA*c-L-Ala-D-Glu-*meso*DAP-D-Ala-D-Ala as the Transpeptidase Acceptor. Assay conditions: 50 mM BisTris Propane, pH 8.5, 20 mM $MgCl_2$, 0.1 % TritonX-100, 50 µM Amplex Red, 3.5 Units *Rhodotorula gracalis* DAAO, 5.8 Units HRP, 0.2 µM *E. coli* LpoB, transpeptidase donor: 20 mM Lys-LII in 0.1 % TritonX-100, 11 nM *E. coli* PBP1B in 0.2% TritonX-100, transpeptidase acceptor: Mur*N*Ac-L-Ala-D-Glu-*meso*DAP-D-Ala-D-Ala. Blue: + Lys-LII, Orange: without Lys-LII.

In the presence of Lys-LII, a positive rate was observed that is not the case in the absence of Lys-LII. Therefore it is likely that Mur*NA*c-L-Ala-D-Glu-*meso*DAP-D-Ala-D-Ala can function as a transpeptidase acceptor when using Lys-LII as the transpeptidase donor. Next, the three synthesised compounds were tested as transpeptidase acceptors with the same Lys-LII donor (**Figure 6.26**). The three transpeptidase acceptor compounds tested were:

(1) D-Trptophan at position four, with the UDP group: UDP-Mur*NA*c-L-Ala-D-Glu-*meso*DAP-D-Trp-D-Ala

(2) D-Azatryptophan at position four, with the UDP group: UDP-Mur*NA*c-L-Ala-D-Glu-*meso*DAP-D-Azatrp-D-Ala

(3) A variant of (2) without the UDP group: Mur*NA*c-L-Ala-D-Glu-*meso*DAP-D-Azatrp-D-Ala

Compound (**1**) contained D-tryptophan, which could act as a donor fluorophore in the FRET pair with dansDAP-LII. Compounds (**2**) and (**3**) contained the fluorophore D-azatryptophan, both/either of which could be used as part of a FRET pairing with Fluorescamine-labelled LII. For these potential FRET pairs to work, Fluorescamine and Dansyl-labelled DAP-LII had to be active as transpeptidase donors, and the three compounds above had to function as transpeptidase acceptors. The capability of all of these compounds to function in these roles in support of *Ec*PBP1B transpeptidase activity was then analysed using the Amplex Red assay.

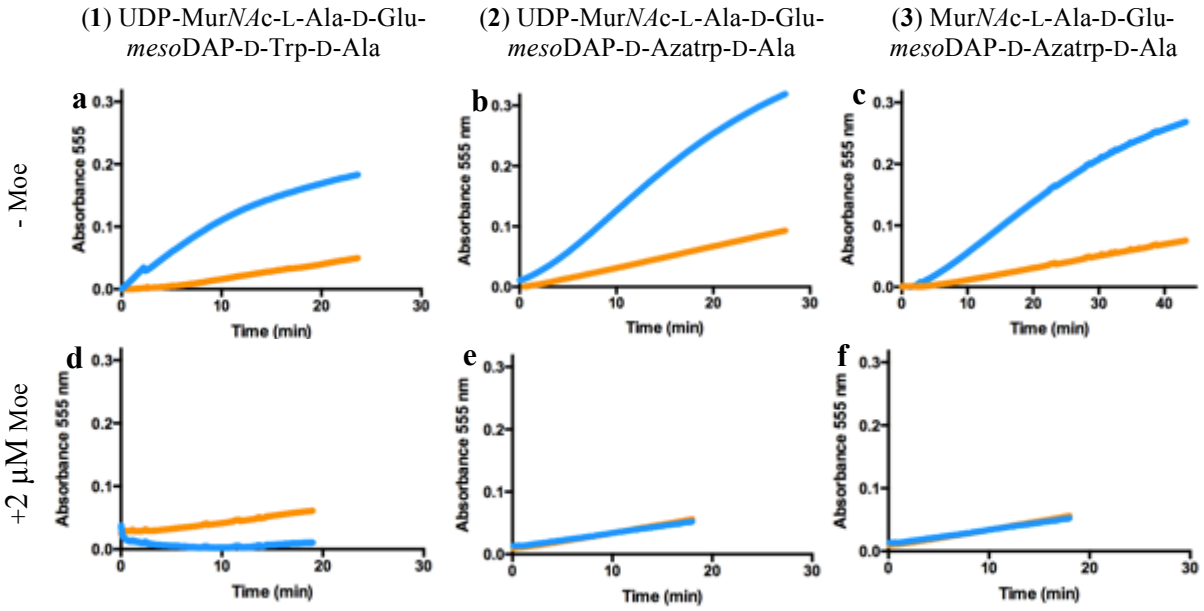

Figure 6.26 The Capability of the Three Synthesised Compounds as Transpeptidase Acceptors, all with Lys-LII as the Donor. (a) and (d) UDP-Mur*NA*c-L-Ala-D-Glu-*meso*DAP-D-Trp-D-Ala as transpeptidase acceptor, (b) and (e) UDP-Mur*NA*c-L-Ala-D-Glu-*meso*DAP-D-Azatrp-D-Ala as transpeptidase acceptor, (c) and (e) Mur*NA*c-L-Ala-D-Glu-*meso*DAP-D-Azatrp-D-Ala as transpeptidase acceptor. (a-c) No Moenomycin (d-f) with 2 µM Moenomycin. Assay conditions: 50 mM BisTris Propane, pH 8.5, 20 mM $MgCl_2$, 0.1 % TritonX-100, 50 µM Amplex Red, 3.5 Units *Rhodotorula gracalis* DAAO, 5.8 Units HRP, 0.2 µM *E. coli* LpoB, transpeptidase donor: 20 mM Lys-LII in 0.1 % TritonX-100, 11 nM *E. coli* PBP1B in 0.2 % TritonX-100, transpeptidase acceptor. Blue: + Lys-LII, Orange: without Lys-LII.

The three compounds tested positive as transpeptidase acceptors when using Lys-LII as the transpeptidase donor. UDP-Mur*NA*c-L-Ala-D-Glu-*meso*DAP-D-Azatrp-D-Ala (**b**) appeared to be turned over the fastest, with Mur*NA*c-L-Ala-D-Glu-*meso*DAP-D-Azatrp-D-Ala second (**c**), and UDP-Mur*NA*c-L-Ala-D-Glu-*meso*DAP-D-Trp-D-Ala (**a**) third. The negative control assays without Lys-LII were inactive, as expected. The assays with the transglycosylase inhibitor Moenomycin added were inhibited suggesting that as was

observed by Bertsche *et al.*, (2005), transglycosylation is required for activity of the transpeptidase domain of *Ec*PBP1B.

6.8.2 Activity of the Synthesised Compounds as Functional Transpeptidase Acceptors, using dansylated DAP-LII as the Transpeptidase Donor

Dansylated DAP-LII was tested as a transpeptidase donor because this compound is one of the four compounds to be used in one of the FRET pairings. Mur*NA*c-L-Ala-D-Glu-*meso*DAP-D-Ala-D-Ala was used as the transpeptidase acceptor using the Amplex Red coupled assay (**Figure 6.27**). DansDAP-LII functions exclusively as a transpeptidase donor because the *meso*DAP D-stereocentre of the DAP residue is shielded by the presence of the dansyl group appended to the ε-amine group of the *meso*DAP.

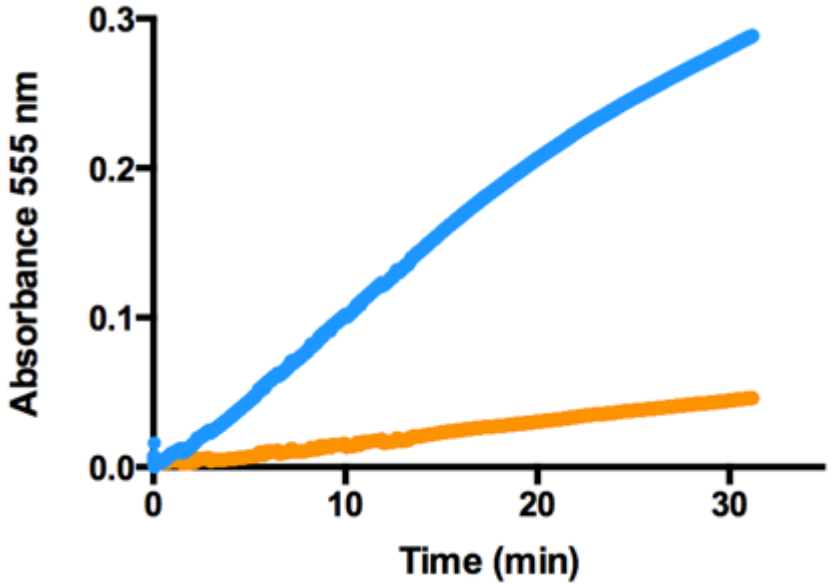

Figure 6.27 The Ability of dansDAP-LII to Function as a Transpeptidase Donor, using Mur*NA*c-L-Ala-D-Glu-*meso*DAP-D-Ala-D-Ala as the Transpeptidase Acceptor. Assay conditions: 50 mM BisTris Propane, pH 8.5, 20 mM $MgCl_2$, 0.1 % TritonX-100, 50 µM Amplex Red, 3.5 Units *Rhodotorula gracalis* DAAO, 5.8 Units HRP, 0.2 µM *E. coli* LpoB, transpeptidase donor: 20 mM dansDAP-LII in 0.1 % TritonX-100, 11 nM *E. coli* PBP1B in 0.2 % TritonX-100, transpeptidase acceptor: Mur*NA*c-L-Ala-D-Glu-*meso*DAP-D-Ala-D-Ala. Blue: + dansDAP-LII, Orange: without dansDAP-LII.

After confirming that dansDAP-LII functioned as a transpeptidase donor with an acceptor (using the pentapeptide that most closely resembles the transpeptidase acceptor *in vivo*: Mur*NA*c-L-Ala-D-Glu-*meso*DAP-D-Ala-D-Ala), dansDAP-LII was tested as a transpeptidase donor with the three synthesised transpeptidase acceptor compounds with

the unusual D-amino acid at the fourth position in the peptide stem using the Amplex Red coupled assay (**Figure 6.28**).

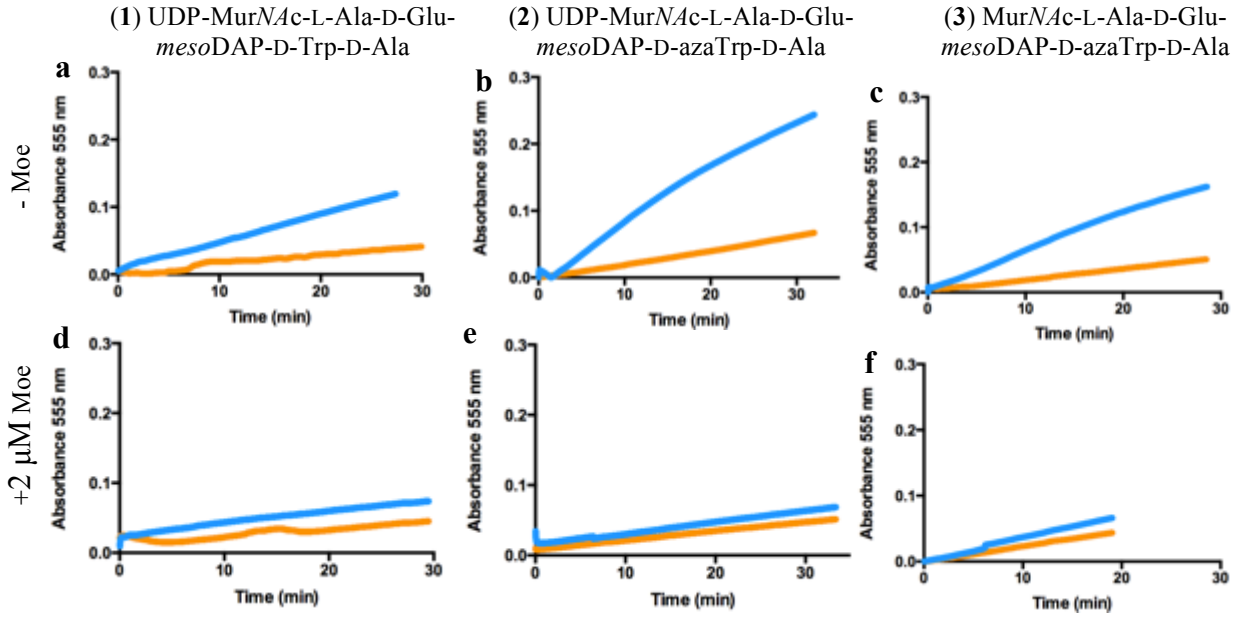

Figure 6.28 Evaluation of the Three Synthesised Compounds as Transpeptidase Acceptors, with dansDAP-LII as the Donor. (a) and (d) UDP-Mur*NA*c-L-Ala-D-Glu-*meso*DAP-D-Trp-D-Ala as transpeptidase acceptor, (b) and (e) UDP-Mur*NA*c-L-Ala-D-Glu-*meso*DAP-D-Azatrp-D-Ala as transpeptidase acceptor, (c) and (e) Mur*NA*c-L-Ala-D-Glu-*meso*DAP-D-Azatrp-D-Ala as transpeptidase acceptor. (a-c) No Moenomycin (d-f) with 2 µM Moenomycin. Assay conditions: 50 mM BisTris Propane, pH 8.5, 20 mM $MgCl_2$, 0.1 % TritonX-100, 50 µM Amplex Red, 3.5 Units *Rhodotorula gracalis* DAAO, 5.8 Units HRP, 0.2 µM *E. coli* LpoB, transpeptidase donor: 20 mM dansDAP-LII in 0.1 % TritonX-100, 11 nM *E. coli* PBP1B in 0.2 % TritonX-100, transpeptidase acceptor. Blue: + dansDAP-LII, Orange: without dansDAP-LII.

All three compounds were active as transpeptidase acceptors, when dansDAP-LII was used as the transpeptidase donor. UDP-Mur*NA*c-L-Ala-D-Glu-*meso*DAP-D-Azatrp-D-Ala (b) appeared to be turned over the quickest (calculate turnover number), with Mur*NA*c-L-Ala-D-Glu-*meso*DAP-D-Azatrp-D-Ala (c) the second best and UDP-Mur*NA*c-L-Ala-D-Glu-*meso*DAP-D-Trp-D-Ala third (a).

6.8.3 Activity of the Synthesised Compounds as Functional Transpeptidase Acceptors, using Fluorescamine-labelled DAP-LII as the Transpeptidase Donor

The final compound to be tested for its capability as a potential substrate for transpeptidation is Fluorescamine-labelled LII as a transpeptidase donor. The most native transpeptidase acceptor (Mur*NA*c DAP-pentapeptide) was initially used with Fluorescamine-LII (**Figure 6.29**).

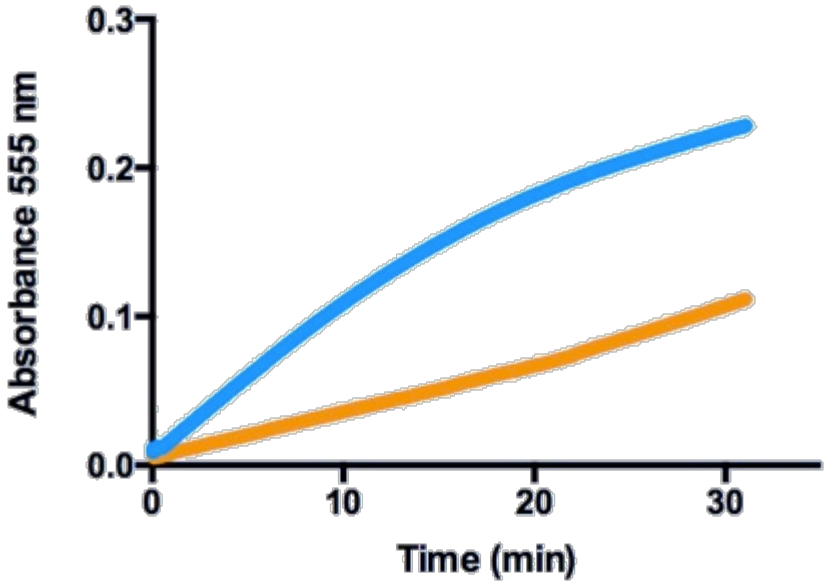

Figure 6.29 The Capability of Fluorescamine-DAP-LII to Function as a Transpeptidase Donor with Mur*NA*c-L-Ala-D-Glu-*meso*DAP-D-Ala-D-Ala as Acceptor. Assay conditions: 50 mM BisTris Propane, pH 8.5, 20 mM $MgCl_2$, 0.1 % TritonX-100, 50 µM Amplex Red, 3.5 Units *Rhodotorula gracalis* DAAO, 5.8 Units HRP, 0.2 µM *E. coli* LpoB, transpeptidase donor: 20 mM Fluorescamine-DAP-LII in 0.1 % TritonX-100, 11 nM *E. coli* PBP1B in 0.2 % TritonX-100, transpeptidase acceptor: Mur*NA*c-L-Ala-D-Glu-*meso*DAP-D-Ala-D-Ala. Blue: + Fluorescamine-labelled DAP-LII, Orange: without Fluorescamine-labelled DAP-LII.

Fluorescamine-DAP-LII is likely to be a viable substrate as a transpeptidase donor, but as the LII may contain some unlabelled species, it cannot be proven that this positive rate is due to Fluorescamine-DAP-LII. The three unusual transpeptidase acceptor compounds with D-Trp or D-Azatrp at position four of the pentapeptide were subsequently tested as transpeptidase acceptors, using Fluorescamine-LII as the donor (**Figure 6.30**).

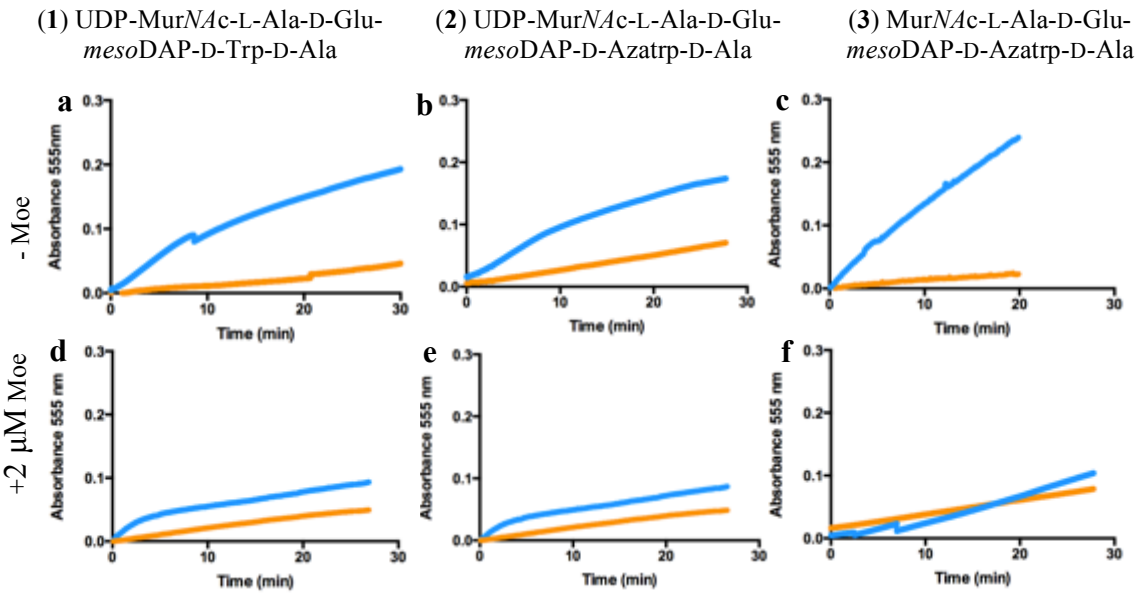

Figure 6.30 The Ability of the Three Synthesised Compounds as Transpeptidase Acceptors, all with Fluorescamine-DAP-LII as the Donor.
(a) and (d) UDP-Mur*NA*c-L-Ala-D-Glu-*meso*DAP-D-Trp-D-Ala as transpeptidase acceptor, (b) and (e) UDP-Mur*NA*c-L-Ala-D-Glu-*meso*DAP-D-Azatrp-D-Ala as transpeptidase acceptor, (c) and (e) Mur*NA*c-L-Ala-D-Glu-*meso*DAP-D-Azatrp-D-Ala as transpeptidase acceptor. (a-c) No Moenomycin (d-f) with 2 µM Moenomycin. Assay conditions: 50 mM BisTris Propane, pH 8.5, 20 mM $MgCl_2$, 0.1 % TritonX-100, 50 µM Amplex Red, 3.5 Units *Rhodotorula gracalis* DAAO, 5.8 Units HRP, 0.2 µM *E. coli* LpoB, transpeptidase donor: 20 mM Fluorescamine-DAP-LII in 0.1 % TritonX-100, 11 nM *E. coli* PBP1B in 0.2 % TritonX-100, transpeptidase acceptor. Blue: + Fluorescamine-DAP-LII, Orange: without Fluorescamine-DAP-LII.

The three compounds tested positive as transpeptidase acceptors when using Fluorescamine-DAP-LII as the transpeptidase donor. Mur*NA*c-L-Ala-D-Glu-*meso*DAP-D-Azatrp-D-Ala (**c**) appeared to be turned over the quickest, UDP-Mur*NA*c-L-Ala-D-Glu-*meso*DAP-D-Trp-D-Ala (**a**) second, UDP-Mur*NA*c-L-Ala-D-Glu-*meso*DAP-D-Azatrp-D-Ala third. The negative control assays without Fluorescamine-DAP-LII were inactive, as expected. The assays with the transglycosylase inhibitor Moenomycin added were inhibited.

In summary, dansDAP-LII and potential Fluorescamine-DAP-LII were both active as transpeptidase donors. The UDP-Mur*NA*c pentapeptides with D-Trp or D-Azatrp at position four in the pentapeptide stem were both active transpeptidase acceptors, with or without the UDP attached in the case of the D-Azatrp pentapeptide. Having confirmed that these compounds are viable transpeptidase substrates, their ability to work as part of a FRET pair is tested.

The compounds were designed as FRET fluorophore pairs, with D-Trp in the pentapeptide stem being the fluorophore donor to the fluorophore acceptor, Dansyl. The other FRET pairing being D-azatrp as the fluorophore donor to the fluorophore acceptor Fluorescamine (**Figure 6.31**).

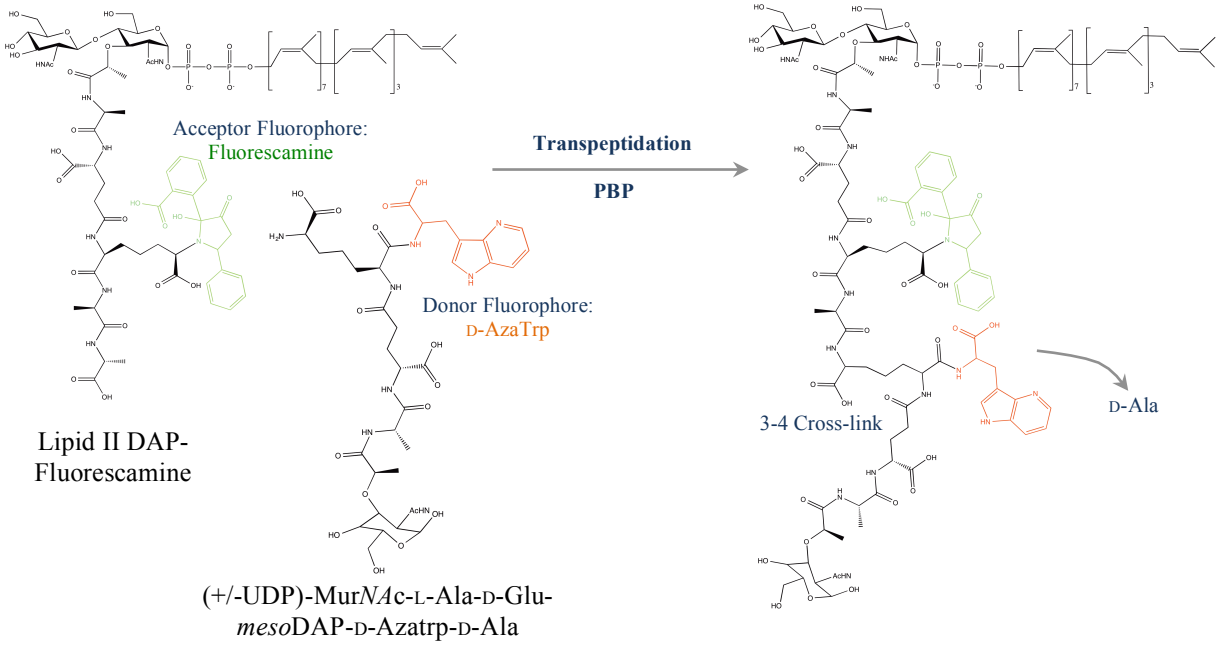

Figure 6.31 Schematic of the Proposed FRET Assay. Upon 3-4 Cross-linking during transpeptidation, fluorescent energy should transfer from the D-Azatrp donor fluorophore, to the Fluorescamine acceptor fluorophore. This schematic represents one of the FRET pairs. In the other pairing, there is a dansyl group in the place of the Fluorescamine moiety, and the D-Azatrp is replaced by D-Trp.

The FRET assay was attempted using the PTI Fluorimeter, but more optimisation is required to show FRET activity between these compounds. Due to the potential for contamination of the fluorescamine-DAP-LII with unlabelled lipid, it is possible that competition by the unlabelled lipid for the transpeptidase acceptor and donor sites reduced the ability of the fluorophore labelled substrates to bind sufficiently to eliminate any detectable FRET interactions.

6.9 Enzymology of Transpeptidation: Kinetic Characterisation of the Transpeptidase Activity of *E. coli* PBP1A and *P. aeruginosa* PBP1A

The penicillin-binding domain of PBPs is responsible for both transpeptidase and carboxypeptidase activity, both of which result in the release of D-alanine. In the past, substrate analogues were used to mimic the donor, and single D-amino acids were used as acceptors in primitive monitoring of transpeptidation. The recent ability to synthesise native substrates *de novo* (Breukink *et al.*, 2003) has encouraged the monitoring of transpeptidation to be detected directly, using radiolabelled peptidoglycan initially (Bertsche *et al.,* 2005) and the native substrate LII more recently (Lebar *et al*., 2013). The reaction products were seaparated either chromographically or by measuring release of the terminal D-alanine. *Ec*PBP1A (Born *et al*., 2006) and *Ec*PBP1B (Bertsche *et al.*, 2005) transpeptidase products were separated by HPLC, analysing the muropeptides by HPLC. The first use of monitoring D-Ala release was by Mirelman *et al*., (1972) through the incorporation of UDPMur*N*Ac-L-Ala-D-Glu-L-Lys-D-Ala-[^{14}C]-D-Ala into *Micrococcus luteus* membranes. A more recent advancement that has somewhat explained previous difficulties in detecting transpeptidase activity, is the role of the lipoproteins *E. coli* LpoA and LpoB in the enhancement of transpeptidase activities of *Ec*PBP1A and 1B, respectively (section 1.5.10.1). *Ec*LpoA was shown to stimulate *Ec*PBP1A catalysed cross-linking by 4.5 fold *in vitro* (Paradis-Bleau *et al*., 2010, Typas *et al*., 2010).

This transpeptidation assay follows the continuous release of the terminal D-Ala from the donor stem peptide. The presence of D-amino acid oxidase, when coupled with Amplex Red and Horse Radish Peroxidase (HRP) gives a quantitative continuous read out of transpeptidation in real time. Addition of an acceptor stimulates the release of the terminal D-Ala on the donor (The transpeptidase donor is esterified at the active site). This released D-amino acid is detected by DAAO and triggers the coupling system (**Figure 6.32)**.

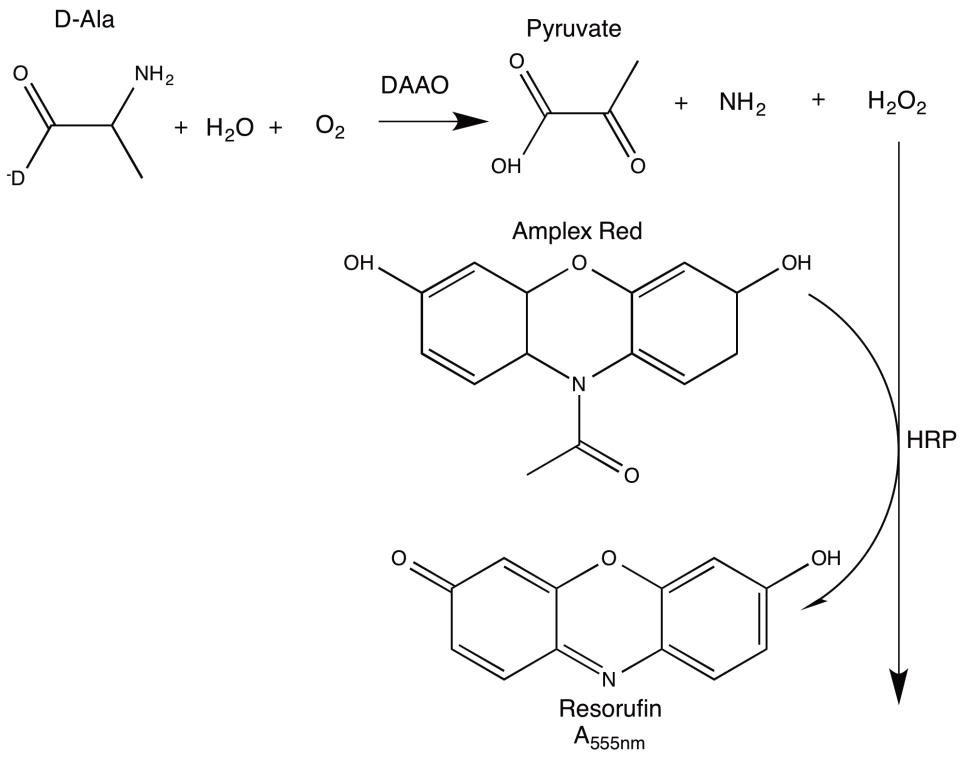

Figure 6.32 A Schematic of the Continuous Transpeptidase coupled Assay. D-Amino acid oxidase oxidises the released D-amino acid to pyruvate and hydrogen peroxide. Horse radish peroxidase (HRP) uses hydrogen peroxide to convert Amplex Red to the chromophore Resorufin, which absorbs strongly at 555 nm.

The spectrophotometric continuous assay was developed by Dr. Adrian Lloyd at The University of Warwick, using *E. coli* PBP1B (sections 2.8.3 and **Figure 6.33**). In each assay, all components were present in the cuvette upon initiation of spectrophotometric monitoring, except for the PBP and the acceptor. A baseline reading was measured for a few minutes, before adding the PBP and finally the acceptor. Assays were monitored at 555 nm, at 30 °C, for 40 minutes. Also, two separate assays were run in parallel, one with the donor present (e.g. Lys-LII, red), and one without the donor (blue) to account for the background rate. This assay was further developed for *E. coli* PBP1A predominantly, as well as *P. aeruginosa* PBP1A subsequently.

6.9.1 The Transpeptidase Activity of *E. coli* PBP1B in the presence and Absence of *E. coli* CpoB

The transpeptidase activity of *E. coli* PBP1B with its necessary cognate stimulatory accessory protein *E. coli* LpoB is shown in **Figure 6.33 a**. Another accessory protein involved in the coordination of cell division and active in the divisome complex is *E.*

coli YbgF, which has recently been renamed in *E. coli* to CpoB. CpoB localises to mid-cell at the onset of constriction, requiring a functional divisome complex. CpoB binds to PBP1B between the UB2H and transpeptidase domains, residues Thr_{751} and Thr_{753} of PBP1B. The affect of the presence of *E. coli* CpoB was tested during transpeptidation (**Figure 6.33 b**).

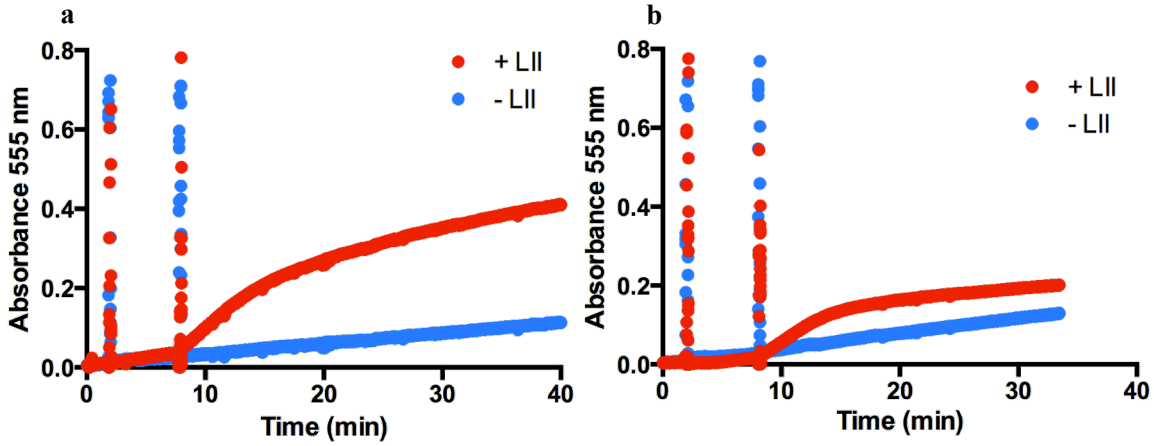

Figure 6.33 The Continuous Spectrophotometric Detection of *E. coli* PBP1B Transpeptidase Activity. (a) *E. coli* PBP1B + *E. coli* LpoB **(b)** *E. coli* PBP1B + *E. coli* LpoB + *E. coli* CpoB (formally YbgF). Assay conditions: 50 mM BisTris Propane, pH 8.5, 20 mM $MgCl_2$, 0.1 % TritonX-100, 50 µM Amplex Red, 3.5 Units *Rhodotorula gracalis* DAAO, 5.8 Units HRP, 0.2 µM *E. coli* LpoB, 0.2 µM *E. coli* CpoB, transpeptidase donor: 20 mM Lys-LII in 0.1 % TritonX-100. First addition: 11 nM *E. coli* PBP1B in 0.2 % TritonX-100, second addition (transpeptidase acceptor): Mur*N*Ac-L-Ala-D-Glu-*meso*DAP-D-Ala-D-Ala. Red: + Lys-LII donor, blue: no Lys-LII donor.

A positive result for the transpeptidase activity of *E. coli* PBP1B was demonstrated in the presence of *E. coli* LpoB, shown to be necessary for transpeptidase activity. However, this assay does not distinguish between DD-carboxypeptidase activity and transpeptidation, owing to the obligation to conduct the assays in duplicate, indicating the comparative background rate in each case. The presence of CpoB during transpeptidation appeared to suppress transpeptidation. Two months before this assay was conducted, Gray *et al.*, 2015 published that *E. coli* CpoB partially inhibited the stimulation of the transpeptidase activity of *Ec*PBP1B by *Ec*LpoB *in vitro,* with a 50% reduction in stimulation (Egan & Vollmer, 2015).

Recently, both TolA and CpoB were shown to interact directly with the PBP1B-LpoB complex *in vitro*, but neither CpoB or TolA affected basal PBP1B transpeptidase activity (Gray *et al.*, 2015). This effect of CpoB is reversed by TolA, which interacts with PBP1B at the region proximal to the membrane. CpoB also had no effect on the

transglycosylase activity of PBP1B, alone or in combination with LpoB (Gray *et al.*, 2015).

6.9.2 The Transpeptidase Activity of *E. coli* PBP1A

The transpeptidase activity of *E. coli* PBP1A (no TM domain) was trialled in the conditions described above for *Ec*PBP1B, with the assay buffer and PBP in 0.2% TritonX-100. However, the *Ec*1A exhibited no activity under these conditions initially. *Ec*PBP1A transpeptidase activity has been shown in CHAPS (Lupoli *et al.*, 2011). The use of Ethylene Glycol Alkyl Ether detergents to investigate transpeptidase activity was suggested by Dr. Adrian Lloyd, due to the nature of these detergents and their published use in the continuous fluorometric transglycosylase assay (Schwartz *et al.*, 2002) and its previous success with transglycosylase activity and *E. coli* PgpB (section 5.6.8.2).

6.9.2.1 Comparing the Transpeptidase Activity of *Ec*PBP1A with and without the Hexa-His tag

The transpeptidase activity of *E. coli* PBP1A with and without the His_6-tag was tested (**Figure 6.34**). The assay was also conducted in the absence of *E. coli* PBP1A, to confirm the dependency of *Ec*PBP1A on transpeptidase activity (**Figure 6.34 c**).

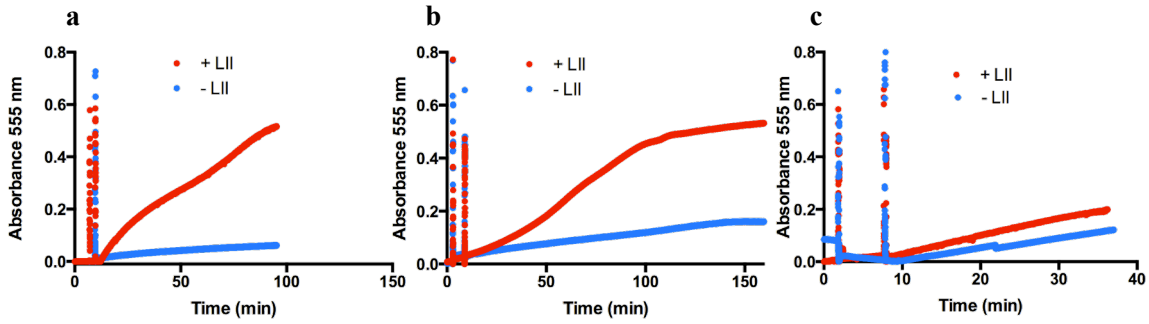

Figure 6.34 The Continuous Spectrophotometric Detection of *E. coli* PBP1A Transpeptidase Activity. (a) *E. coli* PBP1A (+His_6-tag) + *E. coli* LpoA **(b)** *E. coli* PBP1A (no His_6-tag) + *E. coli* LpoA **(c)** No *E. coli* PBP1A, replaced with *Ec*PBP1A storage buffer (25 mM Tris pH 7.5, 10 mM $MgCl_2$, 1M NaCl, 50% glycerol and 20 mM CHAPS). Assay conditions: 50 mM BisTris Propane, pH 8.5, 20 mM $MgCl_2$, 0.39 % E_6C_{12}, 50 µM Amplex Red, 3.5 Units *Rhodotorula gracalis* DAAO, 5.8 Units HRP, 1.16 µM *E. coli* LpoA, transpeptidase donor: 20 µM Lys-LII in 0.026 % E_6C_{12}. Addition 1: 430 nM *E. coli* PBP1A in 20 mM CHAPS, addition 2 (transpeptidase acceptor): 20 µM Mur*N*Ac-L-Ala-D-Glu-*meso*DAP-D-Ala-D-Ala. A final ratio of *Ec*PBP1A : *Ec*LpoA was 1 : 2.7, as a 1:3 ratio advised in Typas *et al.*, 2010) Red: + LysLII donor, blue: no LysLII donor.

E. coli PBP1A appears to show transpeptidase activity with 430 nM *Ec*PBP1A and 1.16 µM *Ec*LpoA (1 : 2.7 ratio). The profile of the activity curve for the PBP1A without a his_6-tag is preferable to the curve observed for that with a his_6-tag. Both sigmoidal and non-sigmoidal kinetic profiles were observed during the continuous transpeptidase activity monitoring of PBP1A. The his_6-tag was removed from all PBP1A preparations for the monitoring of transpeptidation activity.

6.9.2.2 Investigating cryo-preservation and subsequent transpeptidase activity of *E. coli* PBP1A

The concentration of *Ec*PBP1A required to observe a continuous transpeptidation rate was reduced, resulting in 5 µL of a 5.75 µM protein stock, i.e. a final *Ec*PBP1A concentration of 143 nm in each assay. The stability of *E. coli* PBP1A was tested to determine the optimum cryo-preservation storage method. The final step of *Ec*PBP1A purification was dialysis into 50 % glycerol for long-term storage in -80. Assays in **Figure 6.35** were conducted with freshly purified protein, before the protein had undergone any cryo-preservation. An aliquot of *Ec*PBP1A was frozen at -80 °C and at -20 °C and its activity was subsequently tested.

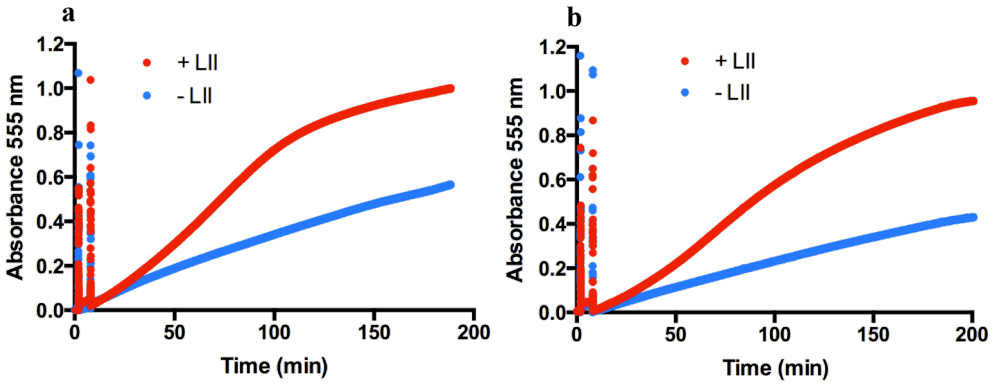

Figure 6.35 The Durability and Stability of *E. coli* PBP1A to withstand one freeze-thaw cycle at -80 or -20 °C. (a) *E. coli* PBP1A stored at -20 °C overnight and then thawed **(b)** *E. coli* PBP1A stored at -80 °C overnight and then thawed. Assay conditions: 50 mM BisTris Propane, pH 8.5, 20 mM $MgCl_2$, 0.39 % E_6C_{12}, 50 µM Amplex Red, 3.5 Units *Rhodotorula gracalis* DAAO, 5.8 Units HRP, 1.16 µM *E. coli* LpoA, transpeptidase donor: 20 µM Lys-LII in 0.026 % E_6C_{12}. Addition 1: 430 nM *E. coli* PBP1A in 20 mM CHAPS, addition 2 (transpeptidase acceptor): 20 µM Mur*N*Ac-L-Ala-D-Glu-*meso*DAP-D-Ala-D-Ala. Red: + LysLII donor, blue: no LysLII donor.

E. coli PBP1A can withstand one freeze-thaw cycle from -80 °C and from -20 °C. A second freeze-thaw cycle was tested, which also demonstrated full activity. Activity became compromised after a third freeze-thaw cycle (data not shown) and no further testing was done, and each aliquot was thawed for single-use only. *Ec*PBP1A can be stored at -20 or -80 in 50% glycerol and remain active after thawing. All 1A PBPs for transpeptidase assays were stored in 50% glycerol in 50 µL aliquots at -80 °C.

6.9.2.3 Determining the Dependency of a Transpeptidase Rate Upon the Presence of *E. coli* PBP1A and *E. coli* LpoA

The dependency of transpeptidase activity on the presence of *E. coli* PBP1A was tested by the presence and absence of this enzyme (**Figure 6.36 a**). In this control, Lys-LII was added to both assays. The necessity to have *E. coli* LpoA present in all transpeptidase assays was also tested (**Figure 6.36 b**).

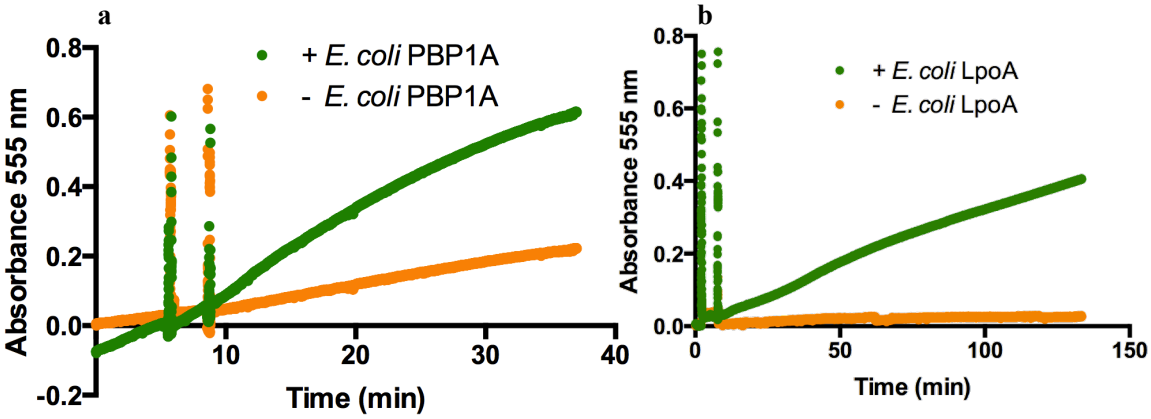

Figure 6.36 The Dependency of Transpeptidase Activity upon the Presence of *E. coli* PBP1A or *E. coli* LpoA. **(a)** +/- *E. coli* PBP1A: LysLII added to both assays with *Ec*PBP1A added to only one. **(b)** +/- *Ec*LpoA. LysLII added to both assays, with *Ec*LpoA added to only one. Assay conditions: 50 mM BisTris Propane, pH 8.5, 20 mM $MgCl_2$, 0.39 % E_6C_{12}, 50 µM Amplex Red, 3.5 Units *Rhodotorula gracalis* DAAO, 5.8 Units HRP, 1.16 µM *E. coli* LpoA or *Ec*LpoA storage buffer, transpeptidase donor: 20 µM Lys-LII in 0.026 % E_6C_{12}. Addition 1: 430 nM *E. coli* PBP1A in 20 mM CHAPS or *Ec*PBP1A storage buffer (25 mM Tris pH 7.5, 10 mM $MgCl_2$, 1M NaCl, 50% glycerol and 20 mM CHAPS), addition 2 (transpeptidase acceptor): 20 µM Mur*N*Ac-L-Ala-D-Glu-*meso*DAP-D-Ala-D-Ala. Green: + (a) *Ec*PBP1A / (b) *Ec*LpoA, orange: no *Ec*PBP1A in (a) or *Ec*LpoA in (b).

In the absence of *E. coli* LpoA the rate of transpeptidation cannot be observed, indicating that either *Ec*PBP1A does not function without *Ec*LpoA or/and the transpeptidation rate is so slow that it cannot be observed. Additionally, no background rate is present in the absence of *Ec*LpoA. One justification for this could be that the

*Ec*LpoA preparation is showing DD-carboxypeptidase activity and triggering the DAAO coupling system, adding to the background rate seen in the negative controls (no Lys-LII) elsewhere.

6.9.2.4 The Sensitivity of *E. coli* PBP1A Transpeptidase Activity to Inhibition by Moenomycin A and Ampicillin

The sensitivity of the assay was tested in the presence of two concentrations of the transpeptidase β-lactam inhibitor ampicillin: a concentration close to the IC_{50} (**Figure 6.37 a**), and the other 10-fold the IC_{50} (**Figure 6.37 b**). Similarly, the potent transglycosylase inhibitor Moenomycin was added to test the ability of *Ec*PBP1A to perform transpeptidation in the presence of a transglycosylase inhibitor (**Figure 6.37 c**).

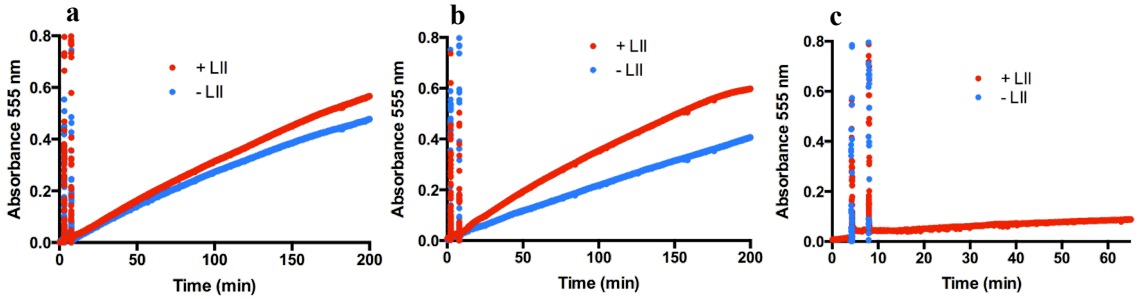

Figure 6.37 Sensitivity of the Transpeptidase assay to Ampicillin or Moenomycin A. **(a)** with 25 µM ampicillin **(b)** with 250 µM ampicillin **(c)** with 25 µM Moenomycin A. Assay conditions: 50 mM BisTris Propane, pH 8.5, 20 mM $MgCl_2$, 0.39 % E_6C_{12}, 50 µM Amplex Red, 3.5 Units *Rhodotorula gracalis* DAAO, 5.8 Units HRP, 1.16 µM *E. coli* LpoA, transpeptidase donor: 20 µM Lys-LII in 0.026 % E_6C_{12}. Addition 1: 430 nM *E. coli* PBP1A in 20 mM CHAPS, addition 2 (transpeptidase acceptor): 20 µM Mur*N*Ac-L-Ala-D-Glu-*meso*DAP-D-Ala-D-Ala. Red: + LysLII donor, blue: no LysLII donor.

The transpeptidase activity was diminished upon the addition of 25 µM ampicillin, which is close to the IC_{50} value for ampicillin, so 10-fold this concentration (250 µM) inhibited any observable transpeptidase activity. In the presence of the transglycosylase inhibitor Moenomycin A, transpeptidation was not observed at all. Without the preceding transglycosylation reaction to form glycan strands, transpeptidation cannot occur. Moenomycin does not affect the Amplex Red coupling reagents at the concentration used and also it does not inhibit DD-carboxypeptidation. 25 µM MoeA sufficiently inhibited the rate demonstrated in its absence, therefore indicating that the rate observed thus far is as a result of transpeptidase activity by *Ec*PBP1A.

6.9.2.5 The Ability of *E. coli* PBP1A to Utilise Structurally Diverse Transpeptidase Acceptor Compounds

Thus far, the transpeptidase donor used in this section has been Lys-LII, and the acceptor Mur*N*Ac-L-Ala-D-Glu-*meso*DAP-D-Ala-D-Ala. Additional acceptors have been tested including the tetrapeptide Mur*N*Ac-L-Ala-D-Glu-*meso*DAP-D-Ala (**Figure 6.38 b**) and the tripeptide Mur*N*Ac-L-Ala-D-Glu-*meso*DAP (**Figure 6.38 c**).

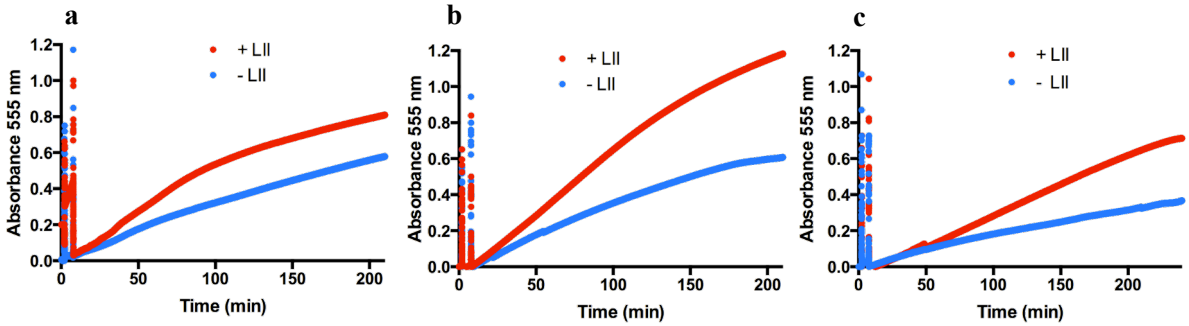

Figure 6.38 The Ability of *E. coli* PBP1A to Utilise Non-Canonical Transpeptidase Acceptor Compounds. **(a)** Using the already tested pentapeptide acceptor 20 µM Mur*N*Ac-L-Ala-D-Glu-*meso*DAP-D-Ala-D-Ala **(b)** with the tetrapeptide acceptor 20 µM Mur*N*Ac-L-Ala-D-Glu-*meso*DAP-D-Ala **(c)** with the tripeptide acceptor 20 µM Mur*N*Ac-L-Ala-D-Glu-*meso*DAP. Assay conditions: 50 mM BisTris Propane, pH 8.5, 20 mM $MgCl_2$, 0.39 % E_6C_{12}, 50 µM Amplex Red, 3.5 Units *Rhodotorula gracalis* DAAO, 5.8 Units HRP, 1.16 µM *E. coli* LpoA, transpeptidase donor: 20 µM Lys-LII in 0.026 % E_6C_{12}. Addition 1: 430 nM *E. coli* PBP1A 20 mM CHAPS, addition 2: chosen transpeptidase acceptor. Red: + LysLII, blue: no LysLII.

The specificity of *E. coli* PBP1A as a transpeptidase enzyme demonstrates its ability to incorporate structurally diverse acceptor substrates in to peptidoglycan including a tetrapeptide acceptor (Mur*N*Ac-L-Ala-D-Glu-*meso*DAP-D-Ala), as well as the tripeptide acceptor Mur*N*Ac-L-Ala-D-Glu-*meso*DAP. Mur*N*Ac-tetrapeptide was not as an efficient acceptor as its pentapeptide equivalent as it appears to have been incorporated at a slower rate. Mur*N*Ac-tripeptide was less efficient again, as the structure is deviating further away from that of the native acceptor *in vivo*. Determining which compounds function as plausible transpeptidase acceptors is important for elucidating further the mechanistic integrity of transpeptidation and could provide novel information on acceptor requirements.

Another compound tested for its potential suitability as a potential acceptor is D-lactate (**Figure 6.39 a**), which is present naturally in the fifth position of the pentapeptide in

strains resistant to vancomycin e.g. vancomycin-resistant *Enterococci* (VRE strains) (Healy *et al.,* 2000). Substitutions in the peptidyl-D-Ala^4-D-Ala^5 extremity of peptidoglycan precursors are selected by glycopeptides because such modifications reduce the affinity of the antibiotics for the target (Nieto & Perkins, 1971). The substrate D,L(*meso*)-DAP-LII was trialed for its ability to function as both a donor and acceptor substrate concurrently (**Figure 6.39 b**). In sections 6.8.2 and 6.8.3, Dansyl-and Fluorescamine-labelled *meso*DAP-LII substrates were tested for potential transpeptidase donor functionality.

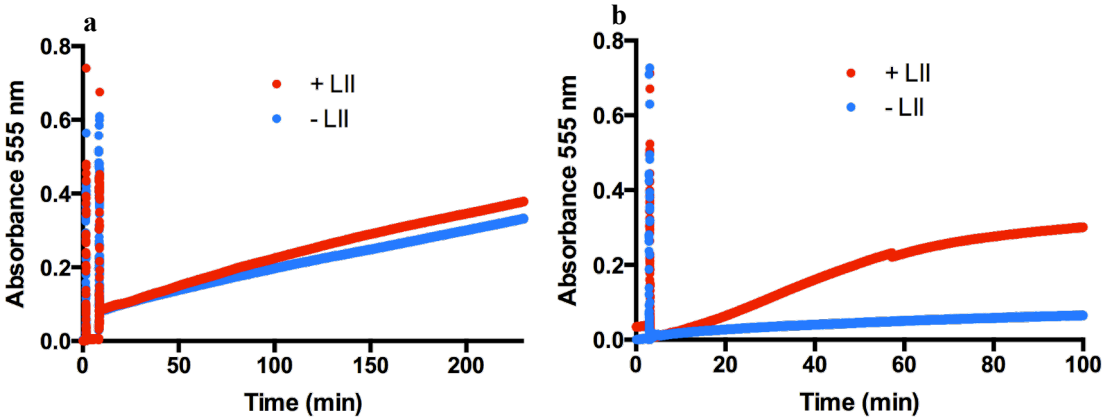

Figure 6.39 The ability of D-lactate to Function as a Transpeptidase Acceptor, and D,L-DAP-LII to Function as both a Transpeptidase Donor and Acceptor. (a) 10 mM D-lactate as a transpeptidase acceptor, with 20 µM L-LysLII in 0.026 % E_6C_{12} as the donor **(b)** D,L-DAPLII as both a transpeptidase donor and acceptor simultaneously. Assay conditions: 50 mM BisTris Propane, pH 8.5, 20 mM $MgCl_2$, 0.39 % E_6C_{12}, 50 µM Amplex Red, 3.5 Units *Rhodotorula gracalis* DAAO, 5.8 Units HRP, 1.16 µM *E. coli* LpoA. Addition 1: 430 nM *E. coli* PBP1A in 20 mM CHAPS, and in (a) only, a second addition: transpeptidase acceptor 10 mM D-lactate. Red: + LII, blue: no LII.

D-lactate did work as a transpeptidase acceptor, but only marginally and was not as successful as the Mur*N*Ac pentapeptides previously tested. D-lactate is a simple acceptor as are D-amino acid residues that can be exchanged naturally in to the fifth position of the pentapeptide stem (Lupoli *et al.*, 2011), however, even with 10 mM D-lactate it was only turned-over very slowly. The substrate D,L-DAP-LII proved to be an efficiently functioning donor and acceptor.

6.9.2.6 Testing *E. coli* PBP1A Catalytic Active Site Transglycosylase and Transpeptidase Mutants in the Continuous Transpeptidase Assay

E. coli PBP1A transglycosylase and transpeptidase active site mutants were tested for their abilities to perform as transpeptidases in the continuous assay (**Figure 6.40**).

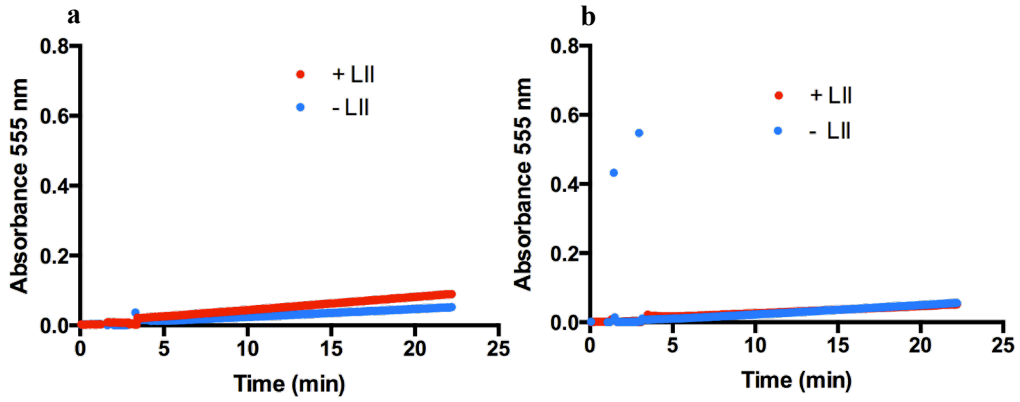

Figure 6.40 *E. coli* PBP1A Transglycosylase and Transpeptidase Catalytic Active Site Mutant Proteins Tested for Transpeptidase Activity (a) *E. coli* PBP1A transglycosylase active site mutant **(b)** *E. coli* PBP1A transpeptidase active site mutant. Assay conditions: 50 mM BisTris Propane, pH 8.5, 20 mM $MgCl_2$, 0.39 % E_6C_{12}, 50 µM Amplex Red, 3.5 Units *Rhodotorula gracalis* DAAO, 5.8 Units HRP, 1.16 µM *E. coli* LpoA. Addition 1: 430 nM *E. coli* PBP1A in 20 mM CHAPS, addition 2: transpeptidase acceptor 20 µM Mur*N*Ac-L-Ala-D-Glu-*meso*DAP-D-Ala-D-Ala. Red: + LII, blue: no LII.

Transpeptidase activity was not observed at all when either the transglycosylase active site residue or the transpeptidase active site residue was mutated to non-catalytic equivalent amino acid residues. This further establishes the imperative functions of the catalytic active site residues in the final peptidoglycan biosynthesis step of transpeptidation. The mutated transglycosylase active site residue prevents glycan polymer formation for subsequent processing *via* transpeptidation.

6.9.3 The Transpeptidase Activity of *P. aeruginosa* PBP1A in the Presence and Absence of *P. aeruginosa* YbgF

Pseudomonas aeruginosa PBP1A was also tested for transpeptidase function, with and without the presence of *Pseudomonas aeruginosa* YbgF (renamed CpoB in *E. coli*) (**Figure 6.41**).

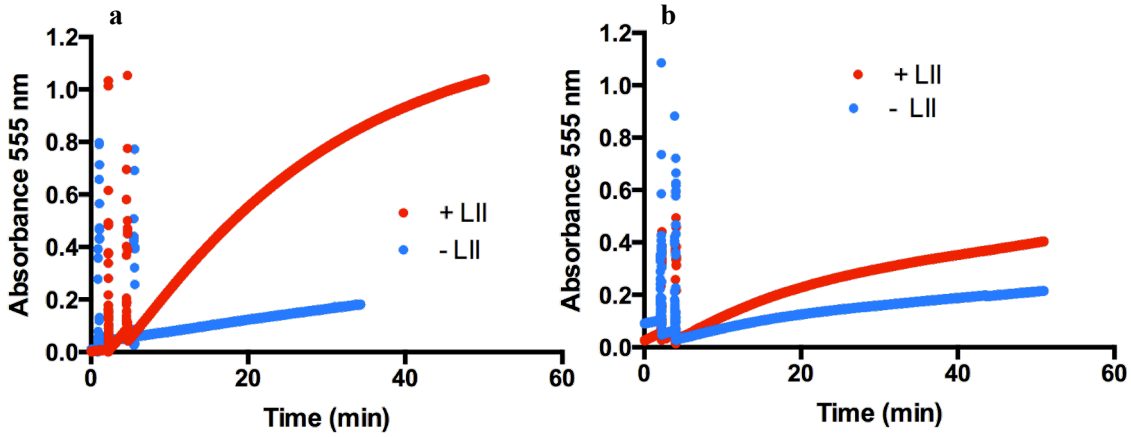

Figure 6.41 The Transpeptidase Activity of *Pseudomonas aeruginosa* PBP1A, with and without *Pa*YbgF. Both assays are stimulated by the presence of *Pa*LpoA **(a)** *P. aeruginosa* PBP1A transpeptidase activity **(b)** *P. aeruginosa* PBP1A transpeptidase activity with *Pa*YbgF. Assay conditions: 50 mM BisTris Propane, pH 8.5, 20 mM $MgCl_2$, 0.39% E_6C_{12}, 50 µM Amplex Red, 3.5 Units *Rhodotorula gracalis* DAAO, 5.8 Units HRP, 1.2 µM *Pa*LpoA. Addition 1: 400 nM *Pa*PBP1A in 20 mM CHAPS, addition 2: transpeptidase acceptor 20 µM Mur*N*Ac-L-Ala-D-Glu-*meso*DAP-D-Ala-D-Ala. Red: + LII, blue: no LII.

A kinetic rate is visible when *P. aeruginosa* PBP1A was tested for transpeptidase activity, signifying a positive observation of transpeptidase activity. No negative controls (apart from without the donor Lys-LII - blue curve in Figure 6.41) with Moenomycin A or ampicillin have been done with *P. aeruginosa* PBP1A thus far. However, the transpeptidase activity of *Pa*PBP1A in TritonX-100 in the same conditions optimised for *E. coli* PBP1B, exhibited comparable activity to *Pa*PBP1A in CHAPS with an alkyl ether detergent assay environment (data not shown).

6.9.3.1 Testing *P. aeruginosa* PBP1A Catalytic Transglycosylase and Transpeptidase Active-Site Mutants in the Continuous Transpeptidase Assay

The *Pa*PBP1A transglycosylase and transpeptidase active site residue mutants were also tested for transpeptidase activity (**Figure 6.42**). The transpeptidase activity of both *P. aeruginosa* mutants was not observed in this assay, suggesting that these are successful active site mutants, with the mutated residue having important catalytic function towards the transpeptidation mechanism.

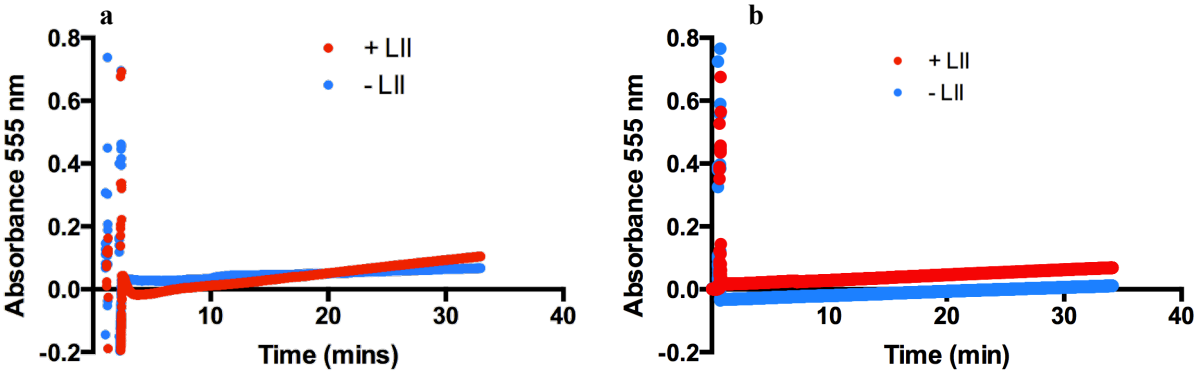

Figure 6.42 *P. aeruginosa* PBP1A Transglycosylase and Transpeptidase Catalytic Active Site Mutant Proteins Tested for Transpeptidase Activity. *Pa*LpoA is present in both assays **(a)** *P. aeruginosa* PBP1A transglycosylase mutant **(b)** *P. aeruginosa* PBP1A transpeptidase active site mutant. Assay conditions: 50 mM BisTris Propane, pH 8.5, 20 mM $MgCl_2$, 0.39 % E_6C_{12}, 50 µM Amplex Red, 3.5 Units *Rhodotorula gracalis* DAAO, 5.8 Units HRP, 1.2 µM *Pa*LpoA. Addition 1: 400 nM *Pa*PBP1A in 20 mM CHAPS, addition 2: transpeptidase acceptor 20 µM Mur*N*Ac-L-Ala-D-Glu-*meso*DAP-D-Ala-D-Ala. Red: + LII, blue: no LII.

A comparison between the assay buffers for the continuous transpeptidase and continuous transglycosylase assays are given in **Table 6.2**.

Table 6.2 A Comparison Between Assay Buffers for Transglycosylation and Transpeptidation for *Ec*PBP1A and *Pa*PBP1A. In the continuous transglycosylase fluorometric assay, the dansLII substrate is resuspended directly into the assay buffer and is stabilised by the decyl-PEG E_8C_{10} detergent present in the buffer, before being aliquoted into wells of a 96-well plate. In the continuous transpeptidase D-Ala release assay, the LII substrate is resuspended in detergent (Triton X-100 or E_XC_Y) prior to addition to the cuvette.

	***E. coli* PBP1a buffer**	***P. aeruginosa* PBP1a buffer**
Continuous **Transglycosylase** Fluorometric Assay	50 mM HEPES pH 7.5 60 mM NaCl 10 mM $MgCl_2$ 10 % (v/v) DMSO 0.085 % (v/v) octa-ethylene glycol monodecyl ether (E_8C_{10}) (+ 4 µg/mL muramidase)	50 mM HEPES pH 7.0 60 mM NaCl 10 mM $MgCl_2$ 10 % (v/v) DMSO 0.085 % (v/v) octa-ethylene glycol monodecyl ether (E_8C_{10}) (+ 4 µg/mL muramidase)
Continuous **Transpeptidase** coupled D-Ala Release Assay	50 mM BisTrisPropane pH 8.5 20 mM $MgCl_2$ z % E_xC_y or 0.1 % TritonX-100 (+ coupling reagents: DAAO, HRP, Amplex Red and accessory protein *Ec*LpoA)	50 mM BisTrisPropane pH 8.5 20 mM $MgCl_2$ z % E_xC_y or 0.1 % TritonX-100 (+ coupling reagents: DAAO, HRP, Amplex Red and accessory protein *Pa*LpoA)

[z] Each E_xC_y detergent has a different CMC, with the percentage used given in each case

The transpeptidase assay buffer did not contain NaCl or DMSO, which are both present in the transglycosylase assay buffer. The E_xC_y detergent used in the transpeptidase buffer was E_6C_{12}, but was E_8C_{10} in the transglycosylase assay buffer (Schwartz *et al*., 2002).

6.10 Discussion

Fluorescamine-DAP-pentapeptide mass spectral analysis showed some unlabelled species present after SepharoseQ purification. A second purification procedure should have been employed here to try to separate the labelled from the unlabelled species, such as a reverse phase column on HPLC may have worked. In light of these mass spec results of the fluorescamine-labelled pentapeptide, the TLC of the purified elutions of Fluorescamine-LII should have contained a DAP-LII (non-labelled) control. As if the compound being purified contained a mixture of fluorescamine labelled and non-labelled species, it may have been easier to identity any non-labelled material on TLC if a sample of DAP-LII was present on the plate. There was limited space on the TLC plate so in retrospect, splitting these samples across two TLC plates and including further control samples would have been preferable.

Although the Fluorescamine-DAP-LII contained some unlabelled species, but it was shown that it functioned as a transpeptidase donor, therefore should have seen some activity in the FRET assay. Or the FRET just didn't work – it doesn't always work.

The continuous spectrophotometric D-Ala release assay was developed by Dr. Adrian Lloyd at The University of Warwick to demonstrate transpeptidase activity in real-time. The success of this assay with *Ec*PBP1B has allowed the characterisation of *P. aeruginosa* and *E. coli* PBP1A transpeptidase activity continuously, for the first time. The rate of *Ec*PBP1B transpeptidase activity was virtually undetectable in the absence of *Ec*LpoB.

6.11 Conclusions

Novel transpeptidase donor and acceptor compounds have been developed to help study the transpeptidase mechanism. Three out of the four compounds were successfully

synthesised, with the Fluorescamine-DAP-LII likely to have been synthesised, indicate in absorbance spectroscopy data. The four synthesised compounds (two transpeptidase donors and two transpeptidase acceptors) were tested for transpeptidase donor and acceptor functionality using the D-Ala release, continuous spectrophotometric transpeptidase activity assay. The two synthesised acceptors showed capability as acceptors with both Lys-LII and dansDAP-LII. Unlabelled DAP-LII was shown to function as both a transpeptidase donor and acceptor simultaneously. Fluorescamine-DAP-LII also showed ability to function as a transpeptidase donor in the continuous fluorometric transglycosylase assay as well as a successful donor in the continuous D-Ala release transpeptidase assay, using the two synthesised transpeptidase acceptors.

The enzymatic activity of the transpeptidase function of Class A PBPs *E. coli* PBP1A has been extensively characterised, and has begun for *P. aeruginosa* PBP1A. The transpeptidase rate exhibited of *E. coli* PBP1A showed sensitivity to both Moenomycin A and ampicillin, and also was able to utilise structurally diverse acceptors including Mur*NA*c-tetrapeptide and Mur*NA*c-tripeptide. *Ec*PBP1A transglycosylase and transpeptidase active site mutants inhibited the transpeptidase rate observed when non-active site mutants were used. *P. aeruginosa* PBP1A also showed a positive rate for transpeptidase activity, as well as its transglycosylase and transpeptidase active site mutants not showing a transpeptidation rate.

6.12 Future Work

Further synthesis work on transpeptidase donors would be useful, including improvements in the purity of Fluorescamine-DAP-LII. LC-MSMS characterisation of the products formed within a transpeptidase FRET assay to confirm the transpeptidase reaction followed by FRET can be detected in terms of a structural identification of the desired transpeptidation product. Further development of the FRET assay also, however, the continuous transpeptidase D-Ala release assay fulfils the requirements of the original brief and duplication is unnecessary.

Further kinetic characterisation of the transpeptidase donors and acceptors would aid in the basic requirements in a transpeptidation mechanism and help in efforts to target transpeptidase activity. The presence of different types of acceptors (e.g. dipeptides vs

single D-amino acids) could have an impact on the rate in which certain donors are incorporated.

Using the D-Ala release transpeptidase assay, investigating whether *E. coli* CpoB or *Pa*YbgF affects the transpeptidase rate of *Ec*PBP1B or *Pa*PBP1B, respectively. The same goes for TolA. TolA is likely to influence the transpeptidation rate of PBP1B, as a consequence of its activation of transglycosylase activity (Gray *et al.*, 2015).

The synthesis of glycan chains through polymerisation of the LII substrate is likely be in close proximity to the membrane, given that transpeptidase cross-linking of these glycan chains must also occur in proximity to bifunctional and monofunctional transpeptidase (PBP) enzymes of the bacterial cell. Although Class a PBPs are membrane associated with a single TM domain, the transglycosylase domain is embedded into the membrane.

Chapter 7
Discussion, Conclusions and Future Work

Class A PBPs are of important relevance to fighting antibiotic resistance pathways at present, particularly those within the group of ESKAPE pathogens, many of which are multi-drug resistant and are capable of 'escaping' the biocidal action of antibiotics and mutually representing new paradigms in pathogenesis, transmission and resistance (Santajit, 2016).

The disruption of the catalytic mechanism of PBPs is bacteriolytic and causes cell wall integrity to be compromised and the cell to lyse. Studying the enzymatic intricacies of bacterial cell wall synthesis is of importance, to help understand how antibiotics interfere with this mechanism and how future potential targets could be designed.

7.1 The Continuous Fluorescence Assay for Transglycosylase Activity

The assay for continuous fluorometric monitoring of real-time transglycosylase activity was used to measure the kinetic constants for 3 Class A bifunctional PBPs (*Ec*PBP1B, *Ec*PBP1A and *Pa*PBP1A) with dansylated variations of LII substrate.

7.1.1 Buffer Conditions for the Continuous Fluorescence Assay

The conditions for optimal transglycosylase activity were determined for *E. coli* PBP1A and *P. aeruginosa* PBP1A. The NaCl concentration optimal for both PBP1A transglycosylase activities was 60 mM, with the optimal pH defined as HEPES pH 7.5 for *Ec*PBP1A and HEPES pH 7.0 for *Pa*PBP1A. Transglycosylase activity for both PBP1A enzymes was observed in TritonX-100, CHAPS and DDM detergents, as well as when tested in a range of ethylene glycol detergents.

7.1.2 Initial Lag-Phase Observed with Class A PBPs

A pre-steady-state lag in the consumption of LII was observed with all three PBPs (*Ec*PBP1B, *Ec*PBP1A and *Pa*PBP1A) during the monitoring of transglycosylase

activity. This initial lag is due to the processivity of the transglycosylase activity of the PBP. During the reaction steady-state, PBPs polymerise in a processive manner, adding LII monomers to a growing polysaccharide chain (Schwartz, 2002). Upon reaction initiation, there is no polymeric substrate to extend and the PBP must synthesise a short oligosaccharide 'primer' to encourage steady-state kinetics. This is a well-known feature of *Ec*PBP1A and PBP1B and was observed in *Pa*PBP1A as well, suggesting that PBP1A in *P. aeruginosa* behaves kinetically similar to *E. coli* PBP1A.

7.1.3 The Pros and Cons of DMSO upon Transglycosylase Activity Assays and Future Work

Further work should be done to reduce the percentage of DMSO or omit this reagent entirely, as it is not necessary for transglycosylase activity in all assays. DMSO was included in the assay buffer for the continuous fluorometric assay because it was present in the published optimal buffer for this technique for *E. coli* PBP1B, and was shown not to interfere with the fluorescence properties of the dansyl reporter group on the pentapeptide stem of LII (Schwartz *et al.,* 2002). The 10 % of DMSO used in the continuous fluorescence assays could help to maintain the low level quantity of synthetic detergent, TritonX-100, required for transglycosylase activity. One occasion where DMSO was useful and necessary was in aiding the migration of transglycosylation products (linear glycan polymers) through a Tris.Tricine polyacrylamide gel matrix to differentiate between varying glycan chain lengths (**Figure 7.1**).

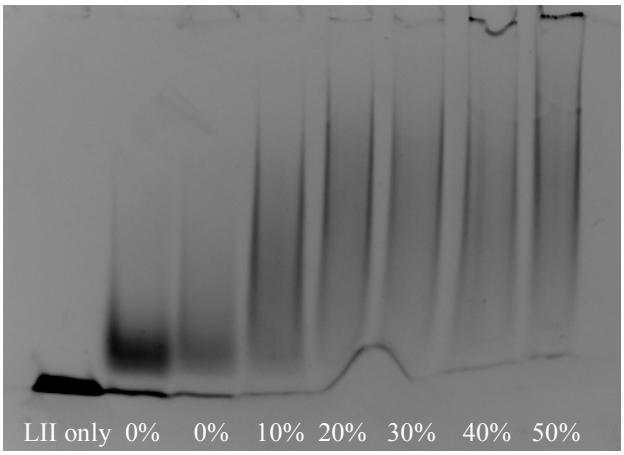

Figure 7.1 The Effect of Increasing Percentage of DMSO upon Glycan Chain Length and Glycan Chain Migration when Analysed by Tris.Tricine SDS-PAGE. A specific Tris-Tricine polyacrylamide gel and dual-buffer system is used (described in section 2.8.1). The dansyl moiety on the LII is visualised through a Short Pass filter. Transglycosylase assay buffer: 10 mM HEPES, 3 mM $MgCl_2$, 150 mM NaCl, 0.18% Triton-X100, + x % DMSO.

It is unclear whether the presence of DMSO in these transglycosylation assays aids in the polymerisation of longer glycan chain or whether its properties means that it acts like a lubricant and physically separates glycan chains, allowing better separation through the polyacrylamide. Further investigation here would be useful to ascertain the involvement of DMSO in transglycosylase activity.

7.1.4 The Kinetic Constants Derived for Class A PBPs, from Transglycosylase Activity

The transglycosylases tested do not require the 55 carbon undecaprenyl moiety, which coincides with results published in Ye *et al.,* 2001, in which they used *E. coli* membranes for transglycosylation activity, rather than purified PBPs. In fact, a shorter polyprenyl chain was a preferred substrate *in vitro* even though the C_{55} chain is the native prenyl chain length. It can be concluded that dansLIIC_{35} was preferred by all three purified PBPs compared to dansLIIC_{55}, most likely due to the substrate with the shorter prenyl chain being more soluble and therefore more accessible to the transglycosylase domain as not surrounded by a synthetic detergent micelle. LII-C_{55} has all the structural features required for recognition but with more desirable physical properties than natural LII. Therefore, it can be used to monitor transglycosylase with a

reduced requirement for synthetic detergent. This continuous fluorometric assay is extremely useful for rapid high-throughput screening to elucidate transglycosylase activity in a range of conditions for comparison, but the substrate(s) used have to report this activity by means of a change in fluorescence or absorbance, resulting in the use of modified substrates.

The full conversion of LII to soluble disaccharide pentapeptide was not assumed, and therefore K_{cat} could not be extracted from the data. Full consumption of LII could be measured and confirmed by HPLC. Ideally the K_{cat}/K_m measure of catalytic efficiency would be calculated to universally compare the affinity between a range of enzymes and substrates obtained through orthogonal assay methods, however, as the full consumption of LII could not be guaranteed with this assay, a reliable K_{cat}/K_m value could not be quantified. Instead $S_{0.5}$, K_m and V_{max} values were calculated for direct comparison between them under the conditions used in this project.

The dependence of Class A PBP1A transglycosylase activity upon LII concentration demonstrated a sigmoidal approach to V_{max}, culminating with a reduction of enzyme activity at higher substrate concentrations. This behaviour was also observed with *S. aureus* MGT (Abrahams, 2011; Bury *et al.*, 2015). It is plausible that Class A bifunctional PBPs also possess two binding sites for the polymerisation of LII into linear glycan chains: one for the elongating glycan chain (donor site) and one for the incoming LII substrate (acceptor site). At time 0, both binding sites will be free of substrate. Upon the addition of substrate, LII binding to the donor site may induce a conformational change, facilitating the binding of the LII substrate at the acceptor site. This would be advantageous if the binding of the two substrates to the donor and acceptor sites occurred in an ordered manner.

The catalytic efficiency values calculated for both *E. coli* PBP1A and *P. aeruginosa* PBP1A were measured by fitting the data to the Hill equation of cooperativity. The catalytic efficiency for dansDAP-LII-C_{35} was >2-fold greater than that for dansDAP-LII-C_{55}, despite the latter being the native substrate. Also this value for dansDAP-LII-C_{55} was 1.5-fold that for dansLys-LII-C_{55} with *P. aeruginosa* PBP1A with no known published values for comparison.

7.1.5 PBP Accessory Proteins and their Impact on Transglycosylase Activity

The affect of the PBP accessory proteins *E. coli* FtsN and PBP2 on the transglycosylase activity of *E. coli* PBP1A and 1B and *P. aeruginosa* PBP1A were discussed in section 4.8.2. It is known that large protein complexes form in *E. coli* to build multifunctional machinery *in vivo*, comprising of inter-dependent and interacting proteins (Leclercq *et al.*, 2017). These initial studies provide the first evidence that the PBP accessory protein PBP2 (albeit the *E. coli* protein) interacts with *P. aeruginosa* PBP1A, pointing to the formation of similar protein complexes in *P. aeruginosa* in addition to *E. coli.* The cloning of the *Pa*PBP2 construct would aid in identifying the effect of the *P. aeruginosa* PBP2 protein on the transglycosylase activity of *Pa*PBP1A. *E. coli* FtsN stimulates the transglycosylase activity of *Ec*PBP1B and it would be interesting to see if *Ec*FtsN stimulates the same activity is *Pa*PBP1B. There is no known FtsN protein in *P. aeruginosa* (except for in *P. fluorescens* F113), but searching the *Pseudomonas* genome by protein BLAST using the *Ec*FtsN gene sequence reveals PA5052 as the only hit, with 28 % identity. Further work to identify the affect of *Ec*FtsN/PA5052 upon the transpeptidase activity of *Pa*PBP1B would be of interest.

7.2 The Oligomeric Status of PBP1A and PBP1B *in vitro*

Kinetic properties observed with PBP1a enzymes are that at low PBP1A concentration and/or low LII substrate concentration, very little transglycosylase reaction rate is observed. Multiple factors could contribute to this observation, including PBP1A requiring a substrate 'primer', i.e. a pre-polymerised glycan chain as a substrate, preferentially to the monomer unit LII substrate. Another factor at play here is that it is possible that PBP1a forms homodimers and so therefore a minimum concentration of PBP enzyme is required (K_D) for optimum transglycosylase function. *E. coli* PBP1A and 1B have both been hypothesised to form independent homodimers *in vivo* (Bertsche, 2005; Born, 2006, Charpentier, 2002, King, 2016) with the K_D value for *Ec*PBP1B dimerisation being determined as $1.27 \pm 0.96 \times 10^{-7}$ M. That being said, the X-ray crystallography structures of *Ec*PBP1B (King, 2016; Sung, 2009) do not obviously represent a 'typical' structure conducive to dimer formation. The dimer prediction software COTH (CO-THreader), a multiple-chain protein-threading algorithm designed to identify dimer templates and recombine protein complex

structures, predicted models of potential dimer formation of *E. coli* PBP1B homodimers (**Figure 7.2**). Although such *in silico* predictions are estimated guesses only and require experimental verification and such predictions could be tested using analytical ultra-centrifugation (AUC) or dynamic light scattering (DLS) in solution.

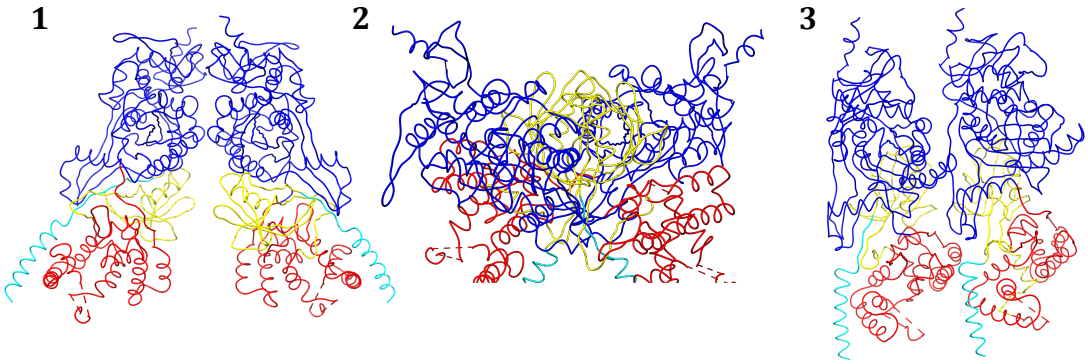

Figure 7.2 Predicted Dimer Conformations for *E. coli* PBP1B Enzymes Calculated using the COTH, models 1, 2 and 3 (Zhang *et al.*, 2011).

These models would not have the space to interact with the known interacting partners of the PBP, e.g. there does not appear to be the necessary space for interacting proteins such as *Ec*LpoB with the UB2H domain of *Ec*PBP1B.

Many proteins are homo-oligomers in solution and monomers self-associate to form non-covalently bound dimers, trimers, etc. *S. pneumoniae* PBP2a was shown to self-associate *in vitro*, TM-domain dependent (Helassa *et al*., 2012). SDS-PAGE analysis only shows the monomer because non-covalent interactions are disrupted by SDS detergent. However, dimeric *E. coli* PBP1B in particular has been observed frequently on SDS-PAGE and even more so in anti-His Western Blots (Figure 3.8). If dimers do indeed form, they are not between disulphide bridges, as potential dimers have been observed in an SDS (reducing) environment and after sample incubation with β-mercaptoethanol. It is still disputed whether PBP1A and/or PBP1B form homodimers *in vivo*, and further work is need to confirm or disprove this theory. A further investigation of enzyme concentrations either side of the published K_D for *E. coli* PBP1B with dansDAP-LII to test whether dimerisation affects cooperativity, or vice versa.

7.3 The PgpB Assay

7.3.1 Kinetic Measurements of Transglycosylation using *E. coli* PgpB

A continuous spectrophotometric assay using native LII substrate had been previously developed and optimised for use with *S. aureus* MGT and *S. pneumoniae* PBP1a by Dr. Kat Abrahams and Dr. Darren Braddick at The University of Warwick. This assay was extended for use with *Ec*PBP1B, *Ec*PBP1A and *Pa*PBP1A. The phosphatase PgpB was used to cleave the terminal phosphate from undecaprenyl pyrophosphate that was generated from the transglycosylase activity of PBPs. The native substrate of *E. coli* PgpB is undecaprenyl pyrophosphate, but diacylglycerol pyrophosphate is a preferable substrate with the K_m for UPP being 1.5-fold that for DGPP. *E. coli* PgpB was able to indirectly report the generation of undecaprenyl pyrophosphate from the capability of all three Class A enzymes to form linear glycan strands. The substrate preference between DAP- and Lys-LII was also confirmed for all three PBPs as the native, Gram-negative substrate DAP-LII. The kinetic profile of the transglycosylase activity of all three proteins were generated, giving K_m values for their affinity to DAP-LII, rather than the K_m values in Chapter 4 calculated using the continuous fluorometric assay and dansDAP-LII. The K_m values extracted from *Ec*PgpB indirectly reporting transglycosylase activity were much higher than the values defined using the continuous fluorometric assay.

7.3.2 *E. coli* PgpB Detergent Screening

Due to *E. coli* PgpB being kinetically slow in this assay, the assay conditions were altered to measure the affect of using different detergents. As ethylene glycol alkyl ether detergents were successful in the elucidation of transglycosylase activity in the continuous fluorometric assay as well as for transpeptidase activity in the continuous spectrophotometric transpeptidase assay, *E. coli* PgpB phosphatase activity was tested in the environment of these ethylene glycol alkyl ether detergents. E6C12 was found to be the optimum detergent from the series of E_xC_y range. Also, the presence and absence of $MgCl_2$ with each detergent was tested and proved that $MgCl_2$ was absolutely essential for *E. coli* PgpB activity under the conditions tested. This finding echoes and

confirms those of other who have extensively worked on *E. coli* PgpB (Touzé *et al.,* 2008).

7.3.3 Limitations of the Current PgpB Assay Protocol

The most limiting factor in this assay is the kinetic speed of *Ec*PgpB, but it has been shown that cardiolipin and phosphatidyl glycerol enhances PgpB activity (Touzé, 2008). At present, the assay set up involves a 15 µL LII polymerisation reaction, which is diluted in to a 200 µL continuous, coupled assay. The dilution of the transglycosylation product of interest (UPP) is unnecessary and could be improved. Reducing the volume of the continuous assay from 200 to 50 µL would be advantageous. Subsequently the assay format could be translated from a cuvette in to a plate-reader well, which would allow the rapid screening of a multitude of parameters and conditions optimised (NaCl, pH, inhibitors, divalent ion concentration, etc.).

7.3.3.1 The Development of a Continuous Assay

Importantly, given that the transglycosylase activity of the Class A PBPs has shown to be substantial and sufficient, and that *Ec*PgpB expresses well, this assay has the potential to measure transglycosylation continuously. Attempts and observing a continuous rate were trialled but no rate was observed. As the focus of this study with PgpB was on *E. coli* PBP1A and *P. aeruginosa* PBP1A and these PBPs are known to prefer a primer substrate for transglycosylase activity to reach steady-state kinetics, adding something to the assay that stimulates the transglycosylase activity of PBP1A or that aids in the formation of a oligosaccharide primer substrate, would be extremely advantageous in the advancing of this assay towards a continuous rate of simultaneous transglycosylation and phosphatase activity.

7.4 No Activity Observed of *P. aeruginosa* PBP1B

Thus far, an in-frame construct of *Pa*PBP1B (W^{23}-N^{744}) was successfully cloned, expressed well in C43(DE3) *E. coli* cells, and purified in high quantities to a high purity by IMAC. The protein was shown to positively bind the BOCILLIN FL™ and also indicated correct folding by circular dichroism. Nonetheless this particular construct did

not show sufficient transglycosylase or transpeptidase activity in any conditions tested. Engineering an active *Pa*PBP1B construct would be of use to compare such interactions between *P. aeruginosa* and *E. coli* as well as define values for kinetic constants for *Pa*PBP1B, which have not been published thus far. If transglycosylase activity could be observed for *Pa*PBP1B, it would be interesting to test the effect of the Lpo lipoproteins on the transglycosylase and transpeptidase activities of this enzyme, however, there is no known LpoB homologue protein in *P. aeruginosa* at present.

7.4.1 The Lack of LpoB in *P. aeruginosa*

Due to the *P. aeruginosa* genome lacking a gene for LpoB, a 'pull-down' experiment was planned in the quest to search for the equivalent protein in *Pseudomonas aeruginosa*. An experiment to seek for a potential LpoB-like protein in *P. aeruginosa* could involve using cyanogen bromide (CNBr) resin to which PaPBP1B would bind and act as the 'bait' protein. Positive control proteins include *Pa*PBP3 and *Pa*YbgF, which are both known to bind to PBP1B. Also the putative FtsN homologue PA5052 is likely to positively bind to PBP1B as does FtsN to PBP1B in *E. coli*, if it is a true homologue of FtsN. Negative controls could include the proteins *Pa*PBP1A, *Pa*LpoA and FtsZ. In the hunt for a new binding partner, exploratory fractions to pass over the *Pa*PBP1B-resin could include *P. aeruginosa* membranes and the isolated *P. aeruginosa* periplasm, as this is where LpoB resides in *E. coli*.

7.5 The FRET Transpeptidase Assay

Four compounds were synthesised, three with mass spectrometry confirmation while Fluorescamine-labelled LII although did not ionise readily for detection in mass spectrometry, the compound was polymerised by *E. coli* PBP1B, with the fluorescence emission wavelength measured for that of fluorescamine (470 nm) (Figure 5.22). The synthesised transpeptidase acceptor compounds were both confirmed as functional transpeptidase acceptors in the continuous, coupled spectrophotometric D-Ala release assay.

Lys-LII was shown to act as a transpeptidase donor and all three synthesised transpeptidase acceptors were capable acceptors when using both Lys-LII and DAP-LII

as the transpeptidase donor. DansDAP LII was also able to function as a transpeptidase donor, as well as all three compounds being positive for transpeptidase acceptor ability. The other transpeptidase donor compound (Fluorescamine-labelled LII) was confirmed to be able to function as a transpeptidase donor with all three acceptor compounds.

The FRET assay to elucidate transpeptidase activity was trialled using fluorescamine-labelled LII as the transpeptidase donor and Mur*N*Ac-L-Ala-D-Glu-*meso*DAP-D-azatryptopthan-L-Ala as the transpeptidase acceptor peptide. The results observed were similar to those observed during a continuous fluorometric transglycosylation reaction, i.e. a steady decrease in fluorescence over time. The fluorescamine-labelled LII was likely being polymerised, but in the FRET assay conditions, there was no muramidase present like in a traditional transglycosylation-monitoring assay. Further optimisation of this technique and the relevant controls are required to progress this assay to be able to visualise a true FRET event between FRET fluorophore donor and acceptor.

7.6 The Continuous Transpeptidation D-Ala Release Assay

This is the first conclusive evidence of the continuous visualisation of transpeptidase activity *in vitro*, of PBP1A from *E. coli* and *P. aeruginosa*. There are multi-drug resistant (MDR) *P. aeruginosa* isolates that are resistant to β-lactams due to alteration of their PBP transpeptidase active site. Understanding the intricacies of the transpeptidase mechanism has been a persistent biochemical question towards which this assay can contribute solutions.

This assay was shown to be substrate-dependent as well as enzyme-dependent and also demonstrated sensitivity to the inhibitors moenomycin and ampicillin. The assay reagents were shown not to disrupt the coupling system. The initial lag-phase observed in these assays is a running feature throughout Class A PBP kinetics, especially with PBP1A, with it having a definite preference for polymeric LII glycan chains as its substrate.

The final reaction rate observed in this assay is a result of simultaneous DD-carboxypeptidation and transpeptidation. The rate of DD-carboxypeptidation was measured upon the addition of the PBP, prior to the addition of acceptor, generating a

rate comprising of both transpeptidation and DD-carboxypeptidation, combined with the rate of transpeptidation able to be calculated by subtracting the initial DD-carboxypeptidase rate away from the final reaction rate.

The assay buffer used for transpeptidase activity did not contain NaCl or DMSO, like the assay buffer for the continuous fluorometric transglycosylase assay buffer. The transglycosylase activity of PBP1A in transpeptidase assay buffer, using the continuous fluorometric transglycosylase assay to determine activity, should be considered. However, as transglycosylation precedes transpeptidation, the PBP present in the transpeptidase assay is conducting transglycosylation and transpeptidation concurrently and this would not occur if the PBP was unstable in the buffer selected for transpeptidase activity. Nevertheless the transpeptidase assay buffer should be tested in a continuous transglycosylase format to confirm this further. Also, the assay buffer used for transglycosylation (the discontinuous part) of the PgpB assay is slightly different again (20 mM Tris.HCl pH 7.6 and 10 mM $MgCl_2$, with the LII resuspended in 0.1 % DDM and the *Ec*PgpB delivered in DDM). With confirmation that both *P. aeruginosa* and *E. coli* PBP1A perform transglycosylation in a few different yet specific buffer conditions, it is likely that continuous transglycosylase activity can be observed in the transpeptidase assay buffer.

7.7 Thesis Summary

This project involved the biochemical characterisation of the membrane-associated PBPs that mediate resistance to the β-lactam class of antibiotics. A number of published assays are limited in some way whether they are qualitative, discontinuous or use modified (fluorescently tagged or radiolabelled) substrate. The major component of this project was assay development for enzymatic characterisation of Class A PBPs. Two assays for transglycosylation and two for transpeptidation were developed and optimised using *P. aeruginosa* PBP1A and *E. coli* PBP1A. Kinetic characterisations of both activities of bifunctional *Pa*PBP1A and *Ec*PBP1A were performed and assay conditions optimised to emulate the environment *in vivo*.

A previously published fluorescence assay to continuously monitor transglycosylation (Schwartz *et al.*, 2002) was developed and optimised for characterisation of the PBP1A

enzymes. The substrate-enzyme interactions involved are paramount in elucidating the full mechanism of peptidoglycan biosynthesis and aiding in the search for new antimicrobials. Both enzymes showed preference for DAP LII over Lys-LII and also demonstrated preference for the non-native C_{35} prenyl chain length over C_{55}. *Ec*PBP1A and *Pa*PBP1A transglycosylase kinetic data fitted for readily to a non-Michaelis-Menten equation that accounts for two substrates: a donor substrate and an acceptor substrate. *Ec*PBP1A was used as a control enzyme to compare *Pa*PBP1A transglycosylase activity, which appeared to behave in the same manner as *Ec*PBP1A *Ec*PBP2 and *Ec*FtsN were shown to stimulate the activity of *Pa*PBP1A, pointing to the formation of protein complexes in *P. aeruginosa*, similar to those in *E. coli*.

Transglycosylase assay of native substrates was the first time developed for Gram-negatives. The coupled spectrophotometric assay for transglycosylation using the phosphatase PgpB that is discontinuous, but uses native LII. This spectrophotometric assay was optimised to study the enzymology of transglycosylase activity of the PBPs with their natural substrate, LII.

A FRET assay was developed to show transpeptidation, in which novel donor and acceptor transpeptidase compounds were synthesised. Non-canonical dipeptides were incorporated at the terminus of the pentapeptide stem, demonstrating flexible promiscuity of the MurF ligase.

A novel spectrophotometric transpeptidase assay generated continuous data of transpeptidation and this thesis has the first illustration of continuously-monitored PBP1A transpeptidase activity. *Ec*PBP1A and *Pa*PBP1A demonstrated transglycosylase and transpeptidase activity in both TritonX-100 and CHAPS PBPs showed transglycosylase activity and transpeptidase activities with a range of structurally different substrates. *Ec*PBP1A was able to utilise a variety of transpeptidase acceptor compounds. *Pa*LpoA was shown to stimulate *Pa*PBP1A transpeptidase activity, like *Ec*LpoA stimulates *Ec*PBP1A.

Active-site mutants of transglycosylase and transpeptidase inactive domains did not enhance the functionality of the active domain. TP active-site mutants still underwent transglycosylation but transglycosylation mutants did not perform transpeptidation.

*Pa*PBP1A transglycosylase and transpeptidase active-site mutants were made and showed a lack of activity.

*Pa*PBP1A and *Ec*PBP1A were both subjected to crystal trials for structural characterisation. *Pa*PBP1B activity was not detected at a level necessary to kinetically characterise the enzyme and it is possible that this PBP has an as yet undetermined stimulatory cofactor.

Appendix 1

A table of oligos for gene synthesis or site-directed mutagenesis. Bases highlighted in bold are the restriction sites in the primers for gene synthesis and highlight the mutated codon in mutagenic primers. All sequences are 5' → 3'.

E. coli PBP1B 58-804	TTT GCG **CAT ATG** AAG CCT CGT GGC AAA CGC GGC TGG CTA TGG CTA CTG CTG TGC **CAG CAG** AGC GAG ATG CAG CAG CAG CCG TCA TAA TTT GGG GGA TCC TTA TGA CGG CTG CTG CTG CAT CTC GCT CTG CTG GCA CAG
E. coli PBP 1A (Full-length)	GCG TTT GCG **CAT ATG** ATG AAA CTA AAT GGG AAA TTT CCA GTG AAG TTC GTA AAG CGC TTT GCG **GCG GCC GC** TCA GAA CAA TTC CTG TGC CTC GCC ATT ATC GAT AAT
Pseudomonas aeruginosa PBP 1A (Full-length)	GCG TTT GCG **CAT ATG** ATG CGC CTG CTG AAG TTC CTG TGG TGG ACT TGC GTC ACC GCG TTT GCG **GCG GCC GC** TCA GAA CAG GTC GAT CGG CGC GCC TTC GTC ATC CGG
E. coli PBP1B TG Active Site Mutant: E233Q	ACT TTG CTG GCG ACA **CAG** GAC CGT CAT TTT TAC GTA AAA ATG ACG GTC **CTG** TGT CGC CAG CAA AGT
E. coli PBP1B TP Active Site Mutant: S510A	CGT CGT TCG ATT GGT **GCG** CTT GCA AAA CCA GCG CGC TGG TTT TGC AAG **CGC** ACC AAT CGA ACG ACG
E. coli PBP1A TG Active Site mutant: E94Q	AGC CTT TAT CGC GAC ACA AGA **CAG** CCG CTT CTA CG TCG TAG AAG CGG **CTG** TCT TGT GTC GCG ATA AAG GC
E. coli PBP1A TP Active Site mutant:S473A	TG CGT CAG GTG GGT **GCC** AAC ATC AAA CCG TTC C AA CGG TTT GAT GTT **GGC** ACC CAC CTG ACG CAG TGC
PaPBP1B TG Active site mutant E190Q	ACC CTG GTC GCG GTC **CAG** GAT CGC GAC TTC TGG CCA GAA GTC GCG ATC **CTG** GAC CGC GAC CAG GGT
PaPBP1B TP Active site mutant S468A	GTG CGG CCG ATC GGT **GCC** CTG ATC AAG CCG GCG CGC CGG CTT GAT CAG **GGC** ACC GAT CGG CCG CAC

PaPBP1A TG Active site mutant: E86Q	GCC CTG CTG TCC GCC **CAG** GAC GAC AAT TTC GCC GGC GAA ATT GTC GTC **CTG** GGC GGA CAG CAG GGC
PaPBP1A TP Active site mutant S461A	AAG CGC CAG CCG GGC **GCC** AGT TTC AAG CCG TTC GAA CGG CTT GAA ACT **GGC** GCC CGG CTG GCG CTT
Pseudomonas aeruginosa PBP 1B (W23 – N775)	GCG TTT GCG **CAT ATG** TGG CTC AGC TGG GCT CTC AAG CTC GGC CTC GTC GGC CTG GCG TTT GCG **GCG GCC GC** TCA ATT CAG CCA GCC ACG TAC CCA GTC CAT CAC CTC
PaPBP1B *P. putida* expression plasmid pVZ101	TTT GCG **AAG CTT** TAA GGA GGT TCT TGA ATG GAC CCG TCC GCG CTC TCC GCG TTC TCG TTT GCG **TCT AGA** TCA ATG ATG ATG ATG ATG ATG ATT CAG CCA ACC ACG AAC CCA GTC CAT
E. coli PBP3 (Full length gene)	5′ TTT CG**G GAT CC**T ATG AAA GCA GCG GCG AAA ACG CAG AAA CCA AAA CGT 3′ 5′ TTT GCG **GAG CTC** TTA CGA TCT GCC ACC TGT CCC CTC GCC TTG ATT AAT 3′
E. coli PBP3 (no N-terminal TM domain) from AA W44.	5′ TTT CG**G GAT CC**T TGG TTA CAA GTT ATC TCC CCG GAT ATG CTG GTG AAA 3′ End primer is the same as the full-length gene
*Pa*LpoA	5′ TTT GCG **CAT ATG** GCG ACC TCG TCC AAT TCC GGA CTG GGC GAA CTT CCC 3′ 5′ TTT GCG **GCG GCC GC** TCA AAA GCT GCT GGT CCC CAG CGG CTG GAC CTG GCC 3′
P. aeruginosa PBP3 (Full length gene)	5′ TTT CG**G GAT CC**T ATG AAA CTG AAT TAT TTC CAG GGC GCC CTC TAC CCA 3′ 5′ TTT GCG **GAG CTC** TCA GCC ACG CCC TCC TTT TGC GGG CGC AGC ATT GAC 3′
P. aeruginosa PBP3 (no N-terminal TM domain) from A35	5′ TTT CG**G GAT CC**T GAC CTG CAC GTG ATC GAC CAT GAC TTC CTC AAG GGC 3′ End primer is the same as the full-length gene

Appendix 2

The percentages and concentrations of each detergent used in extraction (solubilisation) and purification of PBPs.

		Extraction		Purification	
Detergent	**Detergent CMC**	**% Detergent used**	**mM Detergent used**	**% Detergent used**	**mM Detergent used**
CHAPS	0.49 % / 6-10 mM	0.15 %	1.5 mM	0.15 %	1.5 mM
DDM	0.0087 % / 0.12-0.3 mM	0.04 %	0.75 mM	0.03 %	0.5 mM
LDAO	0.023 % / 0.14-1 mM	0.07 %	2.5 mM	0.06 %	2 mM
TritonX-100	0.02 % / 0.2-0.25 mM	1 %	N/D	0.2 %	N/D

Appendix 3 : Derivation of the 'dual substrate' Equation

Introducing a Kinetic Model for Two transglycosylation substrates, a donor and an acceptor, both of which are LII.

The derivation of kinetics for a two-substrate system, which takes into account the participation of a donor and acceptor where both are LII. A K_m for both the donor and acceptor are derived here, K_{mA} and K_{mB}.

$$[E] + [S] \underset{}{\overset{K_{mA}}{\rightleftharpoons}} [ES] \underset{- [S]}{\overset{K_{mB} + [S]}{\rightleftharpoons}} [ES_2] \xrightarrow{K_{cat}} [E] + [P]$$

The change in rate of product formation over time is equivalent to the initial rate of reaction (v_0):

(1) $$\frac{dP}{dt} = v_0 = K_{cat}\,[ES_2]$$

When all of the substrate is bound to the total available amount of enzyme $[E_T]$, $[ES_2] = [E_T]$. All the catalytic sites are saturated with substrate and V_{max} can be defined as:

(2) $$V_{max} = K_{cat}\,[E_T]$$

The two kinetic constants for transglycosylase donor and transglycosylase acceptor can be derived as:

(3a) $$K_{mA} = \frac{[E][S]}{[ES]}$$ **(3b)** $$K_{mB} = \frac{[ES][S]}{[ES_2]}$$

The total concentration of enzyme in the system is the sum of all bound and unbound catalytic sites and can be defined as:

(4) $$[E_T] = [E] + [ES] + [ES_2]$$

The terms in equation (4) can be written to define [E] in terms of [ES], and [ES] in terms of $[ES_2]$:

$$[E] = \frac{K_{mA}\,[ES]}{[S]} \qquad [ES] = \frac{K_{mB}\,[ES_2]}{[S]}$$

Substituting [ES] in to [E], gives:

$$[E] = \frac{K_{mA}\left(\frac{K_{mB}\,[ES_2]}{[S]}\right)}{[S]}$$

$$[E] = \frac{K_{mA}\, K_{mB}\, [ES_2]}{[S]^2}$$

Substituting the above equations in to equation 4, describes $[E_T]$ in terms of the kinetic constants [S] and $[ES_2]$.

(5) $$[E_T] = \frac{K_{mA}\, K_{mB}\, [ES]\, [ES_2]}{[S]^2} + \frac{K_{mB}\, [ES_2]}{[S]} + [ES_2]$$

(6) $$[E_T] = [ES_2] \left(\frac{K_{mA}\, K_{mB}}{[S]^2} + \frac{K_{mB}}{[S]} + 1 \right)$$

Multiply by K_{cat}:

(7) $$K_{cat}\, [E_T] = K_{cat}\, [ES_2] \left(\frac{K_{mA}\, K_{mB}}{[S]^2} + \frac{K_{mB}}{[S]} + 1 \right)$$

Substituting equation (1) for V_0 and equation (2) for V_{max} in to (7), gives:

(8) $$V_{max} = V_0 \left(\frac{K_{mA}\, K_{mB}}{[S]^2} + \frac{K_{mB}}{[S]} + 1 \right)$$

Rearrange (8) to make V_0 the subject:

(9) $$v_0 = \frac{V_{max}}{\left(\frac{K_{mA}\, K_{mB}}{[S]^2} + \frac{K_{mB}}{[S]} + 1 \right)}$$

(10) $$V_0 = \frac{V_{max}\, [S]^2}{K_{mA}\, K_{mB} + K_{mB}\, [S] + [S]^2}$$

Thesis Bibliography

Adam, M., Damblon, C., Jamin, M., Zorzi, W., Dusart, V., Galleni, M., el Kharroubi, A., Piras, G., Spratt, B. G., Keck, W. *et al*., (1991) Acyltransferase activities of the high-molecular mass essential penicillin binding proteins. *Biochem J.* **15** (279-Pt 2) pp601-4

Arenz, S. & Wilson, D. N. (2016) Bacterial Protein Synthesis as a Target for Antibiotic Inhibition. *Cold Spring Harb Perspect Med* **6**(9): pii: a025361

Babu, M. (2011) Genetic interaction maps in *Escherichia coli* reveal functional crosstalk among cell envelope biogenesis pathways. *PLoS Genet.* **7** e1002377

Bagga, S. (2004) Development of Fluorescence Assays for lipid-linked steps of Bacterial Peptidoglycan Biosynthesis, PhD Thesis, The University of Warwick.

Barreteau, H., Kovac, A., Boniface, A., Sova, M., Gobec, S. and Blanot, D. (2008) Cytoplasmic steps of peptidoglycan biosynthesis *FEMS Microbiol Rev* **32**: 168-207

Barrett, D., Wang, T. S., Yuan, Y., Zhang, Y., Kahne, D., Walker, S. (2007) Analysis of glycan polymers produced by peptidoglycan glycosyltransferases, *journal of Biological Chemistry* **282**(44)pp31964

Banzhaf, M, Cooperativity of peptidoglycan synthases active in bacterial cell elongation. *Mol Microbiol*, 2012. *85*(1): *p. 179*-194.

Batson, S. (2010). Structural enzymology of peptidoglycan biosynthetic D-amino acid dipeptide ligases. Unpublished Ph.D., University of Warwick.

Berezin, M. Y. and Achilefu, S. (2010) Fluorescence Lifetime Measurements and Biological *Imaging Chem Rev* 110 (5) 2641-2684

Bertsche, U., Kast, T., Wolf, B., Fraipont, C., Aarsman, M. E., Kannenberg, K., von Rechenberg, M., Nguyen-Disteche, M., den Blaauwen, T., Holtje, J. V., Vollmer, W. (2006) Interaction between two murein (peptidoglycan) synthases, PBP3 and PBP1B, in *Escherichia coli*. *Mol Microbiol*, *61*, 675.

Biboy, J., Bui, N. K., Vollmer, W. (2013) In Vitro Peptidoglycan Synthesis Assay with Lipid II Substrate Anne H. Delcour (ed.), *Bacterial Cell Surfaces: Methods and Protocols,* Methods in Molecular Biology, vol. **966**, Springer Science New York.

Bickford, J. S. Nick, H. S. Conservation of the PTEN catalytic motif in the bacterial undecaprenyl pyrophosphate phosphatase, BacA/UppP (2013) *Microbiology* **159** 2444-2455

Born P, Breukink E, Vollmer W. (2006) *In vitro* synthesis of cross-linked murein and its attachment to sacculi by PBP1A from *Escherichia coli. J. Biol. Chem*. 281:26985-93

Breukink, E., van Heusden, H. E., Vollmerhaus, P. J., Swiezewska, E., Brunner, L., (2003) Lipid II is an intrinsic component of the pore induced by nisin in bacterial membranes.

Brooks, G. Edwards, P. D., Hatto, J. D. I. Smale, T. C. Southgate, R. (1995) Synthesis of Derivatives of Muramic Acid and C-1 Homologated a-D-Glucose as Potential Inhibitors of Bacterial Transglycosylase. *Tetrahedron* 51, 7999-8014

Broome-Smith, J. K. Edelman, A., Yousif, S, Spratt, BG *et al.*, (1985) The nucleotide-sequences of the ponA and ponB gene encoding penicillin-binding protein 1A and 1B of *Escherichia coli. The European Journal of biochemistry* **14***7*, 437-446.

Brotz, H., Bierbaum, G., Reynolds, P.E. and Sahl, H. G. (1997) The lantibiotic mersacidin inhibits peptidoglycan biosynthesis at the level of transglycosylation. *Eur J Biochem* **246** 193-199

Brown, E. D. & Wright G. D. (2016) Antibacterial Drug Discovery in the Resistance Era *Nature Rev* **529** p336-343

Brown, E. D. and Wright, G. D. (2005) New Targets and Screening Approaches in Antimicrobial drug discovery *Chem Rev* **105** p759-774

Bugg, T. D. H. **(1999)** Bacterial peptidoglycan biosynthesis and its inhibition. *Comprehensive Natural Products Chemistry* **3** P41-294

Bury, D., Dahmane, I., Derouaux, A., Dumbre, S., Herdewijn, P., Matagne, A.,Breukink, E., Mueller-Seitz, E., Petz, M., and Terrak, M., (2015). Positive Cooperativity Between Acceptor and Donor Sites of the Peptidoglycan Glycosyltransferase. *Biochemical Pharmacology* **93** (2): 141–150.

Butaye, P., Devriese, L. A., Haesebrouck, F. (2003) Antimicrobial growth promoters used in animal feed: effects of less well known antibiotics on gram-positive bacteria *Clin Microbiol Rev* **16** p175

Center for Disease Control and Prevention. Emerging Infections Program Network Active Bacterial Core Surveillance Report: Methicillin-Resistant *Staphylococcus aureus*. (2014):1-3

Chang, H.-Y., Chou, C.-C., Hsu, M.-F. and Wang, A. H. J. (2014) Proposed Carrier Lipid-binding Site of Undecaprenyl Pyrophosphate Phosphatase from *Escherichia coli. Journal of Biological Chemistry* **289** p18719-18735

Charpentier, X., Chalut, C., Remy, M.-H., Masson, J.-M. (2002) Penicillin-Binding Proteins 1a and 1b Form Independent Dimers in *Escherichia coli J. Bacteriol.* **184** (13) 3749-3752

Chen, W., Zhang, Y.-M. Davies, C (2017) Penicillin-Binding Protein 3 is essential for Growth of *Pseudomonas aeruginosa. Antimicrobial Agents and Chemotherapy* **61**(1) e01651-16

Chen, R. F., Smith, P. D., Maly, M. (1978) The fluorescence of fluorescamine-amino acids *Archives of Biochemistry and Biophysics* **189**(2) p241-250

Cheng, T-J. R., Sung, M-T., Liao, H-Y., Chang, Y-F., Chen, C-W., Huang, C-Y., Chou, L-Y., Wu, Y. D., Chen, Y. H., Cheng, Y. S., Wong, C. H., Ma, C., Cheng, W.C., (2008). Domain Requirements of Moenomycin Binding to Bifunctional Transglycosylases and Development of High-Throughput Discovery of Antibiotics. *Proc Natl Acad Sci* USA **105** (2): 431–436.

Cho, H., Wivagg, C. N., Kapoor, M., Barry, Z., Rohs, P. D., Suh, H., Marto, J. A., Garner, E. C., Bernhardt, T. G. (2016) Bacterial cell wall biogenesis is mediated by SEDS and PBPs polymerase families functioning semi-autonomously *Nat Microbiol* **1**:16172

Corry, B., Jayatilaka, D. and Rigby, P. (2005) A Flexible Approach to the Calculation of Resonance Energy Transfer Efficiency between Multiple Donors and Acceptors in Complex Geometries, *J. Biophys.* 89(6) p3822-3836

Cox, G., Sieron, A., King, A. M., De Pascale, G., Pawlowski, A. C., Koteva, K., Wright, G. D. (2017) A Common Platform for Antibiotic Dereplication and Adjuvant Discovery *Cell Chem Biol* **24**(1) 98-109

Culp, E. & Wright G (2016) Bacterial proteases, untapped antimicrobial drug targets *The Journal of Antibiotics 1-12*

Daub, E., Zawadzke, L. E., Botstein, D., and Walsh, C. T. (1988) Isolation, cloning, and sequencing of the Salmonella typhimurium ddlA gene with purification and characterization of its product, D-alanine: o-aianine ligase (ADP forming). *Biochemistry* **27**.3701-3708.

Davies, T. A., Shang, W., Bush, K. & Flamm, R. K. (2008). Affinity of doripenem and comparators to penicillin-binding proteins in *Escherichia coli* and *Pseudomonas aeruginosa. Antimicrob. Agents Chemother*.**52**, 1510–1512.

De Bernardo, S., Weigele, M., Toome, V., Manhart, K., Leimgruber, W., Bohlen, P., Stein, S., Undenfriend, S. (1974) Studies on the reaction of fluorescamine with primary amines Archives of Biochemistry and Biophysics **163** (1) p390-399

Delcour, A. H. (2009) Outer membrane Permeability and Antibiotic Resistance *Biochem Biophys Acta* **1794**(5) 808-816

Derouaux, A. Sauvage, E. Terrak, M. (2013**)** Peptidoglycan glycosyltransferase substrate mimics as templates for the design of new antibacterial drugs. *Front Immunol***. 4** p78

Derouaux, A. & Terrak, M. (2008) The monofunctional glycosyltransferase of *E. coli* localises to the cell Division site and interacts with PBP3, and FtsN, *J. Bacteriol* **190**(5) 1831-4

Dumbre, S. Derouaux, A. Lescrinier, E., Piette, A., Joris, B., Terrak, M. and Herdewijn, P. (2012) Synthesis of modified peptidoglycan precursor analogues for the inhibition of glycosyltransferase. *J. Am. Chem. Soc.* **134** 9343–9351

Egan A.J.F., Jean, NL, Koumoutsi, A., Bougault, C. M., Biboy, J., Sassine, J., Solovyovar, A. S. Breukink, E., Typas, A., Vollmer W. (2014) Outer-membrane lipoprotein spans the periplasm to stimulate the peptidoglycan synthase PBP1B *PNAS* **111**(22) pp8197-8202

Egan, A. J.; Vollmer, W. (2013) The physiology of bacterial cell division. *Annals of the New York Academy of Sciences*, *1277*, 8.

El-Abadla, N., Lampilas, M., Hennig, L., Findeisen, M., Welzel, P., Müller, D., Markus, A., van Heijenoort, J. (1999) Moenomycin A: The Role of the Methyl Group in the Moenuronamide Unit and a General Discussion of Structure-Activity Relationships *Tetrahedron* **55** p699

El Ghachi, M., Bouhss, A., Blanot D., Mengin-Lecreulx D. (2004) The bacA gene of *Escherichia coli* encodes an undecaprenyl pyrophosphate phosphatase activity. *J Biol Chem* **279** (29) p30106

El Ghachi, M., Derbise, A., Bouhss, A., and Mengin-Lecreulx, D. (2005) Identification of multiple genes encoding membrane proteins with undecaprenyl pyrophosphate phosphatase (UppP) activity in *Escherichia coli. J. Biol. Chem*. **280**, 18689–18695

Fagerberg L, Jonasson K, von Heijne G, Uhlen M, Berglund L (2010) Prediction of the human membrane proteome. *Proteomics* 10: 1141-1149

Farha, M.A. & E.D. Brown. 2013. Discovery of antibiotic adjuvants. *Nat. Biotechnol.* **31**: 120–122.

Fan, J., Jiang, D., Zhao, Y., Liu, J., Zhang, X. C. (2014) Crystal Structure of lipid phosphatase *Escherichia coli* phosphatidylglycerophosphate phosphatase B *PNAS* **111** p7636-40

Fournier, B., Zhao, X., Lu, T., Drlica, K. and Hooper, D. C. (2000) Selective Targeting of Topoisomerase IV and DNA gyrase in Staphylococcus aureus: Different Patterns of Quinolone-Induced Inhibition of DNA Synthesis *Antimicrob Agents Chemother* **44**(8) pp2160-65

Fragneto, G., Lu, J. R., McDermott, D. C. and Thomas, R. K. (1996) Structure of Monolayers of Tetraethylene Glycol Monododecyl Ether Adsorbed on Self-Assembled Monolayers on Silicon: A Neutron Reflectivity Study *Langmuir*, **12**(2) pp477–486

Fraipont, C., Alexeeva, S., Wolf, B., van der Ploeg, R., Schloesser, M., den Blaauwen, T. and Nguyen-Disteche, M. (2011) The integral membrane FtsW protein and peptidoglycan synthase PBP3 from a subcomplex in *E. coli*. *Microbiology* **157** (Pt 1) pp251-259.

Funk, C. R., Zimniak, L. and Dowhan, W. (1992) The pgpA and pgpB genes of *Escherichia coli* are not essential: evidence for a third phosphatidylglycerophosphate phosphatase. *J. Bacteriol* **174** p205-213

Fuse, S., Tsukamoto, H., Yuan, Y., Wang, T.-S. A., Zhang, Y., Bolla, M., Walker, S., Sliz, P. and Kahne, D. (2010) Functional and Structural Analysis of a Key region of the cell wall inhibitor Moenomycin ACS Chem Biol **5**(7) pp701-711

Gampe, C. M., Tsukamoto, H., Wang, T. S., Walker, S., Kahne, D. (2011) Modular synthesis of diphospholipid oligosaccharide fragments of the bacterial cell wall and their use to study the mechanism of moenomycin and other antibiotics Tetrahedron **67**(51) pp 9771-9778

Gampe, C. M., Tsukamoto, H., Doud, E. H., Walker, S., and Kahne, D., (2013). Tuning the Moenomycin Pharmacophore to Enable Discovery of Bacterial Cell Wall Synthesis Inhibitors. *Journal of the American Chemical Society* **135** (10): 3776–3779.

Garneau, s. L. Qiao, L. Chen, S. Walker, J.C. Vederas, (2004) Synthesis of mono- and disaccharide analogs of moenomycin and lipid II for inhibition of transglycosylase activity of penicillin-binding protein 1b. *Bioorg. Med. Chem.* **12** 6473–6494

Ghuysen, J.-M. (1991) Serine β-Lactamases and penicillin-binding proteins *Annu. Rev. Microbiol.* **45**: 37-67

Godfrey, A. J., Bryan, L. E. & Rabin, H. R. (1981). Beta-lactam-resistant Pseudomonas aeruginosa with modified penicillin-binding proteins emerging during cystic fibrosis treatment. *Antimicrob. Agents Chemother*. **19**, 705–711.

Goffin, C. & Ghuysen, J. M. (1998) Multimodular penicillin-binding proteins: an enigmatic family of orthologs and paralogs *Microbiol Mol Biol Rev* **62**(4) 1079-93

Goffin, C. & Ghuysen, J. M. (2002) Biochemistry and comparative genomics of SxxK superfamily acyltransferases offer a clue to the mycobacterial paradox: presence of penicillin-susceptible target proteins versus lack of efficiency of penicillin as therapeutic agent. *Microbiol Mol Biol Rev* **66**(4) 702-738

Goldman, R. C. & Grange D (2000) Inhibition of transglycosylation involved in bacterial peptidoglycan synthesis *Curr Med Chem* **7**(8) 801-820

Gotoh, N., Nunomura, K. & Nishino, T. (1990). Resistance of *Pseudomonas aeruginosa* to cefsulodin: modification of penicillin-binding protein 3 and mapping of its chromosomal gene. *J. Antimicrob. Chemother*. **25**, 513–523.

Grandchamps, J., Nguyen-Disteche, M., Damblon, C., Frere, J. M., Ghuysen J.M. (1995) Streptomyces K15 active-site serine DD-transpeptidase: specificity profile for peptide, thiol ester and ester carbonyl donors and pathways of the transfer reactions *Biochem J* **307** Pt 2 p335-9.

Gray, A. N., Egan, A. J. F., van't Veer, I. L., Verheul, J., Colavin, A., Koumoutsi, A., Biboy, J., Altelaar, M. A. F., Damen, M. J., Huang, K. C., Simorre, J.-P., Breukink, E., den Blaauwen, T., Typas, A. Gross, C. A., Vollmer, W. (2015) Coordination of peptidoglycan synthesis and outer membrane constriction during *Escherichia coli* cell division *ELife* **7**(4) e07118

Halliday, J., McKeveney, D, M., Muldoon, C., Rajaratnam, P. and Meutermans, E. (2006) Targeting the forgotten transglycosylases *Biochem Pharmacol* **17**(7) p957-67

Han, S.; Caspers, N.; Zaniewski, R. P.; Lacey, B. M.; Tomaras, A. P.; Feng, X.; Geoghegan, K. F.; Shanmugasundaram, V. (2011) Distinctive attributes of β-lactam target proteins in Acinetobacter baumannii relevant to development of new antibiotics. *J. Am. Chem. Soc.* **133**, pp20536−20545.

Hancock, R. E. W. & Speert, D. P. (2000) Antibiotic Resistance in *Pseudomonas aeruginosa:* mechanisms and impact on treatment. Drug Resist Update **3**(4) p247-255

Healy, V. L., Lessard, I. A. D., Roper, D. I., Knox, J., and Walsh, C., (2000).Vancomycin Resistance in Enterococci: Reprogramming of the D-Ala-D-Ala Ligases in Bacterial Peptidoglycan Biosynthesis. *Chemistry & Biology* **7** (5): 109–119.

Hecker, S. J, Minich, M. L., Lackey, K. (1990) Synth Synthesis of compounds designed to inhibit bacterial cell wall transglycosylation. *J. Org Chem*. **55**(16) p4902-4911

van Heijenoort, Y., Derrien, M. and Van Heijenoort, J. (1978) Polymerisation by transglycosylation in the biosynthesis of the peptidoglycan of *Escherichia coli* K12 and its inhibition by antibiotics. *FEBS Letters* **89** pp141–144.

Helassa, N., Vollmer, W., Breukink, E., Vernet, T. and Zapun, A. (2012) The membrane anchor of penicillin-binding protein PBP2a from *Streptococcus pneumoniae* influences peptidoglycan chain length *The FEBS Journal* **279** p2071

Huang, C. Y., Shih, H. W., Lin, L. Y., Tien, Y. W., Cheng, W. C., Wong, C. H. and Ma, C. (2012) Crystal structure of *Staphylococcus aureus* transglycosylase in complex with a lipid II analogue and elucidation of peptidoglycan synthesis mechanism. *PNAS* **109** p6496

Jameson, D. M. and Reinhart, G. D. (2012) Fluorescent biomolecukes: Methodologies and Applications Springer Science & Business Media p75-77

Jean, NL, Bougault, CM, Lodge, A, Derouaux, A, Callens, G., Egan, AJ, Ayala, I, Lewis RJ, Vollmer W, Simorre, JP (2014) Elongated Structure of the outer-membrane activator peptidoglycan synthesis LpoA: Implications for PBP1A Structure. *Structure* **22**(7) 1047-54

Jha, R. K. and de Sousa, S. M. (2006) Microplate assay for inhibitors of the transpeptidase activity of PBP1B of *Escherichia coli*. *J. Biomol Screen* **11** (8) p1005-14.

Johnson, J. W., Fisher, J. F., Mobashery, S (2013) Bacterial Cell Wall Recycling *Annual New York Academy Sciences* **1277** p54-75

Jones DT. (1999) Protein secondary structure prediction based on position-specific scoring matrices. J. Mol. Biol. 292: 195-202.

Kempin, U., Hennig, L., Welzel, P., Marzian, S., Müller, D., Fehlhaber, H.-W., Markus, A., van Heijenoort, Y. and van Heijenoort, J. (1995) Introduction of a terminal hydroxyl group into the lipid part of a moenomycin-type transglycosylase inhibitor suppresses antibiotic activity *Tetrahedron* **51** p8471

Kim, J., Kin., H., Park, S. B., (2014) Privileged structures: efficient chemical 'navigators' toward unexplored biologically relevant chemical spaces *J Am Chem Soc* **136** 14629-14638

King, D. T., Wasney, G. A., Nosella, M., Fong, A. Strynadka, N. (2016) *Escherichia coli* Penicillin-Binding Protein 1B: Structural Insights into Inhibition, JBC In Press.

Kohira N, West J, Ito A, *et al*. (2016) *In vitro* antimicrobial activity of a siderophore cephalosporin, S-649266, against *Enterobacteriaceae* clinical isolates, including carbapenem-resistant strains. *Antimicrob Agents Chemother*. **60** (2) pp729–734

Krachler, A. M., Sharma, A., Cauldwell, A., Papadakos, G. and Kleanthous, C. (2010) TolA Modulates the Oligomeric Status of YbgF in the Bacterial Periplasm *J Mol Biol* **403** p270-285

Kumar, A. & Schweizer, H. P (2005) Bacterial Resistance to Antibiotics: Active Efflux and reduced uptake. Adv Drug Deliv Rev **57**(10) pp1486-513

Kumar, V. P, Basavannacharya, C. and de Sousa, S. M. (2014) A microplate assay for the coupled transglycosylase-transpeptidase activity of the penicillin binding proteins; a vancomycin-neutralizing tripeptide combination prevents penicillin inhibition of peptidoglycan synthesis. *Biochem Biophys Res Commun* **450**(1) pp347-352

Kuru, E., Hughes, H. V., Brown, P. J., Hall, E., Tekkam, S., Cava, F., de Pedro, M.A., Brun, Y. V., and VanNieuwenhze, M. S., (2012). In Situ Probing of Newly Synthesized Peptidoglycan in Live Bacteria with Fluorescent D-Amino Acids. *Angew. Chem. Int. Ed.* **51** (50): 12519–12523.

Lairson, L. L. Henrissat, B., Davies, G. J. and Withers S. G. (2008) Glycosyltransferases: Structures, Functions and Mechanisms *Annu Rev Biochem* **77** pp521-55

Lam, S. J., O'Brien-Simpson, N. M., Pantarat, N., Sulisto, A., Wong, E. H., Chen, Y. Y., Lenzo, J. C., Holden, J. A., Blencowe, A., Reynolds., E.C., Qiao, G. G. (2016) Combating multidrug-resistant Gram-negative bacteria with structurally nano-engineered antimicrobial peptide polymers *Nat Microbiol*. 1 (11) p16162

Lamers, R. & Burrows, L. (2016) *Peptidoglycan aeruginosa*: Targeting Cell Wall Metabolism for New Antibacterial Discovery and Development *Future Med Chem* **8** p975-92

Leclercq, S., Derouaux, A., Olatunji, S., Fraipont, C., Egan, A. J., Vollmer, W., Breukink, E. and Terrak, M (2017) Interplay between Penicillin-binding proteins and SEDS proteins promotes bacterial cell wall synthesis. *Sci Rep* 7:43306

Lewis, K. (2013) Platforms for Antibiotic Discovery Nature Reviews Drug Discovery 12, 371–387

Liao X, Hancock RE. (1997) Susceptibility to beta-lactam antibiotics of *Pseudomonas aeruginosa* overproducing penicillin-binding protein 3. *Antimicrob Agents Chemother* **41** pp1158-61

Lim, D. & Strynadka, N. C. (2002) Structural basis for the beta-lactam resistance of PBP2a from methicillin-resistant Staphylococcus aureus. Nat Struct Biol ***9****(11) pp870-876*

Ling, L. L., Schneider, T., Peoples, A. J., Spoering, A. L., Engels, I., Conlon, B. P., Mueller, A., *et al.*, (2015) A New Antibiotic Kills Pathogens Without Detectable Resistance. *Nature* **517** pp455-474

Lebar, M. D., Lupoli, T. J., Tsukamoto, H., May, J. M., Walker, S., and Kahne, D., (2013). Forming Cross-Linked Peptidoglycan From Synthetic Gram-Negative Lipid II. *Journal of the American Chemical Society* **135** (12): 4632–4635.

Liu, C.Y., Guo, C. W. *et al.*, (2010) Synthesis and evaluation of a new fluorescent transglycosylase substrate: lipid II-based molecule possessing a dansyl-C20 polyprenyl moiety. *Org Lett* **12**(7) pp1608-11

Liu, H., and Wong, C-H., (2006). Characterization of a Transglycosylase Domain of *Streptococcus pneumoniae* PBP1b. *Bioorganic & Medicinal Chemistry* **14** (21): 7187– 7195.

Lohner, K. (2017) Membrane-Active Antimicrobial Peptides as Template Structures for Novel Antibiotic Agents *Curr Top Med Chem* **17**(5) 508-519

Lovering, A. J., de Castro, L. H., Lim, D. and Strynadka, N. C. (2007) Structural Insights into the transglycosylation step of bacterial cell wall biosynthesis *Science* **315**(5817) 1402-5

Lovering and Strynadka (2008) Structural details of the glycosyltransferase step of peptidoglycan assembly *Curr Opin Struct Biol* **18** p534

Lovering, A. L., Safadi, S. S., Strynadka, N. C. J. (2012) Structural Perspective of Peptidoglycan Biosynthesis and Assembly *Annual Review of Biochemistry* **81** p451

Lupoli, T. J., Hirokazu Tsukamoto, Emma H. Doud, Tsung-Shing Andrew Wang, Suzanne Walker, and Daniel Kahne (2011) Transpeptidase-Mediated Incorporation of D-Amino Acids into Bacterial Peptidoglycan *JACS* **133** p1074

Lupoli, T. J., Lebar, M. D., Markovski, M., Berhardt, T., Kahne, D., Walker, S. (2014) Lipoprotein Activators Stimulate Escherichia coli Penicillin-Binding Proteins by Different Mechanisms *JACS* **136** 52-55

Manat G, Roure S, Auger R, Bouhss A, Barreteau H, Mengin-Lecreulx D, Touzé T. (2014) Deciphering the Metabolism of Undecaprenyl-Phosphate: The Bacterial Cell-wall unit carrier at the membrane Frontier *Microb Drug Resist*. **20**(3) pp199-214

Mark BL, Vocadlo DJ, Oliver A. (2011) Providing β-lactams a helping hand: Targeting the AmpC β-lactamase induction pathway. *Future Microbiol.* 6 p1415-1427

Marr, A. K. Gooderham, W. J. and Hancock, R. E. (2006) Antibacterial peptides for therapeutic use: obstacles and realistic outlook. *Curr. Opin. Pharmacol* **6**, 468–472.

Massova, I & Mobashery, S. (1998) Kinship and diversification of bacterial penicillin-binding proteins and beta-lactamases *Antimicrob Agents Chemother* **42**(1) 1-17.

McGowen, J. E. (2006) Resistance in non-fermenting Gram-negative bacteria: Multidrug resistance to the maximum *American Journal of Infection Control* **34** pS29-S37

Meeske, A. J., Riley, E. P., Robins, W. P., Uehara, T., Mekalanos, J. J., Kahne, D., Walker, S., Kruse, A. C., Bernhadt, T. G., Rudner, D. Z. (2016) SEDS Portiens are a widespread family of bacterial cell wall polymerises. *Nature* **537**(7622) p634-638

Meisel, U.; Holtje, J. V.; Vollmer, W. (2003) Overproduction of inactive variants of the murein synthase PBP1B causes lysis in *Escherichia coli. J Bacteriol*, **185**, 5342.

Mesleh, M. F., Rajaratnam, P. R., Conrad, M., Chandrasekaran, V,M Liu, C, M., Pandya, B. A., Hwang, Y. S., Rye, P. T., Muldoon, C., Becker, B., Zuegg, J., Meutermans, W. and Moy, T. I. (2016) Targeting Bacterial Cell Wall Peptidoglycan Synthesis by Inhibition of Glycosyltransferase Activity. *Chemical Biology & Drug Design* **87**(2) p190-9.

Miller, S. I. (2016) Antibiotic Resistance and Regulation of the Gram-Negative Bacterial Outer membrane Barrier by Host Innate Immune Molecules *mBio* **7**(5) *e01541-16*

Miller, C., Thomsen, L. F., Gaggero, C., Mosseri, R., Ingmer, H. and Cohen, S. N. (2004) SOS response induction by beta-lactams and bacterial defense against antibiotic lethality. *Science* **305**(5690) 1629-31

Minasov, G., Wawrzak, Z., Shuvalova, L., Kiryukhina, O., Dubrovska, I., Grimshaw, S., Kwon, K., Anderson, W. F. (2017) To be published. Centre for structural Genomics of Infectious Diseases. *H. influenzae* Xtal structure Dec 2016.

Miroux B, Walker JE (1996) Over-production of proteins in *Escherichia coli*: mutant hosts that allow. *J Mol Biol* 260: 289-298

Miyake, M., Asano, A. and Einaga, Y. (2008) Size Change of the Wormlike Micelles of Pentaoxyethylene, Hexaoxyethylene, and Heptaoxyethylene Dodecyl Ethers with Uptake of n-Dodecane *J. Phys. Chem. B* **112** pp4648

Moellering R. C. J (2012) MRSA: the first half century *Antimicrob Chemother* **67** p4-11

Mohammadi, T., van Dam, V., Sijbrandi, R., Vernet, T., Zapun, A., Bouhss, A., Diepeveen-de Bruin, M., Nguyen-Disteche, M., de Kruijff, B. and Breukink, E. (2011) Identification of FtsW as a transporter of lipid-linked cell wall precursors across the membrane *J. EMBO* **30**(8) pp1452-1432

Möller, U., Hobert, K., Donnerstrag, A., Wagner, P., Muller, D., Fehlhaber, H.-W., Makus, A., and Welzel, P. (1993) MoenomycinA – Structure activity relations synthesis of the D-galacturonamide analogue of the smallest antibiotically active degradation product of Moenomycin A *Tetrahedron* 49 p1635

Morrison, K.A.,Akram, A., Matthews, A., Khan, Z. A., Patel, J. H., Zhou, C., Hardy, D. J., Moore-Kelly, C., Patel, R., Odiba, V., Knowles, T. J., Javed, M. U., Chmel, N. P., Dafforn T. R. and Rothnie, A. (2016) Membrane Protein Extraction and purification using styrene-maleic (SMA) copolymer: effect of variations in polymer structure *J Biochem* **473** 4349-4360

Moya, B., Beceiro, A., Cabot, G., Juan, C., Zamorano, L., Alberti, S., Oliver, A (2012) Pan-β-lactam resistace development in *Pseudomonas aeruginosa* clinical strains: molecular mechanisms, penicillin-binding protein profiles and binding affinities *Antimicrob Agents Chemother* **56** p4771

Moya, B., Dötsch, A., Juan, C., Blázquez, J., Zamorano, L., Haussler, S. and Oliver, A. (2009) β-Lactam Resistance Response Triggered by Inactivation of a Nonessential Penicillin-Binding Protein *PLOS Pathogens* **5** e1000353

Mukherjee, S. & Zhang, Y. (2011) Protein-protein complex structure predictions by multimeric threding and template recombination *Structure* **19**(7) 955-966

Müller, P., Ewers, C., Bertsche, U., Anstett, M., Kallis, T., Breukink, E., *et al.* (2007) The essential cell division protein FtsN interacts with the murein (peptidoglycan) synthase PBP1B in *Escherichia coli. J Biol Chem* **282**: 36394-36402

Münch, D., Engels, I., Müller, A., Reder-Christ, K., Falkenstein-Paul, H., Bierbaum, G., Grein, F., Bendas, G., Sahl, H. G., Schneider, T. (2015) Structural Variations of the cell wall precursor Lipid II and their influence on binding and activity of the lipoglycopeptide antibiotic oritavancin *Antimictob Agents Chemother* **59**(2) p772-81

Mushtaq S, Woodford N, Hope R, *et al*. (2013) Activity of BAL30072 alone or combined with beta-lactamase inhibitors or with meropenem against carbapenem-resistant *Enterobacteriaceae* and non-fermenters. *J Antimicrob Chemother*. **68**(7) pp1601-1608

National action plan for combating antibiotic-resistant bacteria. The White House, Washington DC, USA: March 2015:1-63.

Newby ZE (2009) A general protocol for the crystallization of membrane proteins for X-ray. 4: 619-637

Nicola, G., Tomberg, J., Pratt, R. F., Nicholas, R. A. and Davies, C. (2010) Crystal Structures of Covalent Complexes of B-lactam antibiotics with E. coli penicillin-binding protein 5: toward an understanding of antibiotic specificity *Biochemistry* **49** p8094-8104

O'Callaghan, C. H., Acred, P., Harper, P. B., Ryan, D. M., Kirby, S. M. & Harding, S. M. (1980). GR20263, a new broad-spectrum cephalosporin with anti-pseudomonal activity. Antimicrob. Agents Chemother. 17, 876–883.

Ochs, M. M., McCusker, P., Bains, M. and Hancock, R. E. W (1999) Negative Regulation of the Pseudomonas aeruginosa outer Membrane Porin OprD Selective for Imipenem and basic Amino Acids *Antimicrob Agents Chemother* **43**(5) 1085-1090

Ostash, B & Walker, S. (2005) Bacterial Transglycosylase Inhibitors *Curr Opin Chem Biol* **9**(5) 459-46.

Ostash, B. & Walker, S. (2010) Moenomycin family antibiotics: chemical synthesis, biosynthesis, and biological activity *Nat Prod Rep* **27** p1594

Ostash, B., Campbell, J., Luzhetsky A., Walker, S. (2013) MoeH5: a natural glycorandomizer from the moenomycin biosynthetic pathway. *Mol Microbiol* **90** p1324

Paradis-Bleau, C. Markovski, M., Uehara, T,M Lupoli, T., Walker, S., Kahne, D. E. and Bernhardt T. G. (2010) Lipoprotein cofactors located in the outer membrane activate bacterial cell wall polymerases *Cell* **143**(7) p1110-1120

Perlstein, D. L. Wang, T.-S. A., Doud, E. H., Kahne, D. E. (2010) The Role of the Substrate Lipid in Processive Glycan Polymerization by the Peptidoglycan Glycosyltransferases *JACS* **132** p48

Philippon A., Redjeb, S., Fournier, G. and Ben Hassen, A. (1989) Epidemiology of extended spectrum beta-lactamases. *Infection* **17**(5) 347-54.

Pillai, B., Cherney, M.M., Diaper, C. M., Sutherland, A., Blanchard, J. S., Vederas, J. C. and James, M. N. G. (2006) Structural insights into stereochemical inversion by diaminopimelate epimerase: An antibacterial drug target *PNAS* **103** (23) pp8668-8673

Pinho, M. G., Kjos, M. Veening, J. W. (2013) How to get around: Mechanisms controlling growth and division of coccoid bacteria Nature Reviews Microbiology 11 p601-614

Pollock J.J., Ghuysen J.M., Linder R., Salton M.R., Perkins H.R., Nieto M., Leyh-Bouille M., Frere J.M., Johnson K. (1972) Transpeptidase activity of *Streptomyces* d-alanyl-d carboxypeptidases. Proc. Natl. Acad. Sci. USA. **69** p662–666

Popham, D. L. & Young, K. D. (2003) Role of penicillin-binding proteins in bacterial cell morphogenesis *Curr Opin Microbiol* **6**(6) 594-599

Pratt G. J. (1952) *Acta Cryst*. **5** 770-779 Prescott, Harley & Klein's Microbiology 7th Ed, 2008, authored by Willey, J., Sherwood, L. and Woolverton, C.

Qiao, L. & Vederas, J. C. (1993) Synthesis of a C-phosphonate disaccharide as a potential inhibitor of peptidoglycan polymerization by transglycosylase *J. Org. Chem.*, **58**(13) pp 3480–3482

Rossolini GM, Arena F, Pecile P, Pollini S. (2014) Update on the antibiotic resistance crisis. *Clin Opin Pharmacol*. **18**:56–60

Roy, R., Hohng, S., and Ha, T. (2008). A practical guide to single-molecule FRET. *Nature* methods **5,** 507-516.

Santajit, S. & Indrawattana, N. (2016) Mechanisms of Antimicrobial Resistance in ESKAPE Pathogens *Biomed Res Int.* 2475067

Sarkar, S. K., Dutta, M., Kumar, A., Mallik, D., and Ghosh, A. S. (2012) Sub-inhibitory cefsulodin sensitization of *E. coli* to β-lactams is mediated by PBP1B inhibition. *PLoS One* **7**, e48598

Sauvage, E. & Terrak. M. (2016) Glycosyltransferases and Transpeptidases/Penicillin-Binding Proteins: Valuable Targets for New Antibacterials *Antibiotics* **5**(1) pii E12.

Schagger, H. & von Jagow, G. (1987) Tricine-sodium dodecyl sulfate-polyacrylamide gel electrophoresis for the separation of proteins in the range from 1 to 100 kDa. *Analytical Biochemistry* **166** p368

Schouten, J. A., Bagga, S., Lloyd, A. J., de Pascale, G., Dowson, G. D., Roper, D. I. and Bugg, T. D. H. (2006) Fluorescent reagents for *in vitro* studies of lipid-linked steps of bacterial peptidoglycan biosynthesis: derivatives of UDPMurNAc-pentapeptide containing D-cysteine at position 4 or 5 *Mol. Biosyst.*, 2 484-491

Schwartz, B., Markawalder, J. A. and Yi, W. (2001) Lipid II: Total Synthesis of the Bacterial Cell Wall Precursor and Utilization as a Substrate for Glycosyltransfer and Transpeptidation by Penicillin Binding Protein (PBP) 1b of *Eschericia coli. JACS* **123** 11638-43

Schwartz, B. J., Markwalder, A., Seitz, S. P., Wang, Y., and Stein, R. L., (2002). A Kinetic Characterization of the Glycosyltransferase Activity of Eschericia coli PBP1b

and Development of a Continuous Fluorescence Assay. Biochemistry 41: 12552–12561.

Segel, I. H., (1993). Enzyme Kinetics. 2nd edn. Edited by Segel, I. John Wiley & Sons.

Sham, L. T., Butler, E. K., Lebar, M. D., Kahen, D., Bernhardt, T. G., Ruiz, N (2014) Bacterial cell wall. MurJ is the flippase of lipid-linked precursors for peptidoglycan biogenesis. *Science* **345**(6193) 220-222

Shaw, K. J., Rather, P. N., Hare, R. S. and Miller, G. H. (1993) Molecular genetics of aminoglycoside resistance genes and familial relationships of the aminoglycoside-modifying enzymes *Microbiol Rev* **57**(1) p138-63

Shih, H. W., Chen, K. T., Cheng, T. J., Wong, C. H., Cheng, W. C. (2011) A new synthetic approach toward bacterial transglycosylase substrates, Lipid II and Lipid IV. *Org Lett* **13** p4600

Shih, W. H. Chang, Y.F. Li, W.J. Meng, F.C. Huang, C.Y. Ma, C. Cheng, T.J. Wong, C.H. Cheng, W.C. (2012) Effect of the peptide moiety of Lipid II on bacterial transglycosylase. *Angew. Chem. Int. Ed. Engl*. **51** pp10123–10126.

Shirai, S., Yoshimura, S. and Einaga, Y. (2006) Intrinsic Viscosity of Polyoxyethylene Alkyl Ether CiEj Micelles. *Polymer Journal* **38**(1) pp37-43

Siewert, G., and Strominger, J. L. (1967) Bacitracin: An inhibitor of the dephosphorylation of lipid pyrophosphate, an intermediate in the biosynthesis of the peptidoglycan cell walls *PNAS* **57** 767-773

Silhavy, T. J., Kahne, D. K., Walker, S. (2010) The Bacterial Cell Envelope *Cold Spring Harb Perspect Biol* **2**(5) 1000414

Sofia, M. J. et al., (1999) Discovery of novel disaccharide antibacterial agents using a combinatorial library approach. *J. Med Chem* **42**(17) 3193-3198

Spratt, R. F. (2008) Substrate Specificity of bacterial DD-Peptidases (penicillin-binding proteins) *Cell. Mol. Life Sci.* **65**: 2138-2155

Stein, S., Bohlen, P. and Udenfriend, S. (1974) Studies on the Kinetics of Reaction and Hydrolysis of Fluorescamine *Arch Biochem Biophys* **163**(1) pp400-403

Starr, J., Brown, M. F., Aschenbrenner, L., Caspers, N. *et al.,* (2014) Siderophore Receptor-Mediated Uptake of Lactivicin Analogues in Gram-Negative Bacteria *J Med Chem* **57** 3845-3855

Stockhert, J. C., Blazquez, A., L., Galaz, S., Juarranz, A. (2008) A mechanism for the fluorogenic reaction of amino groups with fluorescamine and MDPF. *Acta Histochem,* **110**(4) 333-340

Sung, M.-T., Lai, Y.-T., Huang, C.-Y., Chou, L.-Y., Shih, H.-W., Cheng, W.-C., Wong, C.-H. and Ma, C. (2009) Crystal structure of the membrane-bound bifunctional transglycosylase PBP1B from *Escherichia coli*. *PNAS* **106**(22) pp 8824-8829.

Sutcliffe JA, O'Brien W, Fyfe C, *et al*. (2013) Antibacterial activity of eravacycline (TP-434), a novel fluorocycline, against hospital and community pathogens. *Antimicrob Agents Chemother*. **57**(11) pp5548–5558

Taylor, J. G., Li, X., Oberthür, M., Zhu, W. and Kahne, D. E. (2006) The Total synthesis of Moenomycin A, *JACS* **128**(47) 15084-5.

Terrak M, Ghosh TK, van Heijenoort J, Van Beeumen J, Lampilas M, *et al*. 1999. The catalytic, glycosyl transferase and acyl transferase modules of the cell wall peptidoglycan-polymerizing penicillin-binding protein 1b of *Escherichia coli. Mol. Microbiol*. **34**:350–64

Terrak, M. (2008) Peptidoglycan Glycosyltransferase Inhibition: New Perspectives for An Old Target *Anti-Infective Agents Med. Chem.* **7** *p*180–192.

Testa R, Cantón R, Giani T, *et al.* (2015) *In vitro* activity of ceftazidime, ceftaroline and aztreonam alone and in combination with avibactam against European gram-negative and gram-positive clinical isolates. *Int J Antimicrob Agents* **45**(6) pp641–646.

Tipper, D. J. & Strominger, J. L. (1965) Mechanism of action of penicillins: a proposal based on their structural similarity to acyl-D-alanyl-D-Alanine *PNAS: Microbiology* **54**: 1133-1141

Tong, S., Lin, Y., Lu, S., Wang, M., Bogdanov, M. and Zheng, L. (2016) Structural Insight into Substrate Selection and Catalysis of Lipid Phosphate Phosphatase PgpB in the Cell Membrane *The Journal of Biological Chemistry* **291***,* 18342-18352.

Touze, T. and Mengin-Lecreulx D. (2008) Undecaprenyl Phosphate Synthesis *EcoSal Plus.* **3**(1)

Typas, A., Banzhaf, M.,van den Berg vab Saparoea, B., Verheul, J., Biboy, J., Nichols, R. J., Zietek, M., Beilharz, K., Kannenberg, K., von Rechenberge, M., Breukink, E., den Blaaauwen, T., Gross, C. A. and Vollmer W. (2010) Regulation of peptidoglycan synthesis by outer membrane proteins *Cell* **143**(7) 1097-1109

Udenfriend, S., Stein, S., Bohlen, P., Dairman, W., Leimgruber, W., Weigele, M. (1972) Fluorescamine: A reagent for assay of amino acids, peptides, proteins and primary amines in the picomole range *Science*, **178** (4063) p871-2

van Dam, V., Sijbrandi, R., Kol, M., Swiezewska, E., de Kruijff, B., and Breukink, E., (2007). Transmembrane Transport of Peptidoglycan Precursors Across Model and Bacterial Membranes. *Molecular Microbiology* **64** (4): 1105–1114.

Van den Berg, B., Bhamidimarri, S. P., Prajapati, J. D., Kleinekathofer, U., Winterhalter, M. (2015) Outer-membrane translocation of bulky small molecules by passive diffusion *PNAS* **112**(23) pE2991-E2999

van der Ploeg, R., Verheul, J., Vischer, N. O., Alexeeva, S., Hoogendoorn, E., Postma, M., Banzhaf, M., Vollmer, W. & den Blaauwen, T. 2013. Colocalization and interaction between elongasome and divisome during a preparative cell division phase in *Escherichia coli*. *Mol Microbiol* **87**:1074-87

VanNieuwenhze, M. S., Mauldin, S. C., Zia-Ebrahimi, M., Winger, B. E., Hornback, W. J., Saha, S. L., Aikins, J. A., and Blaszczak, L. C., (2002). The First Total Synthesis of Lipid II: the Final Monomeric Intermediate in Bacterial Cell Wall Biosynthesis. *Journal of the American Chemical Society* **124** (14): 3656–3660.

Vega, D. & Ayala, J. A. (2006) The DD-Carboxypeptidase activity encoded by PBP4 is not essential for the cell growth of *Escherichia coli. Arch Microbiol* **185**(1) 23-7

Vinatier, V., Blakey, C. B., Braddick, D., Johnson, B. R. G., Evans, S. D., and Bugg, T. D. H., (2009). *In Vitro* Biosynthesis of Bacterial Peptidoglycan Using D-Cys-

Containing Precursors: Fluorescent Detection of Transglycosylation and Transpeptidation. *Chemical Communications,* **27**: 4037–4039.
Vivian, J. T. & Callis, P. R. (2001) Mechanisms of Tryptophan Fluorescence Shifts in Proteins *Biophysical Journal*, **80**(5) p2093-2109

Vollmer, V., Blanot, D. and de Pedro, M. A. (2008) Peptidoglycan structure and architecture *FEMS Microbiol Rev* **32**:149-167

Vollmer, W.; von Rechenberg, M.; Holtje, J. V. (1999) Demonstration of Molecular Interactions between the Murein Polymerase PBP1B, the Lytic Transglycosylase MltA, and the Scaffolding Protein MipA of *Escherichia coli. J Biol Chem*, **274**, 6726.

Waggoner AS, Stryer L. (1970) Fluorescent probes of biological membranes. *Proc. Natl. Acad. Sci*. U S A. **67**:579–589

Walker, S., Heck, A. J. R., and de Kruijff, B., (2003). Lipid II Is an Intrinsic Component of the Pore Induced by Nisin in Bacterial Membranes. *The Journal of Biological Chemistry* **278** (22): 19898–18903.

Walkty A, Adam H, Baxter M, *et al*. (2014) *In vitro* activity of plazomicin against 5,015 Gram-negative and gram-positive clinical isolates obtained from patients in Canadian hospitals as part of the CANWARD study, 2011–2012. *Antimicrob Agents Chemother*. **58**(5) pp2554-2563

Walsh, C. T. (1996) Bacterial Resistance to Vancomycin: five genes and one missing hydrogen bond tell the story. *Chemistry and Biology* **3**(1) pp21-28

Walsh, C. T. (2000) Molecular Mechanisms that confer antibacterial drug resistance *Nature*, **406**, 775-781

Walsh, C. (2003) Antibiotics: Actions, Origins, Resistance. Washington, DC: *ASM Press*. pp345

Walsh, C. T. (2004) Polyhetide and non-ribosomal peptide antibiotics: Modularity and Versatility. *Science* **202**(5665) p1805-10

Welzel, P. (2005) Syntheses around the Transglycosylation Step in Peptidoglycan Biosynthesis *Chem Rev* **105** p4610

Welzel, P., Kunisch, F., Kruggel, F., Stein, H., Scherkenbeck, J., Hiltmann, A., Duddeck, H., Müller, D., Scherkenbeck, J. E. Fehlhaber, H.-W., Seibert, G., van Heijenoort, Y., van Heijenoort, J. (1987) Moenomycin A – Minimal Structural Requirements for Biological Activity *Tetrahedron* **43** p585-598

Willard, D. M., Carillo, L. L., Jung, J. and Orden, V. (2001) Quantum Dots as Resonance Energy Transfer Donors in a Model Protein-Protein Binding Assay *Nano Letters* **1** p469

Worthington, R.J. & C. Melander. (2013) Combination approaches to combat multidrug-resistant bacteria. *Trends Biotechnol*. **31**: 177–184

Yang, G., Hennig, L., Findeisen, M., Oehme, R. Giesa S. and Welzel, P. (2004) Studies on the Synthesis of Trisaccharide Analogues of the Antibiotic Moenomycin A *Helvetica Chimica Acta* **87** p1794

Yang, J.-C., van den Ent, F., Neuhaus, D., Brevier, J., Löwe, J. (2004) Solution structure and domain architecture of the divisome protein FtsN. *Molecular Microbiology* **52**(3), pp651-660

Yang, J. & Zhang Y. (2015) Protein Structure and Function Prediction using I-TASSER *Current Protoc Bioinformatics* **52** 5.8.1-5.815

Yau, W.-M., Wimley, W. C., Gawrisch, K. and White, S. H. (1998) The Preference of Tryptophan for Membrane Interfaces *Biochemistry* **37**(42) pp14713-14718

Ye, X.-Y., Lo, M.-C., Brunner, L., Walker, D., Kahne, D., Walker, S. (2001) Better Substrates for Bacterial Transglycosylases *JACS* **123** p3155

Yim, G., Thaker, M. N., Koteva, K. and Wright, G. (2014) Glycopeptide antibiotic Biosynthesis *The journal of Antibiotics* **67** pp31-41

Yuan, Y., Barrett, D., Zhang, Y., Kahne, D., Sliz, P. and Walker, S. (2007) Crystal structure of a peptidoglycan glycosyltransferase suggests a model for processive glycan chain synthesis. *PNAS* **104** p5348

Yuan, Y., Fuse, S., Ostash, B., Sliz, P., Kahne, D. & Walker, S. (2008) Structural Analysis of the Contacts Anchoring Moenomycin to Peptidoglycan Glycosyltransferases and Implications for Antibiotic Design *ACS Chem Biol* **7** p429

Zhang Y, Bao Q, Gagnon LA, Huletsky A, Oliver A, Jin S, Langaee T. (2010) *ampG* gene of *Pseudomonas aeruginosa* and its role in β-lactamase expression. *Antimicrob Agents Chemother*. **54** pp4772–4779